Broome 2003

International Crystallography Meetings

- AsCA'03/Crystal-23 Conference Aug 10-13
- Biological Structure Workshop Aug 13-15
- Sagamore XIV Conference Aug 13-18

Broome2003
International Crystallography Meetings

AsCA'03/Crystal-23

Joint conference of the
Asian Crystallographic Association and the
Society of Crystallographers in Australia and New Zealand

Biological Structure Workshop

Meeting of the ***IUCr Commission on Biological Macromolecules***

Sagamore XIV

Meeting of the ***IUCr Commission on Charge, Spin and Momentum Densities***

ISDN 1 74052 099 8

Printed by Lamb Printers, 9 Robertson Street, Perth 6000, Australia

Contents

Committees

Organising

Syd Hall (Chair)
Mitchell Guss
Trevor Hambley
Brian O'Connor
Brian Skelton
Mark Spackman
Allan White
Matthew Wilce

AsCA/Crystal Program

Mitchell Guss (Chair)
Jenny Martin (Co-chair BioWshop)
Mark Spackman (Chair Sagamore)
Matthew Wilce (Co-chair BioWshop)
Ted Baker
Yuji Ohashi
Allan White
M Vijayan
Brendan Kennedy
Yu Wang
Ian Williams

Sagamore XIV Program

Mark Spackman (Chair)
Arun Bansil
Pierre Becker
Joanne Etheridge
Carlo Gatti
Heinz Graafsma
Arsen Gukasov
Bo Iversen
Dylan Jayatilaka
Wim Klooster
Claude Lecomte
Thomas Lippman
Seppo Manninen
Rob Robinson
John Spence
Francis Tasset
Erich Weigold
Jian-Min Zuo

Sponsors & Exhibitors

International Union of Crystallography
Asian Crystallographic Association
Society of Crystallographers in Australia and New Zealand
Australian Synchrotron Project

marresearch
Bruker Nonius
Rigaku/MSC

Oxford Cryosystems
CCP4
Fluidigm
PANalytical
John Morris Scientific
Moreton Bay Scientific

Meeco
Sietronics
Biolab Australia
Hampton Research
Discovery Partners International
deCODE genetics – BioStructures Group

Institute of Physics Publishing
Royal Society of Chemistry – CrystEngComm
Australian Synchrotron Research Program
Australian Nuclear Science & Technology Organisation
Protein Data Bank

Broome Aviation
Willie Creek Pearls

General Information

Meeting Dates & Venue

Three international crystallography meetings will be held at the Cable Beach Club resort in Broome from August 10-18 2003.

The joint conference **AsCA'03/Crystal-23** of the *Asian Crystallographic Association* and the *Society of Crystallographers in Australia and New Zealand* will be held as parallel sessions in the Sam Male rooms A and B at the Cable Beach Club resort held from August 11-13.

The **Biological Structure Workshop** is held under the auspices of the *IUCr Commission on Biological Macromolecules* as a single session in the Sam Male room A at the Cable Beach Club resort held from August 14-15.

The **Sagamore XIV Meeting** is held under the auspices of the *IUCr Commission on Charge, Spin and Momentum Densities* as a single session in the Sam Male room B at the Cable Beach Club resort held from August 14-18.

The dates for the scientific sessions for all three meetings are summarised below.

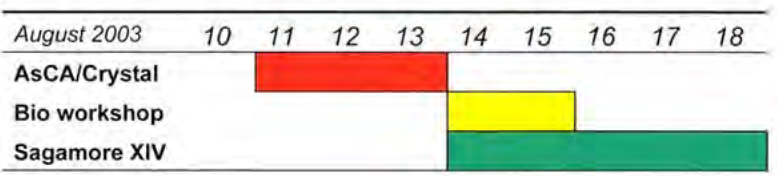

Note: Detailed program timetables of the scientific sessions for each meeting are given in the respective program sections edged with these colours.

Evening Functions

Bruker-Nonius Welcoming Reception (R)

Sunday August 10th at 18:00

A social mixer will be held for AsCA'03/Crystal-23 registrants at the *Club Pool*. Music by the Steve Pigrim Trio.

marresearch Sunset Dinner (D)

Wednesday August 13th at 18:00

The farewell dinner for AsCA'03/ Crystal-23 participants, and the welcome to Bio Workshop and Sagamore XIV registrants, will be held at the *Cable Beach Amphitheatre*. Music by Mick Manolis.

Rigaku/MSC Aussie Barbecue (B)

Friday August 15th at 18:00

A barbecue will be held at the *Kimberley BBQ at the Club Pool* for all Biological Workshop and Sagamore XIV registrants. Music by Alana Pigrim and Calib.

Asian Buffet (A)

Sunday August 17th at 18:00

A farewell Asian buffet dinner will be held at the *Club Pool* for all registrants of the Sagamore XIV meeting.

The registrant entitlements for the evening social functions are summarised below. Name badges will be required for entry into each of these functions.

August 2003	*10*	*11*	*12*	*13*	*14*	*15*	*16*	*17*	*18*
AsCA/Crystal	**R**			**D**					
Bio workshop				**D**		**B**			
Sagamore XIV				**D**		**B**		**A**	

Conference Office

The Conference Office for all three meetings is located at the CBC room close to the Sam Male lecture rooms. It will be open in the mornings from 9:00-12:00, August 11-15. For phone contact call 9192 0400 (international 61 8 9192 0400) and the call will be directed to the conference office.
Faxes should be sent to (61) 8 9192 3417.
For other enquiries contact a member of the organising committee (they have a red dot on their name tags).

Name Badges

Name badges are required for entry into all scientific sessions, lunches and evening functions.

Meals

Evening functions, lunches and mid-morning and poster refreshments are part of the registration package for full, student and accompanying members. Lunches are on the Sam Male veranda from 13:00-13:45 from August 11-18. For other meals see the information about places to eat at Cable Beach and in Broome on page 10.

Medical and Emergency Contacts

The phone number for an urgent emergency in Australia is **000**. This will connect you immediately to POLICE, FIRE and MEDICAL services. State the problem and your location clearly, and assistance will be sent immediately. This number should be used ONLY for emergency help.

For the Broome Hospital call **9192 2222**.

For non-emergency medical assistance contact:
Dakas Street Medical Centre and Pharmacy
Phone 9192 6311

Broome Medical Centre
Phone 9192 2022

AMCAL Pharmacy
Broome Boulevard Shopping Centre
Phone 9192 1866

Phone, Fax and Post

All communications for you sent to the conference hotel will be posted on a Communications poster board at the entrance of the Sam Male lecture halls. When you are phoning overseas numbers from Australia remember to precede the *country code* with **0011**.

Broome's time zone is +8:00GMT. Here are the relative time differences for some cities when making phone calls.

Singapore	0h	London	-7h
Tokyo	+1h	New York	-12h
Sydney	+2h	Chicago	-13h
Frankfurt	-6h	Los Angeles	-15h

Email and Internet

Email and Internet services are not available as part of the conference facilities. The phone jack in your hotel may be suitable for a personal computer connection. Check if your hotel has a business centre for your use.

Banking and Currency Exchange

The Cable Beach Club resort reservation desk will exchange currency and travellers cheques, and an ATM (automatic teller machine) that accepts most credit cards is available in the gift shop. Exchange facilities are available at banks in Broome. Banking hours are usually between 10:00 and 16:00 Monday to Friday only.
Most shops and restaurants in Broome will accept international credit cards for payment.

Restaurants

Beer & Satay Hut
Palms Resort, Walcott Street
Burgers, seafood, pizza and more, in outdoor garden setting. A fun place to eat, drink, and meet with friends. Tel: 9192 1898

Cafe Carlotta
Wood-fired pizzas and pasta (hosts: Charlotte and Mick)
Tel: 9192 7606

Charters Restaurant
Mangrove Hotel, Carnarvon Street
Full range menu in comfortable air conditioned setting with magnificent view of Roebuck Bay. Tel: 9192 1303

Club Restaurant
Cable Beach Club Resort
Award winning dining in elegant ambience, indoors or outdoors al fresco on the boardwalk. Reservations essential. Tel: 9192 0411

Conti Bar & Bistro
Mercure Inn Continental Hotel, Weld Street
Breakfast lunch and dinner 7 days a week. Great value family dining. Tel: 9192 1002

Kimberley BBQ
Cable Beach Club Resort
An Australian outdoors a la carte restaurant serving the best in local bush specialties, including Kimberley beef, emu, crocodile and barramundi. Live entertainment every evening. Call for reservations. Tel: 9192 0413

Lord Mac's
Cable Beach Club Resort
Breakfast, a la carte lunch and theme smorgasbord dinner 7 days a week. The Saturday night seafood buffet is a local favourite.
Tel: 9192 0470

Matso's Cafe & Brewery
Hamersley Street
Open 7 days breakfast, lunch & dinner. Choose from a selection of coffees, cakes, fresh juices, shakes and meals. Refresh yourself with a real beer, brewed on site using time-honoured techniques or choose a fine wine. Sit back on the verandah overlooking Roebuck Bay & watch "Broometime" go by
Tel: 9193 5811

Noodlefish
Shop 2/6 Hammersley Street
Best Thai in town, sit on the verandah, have a private party for 12 in the garden or take it away. It's BYO. All entrees under $10 and mains under $20. Open: Mon-Sat 5.30pm-late. No credit cards; No booking. Tel: 9192 5529

Pure Steel Restaurant & Bar
Tropicana Inn, Robinson Street
Great value counter meals and Governor Bar. Friday night seafood buffet and Sunday night carvery. Tel: 9192 1204

Sandbar and Grill
Cable Beach beachfront (close to the CBC)
Casual cafe with inexpensive food and drinks. Open 7 Days. No bookings.

Sheba Lane Garden Restaurant
Napier Terrace, Chinatown
Enjoy alfresco dining or airconditioned comfort for lunch and dinner. Extensive menu ranging from Japanese, Thai dishes, Kimberley steak and fish to Chilli Mud Crab. Fully licensed. Open 7 Days. Tel: 9193 6036

The Icecreamery
Carnarvon Street, Chinatown
Specialising in homemade all natural ice creams, sundaes, smoothies, shakes and juices. Open 7 days. Tel: 9193 5400

The Old Zoo Cafe
Challenor Drive, Cable Beach
Open for breakfast and lunch 7 days a week. Great sandwiches, cakes and coffees in the tropical setting of the old Pearl Coast Zoological Gardens. Tel: 9193 6200

The Tides Garden Restaurant
Mangrove Hotel, Carnarvon Street
Take in the panoramic views of Roebuck Bay while enjoying a scrumptious meal, a hot coffee or an ice cold drink. The menu is extensive, fresh and simply delicious. Open for lunch, Dinner, Coffee & Cake. 7 Days.
Tel: 9192 1303

Tours & Attractions

With its exotic history, pearling industry and natural features, you'll find plenty of sights and attractions in and around Broome. Whether your interests lean toward art and culture, history or exploring the great outdoors, there's something for everyone.

Most of the attractions listed below are free and open to the public. Others have specific open hours and may have an entry fee. Where phone numbers are provided, it's a good idea to check ahead for hours and details.

The **Shinju Matsuri Festival of the Pearl** runs in the Broome township from Aug 15-24, and the **Staircase to the Moon** from Aug 12-15.

A visit to the Tour Office at the CBC (phone 9192 0417), or the **Visitor Centre** in the Broome (phone 9192 2222), is a good starting point for expert advice and information on the sights and attractions. In addition to information, the staff provide a booking service for all your needs.

Have fun and don't forget a relaxing sunset walk along Cable Beach!

ANASTASIA'S POOL
Located at Gantheaume Point and built by a former lighthouse keeper for his wife, Anastasia, who was crippled with arthritis and found relief in the pool.

LIONS PIONEER PARK
Located at Town Beach (end of Robinson Street). This is a pleasant picnic and recreation area, and a great spot to watch the Staircase to the Moon August 12-15.

ART GALLERIES
Broome is home to a vast array of art galleries specialising in local and indigenous art.

BEAGLE BAY
Located 118 kms north of Broome, the Beagle Bay church was built by Pallotine Monks with raw materials from the area and completed in 1918. It features a unique altar beautifully decorated with pearl shell. Visitors must contact the office on arrival and a fee of $5 is charged for entry to the community. Access is by 4WD only. Tours are available.

BEDFORD PARK
Situated overlooking beautiful Roebuck Bay on Hamersley Street is the site of Broome's War Memorial. The park features an array of memorabilia, including a replica of one of explorer William Dampier's sea chests and an old train coach once used on a railway that connected the original jetty at Town Beach to Chinatown.

BROOME BIRD OBSERVATORY
Located 18 kms from Broome on the shores of beautiful Roebuck Bay, visitors will share the amazing story of Broome's migratory shorebirds from Siberia. The North West is regarded as the most significant site in Australia for shorebirds, as over 800,000 use the area annually. Self interpretive walks. Phone 9193 5600.

BROOME BREWERY
Broome's first boutique brewery opened in 1997 and is situated in Matso's Gallery. It is the only brewery in the Kimberley and the Brewhouse is always open for viewing. Meals are served all day from 8am. Phone 9193 5811.

BROOME CROCODILE PARK
The park is home to over 1500 dangerous salt water crocodiles as well as Australian fresh water crocodiles, New Guinea freshwater crocodiles, South American Caimans and American Alligators. Don't miss the afternoon feeding! Phone 9193 7824.

BROOME GOLF CLUB
The only 18 hole fully grassed course between Geraldton and Darwin! Open to the public. Hire clubs, club house facilities. Call 9192 2092.

BROOME HISTORICAL SOCIETY MUSEUM
Definitely one of the best regional museums in Australia - a must see when visiting! Features a display on pearling and a large collection of photographs and files that piece together the fascinating history of Broome. Located in the old Custom's House behind the Seaview Shopping Centre. Phone 9192 2075.

BUCCANEER ROCK
Broome legend has it that Buccaneer explorer, William Dampier, came to the present town anchorage, landed a treasure chest of pirated pieces of eight and buried it at Buccaneer Rock. His ghost is said to be seen there on a misty night with a lantern looking for the lost loot. A great legend but, alas, the treasure seems only an often repeated myth. The Rock is located in Roebuck Bay opposite the Mangrove Hotel.

CAPTAIN GREGORY'S HOUSE
Built in 1917 for Captain A.C. Gregory, who operated one of Broome's most successful pearling businesses. A fine example of early Broome architecture and has now been converted to an art gallery. Situated on the corner of Hamersley and Carnarvon Streets in the same grounds as Matso's Gallery and Broome Brewery. Phone 9193 5811.

CHINATOWN
Take a wander through the original commercial centre of Broome, which was once the bustling hub of pearl sheds, billiard saloons, entertainment houses and Chinese eateries. Chinatown is now home to some of the worlds finest pearl showrooms, along with a variety of retail outlets. Sidewalk cafes add a splash of colour to the pavements.

CHINESE CEMETERY
The resting place for members of Broome's Chinese community, situated on Port Drive.

COURTHOUSE and COURTHOUSE MARKETS
Built in distinctive "Broomestyle" architecture, the courthouse was the original Cable House, where the Broome end of the oceanic telegraph cable terminated. Browse through the gardens or visit the popular Courthouse Markets held on Saturday mornings from 8am - 1pm all year. Located on the corner of Frederick and Hamersley streets.

CULTURED PEARLING MONUMENT
Mr. Tokuichi Kuribayashi, originally from Nippon Pearl Company, Tokyo, Mr. Hiroshi Iwaki and Keith Francis Dureau from Pearl Prop. Ltd. were pioneers in the cultured pearl industry in Broome. The three lifesize statues are now on display on the grassed area of Carnarvon Street in Chinatown.

DAMPIER PENINSULA
The Dampier Peninsula is a unique area north of Broome featuring spectacular red pindan cliffs, azure waters and an amazing variety of flora and fauna. Several Aboriginal communities offer bush tucker walks and mud-crabbing tours. Access is by 4WD only. A variety of day tours are available from Broome - contact Broome Tourist Bureau for details.

DINOSAUR FOOTPRINTS
Dinosaur footprints over 120 million years old can be seen at Gantheaume Point at very low tide. As the reef area is very fragile, care must be taken when exploring this area. For the benefit of visitors, a plaster cast of the tracks has been embedded at the top of the cliff.

DIVING
Beneath the sparkling tropical waters that surround Broome is a diverse aquatic habitat that is fast developing a reputation as a unique diving experience. Half day, full day and extended dive trips are available. Charters are also available to the Rowley Shoals. Situated approximately 260 kilometres west of Broome on the edge of the Continental shelf, the Rowley Shoals is one of the best diving areas in the world where the magnificent coral gardens, giant clams and large reef fish astound visitors. For a list of dive operators contact the Broome Tourist Bureau.

FISHING
Broome waters boast an abundance of different varieties of fish including the elusive sailfish. Full, half day or extended fishing charters available and tournaments are held annually. For a list of fishing charter operators contact the Broome Tourist Bureau.

FLYING BOAT WRECKS
These wrecks remain as evidence of the flying boats sunk by the Japanese air raid on Broome during WWII. Located approximately 1 km offshore from Town Beach and visible only on minus tides. Check with Broome Tourist Bureau for tide times and viewing information.

GANTHEAUME POINT
Located approximately 6 km from town, this is a scenic area of red, craggy cliffs providing a stark contrast to the azure water below. Dinosaur footprints over 120 million years old can be seen here when tides are less than 1.5 metres. As the reef area is very fragile, care must be taken when exploring this area. For the benefit of visitors a plaster cast of the tracks has been embedded at the top of the cliff.

HARD HAT DIVER
This life size statue of the Hard Hat Pearl Diver adjacent to the Cultured Pearling Monument in Chinatown, was erected in 1999 to pay tribute to the

role that the Hard Hat Diver played in establishing Broome as the centre of the world's pearling industry in the early 1900's. These early Pearl Divers came from diverse cultural backgrounds, and this resulted in Broome being exempted from the White Australia Policy, making the town a pioneer of multiculturalism in Australia. Around 50 of these divers along with many of their ancestors still reside in Broome today.

JAPANESE CEMETERY
A testimony to the perils of the early pearl diving and the final resting place of over 900 pearl divers. Situated on Port Drive.

LIBRARY
Broome boasts a modern library situated in the Civic Centre gardens on Hamersley Street. Visitors welcome to borrow books. Open hours: Mon/Wed/Fri 10am-5pm; Tue/Thu 10am-7pm; Sat 9am-12noon; Closed Sunday.

MATSO'S GALLERY AND COFFEE HOUSE
Matso's Gallery houses the largest and most diverse collection of artwork in the Kimberley. The Gallery has a wide range of Aboriginal art and artifacts with artwork from all of the major art communities in the Western Desert. The Coffee House serves a range of light meals and drink throughout the day from 8am. A range of boutique beers is also available from the Broome Brewery which is also located in Matso's Store. Phone 9193 5811.

PEARL SHOPS
As the home of some of the most precious pearls in the world, Broome has a good selection of pearl shops catering to all budgets.

PEARL LUGGERS
Experience more than 140 years of Broome's unique maritime heritage. Take an historical journey through the life and times of the pearl divers on two of the last surviving perfectly restored pearl luggers. Brought to life through 1 hour guided tours. Phone 9192 2059.

PIONEER CEMETERY
Located at Lions Pioneer Park, near Town Beach. Resting place of some of Broome's early settlers.

REDDELL BEACH
This spectacular stretch of beach is an ideal place to observe the red pindan cliffs of Broome's peninsula coastline. Named after Captain Reddell, who was murdered by his mutinous crew in 1899. Great for swimming and picnicking. Located 8 km from the town centre.

ROWLEY SHOALS
Situated approximately 260 kilometres west of Broome on the edge of the Continental shelf, Rowley Shoals is one of the best diving areas in the world where the magnificent coral gardens, giant clams and large reef fish astound visitors. Extended dive charters are available. For a list of dive operators contact the Broome Tourist Bureau.

THE SHELL HOUSE OF GUY STREET
A museum and retailer of seashells, shell products and mother of pearl. Handcrafting of pearl shell carried out on the premises. Phone 9192 1423. No entry fee.

STAIRCASE TO THE MOON (August 12-15)
This natural phenomenon is caused by a full moon rising over the exposed mudflats of Roebuck Bay at extremely low tides, creating a beautiful optical illusion of a staircase reaching to the moon. Great locations to view the Staircase include the outdoor bar at the Mangrove Hotel and Town Beach. Staircase Markets take place during most staircase dates at Town Beach, and feature a great selection of foods and crafts.

SUN PICTURES
A unique movie experience! Officially opened in 1916, it is believed to be the oldest operating picture garden in the world. This indoor/outdoor theatre has withstood the ravages of war, cyclones and king tides. Housed in the foyer is an excellent display of movie memorabilia. Taking in a movie under the stars at Sun Pictures is a must do when visiting Broome! Located in Chinatown. Current movies are shown every night. Phone 9192 3738.

TESLING TROPICAL FRUIT & MANGO WINE
An innovative new wine producer, Mango Wine of Broome has enjoyed rapid expansion to meet the growing demand from locals and visitors alike, eager to tantalise their palate with the unique blend of succulent flavour contained within the Kensington Pride Mango. Situated 19 km from Broome. Tasting available for small fee. Phone 9192 1433.

TOWN BEACH
Ideal relaxing picnic and swimming spot located at the end of Robinson Street. Cafe facilities available. Also a great spot to watch the *Staircase to the Moon* and enjoy the Staircase Markets.

WILLIE CREEK PEARL FARM
Discover how some of the world's largest and most highly prized gems are produced. The managers of the pearl farm demonstrate the intricate process of cultured pearling, including live oyster seeding. There is a great educational demonstration for those interested in the pearling industry. Their showroom houses an extensive display of locally handcrafted jewellery and loose pearls for purchase at very competitive prices. Located 38 kms north of Broome. Coach or self drive tours available - times vary depending on the season. Phone 9193 6000 for tour times and details. Bookings are essential.

AsCA'03/Crystal-23 Program

August	10 Sunday	11 Monday		12 Tuesday		13 Wednesday	
8:30		Plenary 1		Plenary 3			
9:00							
9:30		Plenary 2		Plenary 4		AWe1A	AWe1B
10:00							
10:30		Coffee/Tea		Coffee/Tea		Coffee/Tea	
11:00							
11:30		AMo1A	AMo1B	ATu1A	ATu1B	AWe2A	AWe2B
12:00							
12:30							
13:00		Lunch		Lunch		Lunch	
13:30							
14:00							
14:30		A	B	A	B	A	B
15:00		*ASPW*	*TwinW*	*MSW*		*SCANZ*	
15:30							
16:00	Registration					Plenary 5	
16:30							
17:00						Plenary 6	
17:30		POSTERS		POSTERS			
18:00							
18:30	Bruker-Nonius					marresearch	
19:00	Welcoming					Sunset	
19:30	Reception					Dinner	
20:00							
20:30		AMo2A	AMo2B	ATu2A	ATu2B		
21:00							

ASPW = Australian Synchrotron Project Workshop; *TwinW* = Twinning Workshop

MSW = Modulated Structures Workshop; *SCANZ* = SCANZ General Meeting

Plenary session

Chair: Mark Spackman

8:30 PL-1 **COHERENT X-RAY DIFFRACTION FOR PHASING IN CRYSTALLOGRAPHY**
Ian Robinson *(Maslen 1987 Fellow)*

Chair: Bill Duax

9:30 PL-2 **CONTROLLING THE VAN DER WAALS INTERPLAY OF FULLERENE C60**
C. L. Raston, J. L. Atwood, L. J. Barbour, & M. W. Heaven

10:30 Coffee Break

Oral session 1A: *Nucleic acids and their protein complexes* Room A

Chair/Co-chair: Akio Takénaka, Adrienne Adams

11:00 Introduction: Adrienne Adams

11:10 AMo1A-1 **STRUCTURE OF T7 RNA POLYMERASE ELONGATION COMPLEX AT 2.9Å RESOLUTION**
Dmitry G. Vassylyev, Tahir H. Tahirov, Dmitry Temiakov, Michael Anikin, Vsevolod Patlan, William T. McAllister, and Shigeyuki Yokoyama

11:40 AMo1A-2 **CRYSTAL STRUCTURES OF THE REPLICATION TERMINATION PROTEIN BOUND TO DNA REVEAL A MODE OF POLAR REPLICATION FORK ARREST**
J. P. Vivian, C. J. Porter, J. A. Wilce, and M. C. J. Wilce

12:00 AMo1A-3 **TWO CRYSTAL STRUCTURES OF D(GICGAGAGC) SUGGEST THAT POTASSIUM IONS MEDIATE TO FORM DNA OCTAPLEX WITH I-MOTIF OF GUANINE QUARTET**
Jiro Kondo, Shun-ichi Umeda, Tomoko Sunami, and Akio Takénaka

12:20 AMo1A-4 **BACTERIAL OFFENSE AND DEFENSE MECHANISMS USING NON-SPECIFIC ENDONUCLEASES**
Hanna S. Yuan, Chia Lung Li, Kuo-Chiang Hsia, and Woei-Chyn Chu

12.40 AMo1A-5 **STRUCTURE OF MYCOBACTERIUM TUBERCULOSIS SINGLE-STRANDED DNA-BINDING PROTEIN. VARIABILITY IN QUATERNARY STRUCTURE AND ITS IMPLICATIONS**
K. Saikrishnan, J. Jeyakanthan, J. Venkatesh, N. Acharya, K. Sekar, U. Varshney, and M. Vijayan

13:00 Lunch

Oral session 1B: *Structural chemistry* Room B

Chair/Co-chair: Colin Raston, Yu Wang

11:00 AMo1B-1 **X-RAY ANALYSIS OF VARIOUS REACTION PATHWAYS OBSERVED FOR UNSTABLE NITRENES**
Yuji Ohashi, Takahiro Mitsumori, Terufumi Takayama, Hidehiro Uekusa, and Masaki Kawano

11:30 AMo1B-2 **HYDROTHERMAL SYNTHESIS, CRYSTAL STRUCTURES, AND SOLID STATE NMR SPECTROSCOPY OF METAL SILICATES**
Kwang-Hwa Lii

11:55 AMo1B-3 **POWDER NEUTRON DIFFRACTION STUDY OF UNSATURATED THIOAMIDE DERIVATIVE**
Takashi Ohhara, Susumu Ikeda, Kenichi Oikawa, Akinori Hoshikawa, Takashi Kamiyama, Takaaki Hosoya, and Yuji Ohashi

12:15 AMo1B-4 **PHASE TRANSITION OF DEHYDRATED CALCINED ALPO4-5 INVESTIGATED BY IN-SITU SYNCHROTRON XRD**
Hwo-Shuenn Sheu, Jey-Jau Lee, Khin Win Phyu, Kuei-Jung Chao

12.35 AMo1B-5 **COMPLEXES OF SIMPLE ALKALI METAL SALTS WITH N,N'-AROMATIC BIDENTATE LIGANDS**
Allan H. White, Jarrod N. Buttery, Effendy, George A. Koutsantonis, Siti Mutrofin, Neil C. Plackett, Brian W. Skelton, and Claire R. Whitaker

13:00 Lunch

14:00 **Australian Synchrotron Project Workshop** Room A
Convener: Richard Garrett *(see p380 for program)*

14:00 **Twinning Workshop** Room B
Convener: Victor Young *(see p381 for program)*

Oral session 2A: *Computational biology and methods* Room A

Chair/Co-chair: Janet Smith, Bret Church

20:00 AMo2A-1 **CADB: CONFORMATION ANGLES DATABASE OF PROTEINS**
K. Sekar, G. Ramya Bhargavi, P. Ananthalakshmi, and S. S. Sheik

20:25 AMo2A-2 **USING STRUCTURAL INFORMATION IN FUNCTIONAL GENOMICS: IDENTIFICATION OF PROTEIN KINASE SUBSTRATES**
Bostjan Kobe, Robert A. Breinl, and Ross I. Brinkworth

20:45 AMo2A-3 **CAN YOU PREDICT WHETHER A PROTEIN WILL CRYSTALLISE FROM THE PRIMARY SEQUENCE?**
Adrian H. Batchelor

21:05 AMo2A-4 **CYSTEINE DISTRIBUTION AND THE EVOLUTION OF SHORT CHAIN OXIDOREDUCTASE ENZYMES: COVARIANCE AND DISULFIDE BOND POTENTIAL**
W. L. Duax, V. Pletnev, and R. Huether

21:30 Close

Oral session 2B: *Supramolecular chemistry & crystal engineering* Room B

Chair/Co-chair: Peter Turner, Yoshio Matsui

20:00 AMo2B-1 **THREE NOVEL POLYMERIC NETWORK OF COPPER(II) CONSTRUCTED WITH SUCCINATO LIGAND AND THE INFLUENCES OF WEAK INTERACTIONS ON THEIR CRYSTAL PACKING**
Tian-Huey Lu, G. Mostafa, and N. Ray Chaudhuri

20:30 AMo2B-2 **NEW BOROPHOSPHATES IN MAIN GROUP ELEMENT Al, Ga AND In SYSTEMS : SYNTHESES AND STRUCTURES**
J.-T. Zhao, and R. Kniep

20:50 AMo2B-3 **IN-SITU SINGLE CRYSTAL X-RAY DIFFRACTION STUDIES OF GUEST-EXCHANGE IN NANOPOROUS FRAMEWORK MATERIALS**
Gregory J. Halder, Cameron J. Kepert, Boujemaa Moubaraki, Keith S. Murray, and John D. Cahsion

21:10 AMo2B-4 **CHANNELS IN 3-DIMENSIONAL COORDINATION POLYMERS: ZINC SACCHARATE AND LANTHANUM MUCATE**
Michael Moylan, Brendan Abrahams, Simon Orchard, and Richard Robson

21:30 Close

Poster session 17:00 – 18:30 Veranda

AMoP-01 **EXPERIMENTAL CHARGE DENSITIES IN STRONGLY HYDROGEN-BONDED AROMATICS**
Ross O. Piltz, David E. Hibbs and Peter Williams

AMoP-02 **A WAVEFUNCTION CONSTRAINED JOINTLY TO X-RAY AND POLARISED NEUTRON DIFFRACTION DATA FOR THE Cs_3CoCl_5 CRYSTAL**
Dylan Jayatilaka

AMoP-03 **USING THE HIRSHFELD SURFACE TO INVESTIGATE CRYSTAL PACKING IN POLYMORPHS AND CRYSTALS WITH Z'>1**
Joshua McKinnon, and Mark Spackman

AMoP-04 **A NEW HYBRID MATERIAL WITH THREE DIMENSIONAL Na-O-Cu CONNECTIVITY AND ITS NANOSTRUCTURES BY ANNEALING**
G. Mostafa, Tian-Huey Lu, and N. Ray Chaudhuri

AMoP-05 **PROTEIN CRYSTALLIZATION IN SPACE USING COUNTER-DIFFUSION TECHNIQUE**
Hiroaki Tanaka, Koji Inaka, Sachiko Takahashi, Satoshi Sano, Masaru Sato, and Susumu Yoshitomi

AMoP-06 **PROTEIN CRYSTAL GROWTH WITH STIRRING SOLUTION**
Hiroaki Adachi, Kazufumi Takano, Masashi Yoshimura, Yusuke Mori, and Takatomo Sasaki

AMoP-07 **A STRUCTURAL STUDY ON THE POLYMORPH OF ICOSANE-1,20-DIOL**
K. Uno, N. Nakamura, and Y. Ogawa

AMoP-08 **HYDROTHERMAL SYNTHESIS OF SINGLE-PHASE HYDROXYAPATITE WHISKERS AND CRYSTAL STRUCTURE CHARACTERISATION BY HRTEM AND IMAGE SIMULATION**
Z. L. Dong, and T. J. White

AMoP-09 **THE EFFECT OF MIXED Mn VALENCES ON Li MIGRATION IN $LiMn_2O_4$: MOLECULAR DYNAMICS SIMULATIONS**
Kenji Tateishi, Douglas du Boulay, and Nobuo Ishizawa

AMoP-10 **MECHANISM FOR PIEZOELECTRICITY OF LANGASITE CRYSTAL UNDER HIGH PRESSURE**
N. Araki, T. Iwataki, K. Kakimoto, H. Ohsato, T. Kuribayashi, Y. Kudoh, and H. Morikoshi

AMoP-11 **IMIDE-AMIDE BETWEEN KEMP'S ACID AND L-PROLINOL AND THE HYDROGEN BONDING**
M. Kawaminami, Y. Odo, T. Shimo, and K. Somekawa

AMoP-12 **STRUCTURE ANALYSIS BEFORE AND AFTER ACCELERATED EXAMINATION FOR DETERIORATION OF BAM, BLUE PHOSPHOR**
H. Imura, T. Honma, I. Hirosawa, Y. Shimomura, and N. Kijima

AMoP-13 **CRYSTAL STRUCTURE OF A STREPTOCOCCAL SUPERANTIGEN, SPE-J**
Heather M. Baker, Vickery L. Arcus, Thomas Proft, Melissa Nicholson, John D. Fraser, and Edward N. Baker

AMoP-14 **STRUCTURAL GENOMICS OF MOUSE MACROPHAGE PROTEINS**
Nathan Cowieson, Pawel Listwan, Christine Wells, Thomas Huber, Timothy Ravasi, Anna Aagaard, Bostjan Kobe, and Jenny Martin

AMoP-15 **CRYSTALLOGRAPHIC STUDIES ON HEN SERUM TRANSFERRIN**
Piyali Guha Thakurta, Debi Choudhury, Rakhi Dasgupta, and J. K. Dattagupta

AMoP-16 **BIOPHYSICAL STUDIES OF A NOVEL RNA BINDING PROTEIN**
Corrine J. Porter, Lois A. Balmer, Peter J. Leedman, Matthew C. J. Wilce, and Jackie A. Wilce

AMoP-17 **DETAILED STRUCTURE OF L-METHIONINE g-LYASE FROM PSEUDOMONAS PUTIDA BASED ON THE RESULT OF 1.8 Å RESOLUTION X-RAY CRYSTAL STRUCTURE DETERMINATION**
Shintaro Misaki, Tomoaki Takakura, Takayuki Yoshioka, Robert M Hofman, Shigeo Yagi, Kenji Inagaki, and Akio Takimoto

AMoP-18 **THE EAFP CRYSTAL GROWTH OBSERVED BY ATOMIC FORCE MICROSCOPY**
Sheng Wang, Ye Xiang, and Dacheng Wang

AMoP-19 **CRYSTAL STRUCTURE OF ESCHERICHIA COLI ATASE N-TERMINAL DOMAIN**
Yibin Xu, Rongguang Zhang, Paul D. Carr, and David L. Ollis

AMoP-20 **1.7Å AND 2.1Å X-RAY STRUCTURES OF HEMOGLOBIN E AND HEMOGLOBIN A2, ISOLATED FROM THE BLOOD SAMPLES OF THALASSEMIC PATIENTS**
J. K. Dattagupta, Udayaditya Sen, Debi Choudhury, and Jhimli Dasgupta

AMoP-21 **STRUCTURAL AND KINETIC IMPLICATIONS OF SUBSTRATE INHIBITION IN THE HUMAN SULFOTRANSFERASE 1A1 ENZYME**
Niranjali U. Gamage, Ronald G. Duggleby, Amanda C. Barnett, Michael Tresillian, Catherine F. Latham, Nancy E. Liyou, and Jennifer L. Martin

AMoP-22 **SERA PROTEINS: ARE THEY CYSTEINE OR SERINE PROTEASES?**
Robyn L. Malby, Anthony N. Hodder, and Brendan S. Crabb

AMoP-23 **STRUCTURAL FEATURES OF MORACEAE LECTINS**
K. Sekar, J. V. Pratap, A. A. Jeyaprakash, A. Surolia, and M. Vijayan

AMoP-24 **THE CRYSTAL STRUCTURE OF A NOVEL CALCIUM BINDING PROTEIN ATCBL2 FROM ARABIDOPSIS THALIANA**
Masamichi Nagae, Akira Nozawa, Nozomu Koizumi, Hiroshi Sano, Mamoru Sato, and Toshiyuki Shimizu

AMoP-25 **EXPRESSION, PURIFICATION AND CRYSTALLIZATION OF DEUTERATED PROTEINS FOR NEUTRON DIFFRACTION**
Kyoko Suto, Noritake Yasuoka,and Hiroshi Mizuno

AMoP-26 **CRYSTAL STRUCTURE OF FLINC4, AN INTRAMOLECULAR LMO4:LDB1 COMPLEX**
Janet E. Deane, Megan Maher, J. Mitchell Guss, and Jacqueline M. Matthews

AMoP-27 **CATCHING CATALYSIS IN THE ACT: USING SINGLE CRYSTAL KINETICS TO TRAP METHYLAMINE DEHYDROGENASE REACTION INTERMEDIATES FOR STRUCTURAL STUDIES**
Arwen R. Pearson, Teresa De la Mora Rey, Kevin T. Watts, Ed Hoeffner, and Carrie M. Wilmot

AMoP-28 **AURACYANIN B STRUCTURE IN SPACE GROUP $P6_5$**
Mihwa Lee, Megan J. Maher, Robert E. Blankenship, and Hans C. Freeman

AMoP-29 **THE STRUCTURE OF THE LYSYL OXIDASE FROM PICHIA PASTORIS - A COPPER-CONTAINING AMINE OXIDASE THAT CAN OXIDISE LYSINE-CONTAINING PEPTIDES**
Anthony P. Duff, Paul J. Ellis, Aina E. Cohen, Jason A. Kuchar, David Langley, David M. Dooley, Hans C. Freeman, and J. Mitchell Guss

AMoP-30 **INSECT CELL EXPRESSION OF A PLANT DISEASE RESISTANCE PROTEIN CF-9 FOR STRUCTURAL STUDIES**
T. Teh, S. Lang, and D. A. Jones

AMoP-31 **THE COMPARISON OF THE LOOP STRUCTURES OF MEMBRANE BINDING SITES BETWEEN HUMAN AND BOVINE ANNEXINS IV**
Michiko Konno, Yae Kanzaki, Kayoko Mochizuki, Nahomi Fushinobu, Ayano Sato, Kyoko Aikawa, and Isamu Matsumoto

AMoP-32 **THE CRYSTAL STRUCTURE OF 9-AMINO-[N-(2-DIMETHYL-AMINO)PROPYL]ACRIDINE-4-CARBOXAMIDE BOUND TO D(CGTACG)2: A COMPARISON OF STRUCTURES OF D(CGTACG)2 COMPLEXED WITH INTERCALATORS IN THE PRESENCE OF COBALT**
Adrienne Adams, J. Mitchell Guss, William A. Denny, and Laurence P. G. Wakelin

AMoP-33 **STRUCTURAL GENOMICS STUDIES OF MENAQUINONE BIOSYNTHESIS PROTEINS FROM MYCOBACTERIUM TUBERCULOSIS: INSIGHTS FROM THE STRUCTURES OF MENG AND MENB**
J. M. Johnston, V. Arcus, and E. N. Baker

AMoP-34 **CRYSTAL STRUCTURES OF RESTRICTION ENDONUCLEASE ECOO109I**
Hiroshi Hashimoto, Tsuyoshi Imasaki, Matsuri Kato, Toshiyuki Shimuzu, Mamoru Sato, and Keiko Kita

AMoP-35 **CRYSTAL STRUCTURE OF THERMOSTABLE ENDO-1,5--L-ARABINASE FROM BACILLUS THERMODENITRIFICANS TS-3**
Asako Yamaguchi, Toshiji Tada, Tetsuko Nakaniwa, Makoto Takao, Takuo Sakai, and Keiichiro Nishimura

AMoP-36 **STRUCTURAL BASIS OF LIPID BINDING IN RICE NON-SPECIFIC LIPID TRANSFER PROTEIN COMPLEXES**
Yuh-Ju Sun, Hui-Chun Cheng, Peiyu Peng, and Ping-Chiang Lyu

AMoP-37 **REFINEMENT OF THE 7/2-AND 10/3-HELICAL STRUCTURES BASED ON THE FIBER DIFFRACTION PATTERN FROM NATIVE COLLAGEN**
K. Okuyama, X. Xu, and K. Noguchi

AMoP-38 **INTERSUBUNIT SALT BRIDGES AND OLIGOMERIZATION DO NOT CONTRIBUTE TO THE HIGH THERMAL STABILITY OF A HYPERTHERMOPHILIC PROTEIN FROM *PYROCOCCUS FURIOSUS***
Jai K. Kaushik, Yuriko Yamagata, Kyoko Ogasahara, and Katsuhide Yutani

AMoP-39 **STRUCTURAL CHARACTERISATION OF THE INI OPERON OF MYCOBACTERIUM TUBERCULOSIS**
J. Shaun Lott, Moyra M. Komen, Tet Verne Lee, Clare Scott, Joel McKay, Edward N. Baker, and Vickery L. Arcus

AMoP-40 **STUDIES OF PROTEINS OF THE FOLATE BIOSYNTHESIS PATHWAY**
Jacqueline F. Satchell, Brian J. Smith, Jonathan Baell, and Peter M. Colman

AMoP-41 **IDENTIFYING ANTAGONISTS TOWARDS A G-PROTEIN COUPLED RECEPTOR USING THE STRUCTURE OF A HORMONE COMPLEXED TO A NEUTRALISING MONOCLONAL ANTIBODY**
Patricia W. M. Ho, Craig J. Morton, Koh Sato, Etsuro Onuma, Matthew T. Gillespie, T. John Martin, and Michael W. Parker

AMoP-42 **RECENT DEVELOPMENTS AT ASRP X-RAY DIFFRACTION FACILITIES**
James R Hester, and David Cookson

AMoP-43 **COMPARISON OF THE FR-E AND RU-H2R X-RAY SOURCES FOR PROTEIN CRYSTALLOGRAPHY APPLICATIONS**
Karl A. Byriel, Anna Aagaard, Christine L. Gee, Nirajali Gamage, and Jennifer L. Martin

AMoP-44 **EVALUATION OF MICROSTRUCTURE PARAMETERS FROM POWDER X-RAY DIFFRACTION DATA**
Takashi Ida, and Hideo Toraya

AMoP-45 **THEORETICAL AND EXPERIMENTAL STUDY OF THE NEWEST HIGH BRILLIANCE ROTATING ANODE GENERATORS AND CMF OPTICS**
K. F. Tesh, A. R. Criswell, C. Yang, D. A. Courville, J. D. Ferrara, M Kuribayashi, B. Verman, and L Jiang

AMoP-46 **PHASE TRANSITION OF LANTHANUM TITANATE PEROVSKITES**
Masatomo Yashima, Mizuki Mori, Koh Saitoh, Kenji Tsuda, Takashi Kamiyama, Ken-ichi Oikawa, Akinori Hoshikawa, Shuki Torii, Masahiko Tanaka, Takeharu Mori, Ken-ichi Kato, Shinobu Aoyagi, Masaki Takata, and Eiji Nishibori

AMoP-47 **PRECISE MEASUREMENT OF THE LATTICE SPACING OF LaB_6 STANDARD BY POWDER DIFFRACTION AND THE X-RAY EXTENDED RANGE TECHNIQUE USING SYNCHROTRON RADIATION**
C. T. Chantler, Z. Barnea, C. Q. Tran, and D. J. Cookson

AMoP-48 **ANALYSIS OF THE DEPTH DEPENDENCE ON THE POLY-CRYSTAL STRUCTURE NEAR THE SURFACE BY THE USE OF SCATTERED X-RAY AT SMALL GLANCING ANGLE INCIDENCE**
Y. Fujii, A. Tao, T. Komai, and K. Ikeda

AMoP-49 **THE USE OF PARENT SYMMETRY TO IDENTIFY SPACE GROUP OPTIONS FOR TWINNED/DISORDERED PSEUDO SYMMETRIC CRYSTAL STRUCTURES**
A. David Rae

AMoP-50 **PHASE TRANSITION AND STRUCTURE OF $C_6H_{20}NX_n.nCH_4N_2S$ (X=I, Br, Cl, n=2, 4, 5)**
H. Ishigami, M. Sumita, Y. Tsunashima, S. Sato, M. Shiro, and T. Hikita

AMoP-51 **TRANSMISSION ELECTRON MICROSCOPE STUDY OF $RuSr_2Gd_{1.5}Ce_{0.5}Cu_2O_{10-d}$ MAGNETO-SUPERCONDUCTOR**
Yoshio Matsui, Tadahiro Yokosawa, Veer Pal Singh Awana, Koji Kimoto, Eiji Takayama-Muromachi, Maarit Karppinen, and Hisao Yamauchi

AMoP-52 **X-RAY DIFFRACTION STUDY ON THE PHASE TRANSITIONS OF $BaTiO_3$ SINGLE CRYSTAL**
Y. Yoshimura, N. Tokunaga, H. Iwasaki, A. Kojima, H. Sasou, and K. Tozaki

AMoP-53 **ALKALI METAL COMPLEXES OF AROMATIC POLYCARBOXYLATES - A BALANCE OF PI-STACKING AND COORDINATE BONDING INTERACTIONS?**
G. A. Koutsantonis, S. Burnet, A.K. Hall, J.M. Harrowfield, V. Sanford, D. Sauter, B.W. Skelton, and A.H. White

AMoP-54 **COMPLEX COINAGE METAL(I) THIOSULFATES**
E. J. Chan, B. W. Skelton, and A. H. White

AMoP-55 **STRUCTURE DETERMINATION OF ADDUCTS OF LEAD(II) IODIDE WITH N-METHYL SUBSTITUTED ETHYLENEDIAMINE AT LOW AND ROOM TEMPERATURES (123, 209 AND 295 K)**
Hiroshi Miyamae, Kouichirou Enomoto, Youhei Maruyama, and Goro Hihara

AMoP-56 **UNEXPECTED PIPERAZINE DERIVATIVE LIGANDS FROM A MIXTURE OF $CuCl_2.2H_2O$, Na_2CO_3, AND TRIETHYLENETETRAMINE TETRAHYDRO-CHLORIDE**
Norihiro Tamura, Masato Sakai, Katsuya Kudoh, and Hiroshi Miyamae

AMoP-57 **ANALYSIS OF PHASE TRANSITION MECHANISM OF ACYLUREA DERIVATIVE CRYSTAL BY A DETAILED TEMPERATURE RESOLVED MEASUREMENT OF POWDER X-RAY DIFFRACTION**
Daisuke Hashizume, Masaru Ogawa, Yasuhiro Iimura, Masanori Yasui, Eiji Nishibori, Masaki Takata, and Fujiko Iwasaki

AMoP-58 **OBSERVATION OF THE PHOTO-EXCITED STRUCTURE OF PLATINUM COMPLEXES**
Nobuhiro Yasuda, Hidehiro Uekusa, and Yuji Ohashi

AMoP-59 **DISORDER IN STRUCTURAL CRYSTALLOGRAPHY**
S. Banerjee, and A. K. Mukherjee

AMoP-60 **NOVEL CRYSTAL STRUCTURES OF VANADYL GALLOPHOSPHATES**
Sue-Lein Wang

AMoP-61 **ON THE DIELECTRIC CONSTANT OF $Ba_{6-3x}R_{8+2x}Ti_{18}O_{54}$(R=Sm,Nd) SOLID SOLUTIONS: CRYSTAL STRUCTURAL ANALYSIS**
H. Sakashita, H. Ohsato, N. Araki, and K. Kakimoto

AMoP-62 **DEUTERIUM TRANSFER MECHANISM IN CHIRAL THIOLACTAM FORMATION BY NEUTRON DIFFRACTION MEASUREMENT USING BIX-III DIFFRACTOMETER**
Takaaki Hosoya, Hidehiro Uekusa, Yuji Ohashi, Takashi Ohhara, Ichiro Tanaka, and Nobuo Niimura

AMoP-63 **STRUCTURE OF THE PSEUDORHOMBOHEDRAL $InFe_{1-x}Ti_xO_{3+x/2}$ COMPOSITE CRYSTAL**
Yuichi Michiue, Mitsuko Onoda, Francisco Brown, Noboru Kimizuka, and Mamoru Watanabe

AMoP-64 **USING THE HREM TO STUDY MORPHOLOGY AND STRUCTURE OF NANOMATERIAL Ta AND TaN_x**
Vo Vong, Luu tien Hung, Steffen Schulze, and Michael Hietschold

AMoP-65 **STRUCTURE–BASED DESIGN OF ANTI-INFLAMMATORY AGENTS: CRYSTAL STRUCTURE OF A COMPLEX FORMED BETWEEN COBRA VENOM PHOSPHOLIPASE A2 AND A DESIGNED POTENT PEPTIDE INHIBITOR VAL-ALA-PHE-ARG-SER- (VAFRS) AT 1.9 Å RESOLUTION.**
R. K. Singh, J. Makker, P. Vikram, M. Paramsivam, T. Jabeen, S. Sharma, S. Dey, P. Kaur, A. Srinivasan, and T. P. Singh

Plenary session

Chair: Brendan Kennedy

8:30 PL-3 **ULTRA-HIGH SPEED NEUTRON DIFFRACTION STUDIES: COMBUSTION SYNTHESIS OF TI3SIC2 AND RELATED COMPOUNDS**
Erich H. Kisi, and Daniel P. Riley

Chair: Yuji Ohashi

9:30 PL-4 **ELECTRON MICROSCOPY TECHNIQUES: MICROSCOPY, DIFFRACTION AND SPECTROSCOPY**
Michiyoshi Tanaka

10:30 Coffee Break

Oral session 1A: *Enzyme structure, function & catalysis*

Room A

Chair/Co-chair: Jose Varghese, Jenny Martin

11:00 ATu1A-1 **CATALYSIS AND ALLOSTERIC REGULATION IN PHOSPHORIBOSYL DIPHOSPHATE SYNTHASE; THE ROLE OF TWO MAGNESIUM IONS**
Sine Larsen, and Frank B. Nygaard

11:30 ATu1A-2 **ENZYMES OF RIBOSE METABOLISM: STRUCTURE AND MECHANISM**
Sherry L. Mowbray, C. Evalena Andersson, Annette Roos, and T. Alwyn Jones

11:55 ATu1A-3 **CRYSTAL STRUCTURE OF TWO KNOTTED PROTEINS: ACETOHYDROXY ACID ISOMEROREDUCTASE AND tRNA(m1G37)METHYLTRANSFERASE**
Se Won Suh, Hyung Jun Ahn, Jin Kuk Yang, Byung Il Lee, and Hye-Jin Yoon

12:20 ATu1A-4 **SUPEROXIDE DISMUTASES FROM HYPERTHERMOPHILES**
Geoffrey B. Jameson, Julian J. Adams, Paul D. Hempstead, James W. Whittaker, Edward N. Baker, and Bryan F. Anderson

12.40 ATu1A-5 **X-RAY ANALYSES OF FAMILY 8 CHITOSANASE FROM BACILLUS SP. K17**
Wataru Adachi, Shinji Shimizu, Tomoko Sunami, Tesuya Fukazawa, Mamie Suzuki, Rie Yatsunami, Satoshi Nakamura, and Akio Takénaka

13:00 Lunch

Oral session 1B: *Synchrotron and neutron science* Room B

Chair/Co-chair: Brendan Kennedy, Y. Kubota

11:00 ATu1B-1 **EXPERIMENTAL SYSTEM FOR X-RAY MAGNETIC DIFFRACTION UNDER EXTREME CONDITIONS**
Etsuo Arakawa, Masahisa Ito, Naoki Ishimatsu, Motohiro Suzuki, Naomi Kawamura, Hiroshi Sakurai, Fumitake Itoh, Yoshiya Honma, Akira Ochiai, Yuichi Akahama, Kazuyuki Matsuda, Yoh Kohori, Shunji Kishimoto, Keiichi Hirano, Hiroshi Maruyama, Kazumichi, Namikawa and Osamu Shimomura

11:30 ATu1B-2 **ELECTRONIC DIPOLE-MOMENT OF HYDROGEN ATOM IN A HYDROGEN-BOND STUDIED BY X-RAY AND NEUTRON**
Yukio Noda, Ryoji Kiyanagi, Masashi Watanabe, Hiroyuki Kimura, Akiko Kojima, Tomoyuki Mochida, and Tadashi Sugawara

11:50 ATu1B-3 **THREE-BEAM DIFFRACTION ANOMALOUS FINE STRUCTURE OF GALLIUM ARSENIDE**
Shih-Lin Chang, Yen-Ru Lee, Yu. P. Stetsko, Sen-Yuan Cheng ,Guin-Gi Lin and Wen-Shien Sun

12:10 ATu1B-4 **THE NEW QUASI-LAUE DIFFRACTOMETER AT THE REPLACEMENT RESEARCH REACTOR**
Wim T. Klooster

12.30 ATu1B-5 **VALENCE AND STRUCTURAL PHASE TRANSITIONS IN THE SERIES $Ba_2PrRu_{1-x}Ir_xO_6$**
Brendan J. Kennedy, Leqing Li, Christopher J. Howard and Brett A. Hunter

13:00 Lunch

14:00 **Modulated Structures Workshop** **Room A**
Convener: Siegbert Schmid *(see p382 for program)*

Oral session 2A: *Structural genomics* Room A

Chair/Co-chair: Ted Baker, Bostian Kobe

20:00 ATu2A-1 **STRUCTURE OF THE PUTATIVE ANTITERMINATOR PROTEIN RV1626 FROM *MYCOBACTERIUM TUBERCULOSIS***
J. P. Morth, V. Feng, L. J. Perry, and P. A. Tucker

20:20 ATu2A-2 **STRUCTURAL STUDIES OF LATEXIN, A NOVEL CARBOXYPEPTIDASE INHIBITOR**
Anna Aagaard, Pawel Listwan, Nathan Cowieson, Thomas Huber, Christine Wells, Timothy Ravasi, Bostjan Kobe, and Jennifer Martin

20:40 ATu2A-3 **CRYSTAL STRUCTURE OF AN ANCIENT CONSERVED DOMAIN**
J. Shaun Lott, Mark J. Banfield, Jill Sigrell, and Edward N. Baker

21:00 ATu2A-4 **RIKEN STRUCTURAL GENOMICS/PROTEOMICS INITIATIVE**
S. Yokoyama

21:30 Close

Oral session 2B: *Modulation, disorder & twinning* Room B

Chair/Co-chair: Victor Young, Siegbert Schmid

20:00 ATu2B-1 **DETERMINATION AND REFINEMENT OF A DISORDERED HOST-GUEST CRYSTAL STRUCTURE USING AN EVOLUTIONARY ALGORITHM IN COMBINATION WITH MONTE CARLO METHODS**
H.-B. Bürgi, and T. Weber

20:30 ATu2B-2 **THE IMPORTANCE OF MULTISITE CORRELATIONS IN DISORDERED STRUCTURES**
T. R. Welberry, and R. L. Withers

20:50 ATu2B-3 **STRUCTURE SOLUTION AND REFINEMENT OF $KNbOB_2O_5$ A COMMENSURATE MODULATED STRUCTURE**
Siegbert Schmid

21:10 ATu2B-4 **APPLICATION OF A SIX-DIMENSIONAL TWIN REFINEMENT TECHNIQUE TO MULTIPLE-TWINNED CRYSTALS OF Cu_2Sn_{23}, Cu_8GeS_6 AND Ag_7Ta_6**
M.Onoda, H.Wada, X.-a. Chen, A. Sato, and M. Ishii

21:30 Close

Poster session 17:00 – 18:30 **Veranda**

ATuP-01 **ELECTRON MOMENTUM DENSITY STUDY OF ICOSAHEDRAL $Cd_{84}Yb_{16}$**
Y. Sakurai, J. T. Okada, Y. Watanabe, S. Nanao, R. Tamura, S. Takeuchi, Y. Yokoyama, N. Hiraoka, and M. Itou

ATuP-02 **CHARGE DENSITY STUDIES OF Z' = 2 MOLECULES. POSSIBILITIES AND LIMITATIONS**
Dai Hibbs, Mark P. Waller, and Jacob Overgaard

ATuP-03 **CRYSTAL EXPLORER: A GRAPHICAL USER INTERFACE FOR DISPLAYING AND MANIPULATING HIRSHFELD SURFACES AND FINGERPRINTS FOR CRYSTAL ENGINEERING APPLICATIONS**
Dylan Jayatilaka, Daniel Grimwood, and Stephen Wolff

ATuP-04 **CRYSTALLIZATION OF SECRETED PROTEIN BY COMPLEXATION WITH AN ANTIBODY FRAGMENT**
Taro Tamada, Keiko Kurosawa, Uichi Nishiyama, Tomoaki Kuwaki, and Ryota Kuroki

ATuP-05 **CRYSTALLIZATION OF ALPHA-AMYLASE AS A MODEL PROTEIN FOR DEMONSTRATING THE EFFICACY OF THE COUNTER-DIFFUSION TECHNIQUE UNDER MICROGRAVITY CONDITIONS**
Masaru Sato, Hiroaki Tanaka, Koji Inaka, Sachiko Takahashi, Satoshi Sano, Susumu Yoshitomi, and Hiroshi Komatsu

ATuP-06 **INVESTIGATION OF CRYOPROTECTANT CONDITION FOR PROTEIN STRUCTURE ANALYSIS USING CRYOPROTECTANT DATABASE**
Sachiko Takahashi, Takashi Yoshimine, Masaru Sato, Hiroaki Tanaka, Kensaku Hamada, and Susumu Yoshitomi

ATuP-07 **CRYSTAL STRUCTURE OF NONADECANE-1,19-DITHIOL**
H. Shimizu, K. Uno, Y. Ogawa, and N. Nakamura

ATuP-08 **A STRUCTURAL STUDY ON THE MONOSUBSTITUTED FERROCENE DERIVATIVES**
Y. Kawamura, Y. Okada, K. Uno, and N. Nakamura

ATuP-09 **CRYSTAL STRUCTURE OF $Te_{0.4}Se_{0.6}$**
Yuji Soejima, Akie Hoshiko, Hirotoshi Hayashida, Yoshinori Ohmasa, Hirohisa Endo, and Masaru Kawaminami

ATuP-10 **CRYSTAL STRUCTURES OF A BISAZOMETHINE DYE FORMING J-AGGREGATES**
Shinya Matsumoto, Kazuko Shirai, Kimiko Kobayashi, Tatsuo Wada, and Motoo Shiro

ATuP-11 **STRUCTURAL STUDY OF STRESS-INDUCED LUMINESCENT PARTICLE $SrAl_2O_4$:Eu**
Hiroshi Yamada, Hajime Kusaba, Weng-Shen Shi, Keiko Nishikubo, and Chao-Nan Xu

ATuP-12 **POSITIONS OF La AND Ba OF $BaLa_4Ti_4O_{15}$ HOMOLOGOUS COMPOUND**
H. Ohsato, Y. Tohdo, K. Kakimoto, T. Okawa, and H. Okabe

ATuP-13 **RELATIONSHIPS BETWEEN RUTILE STRUCTURES**
Christopher J. Howard, Zhaoming Zhang, and Brendan J. Kennedy

ATuP-14 **STRUCTURAL STUDIES ON JACALIN CARBOHYDRATE COMPLEXES**
K. Sekar, A. A. Jeyaprakash, P. G. Rani, S. Katiyar, A. Surolia, and M. Vijayan

ATuP-15 **PRESENT STATUS OF PHARMACEUTICAL INDUSTRY BEAMLINE AT SPRING-8**
Shintaro Misaki, Kenji Suzuki, Yoshio Katsuya, and Kazumi Nishijima

ATuP-16 **REFINEMENT OF THE CRYSTALLIZATION CONDITIONS OF CONGER EEL GALECTIN, CONGERIN I AND II**
Takashi Yamane, Atsuo Suzuki, Yumiko Miyabe, Yuusuke Niwa, Tomohisa Ogawa, Koji Muramoto, and Mitsuo Ataka

ATuP-17 **NEUTRON PROTEIN CRYSTALLOGRAPHY OF CUBIC INSULIN**
M. Maeda, T. Chatake, I. Tanaka, A. Ostermann, and N. Niimura

ATuP-18 **PREPARATION, CHARACTERIZATION AND CRYSTALLIZATION OF THE COMPLEX COMPOSED OF GRANULOCYTO COLONY-STIMULATING FACTOR AND ITS RECEPTOR**
Eijiro Honjo, Shouhei Mine, Takumi Koshiba, Tomoyuki Okamoto, Taro Tamada, Yoshitake Maeda, Yasuko Matsukura, Akane Horie, Matsujiro Ishibashi, Miharu Sato, Mizue Azuma, Masao Tokunaga, Katsutoshi Nitta, and Ryota Kuroki

ATuP-19 **CRYSTAL STRUCTURE OF DSBG A DISULFIDE BOND ISOMERASE FROM ESCHERICHIA COLI**
Begona Heras, Melissa A. Edeling, Jennifer L Martin, and Satish Raina

ATuP-20 **PROTEIN MODEL BUILDING USING IMAGE PROCESSING TECHNIQUE AND OPTIMIZATION ALGORITHMS**
Osamu Takahashi, and Shigenobu Kobayashi

ATuP-21 **CRYSTAL STRUCTURE OF TBP-INTERACTING PROTEIN (TK-TIP26) FROM HYPERTHERMOPHILIC ARCHAEON THERMOCOCCUS KODAKARAENSIS STRAIN KOD1**
T. Yamamoto, T. Matsuda, H. Matsumura, T. Inoue, M. Morikawa, S. Kanaya, and Y. Kai

ATuP-22 **TOWARDS A MORE USABLE PROTEIN STRUCTURE DATABASE**
W. Bret Church, William M. Shui, Stephen C. Graham, Lawrence K. Lee, and Raymond K. Wong

ATuP-23 **DATA BASE OF HYDROGEN AND HYDRATION IN PROTEINS**
N. Niimura

ATuP-24 **E. COLI DIHYDROOROTASE: STRUCTURE OF THE ENZYME CRYSTALLISED IN THE PRESENCE OF DIHYDROOROTATE. THE POSSIBILITY OF COOPERATIVITY BETWEEN SUBUNITS?**
Mihwa Lee, J. Mitchell Guss, Richard I. Christopherson, and Megan J. Maher

ATuP-25 **THE CRYSTAL STRUCTURE OF RUBREDOXIN FROM DESULFOVIBRIO GIGAS AT ULTRA-HIGH 0.68 Å RESOLUTION**
Chun-Jung Chen, Yi-Ting Chen, Ming-Yih Liu, and Jean Le Gall

ATuP-26 **TUMOUR PEPTIDE PRESENTATION BY MHC CLASS I**
Michelle A. Dunstone, Andrew Z. Webb, Anthony W. Purcell, and Jamie Rossjohn

ATuP-27 **THE CRYSTAL STRUCTURE OF A CORAL POCILLOPORIN**
Pascal G. Wilmann, Travis Beddoe, Mark Prescott, Michael Ling, Aaron J. Oakley, Sophie Dove, and Rodney J. Devenish

ATuP-28 **STRUCTURAL CHARACTERISATION OF MITOCHONDRIAL IMPORT RECEPTORS**
Travis Beddoe, Pascal Wilmann, Simon Bushell, Judy Scoble, Diana Macasev, and Trevor Lithgow

ATuP-29 **MHC CLASS I PEPTIDE PRESENTATION A STRUCTURAL INSIGHT**
L. K. Ely, W. A. MacDonald, C. S. Clements, A. G. Brooks, A. Purcell, J. McCluskey, and J. Rossjohn

ATuP-30 **THE CRYSTALLIZATION AND X-RAY DIFFRACTION OF THE HALOACID DEHALOGENASE DEHIVA FROM THE SOIL BORNE BACTERIUM BURKHOLDARIA CEPACIA MBA4**
Jason W. Schmidberger, Matthew C. J. Wilce, Aaron J. Oakley, and Colin A. Thompson

ATuP-31 **TRYPTOPHAN BIOSYNTHESIS IN MYCOBACTERIUM TUBERCULOSIS**
J. Shaun Lott, Anthony J. Harrison, Emily Parker, Rochelle J. Ramsay, and Edward N. Baker

ATuP-32 **UNDERSTANDING THE FUNCTIONING OF THE COPPER BINDING DOMAIN OF THE AMYLOID PRECURSOR PROTEIN**
G. K. W. Kong, W. J. McKinstry, J. J. Adams, G. Polekhina, N. A. Williamson, D. Cappai, K. J. Barnham, R. Cappai, and M. W. Parker

ATuP-33 **CRYSTALLOGRAPHIC STUDIES OF THE MITOCHONDRIAL FISSION PROTEIN FIS1**
Michael A. Gorman, Diana Stojanovski, Michael T.Ryan, and Jacqueline M. Gulbis

ATuP-34 **THE CRYSTAL STRUCTURE OF T84.66FAB AT 2.2 Å RESOLUTION AND MODELLING THE BINDING OF ANTI-CEA ANTIBODY CONSTRUCTS TO THE CEA ANTIGEN**
Jennifer A. Carmichael, Barbara Power, Albert van Donkelaar, Mark Sherman, Paul Yazaki, Anna M. Wu, and Peter J. Hudson

ATuP-35 **STRUCTURAL STUDIES OF CP PROTEIN AND ITS FRAGMENTS WITH ANDROGEN RECEPTOR-MRNA**
M. Sidiqi, J. Vivian, J. Wilce, and M. Wilce

ATuP-36 **THE SIGNIFICANCE OF INTERACTION BETWEEN O6 HYDROXYL GROUPS OF GLUCOSE RESIDUES OF MALTOORIGOSACCHARIDE AND β-AMYLASE FROM *BACILLUS CEREUS* VER. *MYCOIDES***
Hideo Miyake, Genji Kurisu, Masami Kusunoki, Sigenori Nishimura, and Yasunori Nitta

ATuP-37 **TOWARDS A CATALYTIC MECHANISM OF AMINOPEPTIDASE P**
S. C. Graham, M. H. Lee, M. J. Maher, W.H. Simmons, H. C. Freeman and J. M. Guss

ATuP-38 **CRYSTAL STRUCTURE OF THERMOSTABLE ASPARTASE AND STRUCTURE-BASED EXPLORATION OF FUNCTIONAL SITES IN THE ASPARTASE FAMILY**
Yasuo Hata, Tomomi Fujii, Hisanobu Sakai, and Yasushi Kawata

ATuP-39 **CRYSTAL STRUCTURE OF THE CU-AMINE OXIDASE FROM ARTHROBACTER GLOBIFORMIS IN COMPLEX WITH THE SUICIDE INHIBITOR 4-(2-NAPHTHYLOXY)-2-BUTYN-1-AMINE**
David B. Langley, Eric M. Shepard, Anthony P. Duff, Hans Freeman, David M. Dooley, and J. Mitchell Guss

ATuP-40 **STRUCTURAL GENOMICS OF NOVEL MACROPHAGE PROTEINS ASSOCIATED WITH INFLAMMATORY DISEASE AND CANCER**
Pawel Listwan, Nathan Cowieson, Anna Aagaard, Robert Serek, Timothy Ravasi, Christine Wells, Thomas Huber, David Hume, and Jenny Martin

ATuP-41 **A STRUCTURAL GENOMICS APPROACH TO TUBERCULOSIS**
Edward N. Baker, Vickery L. Arcus, Kristina Backbro, Graeme L. Card, Jodie M. Johnston, Moyra Komen, Nayden Koon, Simon Li, Andrew A. McCarthy, Rochelle J. Ramsay, Miriam L. Sharpe, and J. Shaun Lott

ATuP-42 **HIGH THROUGHPUT APPROACHES FOR CRYSTALLISATION OF BIOLOGICAL MACROMOLECULES**
Christine L. Gee, Richard D. Kidd, Anna Aagaard, Fiona M. McMillan, Niranjali U. Gamage, Paul R. Young, and Jennifer L. Martin

ATuP-43 **THE STRUCTURE AND FUNCTION OF STREPTOLYSIN O**
Julian J. Adams, Susanne C. Feil, Rodney K. Tweten, and Michael W. Parker

ATuP-44 **HIGH RESOLUTION ANALYSIS OF THE NEW INHIBITOR PGD-042 BOUND HUMAN HEMETOPOIETIC PROSTAGLANDIN D SYNTASE**
N. Katsuyama, T. Inoue, Y. Okano, H. Shishitani, N. Okazaki, H. Matsumura, Y. Urade, and Y. Kai

ATuP-45 **THE ROLE OF PROLINE RESIDUES IN THE HINGE REGION OF Cdc2 KINASE SUBUNIT PROTEINS**
J. Kelly, E. A. Williams, and M. J. C. Wilce

ATuP-46 **SAD PHASING USING SULFUR ANOMALOUS SCATTERING WITH CHROMIUM RADIATION**
K. F. Tesh, C. Yang, J. W. Pflugrath, C. N. Stence, D. A. Courville, and J. D. Ferra

ATuP-47 **STRUCTURAL CHARACTERIZATION OF TWO PHOSPHOLIPASE A2 PROTEINS FROM THE VENOM OF THE AUSTRALIAN BROWN SNAKE, PSEUDONAJA AFFINIS AFFINIS**
Roopwant K. Judge, Matthew C. J. Wilce, and Jacqueline A. Wilce

ATuP-48 **X-RAY ANALYSIS OF YEAST LIPOAMIDE DEHYDROGENASE COMPLEXED WITH NAD+**
Wataru Adachi, Kaoru Suzuki, Masaru Tsunoda, Takeshi Sekiguchi, Lester J. Reed, and Akio Takénaka

ATuP-49 **A NEW METHOD FOR PROTEIN CRYSTALLIZATION: SAMPLING PHASE SPACE IN A MICROFLUIDIC ENVIRONMENT**
Kyle Self, Carl L. Hansen, James M. Berger, Stephen R. Quake, Susanna Ng, Shelley Godley, and Joseph Barco

ATuP-50 **MICROSTRUCTURES OF THE FeSiBNbCu SOFT MAGNETIC MATERIAL STUDIED BY HIGH RESOLUTION ELECTRON MICROSCOPY (HREM)**
Vo Vong and Ng.Q.Thang

ATuP-51 **MICRO-ARRAY CHIP FOR HIGH-THROUGHPUT PROTEIN CRYSTALLOGRAPHY**
N. Watanabe, I. Tanaka, C. Nishijima, H. Takeuchi, and T. Iseki

ATuP-52 **STRUCTURES AND PHASE TRANSITION IN THE LAYERED PEROVSKITE $La_{0.6}Sr_{0.1}TiO_3$**
Christopher J. Howard, and Zhaoming Zhang

ATuP-53 **STRUCTURE ESTIMATION OF ORBITAL ORDERED THIN FILMS USING SYNCHROTRON RADIATION**
Y. Wakabayashi, H. Sawa, M. Nakamura, M. Izumi, K. Miyano, and Y. Murakami

ATuP-54 **THIN-FILM CRYSTAL STRUCTURE DETERMINATION OF $Bi_3Fe_5O_{12}$ MEASURED WITH VCIP METHOD**
K. Tanaka, K. Itatsu, N. Adachi, and T. Okuda

ATuP-55 **POLYTYPE POSSIBILITIES ARISING FROM PSEUDO SYMMETRIC CRYSTAL STRUCTURES ALLOWING STACKING FAULTS**
Anthony. C. Willis, A. David Rae, Tory N. Cayzer, and Michael S. Sherburn

ATuP-56 **THE TEMPERATURE DEPENDENCE OF THE CRYSTAL STRUCTURE OF 3,5-DI-T-BUTYLPYRAZOLE**
Alexandre N. Sobolev, and Allan H. White

ATuP-57 **EXPERIMENTAL AND THEORETICAL STUDIES OF THE SULFOXIMINE GROUP [R1-S(=O)(=N-R2)R3]: DETECTION OF POSSIBLE LATTICE EFFECTS**
Gerhard Raabe

ATuP-58 **THE PDF-4/FULL FILE AND PDF-4/ORGANICS DATABASES: NEW DATA MINING TOOLS FOR STRUCTURAL CRYSTALLOGRAPHY AND MATERIALS CHARACTERISATION**
Brian O'Connor, Camden Hubbard, Tim Fawcett, and John Faber

ATuP-59 **HIGH TEMPERATURE LAUE METHOD WITH POLYCHROMATIC SR: ITS APPLICATION TO QUARTZ PHASE TRANSITION**
Kazumasa Ohsumi, Yoshikazu Miyata, Katsuhiro Kusaka, Takeshi Nakagawa, and Kenji Hagiya

ATuP-60 **X-RAY EXTENDED-RANGE TECHNIQUE FOR PRECISION MEASUREMENT OF THE X-RAY MASS ATTENUATION COEFFICIENT AND IM(F) FOR MOLYBDENUM USING SYNCHROTRON RADIATION**
C. T. Chantler, M. de Jonge, Z. Barnea, C. Q. Tran, . B. Dhal, and D. J. Cookson

ATuP-61 **X-RAY MASS ATTENUATION COEFFICIENT OF SILICON: THEORY VERSUS X-RAY EXTENDED-RANGE TECHNIQUE AND OTHER EXPERIMENTS**
C. T. Chantler, C. Q. Tran, and Z. Barnea

ATuP-62 **THE CRYSTAL STRUCTURE OF DOPED PEROVSKITES DERIVED FROM ELECTRON SCATTERING TECHNIQUES**
C. J. Maunders, J. E. Etheridge, C. J. Rossouw, and H. J. Whitfield

ATuP-63 **EFTEM AND HRTEM STUDIES OF META-KAOLINITE AND META-DICKITE**
Sujeong Lee, Youn Joong Kim, Hi-Soo Moon, and Won-Seon Seo

ATuP-64 **DEPENDENCE OF THE ACCURACY OF A CONTINUOUS PHASE TRANSITION TEMPERATURE ON ANGULAR RESOLUTION IN POWDER DIFFRACTOMETRY**
Masatomo Yashima, Mizuki Mori, Roushown Ali, Masahiko Tanaka, and Takeharu Mori

ATuP-65 **A NEW HIGH-TEMPERATURE FURNACE FOR HIGH-RESOLUTION SYNCHROTRON RADIATION POWDER DIFFRACTION STUDY UP TO 1900K**
Masatomo Yashima, Masahiko Tanaka, Takeharu Mori, Kenjiro Ohouchi, and Daiju Ishimura

ATuP-66 **SUB-SECOND X-RAY DIFFRACTION MEASUREMENT AND STRUCTURE ANALYSIS BY MSGC**
Hidehiro Uekusa, Yuji Ohashi, Y. Tsuji, Y. Nishi, T. Tajima, and S. Adachi

ATuP-67 **THE BEAMLINE FOR MACROMOLECULAR ASSEMBLIES OF THE INSTITUTE FOR PROTEIN RESEARCH**
Masato Yoshimura, Eiki Yamashita, Atsushi Nakagawa, Masaki Yamamoto, Shinya Yoshikawa, and Tomitake Tsukihara

ATuP-68 **X-RAY MICRODIFFRACTION SURFACE AREA INVESTIGATIONS OF TUNGSTEN CLAD MAGNESIUM ALLOYS**
Natasha Wright, M. Mandagie, and G. Theodossiou

ATuP-69 **ON THE DESIGN FOR A VERSATILE IMAGING AND HARD X-RAY BEAMLINE FOR MATERIALS SCIENCE, BIOMEDICAL, AND MEDICAL APPLICATIONS AT "BOOMERANG"**
S. W. Wilkins, R. A. Lewis, K. K-W. Siu, A. W. Stevenson, K. A. Nugent, and D. J. Parry

ATuP-70 **DIRECT OBSERVATION OF OXYGEN MOLECULES PHYSISORBED IN A MICROPOROUS COORDINATION POLYMER**
Yoshiki Kubota, Masaki Takata, Makoto Sakata, Ryo Kitaura, Ryotaro Matsuda, Susumu Kitagawa, Tatsuo Kobayashi, Kouichi Kindo, Yoshimi Mita, Akira Matsuo, Michihiro Kobayashi, Ho-Chol Chang, Tadashi Oszawa, and Megumi Suzuki

ATuP-71 **THE SELF-ASSEMBLED STRUCTURE OF A 2,6 DI(ACYLAMINO)-PYRIDINE: FORMATION THROUGH N-H....N and N-H...O=C INTER MOLECULAR INTERACTIONS**
E. Marfo-Owusu and T. Kato

Oral session 1A: *Membrane proteins, macromolecular assemblies and receptors* Room A

Chair/Co-chair: Wah Chiu, Jacqui Gulbis

8:30 AWe1A-1 **SYSTEMATIC APPROACHES FOR MEMBRANE PROTEIN STRUCTURE DETERMINATION**
Ben Hankamer, Rosalba Rothnagel, Alasdair McDowall, Geoff Ericksson, Francis Clark, Jasmine Banks, Bernard Pailthorpe, Charles Sennoga, Andrew Heron, John Seddon, Richard Templer, and David Crout

9:00 AWe1A-2 **STRUCTURAL CHANGES IN AN αβ T-CELL RECEPTOR UPON LIGAND BINDING**
Craig S. Clements, Lars Kjer-Nielsen, Anthony W. Purcell, Andrew G. Brooks, James C. Whisstock, Scott R. Burrows, James McCluskey, and Jamie Rossjohn

9:25 AWe1A-3 **A NEW MODE OF PORE ASSEMBLY BASED ON THE STRUCTURE OF INTERMEDILYSIN, A TOXIN SPECIFIC FOR HUMAN CELLS**
Galina Polekhina, Rodney Tweten, and Michael W. Parker

9:50 AWe1A-4 **HIGH-THROUGHPUT PROTEIN STRUCTURE VALIDATION ALSO FOR INTEGRAL MEMBRANE PROTEINS**
W. Bret Church, and Lawrence K. Lee

10:10 AWe1A-5 **CRYSTAL STRUCTURE OF PEA TOC34 - A NOVEL GTPASE OF THE CHLOROPLAST PROTEIN TRANSLOCON**
Chwan-Deng Hsiao, Yuh-Ju Sun, Farhad Forouhar, and Hsou-min Li

10:30 Coffee break

Oral session 1B: *Charge density – experimental & theoretical approaches* Room B

Chair/Co-chair: Mark Spackman, K. Tanaka

8:30 AWe1B-1 **CHARGE DENSITY STUDY OF AN IRON NITROSYL COMPLEX**
Yu Wang, and J. J. Lee

9:00 AWe1B-2 **FINDING HYDROGEN BY SYNCHROTRON POWDER DIFFRACTION**
Makoto Sakata, Hitomi Sakai, and Eiji Nishibori

9:30 AWe1B-3 **CHARGE DENSITY STUDIES OF POLYMORPHIC ANTI-ULCER AGENTS. THE APPLICABILITY OF THE ELECTROSTATIC POTENTIAL IN DRUG DESIGN**
Jacob Overgaard, Mark P. Waller, and David E. Hibbs

9:50 AWe1B-4 **ELECTRON DENSITY DISTRIBUTIONS ON WEAK INTER-MOLECULAR INTERACTIONS - Br...Br INTERACTIONS**
Masanori Yasui, Kouki Tamakawa, Fujiko Iwasaki, and Daisuke Hashizume

10:10 AWe1B-5 **CHARGE DENSITY ANALYSIS AND DIPOLE MOMENT ENHANCEMENT IN MNA (2-METHYL-4-NITROANILINE)**
Andrew Whitten, Mark Spackman, Peter Turner, Wim Klooster, Ross Piltz, and Masaru Tachibana

10:30 Coffee break

Oral session 2A: *Protein structure, function and evolution*

Room A

Chair/Co-chair: Peter Colman, Jamie Rossjohn

11:00 AWe2A-1 **HOW DO TRANSLATION FACTORS CATALYSE PROTEIN SYNTHESIS?**
Anders Liljas

11:30 AWe2A-2 **EVOLUTION OF AN ORGANOPHOSPHATE DEGRADING ENZYME: A COMPARISON OF NATURAL AND DIRECTED EVOLUTION**
P.D. Carr, H. Yang, S. Yu McLoughlin, J.W. Liu, X. Qiu, R.J. Russell, J.G. Oakeshott, and D.L. Ollis

11:50 AWe2A-3 **CRYSTAL STRUCTURE OF GLUTAMATE-CYSTEINE LIGASE FROM ESCHERICHIA COLI B WITH SUBSTRATES**
T. Hibi, M. Nakayama,H. Nii, and J. Oda

12:20 AWe2A-4 **CRYSTALLOGRAPHIC ANALYSIS OF THE MECHANISM OF HMG-CoA REDUCTASE**
Cynthia V. Stauffacher, Nicklaus Steussy, John W. Burgner, Tim Schmidt, and Victor W. Rodwell

12:40 AWe2A-5 **STRUCTURE AND SIGNALING IN THE EPIDERMAL GROWTH FACTOR RECEPTOR FAMILY**
T. P. J. Garrett, M-Z Lou, N. M. McKern, T. E. Adams, G. O. Lovrecz, R. N. Jorissen, E. C. Nice, A. W. Burgess, and C. W. Ward

13:00 Lunch

Oral session 2B: *Materials and nanoscience* Room B

Chair/Co-chair: Richard Welberry, Christopher Howard

11:00 AWe2B-1 **SYNCHROTRON X-RAY AND MOLECULAR DYNAMICS STUDIES OF $La_{2-x}Sr_xCuO_4$ WITH x~1/8**
Nobuo Ishizawa, Kenji Suzuki, Katsumi Suda, and Douglas du Boulay

11:30 AWe2B-2 **CORRELATION OF METAPRISM TWIST ANGLE WITH DISEQUILIBRIUM IN CALCIUM-LEAD FLUORO-VANADINITE APATITES**
Z. L. Dong, and T. J. White

11:50 AWe2B-3 **NEGATIVE THERMAL EXPANSION IN CYANIDE-BRIDGED COORDINATION FRAMEWORK MATERIALS**
Karena W. Chapman, Andrew L. Goodwin, and Cameron J. Kepert

12:20 AWe2B-4 **PHASE TRANSITION AND STRUCTURAL CHANGE OF TRICALCIUM PHOSPHATE AT HIGH TEMPERATURES UP TO 1900 K**
Masatomo Yashima, Atsushi Sakai, Keisuke Yamamoto, Yoshisato Kimura, Yoshinao Mishima, Masahiko Tanaka, Takeharu Mori, Kenji Ohoyama, and Yasuo Yamaguchi

12:40 AWe2B-5 **IN-SITU STRUCTURE SOLUTION AND PHASE TRANSFORMATION STUDIES OF DRUG POLYMORPHS USING HIGH RESOLUTION SYNCHROTRON POWDER DIFFRACTION**
W. I. F. David, and K Shankland

13:00 Lunch

14:00 **SCANZ General Meeting** Room A

Plenary session

Chair: David Rae

16:00 PL-5 **THE ROLE OF NON-MEROHEDRAL TWINNING IN SOME PHASE TRANSITIONS**
Victor G. Young, Jr., Maren Pink,Neil R. Brooks, and William Brennessell

Chair: Sine Larsen

17:00 PL-6 **MECHANISMS OF SELF-ASSEMBLY AND SWITCHING OF THE BACTERIAL FLAGELLUM**
Keiichi Namba

18:00 **marresearch Sunset Dinner**

Biological Structure Workshop Program

August	13 Wednesday	14 Thursday	15 Friday
9:00			
9:30		BTh1	BFr1
10:00			
10:30		Coffee	Coffee
11:00			
11:30		BTh2	BFr2
12:00			
12:30			
13:00		Lunch	Lunch
13:30			
14:00			
14:30			
15:00			
15:30		CCP4	
16:00		Workshop	
16:30	Registration		
17:00			
17:30			
18:00			
18:30			
19:00			
19:30	marresearch		Rigaku/MSC
20:00	Sunset		Aussie
20:30	Dinner		BBQ
21:00		BTh3	
21:30			
22:00			

Oral session 1: *The need for speed* — Room A

Chair: Jenny Martin

9:00 BTh1-1 **CELL FREE PROTEIN SYNTHESIS AND STRUCTURAL / FUNCTIONAL PROTEOMICS**
Shigeyuki Yokoyama and Takanori Kigawa

9:45 BTh1-2 **A STRUCTURAL GENOMICS APPROACH TO TUBERCULOSIS**
Edward N. Baker, Vickery L. Arcus, Kristina Backbro, Graeme L. Card, Jodie M. Johnston, Moyra Komen, Nayden Koon, Simon Li, Andrew A. McCarthy, Rochelle J. Ramsay, Miriam L. Sharpe, and J. Shaun Lott

10:10 BTh1-3 **STRUCTURAL GENOMICS OF NOVEL MACROPHAGE PROTEINS ASSOCIATED WITH INFLAMMATORY DISEASE AND CANCER**
Pawel Listwan, Nathan Cowieson, Anna Aagaard, Robert Serek, Carmel Walsh, Timothy Ravasi, Christine Wells, Thomas Huber, David Hume, Jenny Martin, and Bostjan Kobe

10:30 Coffee Break

Oral session 2: *Clever stuff* — Room A

Chair: Sine Larsen

11:00 BTh2-1 **ELECTRON CRYOMICROSCOPY OF VIRUS PARTICLES AT SUBNANOMETER RESOLUTION**
Wah Chiu, Z. Hong Zhou, Matthew L. Baker, Wen Jiang, Joanita Jakana, Matthew Dougherty, Brian R. Bowman, Florante A. Quiocho, and Frazer J. Rixon

12:00 BTh2-2 **CATCHING CATALYSIS IN THE ACT: PROBING ENZYME MECHANISMS USING SINGLE CRYSTAL MICROSPECTROPHOTOMETRY AND X-RAY CRYSTALLOGRAPHY**
Arwen R. Pearson and Carrie M. Wilmot

13:00 Lunch

14:00 **CCP4 Workshop** *(see p383 for program)* — Room A

18:00 Close

Oral session 3: *Are we there yet?* Room A

Chair: Mitchell Guss

20:00 BTh3-1 **STRUCTURE MODELLING AND VALIDATION**
T. Alwyn Jones, Mark Harris, and Gerard J. Kleywegt

21:00 BTh3-2 **THE PROTEIN DATA BANK AND STRUCTURAL GENOMICS**
Helen M Berman

22:00 Close

Oral session 1: *Synchrotron beamlines and us!* Room A

Chair: Jose Varghese

9:00 BFr1-1 **CASSIOPEIA - A PROGRESS REPORT FROM THE DEVELOPMENT OF FIVE BEAMLINES AT THE MAX SYNCHROTRON LABORATORY**
Anders Liljas

9:45 BFr1-2 **BUILDING A USER-FRIENDLY BEAMLINE**
Aina Cohen and Paul Ellis

10:30 Coffee Break

Oral session 2: *Synchrotron beamlines and us! Part II* Room A

Chair: Matthew Wilce

11:00 BFr2-1 **NEW BEAMLINES FOR MACROMOLECULAR CRYSTALLOGRAPHY**
Janet L. Smith, Robert F. Fischetti, L. E. Berman, W. Diete, R. Signorato, R. Benn, S. Stepanov, R. Sanishvili, S. Xu, A. Urakhchin, O. Makarov, and W. W. Smith

11:45 BFr2-2 **BIOLOGICAL APPLICATIONS AT THE AUSTRALIAN SYNCHROTRON**
Jose Varghese

12:30 ***Discussion and Q&A with all Friday's speakers***

13:00 Lunch

18:00 ***Rigaku/MSC Aussie BBQ***

Sagamore XIV Program

August	13 Wednesday	14 Thursday	15 Friday	16 Saturday	17 Sunday	18 Monday
8:30						
9:00		STh1	SFr1	SSa1	SSu1	SMo1
9:30						
10:00						
10:30		Coffee	Coffee	Coffee	Coffee	Coffee
11:00						
11:30		STh2	SFr2	SSa2	SSu2	SMo2
12:00						
12:30						
13:00		Lunch	Lunch	Lunch	Lunch	Lunch
13:30						
14:00						
14:30						
15:00						
15:30						
16:00	Registration					
16:30						
17:00						
17:30		Posters	Posters	Posters		
18:00						
18:30						
19:00						
19:30	marresearch		Rigaku/MSC		Asian	
20:00	Sunset		Aussie		Buffet	
20:30	Dinner	STh3	BBQ	SSa3		
21:00						
21:30						
22:00						

Oral session 1: *Charge density studies on heavy-atom materials* Room B

Chair/Co-chair: Claude Lecomte, Yu Wang

8:30 **OPENING REMARKS**
Mark Spackman

8:40 STh1-1 **BONDING EFFECTS IN LARGE METAL CLUSTER MOLECULES**
Piero Macchi, and Angelo Sironi

9:10 STh1-2 **EXPERIMENTAL RESULTS ON COUPLED ANALYSIS OF SPIN AND CHARGE DENSITIES OF Y AND Gd COMPLEXES**
N. Claiser, B. Gillon, M. Souhassou, C. Lecomte, N. K. Hansen, Y. Pontillon, A. Caneschi, D. Gatteschi, C. Carbonera, A. Bencini, A. Cousson, and E. Lelièvre-Berna

9:40 STh1-3 **SCATTERING FACTOR CALCULATIONS AND DISPERSION CORRECTIONS FOR HEAVY ATOMS**
Chris Chantler

10:10 STh1-4 **MULTI-TEMPERATURE EDD MEASUREMENT IN RARE-EARTH HEXABORIDES LB_6 (L=La, Ce, Sm)**
K. Tanaka, S. Funahashi, and S. Takagi

10:30 Coffee Break

Oral session 2: *Instrumentation large and small* Room B

Chair/Co-chair: Fumitake Itoh, Steve Wilkins

11:00 STh2-1 **OPPORTUNITIES FOR RESEARCH AT AUSTRALIA'S REPLACEMENT RESEARCH REACTOR**
R. A. Robinson

11:30 STh2-2 **ENPI - THE EUROPEAN NEUTRON POLARIMETRY NETWORK, A STATUS REPORT**
Francis Tasset

12:00 STh2-3 **CURRENT STATUS AND FUTURE PLANS AT THE AUSTRALIAN SYNCHROTRON PROJECT**
S.W. Wilkins

12:30 STh2-4 **CHARGE DENSITIES OF PHOSPHORUS CONTAINING COMPOUNDS AT 20 K**
Marc Messerschmidt, and Peter Luger

13:00 Lunch

Oral session 3: ***New approaches to measuring magnetisation densities*** **Room B**

Chair/Co-chair: Rob Robinson, Beatrice Gillon

20:00 STh3-1 **EXPERIMENTAL ATTEMPTS TO MEASURE NONCOLLINEAR LOCAL MAGNETISATION**
P.J. Brown

20:30 STh3-2 **MAGNETIC EXAFS AS A TOOL TO MEASURE RADIAL DISTRIBUTION OF SPIN AND ORBITAL MAGNETIC MOMENTS**
Andrei Rogalev, and José Goulon

21:00 STh3-3 **TWISTED STATES OF Fe/Tb MULTILAYERS**
Katsuyoshi Takano, Kazuhiro Ikeuchi, Hiroshi Sakurai, Hiromi Oike, and Fumitake Itoh

21:30 Close

Poster session 17:00 – 18:30 **Veranda**

SThP-01 **THE ATOMISTIC ORIGIN OF THE INVERSE PIEZOELECTRIC EFFECT IN α-SiO_2 AND α-$GaPO_4$**
Jav Davaasambuu, Vasili Kochin, Andreas Pucher, Semen V. Gorfman, Vladimir G. Tsirelson, Peter Blaha and Ullrich Pietsch

SThP-02 **SIMULATION OF COMPTON DOUBLE SCATTERING**
Yukinobu Kakutani, Akihisa Koizumi and Nobuhiko Sakai

SThP-03 **DIRECT PHASE DETERMINATION OF FRACTIONAL REFLECTION IN CHARGE-DENSITY-WAVE CRYSTALS USING X-RAY MULTIPLE DIFFRACTION**
Shih-Lin Chang, Chao-Hong Du, Mau-Tsu Tang, Yu. P. Stetsko, Yen-Ru Lee, Tsong-Tze Lin, Shih-Chang Wong and Wen-Shien Sun

SThP-04 **ELECTROSTATIC PROPERTIES OF THE MOLECULAR SIEVE $AlPO_4$-15**
E. Aubert, F. Porcher, M. Souhassou and C. Lecomte

SThP-05 **VIRTUAL EXPERIMENTS FOR THE BUILDUP OF ASPHERICAL ATOM SCATTERING FACTORS OBTAINED BY A NOVEL PARTITIONING SCHEME AND APPLICATION TO A TRIVALINE STRUCTURE**
Birger Dittrich and Dylan Jayatilaka

SThP-06 **THE NEW QUASI-LAUE DIFFRACTOMETER AT THE REPLACEMENT RESEARCH REACTOR**
Wim T. Klooster

SThP-07 **NEW IONIC MODEL POTENTIAL FOR SEMICONDUCTORS WITH APPLICATION TO Si**
Teiji Kobayasi and Hisashi Nara

SThP-08 **EFFECTS OF ELECTRON CORRELATION ON MAGNETIC COMPTON**
Yasunori Kubo

SThP-09 **CHARGE DENSITY ANALYSIS AND DIPOLE MOMENT ENHANCEMENT IN MNA (2-METHYL-4-NITROANILINE)**
Andrew Whitten, Mark Spackman, Peter Turner, Wim Klooster, Ross Piltz and Masaru Tachibana

SThP-10 **MOLECULAR ELECTRIC PROPERTIES USING HIRSHFELD SURFACES: A NOVEL APPLICATION OF SURFACE INTEGRALS**
Mark Spackman, Andrew Whitten, Joshua McKinnon, Xiaoxiong Meng, and Christopher Radford

SThP-11 **STUDY OF ANISOTROPY IN MOMENTUM DENSITY OF COBALT**
B. K. Sharma, B. L. Ahuja, S. S. Asawat, V. Purvia, Y. Kakutani, A. Koizumi and N. Sakai

SThP-12 **THE STUDY OF THE PHASES OF CDWS UNDER THE APPLICATION OF ELECTRIC FIELDS USING MULTIPLE X-RAY DIFFRACTION**
Chao-Hung Du, Mau-Tsu Tang, Yuri P. Stetsko, Yen-Ru Lee, J. -J. Lee and Shih-Lin Chang

SThP-13 **CHARGE DENSITY STUDIES OF POLYMORPHIC ANTI-ULCER AGENTS. THE APPLICABILITY OF THE ELECTROSTATIC POTENTIAL IN DRUG DESIGN**
Jacob Overgaard, Mark P. Waller and David E. Hibbs

SThP-14 **CHARGE DENSITY ANALYSIS OF β-Si_3N_4**
Doug du Boulay, Nobuo Ishizawa and Victor Streltsov

SThP-15 **CHARGE DENSITY STUDY UNDER HIGH PRESSURE**
Makoto Sakata. Takafumi Itsubo, Eiji Nishibori, Yutakata Moritomo, Norimichi Kojima, Yasuo Ohishi and Masaki Takata

SThP-16 **FERMI SURFACE OF A SHAPE MEMORY ALLOY OF TiNi**
N. Shiotani, I. Matsumoto, H. Kawata, J. Katsuyama, M. Mizuno, H. Araki and Y. Shirai

SThP-17 **PRECISE CHARGE DENSITY STUDY OF CYTOCHROME C-553 BY MAXIMUM ENTROPY METHOD**
Masaki Takata, Kenichi Kato, Hiroshi Tanaka, Atsushi Nakagawa and Makoto Sakata

SThP-18 **AN EXPERIMENTAL CHARGE DENSITY STUDY OF SINGLE-COMPONENT MOLECULAR METALS, $Ni(TMDT)_2$ AND $Au(TMDT)_2$**
E. Nishibori, Y. Fujishiro, M. Takata, M. Sakata, A. Kobayashi, W. Suzuki, E. Fujiwara, H. Tanaka and H. Kobayashi

SThP-19 **MULTIPOLE REFINEMENTS WITH RIGID-BOND AND LINK CONSTRAINTS**
T. Koritsanszky

SThP-20 **STRUCTURAL RELATIONSHIP OF β-SODIUM (X=0.33) AND β/-COPPER (X=0.65) VANADIUM BRONZES $M_xV_2O_5$**
Ruslan Ozerov, Victor Streltsov and Alexander Sobolev

SThP-21 **VALENCE STATE OF VANADIUM ATOMS IN β-$Na_xV_2O_5$ BRONZE**
Ruslan P. Ozerov, Alexandra A. Alexa and Victor A. Streltsov

SThP-22 **DEVELOPMENT OF MEASURING MAGNETIC COMPTON PROFILES BY GRAZING INCIDENT GEOMETRY**
Hiroshi Sakurai, Fumitake Itoh, Minoru Ota, Katsuyoshi Takano, Xioxi Liu and Hiroshi Kawata

SThP-23 **MAGNETIC COMPTON PROFILES OF MAGNETIC THIN FILMS AND ANISOTROPY OF Co/Pd MULTILAYER**
M. Ota, H. Sakurai, F. Itoh, M. Itou and Y. Sakurai

SThP-24 **THE ELECTRON DENSITY TOPOLOGY CHANGES DUE TO THE PHASE TRANSITION IN $KMnF_3$**
Yury V. Ivanov and Kiyoaki Tanaka

SThP-25 **STRUCTURE ANALYSIS OF GAS MOLECULES ADSORBED IN THE NANOCHANNEL OF A COORDINATION POLYMER BY THE MEM/RIETVELD METHOD**
Yoshiki Kubota, Masaki Takata, Makoto Sakata, Ryo Kitaura, Ryotaro Matsuda, Susumu Kitagawa, Tatsuo Kobayashi, Kouichi Kindo, Yoshimi Mita, Akira Matsuo, Michihiro Kobayashi, Ho-Chol Chang, Tadashi Oszawa and Megumi Suzuki

SThP-26 **MOMENTUM TRANSFER DEPENDENCE OF X-RAY RAMAN SCATTERING AT THE BERYLLIUM K-EDGE**
M. Volmer, C. Sternemann, J. A. Soininen, H. Nagasawa, M. Paulus, H. Enkisch, G. Schmidt, M. Tolan and W. Schülke

SThP-27 **CONSTRAINED DENSITY FUNCTIONAL THEORY USING X-RAY DIFFRACTION DATA**
Daniel J. Grimwood

SThP-28 **A WAVEFUNCTION CONSTRAINED JOINTLY TO X-RAY AND POLARISED NEUTRON DIFFRACTION DATA FOR THE Cs_3CoCl_5 CRYSTAL**
Dylan Jayatilaka

SThP-29 **CRYSTAL EXPLORER: A GRAPHICAL USER INTERFACE FOR DISPLAYING AND MANIPULATING HIRSHFELD SURFACES AND FINGERPRINTS FOR CRYSTAL ENGINEERING APPLICATIONS**
Dylan Jayatilaka, Daniel Grimwood and Stephen Wolff

SThP-30 **STUDY OF METAL-INSULATOR TRANSITION IN Rb_4C_{60} BY COMPTON SCATTERING, UNDER PRESSURE**
Genevieve Loupias, A. A. Sabouri-Dodaran, M. Marangolo, Ch. Bellin, F. Mauri, S. Rabii, Th. Buslaps, M. Mezouar and W. Crichton

SThP-31 **ARE ELECTRON CORRELATION EFFECTS OBSERVABLE IN ELASTIC X-RAY SCATTERING EXPERIMENTS?**
Graham Chandler, Ian Bytheway, Brian Figgis, and Dylan Jayatilaka

Oral session 1: *Inelastic X-ray scattering as a probe of highly correlated systems* Room B

Chair/Co-chair: Malcolm Cooper, Keijo Hämäläinen

8:30 SFr1-1 **INELASTIC MAGNETIC X-RAY SCATTERING FROM HIGHLY CORRELATED ELECTRON SYSTEMS**
P. A. Montano, Y. Li, J. F. Mitchell, P. E. Mijnarends, S. Kaprzyk, B. Barbiellini and A. Bansil

9:15 SFr1-2 **ELECTRON CORRELATION EFFECTS IN NOVEL MATERIALS: RECENT STUDIES OF CUPRATES, MANGANITES AND 3D QUANTUM DOTS**
Arun Bansil

10:00 SFr1-3 **SUPERCONDUCTIVITY AND FERROMAGNETISM OF $ZrZn_2$**
Zs. Major, S. B. Dugdale, R. Watts, G. Santi, M. A. Alam, S. M. Hayden, J. A. Duffy, J. W. Taylor, T. Jarlborg, E. Bruno, D. Benea and H. Ebert

10:30 Coffee Break

Oral session 2: *New perspectives in the theory and computation of the electronic structure of solids* Room B

Chair/Co-chair: Dylan Jayatilaka, Andreas Savin

11:00 SFr2-1 **WAVE-FUNCTION-BASED AB INITIO METHODS FOR ELECTRONIC STRUCTURE CALCULATIONS ON INSULATORS**
Alok Shukla

11:40 SFr2-2 **THE SIESTA METHOD: PRESENT STATUS AND FUTURE PROSPECTS**
Julian D. Gale, Emilio Artacho, Alberto Garcia, Javier Junquera, Pablo Ordejón, Daniel Sánchez-Portal and José M. Solerg

12:20 SFr2-3 **SOME NEW DEVELOPMENTS WITH WAVEFUNCTIONS CONSTRAINED TO EXPERIMENTAL SCATTERING DATA**
Dylan Jayatilaka

13:00 Lunch

Poster session 17:00 – 18:30 **Veranda**
(Same posters as Thursday August 14)

18:00 **Rigaku/MSC Aussie BBQ**

Oral session 1: *Density matrices and electron densities: new functions and new directions* Room B

Chair/Co-chair: Julian Gale, Bernardo Barbiellini

8:30 SSa1-1 **POSITION AND MOMENTUM DENSITIES COMPLEMENTARITY AT WORK, REFINING A QUANTUM MODEL FROM DIFFERENT DATA SETS**
J. -M. Gillet, S. Ragot and P. J. Becker

9:00 SSa1-2 **ELF: FOR THE GOOD AND FOR THE BAD**
Andreas Savin

9:30 SSa1-3 **SINGLE-PARTICLE ORBITALS AND MANY-BODY COMPTON SCATTERING**
Bernardo Barbiellini

10:00 SSa1-4 **CHEMICAL INFORMATION FROM THE SOURCE FUNCTION**
C. Gatti, F. Cargnoni and L. Bertini

10:30 Coffee Break

Oral session 2: *Pushing the limits of experimental charge densities* Room B

Chair/Co-chair: Mark Spackman, Masaki Takata

11:00 SSa2-1 **THERMAL MOTION ANALYSIS, A MOLECULAR MEAN FIELD MODEL**
Hans-Beat Bürgi

11:30 SSa2-2 **PSEUDOATOM RADIAL FUNCTIONS FROM THEORETICAL MOLECULAR DENSITIES**
T. Koritsanszky and A. Volkov

12:00 SSa2-3 **MULTIPOLAR REFINEMENT OF PROTEINS : SUCCESS AND PITFALLS**
B. Guillot, C. Jelsch, A. Podjarny and C. Lecomte

12:30 SSa2-4 **CHARGE DENSITY STUDIES OF Z' = 2 MOLECULES. POSSIBILITIES AND LIMITATIONS**
Dai Hibbs, Mark P. Waller and Jacob Overgaard

13:00 Lunch

Poster session 17:00 – 18:30 **Veranda**
(Same posters as Thursday August 14)

Oral session 3: ***Collinear and noncollinear spin densities in electronic materials*** **Room B**

Chair/Co-chair: Jane Brown, Rob Robinson

20:00 SSa3-1 **SPIN DENSITIES IN MOLECULE-BASED MAGNETIC COMPOUNDS: FIRST STUDY OF A PHOTO-INDUCED MAGNETIC STATE**
B. Gillon

20:30 SSa3-2 **ENSEMBLE REPRESENTABLE DENSITIES FOR ATOMS AND MOLECULES: ANALYSIS OF POLARISED NEUTRON EXPERIMENTS WHEN SEVERAL ZEEMAN LEVELS ARE POPULATED**
P. Cassam-Chenaï

21:00 SSa3-3 **OBSERVATION OF ORDERED ORBITAL OF $YTiO_3$ BY THE X-RAY MAGNETIC DIFFRACTION EXPERIMENTS**
Masahisa Ito, Naruki Tuji, Fumitake Itoh, Hiromichi Adachi, Etsuo Arakawa, Kazumichi Namikawa, Hironori Nakao, Youichi Murakami, Yasujiro Taguchi and Yoshinori Tokura

21:30 Close

Oral session 1: *Developments in electron momentum spectroscopy* Room B

Chair/Co-chair: Erich Weigold, Arun Bansil

8:30 SSu1-1 **ELECTRON MOMENTUM SPECTROSCOPY OF SINGLE CRYSTAL SILICON AND NICKEL TARGETS**
M. Vos, C. Bowles, C. Chen, A. S. Kheifets, V. A. Sashin and E. Weigold

9:10 SSu1-2 **ORBITAL MOMENTUM DENSITIES OF CHEMICALLY SIMILAR MOLECULES USING HREMS AND DFT**
M. J. Brunger, K. L. Nixon, L. Campbell, F. Wang, B.Appelbe, M. Hamilton and D. A. Winkler

9:50 SSu1-3 **PROBING ELECTRON MOMENTUM DENSITIES IN MOLECULES USING A NEW MULTICHANNEL (e,2e) SPECTROMETER**
Masahiko Takahashi and Yasuo Udagawa

10:30 Coffee Break

Oral session 2: *Electronic structure measurements using electron scattering techniques* Room B

Chair/Co-chair: Joanne Etheridge, Kenji Tsuda

11:00 SSu2-1 **CHARGE DENSITY MEASUREMENTS OF TRANSITION-METAL OXIDES USING CONVERGENT-BEAM ELECTRON DIFFRACTION**
K. Tsuda, Y. Ogata and M. Tanaka

11:40 SSu2-2 **CALCULATIONS OF ELECTRON ATOMIC SCATTERING FACTORS AND TEMPERATURE DEPENDENT DEBYE-WALLER FACTORS**
Lian-Mao Peng

12:20 SSu2-3 **THE "COMBINATION METHOD" OF QUANTITATIVE CBED AND X-RAY DIFFRACTION APPLIED TO CORUNDUM**
Philip N.H. Nakashima, Victor A. Streltsov and Andrew W.S. Johnson

13:00 Lunch

18:00 **Asian Buffet**

Oral session 1: *Recent developments in Compton scattering*

Room B

Chair/Co-chair: Bal Krishna Sharma, Sohrab Rabii

8:30 SMo1-1 **RECENT MOMENTUM DENSITY STUDY OF NOVEL MATERIALS**
Y. Sakurai and M. Itou

9:00 SMo1-2 **SPIN DENSITIES IN MOMENTUM SPACE**
J. A. Duffy

9:30 SMo1-3 **COMPTON-SCATTERING STUDIES ON ATOMIC AND MOLECULAR SYSTEMS**
S. Huotari, M. Hakala, Sz. Galambosi, S. Manninen, and K. Hämäläinen

10:00 SMo1-4 **COMPTON SCATTERING ON ALKALI-METAL-DOPED SILICON CLATHRATES**
M. Volmer, C. Sternemann, J. S. Tse, D. D. Klug, M. Paulus, C. L. Bull, T. Buslaps, N. Hiraoka, and M. Tolan

10:30 Coffee Break

Oral session 2: *Topological analyses: current state-of-the-art*

Room B

Chair/Co-chair: Carlo Gatti, Tibor Koritsanszky

11:00 SMo2-1 **TOPOLOGICAL ANALYSIS OF 3D GRIDDED ELECTRON DENSITIES**
P. Rabiller, M. Souhassou, C. Katan, S. Dahoui and C. Lecomte

11:30 SMo2-2 **CHARGE-DENSITY STUDY OF THE NON-LINEAR OPTICAL MATERIAL: ZINC (TRIS)THIOUREA SULPHATE**
Jacqueline M. Cole, Shamus L. G. Husheer, Dima S. Yufit, Judith A. K. Howard and Garry J. McIntyre

12:00 SMo2-3 **TOPOLOGICAL CHARACTERIZATION OF INTERMOLECULAR INTERACTIONS**
Yu Wang, Chi-Rung Lee and Chih-Chieh Wang

12:30 SMo2-4 **TOPOLOGICAL FEATURES OF THE ELECTRON DENSITY AND THE BASIN PROPERTIES IN SOLIDS**
A. Martín Pendás

13:00 Closing remarks and Lunch

marresearch

High-performance X-ray data collection systems

marmosaic/marcsc

The only fully integrated endstation for high-throughput crystallography

marusa

www.mar-usa.com

1880 Oak Avenue, Evanston, IL 60201 USA

Toll-free: 1-877-MAR-XRAY (1-877-627-9729)

From outside the U.S.: 1-847-869-1548

Fax: 1-847-869-1587

E-mail: info@mar-usa.com

marresearch

www.marresearch.com

Hans-Boeckler-Ring 17
22851 Norderstedt Germany

Telephone: +49 40 529 884-0

Fax: +49 40 529 884-20

E-mail: info@marresearch.com

Now, something completely NEW for crystallographers.

Introducing the TOPAZ™ Crystallizer: More crystal hits with less protein sample

The TOPAZ™ Crystallizer is creati
quite a buzz. That's because it tak
advantage of free interface diffusi
on small disposable chips. We ca
them Microprocessors because th
metering of fluids takes place with
the device, automatically, by way
tiny pneumatically actuated valve
With the TOPAZ Crystallizer, you ca
run 5760 diffusion trials per wee
with as little as 120µL of startin
protein. The crystals are high
ordered and can be harvested f
diffraction. Don't just talk about th
new TOPAZ Crystallizer. Visit ou
website or call us to find out how yo
can get your lab up and runnin
today.

Fluidigm™

www.fluidigm.com
or call
1.866.FLUIDLINE

X8PROTEUM

X-ray Crystallography Solution for Life Sciences

Bruker Nonius now offers the newest solution for X-ray Crystallogrpahy in Life Science applications - the X8PROTEUM. This remarkable system features:

- FR591 Rotating Anode generator
- Montel200 Multi-layer Graded Optics
- Kappa 4-axis Goniometer
- PROTEUM CCD Detector

Call us now and let us help you specify the solution to your research requirements.

BRUKER NONIUS

BRUKER ADVANCED X-RAY SOLUTIONS

TEL: (+31) 15 2152400 • FAX: (+31) 15 2152500 • http://www.bruker-axs.com

High-Throughput
Protein Crystallography

John Morris Scientific

Vapour Diffusion & High-Throughput Options

- Automates sitting and hanging-drop vapour diffusion crystallography methods
- Pipettes and transfers reagent solutions, greases wells, dispenses protein droplets on the bridge or cover-slip and seals cover-slips on wells
- Create custom procedures or use pre-formulated screens

Reproduce your manual method precisely with improved repeatability and throughput

It's time for Gilson to revolutionise your lab... Again

GILSON
SOLUTIONS AT WORK FOR YOU

John Morris Scientific

Free Call: 1800 251 799
Email: sales@johnmorris.com.au
Web: www.johnmorris.com.au

Sydney ● Melbourne ● Adelaide ● Perth ● Brisbane

Leading With Innovation

MicroMax™-007

The new "standard" rotating anode generator

The MicroMax™-007 sets the new standard of flux for your home laboratory X-ray source. Rigaku generators have long set the standard of excellence in terms of flux and reliability over years of operation. The new MicroMax-007 has dramatically increased the usable flux over an ordinary rotating anode generator while maintaining the Rigaku standard of reliability.

Introducing the MicroMax-007

- Twice the usable flux of an ordinary rotating anode at 800 W loading and a 70 micron focal spot
- Configurable with an Osmic Max-Flux® Confocal optic optimized for your experimental requirements
- Small vacuum chamber and pre-crystallized, pre-aligned filaments for maximum uptime
- The X-ray generator for the Rigaku High-Throughput HomeLab™

Contact Rigaku today to increase your laboratory throughput

www.RigakuMSC.com
US phone: 281-363-1033 fax: 281-364-3628
e-mail: info@RigakuMSC.com

Rigaku

Speed and resolution

X'Celerator redefines X-ray diffraction recording speed

The sea eagle spots its prey from far above the water's surface – compensating for the diffraction of light in water – dives with breathtaking pace and catches it with amazing accuracy.
A solution demanding both speed and resolution.
The X'Celerator, based on RTMS (Real Time Multiple Strip) detection technology, brings the same benefits in X-ray powder diffractometry. It's up to one hundred times faster than a traditional detection system – without any compromise on data quality or ease of use.

Why wait for hours of data collection while you could have your results in only a few minutes?

For more information:
PANalytical
Spectris Australia Pty Ltd
Suite 3 Level 2
410 Chapel Road
Bankstown NSW 2200
Tel: +61 (02) 9790867
Fax: +61 (02) 9790707
E-mail:
info@panalytical.com

www.panalytical.co

Winning by Sharing

PANalytica

18 Years of building Cryostream Coolers – there's no substitute for experience!

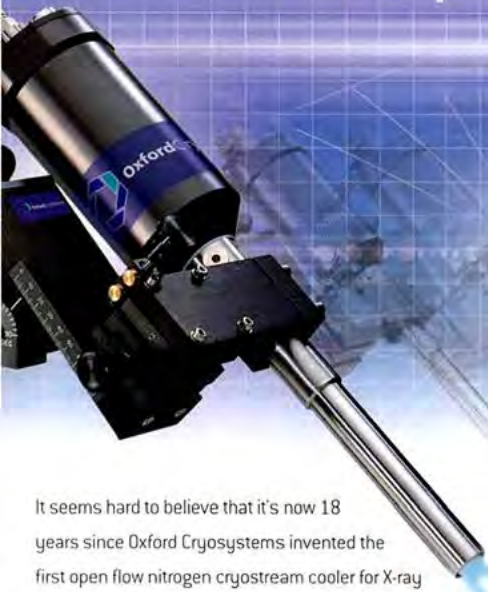

It seems hard to believe that it's now 18 years since Oxford Cryosystems invented the first open flow nitrogen cryostream cooler for X-ray crystallography.

The Cryostream Cooler quickly became the world standard for crystallography labs, combining reliability, low nitrogen consumption, value for money and superb service.

It was always inevitable that other systems would emerge, but we like to think that after 18 years of experience, we still leave our competitors standing. Because Oxford Cryosystems are dedicated to making cryocoolers for X-ray crystallography, our development team spend 100% of their time adapting, improving and adding to our systems to ensure our customers only receive the best product.

From our upgraded, virtually silent, AD51 Dry Air Unit to the exciting new Cryoshutter gas stream deflector for assisted in-stream shock cooling and annealing, the Cryostream is the past, present *and* future of low temperature crystallography.

We look after our technology so you can look after yours!

OxfordCryosystems

North American Office
220 Wood Road · Braintree
MA 02184-2403 · USA
T. 1-866-OXCRYO-8
781-843-5900
F. 781-843-5945
E. Info@OxfordCryosystems.com

Head Office
3 Blenheim Office Park
Lower Road · Long Hanborough
Oxford · OX29 8LN · UK
T. +44 (0)1993 883488
F +44 (0)1993 883988
E. info@OxfordCryosystems.co.uk

www.OxfordCryosystems.com/700series/

CCP4

Collaborative Computational Project Number 4

http://www.ccp4.ac.uk
Contact: ccp4@ccp4.ac.uk

Software Development in Macromolecular Crystallography

for 25 yrs

Current developments in the CCP4 software package include:

- Data Processing Software
- C++ PX libraries (LGPL)
- Molecular Graphics package
- Structure Refinement with Refmac5
- LIMS - MOLE
- Software Parallelisation
- Advanced, Automated Structure Solution Tools

Chair of WG1 and Executive Committee: Professor J. Naismith, St.Andrews, UK
Chair of WG2: Dr P. Evans LMB-Cambridge, UK.
CCP4 is supported by the BBSRC

KOHZU

High Performance Mechanical Systems by KOHZU

Multi-purpose modular goniometric systems

- Precision stages and goniometers (including vacuum compatible)
- Double crystal X-ray monochromators

X-ray diffractometers

- Protein crystallography experimental stations
- Other custom built beamline components

Contact in Australia :
Moreton Bay Scientific PTY Ltd.
166 Gordon Parade Manly 4179 QLD
Phone : +61 7 33 93 59 13 E-mail : mbscientific@hn.ozemail.com.au

KOHZU Precision Co.,Ltd. 2-6-15 Kurigi, Asao-ku, Kawasaki-shi, Kanagawa 215-8521 Japan
Phone:+81-44-981-2131 **Fax**:+81-44-981-2181
Web site http://www.kohzu.co.jp/ **E-mail** sale@kohzu.co.jp

Monday August 11

AsCA'03/Crystal-23

ABSTRACTS

ORAL SESSIONS

COHERENT X-RAY DIFFRACTION FOR PHASING IN CRYSTALLOGRAPHY

Ian Robinson

University of Illinois, 1110 West Green St, Urbana, IL 61801, USA
(robinson@mrl.uiuc.edu)

This lecture will demonstrate how the use of a coherent X-ray beam can produce additional information in a diffraction pattern which can provide phase information. By solving the phase problem, the diffraction can then be inverted to produce images of the crystal under investigation. Coherence is a quality inherent to undulator radiation provided by third-generation synchrotron sources. The resulting diffraction patterns must be oversampled with respect to the spatial Nyquist frequency in order to supply sufficient information. Iterative image reconstruction methods formerly developed by Fienup are then found to converge on a plausible solution.

Three-dimensional images showing the microstructure inside micron-sized gold nanocrystals will be presented [1]. It has been since found that the coherence can be preserved even after moderate focussing of the beam. In this way the resolution of the method can be greatly enhanced and so applied to a wide variety of interesting materials. With the development of X-ray free-electron lasers, we should one day be able to image individual biomolecules without having to grow crystals first.

References

1 Williams, G. J., Pfeifer, M. A., Vartanyants, I. A. and Robinson, I. K. (2003) "Three-dimensional Imaging of Microstructure in Gold Nanocrystals" *Physical Review Letters* **90,** 175501-1.

CONTROLLING THE VAN DER WAALS INTERPLAY OF FULLERENE C_{60}

C. L. Raston,[a] J. L. Atwood,[b] L. J. Barbour,[b] and M. W. Heaven[b]

[a]School of Biomedical and Chemical Sciences, University of Western Australia, Crawley, Perth WA 6009 Australia; [b]Department of Chemistry, University of Missouri - Columbia, Columbia USA. (clraston@chem.uwa.edu.au)

Controlling the way fullerenes assemble has potential in building up material with novel function. Large curved molecules such as calixarenes form inclusion complexes with C_{60} whereby the fullerene can reside *endo*- and/or *exo*-relative to the cavity of the calixarene, and this modulates the van der Waals connectivity and spatial interplay of the fullerenes. The results presented will focus on the use of calix[5]arene to assemble into different arrays. Calix[5]arene, with its C_{5v} symmetry cone conformation has complementarity of size and curvature relative to C_{60}, and the principle axis extremities of C_{70}, as well as potential symmetry matching. A 1:1 C_{60}/calix[5]arene complex crystallises from toluene with the fullerenes organised in a one dimensional zigzag array shrouded by a sheath of calixarenes (*endo*- and *exo*-cavity with respect to each fullerene). The complex forms in the presence of other globular molecules, including C_{70} as the major impurity in fullerite, and thus an impurity facilitates the purification of C_{60}. This finding has implications in controlling the interplay of C_{60} as well as in separation science. Advances in the complexation of C_{70} with calix[5]arene will also be presented. Remarkably the solid-state structure of the C_{60} complex formed from solutions of the pure fullerene has the fullerenes organized in a Z-array comprised of five close packed columns which are shrouded by a sheath of calix[5]arene molecules [1].

References

1 Atwood, J. L., Barbour, L. J. and Raston, C. L. (2002) *Crystal Growth & Design*, **2**, 3-6.

STRUCTURE OF T7 RNA POLYMERASE ELONGATION COMPLEX AT 2.9Å RESOLUTION

Dmitry G. Vassylyev,[a,b] Tahir H. Tahirov,[c] Dmitry Temiakov,[d] Michael Anikin,[d] Vsevolod Patlan,[b] William T. McAllister,[d] and Shigeyuki Yokoyama[a,b,e,f]

[a]Cellular Signaling Laboratory; [b]Structurome Research Group and [c]High Throughput Factory, RIKEN Harima Institute at SPring-8, 1-1-1 Kouto, Mikazuki-cho, Sayo, Hyogo 679-5148, Japan; [d]Morse Institute for Molecular Genetics, Department of Microbiology, SUNY Health Science Center, 450 Clarkson Avenue, Brooklyn, New York, 11203, USA; [e]RIKEN Genomic Sciences Center, 1-7-22 Suehiro-cho, Tsurumi, Yokohama 230-0045, Japan; [f]Department of Biophysics and Biochemistry, Graduate School of Science, University of Tokyo, 7-3-1 Hongo, Bunkyo-ku, Tokyo 113-0033, Japan (dmitry@yumiyoshi.harima.riken.go.jp)

The single-subunit bacteriophage T7 RNA polymerase carries out the transcription cycle in an identical manner to that of bacterial and eukaryotic multi-subunit enzymes. Here we report the crystal structure of a T7 RNA polymerase elongation complex, which shows that incorporation of an 8 bp RNA:DNA hybrid into the active site of the enzyme induces a striking rearrangement of the N-terminal domain. This rearrangement involves alternative folding of ~130 residues and a dramatic reorientation (~130° rotation) of a stable core subdomain, resulting in a structure that provides elements required for stable transcription elongation. A wide opening on the enzyme surface which is likely to be an RNA exit pathway is formed, and the RNA:DNA hybrid is completely buried in a newly-formed deep protein cavity. Binding of 10 bps of downstream DNA is stabilized mostly by long-distance electrostatic interactions. The structure implies plausible mechanisms for the various phases of the transcription cycle, and reveals important structural similarities with the mulitsubunit RNA polymerases.

CRYSTAL STRUCTURES OF THE REPLICATION TERMINATION PROTEIN BOUND TO DNA REVEAL A MODE OF POLAR REPLICATION FORK ARREST

J. P. Vivian,[a] C. J. Porter,[b] J. A. Wilce,[b] and M. C. J. Wilce[a]

[a]School of Medicine and Pharmacology; [b]School of Biomedical and Chemical Sciences, University of Western Australia, Crawley 6009, WA, Australia (jvivian@receptor.pharm.uwa.edu.au)

The final phase of DNA replication in *Bacillus subtilis* begins with the arrest of the replication forks at a distinct region located approximately opposite the origin. This terminus region is characterised by replication termination complexes composed of 30 base pair DNA sequences comprising two overlapping, inverted repeats of 16 base pairs, each capable of binding one dimer of the replication termination protein (RTP). It is thought that the RTP-DNA complex is able to affect the arrest of replication forks by impeding the progression of the leading helicase. Furthermore, the action of the RTP-DNA complex is polar in nature; that is, it allows the replication fork to pass unimpeded if it approaches from one direction yet halts its approach from the other. This in effect forms a "replication fork trap", or section of the chromosome in which the replication forks are forced to fuse. This appears to be essential for the successful transition and timing of the post-replicative processes. Identifying the determinant of this polarity and furthermore the mechanism by which the helicase is impeded has been intensely debated in the literature. Presently, it remains unclear whether polarity emanates through the differential binding affinity of RTP for the overlapping binding sites or whether there are significant conformational changes to the protein upon complex formation. Likewise, it is not well understood whether the terminator complex is acting as a non-specific obstacle to helicase progression or whether the terminator complex may specifically contact the helicase.

In this study crystal structures of RTP in complex with both a symmetrical and a pseudo-symmetrical DNA binding site have been deduced. Comparison of these models reveals a mode of generating the structural asymmetry that underlies the polarity and formation of the functional terminator complex.

TWO CRYSTAL STRUCTURES OF D(G^{I}CGAGAGC) SUGGEST THAT POTASSIUM IONS MEDIATE TO FORM DNA OCTAPLEX WITH I-MOTIF OF GUANINE QUARTET

Jiro Kondo, Shun-ichi Umeda, Tomoko Sunami, and Akio Takénaka

[a]Graduate School of Bioscience and Biotechnology, Tokyo Institute of Technology, Midori-ku, Yokohama 226-8501, Japan (jkondo@bio.titech.ac.jp)

DNA structures have been described in duplex forms, the two strands being aligned in the anti-parallel fashion, in general. As a special case, the telomeric DNA is assumed to form quadruplex with G-quartet and intercalated cytosine motifs (*i*-motif). In DNA replications, triple helix formation is required. Functional DNA would have much more complicated structures. In the present study, the two forms of crystal structures of d(G^{I}CGAGAGC) have been determined by X-ray analyses to investigate the structural basis for such specific functions.

The octamer is crystallized in the two different forms, 5GI-1 and 5GI-2. These crystals belong to the same space group I222, but with different unit-cell dimensions; *a*= 36.2, *b*=36.4, and *c*=63.1Å for 5GI-1, and *a*=34.7, *b*=42.5, and *c*=64.1Å for 5GI-2. In the 5GI-1 crystal, which is obtained at relatively low potassium-ion concentration, the octamers are assembled to form an octaplex (Fig. 1*a*) that has never been found in nucleic acid structures. In the central part of this novel octaplex, the G5 residues are associated around the crystallographic 2-fold axis to form the two G-quartets stacked on each other (Fig. 2*a* and 2*b*). A potassium ion occupies the center of the octaplex for interactions with the eight O6 atoms of the G5 residues. Other two potassium ions interact to the four O6 atoms above and below the double quartets, respectively (Fig. 2*a*). The A4 residues form water-mediated A-quartets (Fig. 2*c*). Here, it is interesting to note that the octaplex is composed of the two quadruplexes, each consisting of the four parallel strands with a G-quartet. The two G-quartets with the opposite strand polarity are intercalated (Fig. 2*a*). The present octaplex is characterized as an *I*-motif of G-quartets.

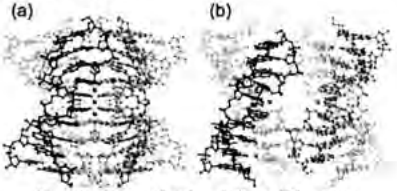

Fig. 1. The octaplex (*a*) and the two split quadruplexes (*b*).

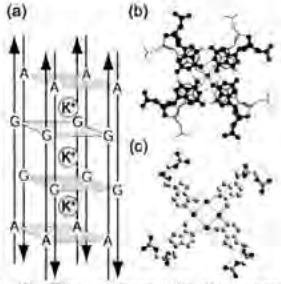

Fig. 2. The schematic diagram of octaplex formation (*a*), stacking of intercalated G5-quartets (*b*) and the water-mediated A4-quartets (*c*).

In the 5GI-2 crystal, which is obtained at relatively high potassium-ion concentration, however, the octaplex is split into two quadruplexes, each of which contains two G-duets bound to a potassium ion (Fig. 1*b*). Above and below them, disordered potassium cations and/or water molecules surround the protruded bases. The two crystal forms suggest a dynamic formation of an octaplex from two quadruplexes in solution.

BACTERIAL OFFENSE AND DEFENSE MECHANISMS USING NON-SPECIFIC ENDONUCLEASES

Hanna S. Yuan,[a] Chia Lung Li,[a] Kuo-Chiang Hsia,[a] and Woei-Chyn Chu[b]

[a]Institute of Molecular Biology, Academia Sinica, Taipei, Taiwan; [b]Institute of Medical Engineering, National Yang-Ming University, Taipei, Taiwan. (hanna@sinica.edu.tw)

Restriction enzymes are probably the most well studied bacterial endonucleases which cleave only short foreign unmethylated DNA with specific sequences and thereby protect the host methylated genome. In prokaryotic organisms, a variety of other types of endonucleases involved in the protection of bacterial cells have been identified but differ from restriction enzymes in that they cleave DNA in a sequence-independent manner. Examples include *Escherichia coli* colicin, ColE7, which is an H-N-H endonuclease that digests chromosomal DNA to kill target cells so the host cells have better survival advantage during times of stress. The crystal structures of the endonuclease domain of ColE7 [1, 2] and its complex with DNA demonstrates how the H-N-H motif mediates its functions in DNA binding and hydrolysis. The structure of the protein-DNA complex also provides the structural basis for non-specific interactions between ColE7 and DNA.

The Vvn from *Vibrio Vulnificus* is another example of a non-specific endonuclease involved in defense. Vvn is located in the periplasm, capable of digesting DNA and RNA, so that it prevents the uptake of foreign DNA during transformation. The crystal structure of the magnesium ion-bound Vvn and that of Vvn mutant H80A in complex with a duplex DNA and a calcium ion were resolved both at 2.3 Å resolution. Vvn has a novel mixed a/b topology bearing no similarity to other endonucleases, however, a known endonuclease motif containing a "bba-metal" fold is identified in the central cleft region. The crystal structure of the mutant Vvn/DNA complex shows that Vvn binds DNA at minor grooves inducing moderate DNA bending and contacts only the phosphate backbones. This result suggests the structural basis for Vvn's sequence-independent recognition of DNA and RNA. In summary, our data provides a solid foundation for a better understanding of the molecular mechanisms of non-specific endonucleases involved in the protection of bacterial cells and the recognition of DNA by sequence-independent DNA-binding proteins.

References

1 Cheng, Y. -S., Hsia, K. -C., Doudeva, L. G., Chak, K. -F. and Yuan , H. S. (2002) *J. Mol. Biol.*, **324**, 227-236.

2 Ko, T. -P., Liao, C. -C., Ku, W. -Y., Chak, K. -F. and Yuan, H. S. (1999) *Structure*, **7**, 91-102.

STRUCTURE OF MYCOBACTERIUM TUBERCULOSIS SINGLE-STRANDED DNA-BINDING PROTEIN. VARIABILITY IN QUATERNARY STRUCTURE AND ITS IMPLICATIONS

K. Saikrishnan,[a] J. Jeyakanthan,[a] J. Venkatesh,[b] N. Acharya,[b] K. Sekar,[c] U. Varshney,[b] and M. Vijayan[a]

[a]Molecular Biophysics Unit; [b]Department of Microbiology and Cell Biology; [c]Bioinformatics Centre, Indian Institute of Science, Bangalore, 560012, India (ksai@mbu.iisc.ernet.in)

Single-stranded DNA-binding protein (SSB) is an essential protein necessary for the functioning of the DNA replication, repair and recombination machineries. The protein binds preferentially to single-stranded DNA (ssDNA). As part of tuberculosis structural genomics project with special emphasis on repair and recombination, we have solved the structure of the DNA-binding domain of *Mycobacterium tuberculosis* SSB (*Mtu*SSB) in four different crystals distributed in two forms. The structure of one of the forms was solved by a combination of isomorphous replacement and anomalous scattering. This structure was used to determine the structure of the other form by molecular replacement. Like most other SSBs, topologically the DNA-binding domain contains the OB-fold. The globular core of the molecule in different subunits in the two forms and those in *Escherichia coli* SSB (*Eco*SSB) and human mitochondrial SSB (HMtSSB) have similar structure, although the three loops exhibit considerable structural variation. However, the tetrameric *Mtu*SSB has an as yet unobserved quaternary association. This quaternary structure with a unique dimeric interface lends the oligomeric protein greater stability, which may be of significance to the functioning of the protein under conditions of stress. Modelling studies indicate a difference in the path adopted by the ssDNA to wrap around *Mtu*SSB, in comparison to *Eco*SSB-ssDNA.

X-RAY ANALYSIS OF VARIOUS REACTION PATHWAYS OBSERVED FOR UNSTABLE NITRENES

Yuji Ohashi, Takahiro Mitsumori, Terufumi Takayama, Hidehiro Uekusa and Masaki Kawano

Department of Chemistry and Materials Science, Tokyo Institute of Technology, Ookayama, Meguro-ku, Tokyo 152-8551, Japan (yohashi@cms.titech.ac.jp)

It has been well known that the triplet nitrenes are produced when the phenyl azides are exposed to UV light. However, the structures have not been reported yet, since they are very unstable and active at room temperature. Many kinds of reaction products from the triplet nitrene have been obtained. Recently the structures of unstable carbenes and radicals were observed by X-ray analysis, we intended to analyse the structures of nitrenes.

The first example is the nitrene produced from *m*-carboxylic phenyl azide, **1**. Since the crystal of **1** was easily broken when it was exposed to the UV light, the host-guest complex between **1** and dibenzylamine was produced. The crystal was irradiated with the Hg lamp through a band path filter. The intensity data before and after the irradiation were collected at 25 K using the vacuum camera at the beam line, BL02B2, at Spring-8. The analysed structure clearly revealed the structure of the nitrene trapped in the host lattice. The bond distance of C-N(nitrene) distance is 1.34(4) Å, which is in good agreement with the theoretical calculation.

The second example is the dimer formation from the nitrene. The dimer formation is most popular pathway when the unstable nitrene is produced in a solution. Since the large molecular motion is necessary to form the dimer, the dimerization is not believed to occur in the solid state. When the polymorphic crystal of the above host-guest complex was exposed to a Hg lamp and the intensity data were collected at 80 K using the SPART-CCD diffractometer. The analysed structure revealed that approximately 10 % of the phenyl azide molecule turned to the dimer structure. In the original crystal lattice, the interatomic distance between the neighbouring nitrogen atoms, which are changed to the nitrene, is 4.067Å. Moreover, the produced dimer structure occupies nearly the same position as those of the monomer molecule before photo irradiation.

The third example is transformation from a nitrene to a hetero-ring. The crystal of 2-nitrophenylazide was exposed to the Hg lamp at 80 K and the intensity data were collected using R-AXIS RAPID. The analysed structure showed no triplet nitrene but the formation of the five-membered ring. However, the characteristic triplet nitrene signal was observed at 5 K, when the ESR measurement of the crystal was performed upon irradiation with the Hg lamp. This suggests that the produced nitrene attacked to the neighbouring oxygen of the nitro group to form the five-membered ring and became benzofuroxan, **2**.

These three examples suggest that the in situ crystal structure analysis at low temperatures make it possible to elucidate the various reaction pathways. Moreover, the time-resolved structure analysis will be very powerful method to make clear the complicated reaction pathway.

HYDROTHERMAL SYNTHESIS, CRYSTAL STRUCTURES, AND SOLID STATE NMR SPECTROSCOPY OF METAL SILICATES

Kwang-Hwa Lii

Department of Chemistry, National Central University, Chungli, Taiwan 320, R.O.C. (liikh@cc.ncu.edu.tw)

Organically templated metal phosphates have been extensively studied because of interesting structural chemistry and potential applications in catalysis. However, in most cases the organic templates cannot be removed without collapse of the frameworks. This is in contrast to the high thermal stability and extensive applications of zeolites in refinery and petrochemical processes. Therefore, studies have been directed to the synthesis of transition metal silicates to produce more stable frameworks [1,2]. Our synthetic methods are 2-fold, namely mild hydrothermal reactions in Teflon-lined autoclaves at 100-200 °C using organic amines as templates and high-temperature, high-pressure hydrothermal reactions in gold ampoules contained in a high-pressure reaction vessel at ca. 550 °C and 150 Mpa using alkali metal cations as templates. In this presentation I shall report the high-temperature, high-pressure hydrothermal synthesis, crystal structures, and solid-state NMR spectroscopy of several new silicates of transition metals and group 13 elements [3-5].

References

1. Francis, R., Jacobson, A. J. (2001) *Angew. Chem. Int. Ed.* **40**, 2879.
2. Wang, X., Liu, L., Jacobson, A. J. (2002) *J. Am. Chem. Soc.* **124**, 7812.
3. Li, C.-Y., Hsieh, C.-Y., Lin, H.-M., Kao, H.-M., Lii, K.-H. (2002) *Inorg. Chem.* **41**, 4206.
4. Kao, H.-M., Lii, K.-H. (2002) *Inorg. Chem.* **41**, 5644.
5. Hung, L.-I., Wang, S.-L., Kao, H.-M., Lii, K.-H. *Inorg. Chem.* in press.

POWDER NEUTRON DIFFRACTION STUDY OF UNSATURATED THIOAMIDE DERIVATIVE

Takashi Ohhara,[a] Susumu Ikeda,[a] Kenichi Oikawa,[a] Akinori Hoshikawa,[a] Takashi Kamiyama,[a] Takaaki Hosoya,[b] and Yuji Ohashi[b]

[a]Institute of Materials Structure Science, KEK, Tsukuba, Ibaraki 305-0801, Japan; [b]Dept. of Chemistry and Materials Science, Tokyo Institute of Technology, Meguro-ku, Tokyo 152-8550, Japan (tohhara@post.kek.jp)

Crystalline-state reaction, which proceeds with retention of single crystal form, is one of the most interesting topics in crystal chemistry and many reactions have been analysed mainly by single crystal X-ray diffraction. Recently, author and co-workers proposed a single crystal neutron diffraction (SND) analysis of a crystalline-state reaction as follows; hydrogen atoms in the reactive part of the reactant molecule are replaced with deuterium atom as markers, then the crystalline-state reaction is proceeded, and finally the migration of the deuterium atoms according to the reaction is observed by SND. This analytical method is very powerful to analyse the mechanism of crystalline-state reaction[1]. However, since SND requires a very large single crystal, it is much more difficult to keep the single crystal form during the reaction than single crystal X-ray diffraction study. So, we proposed to apply powder neutron diffraction (PND) instead of SND. In PND, retention of a large single crystal form is not necessary. Even though the accuracy of the structure of an organic molecule determined by PND is worse than that by SND, we expected that the distribution of H and D atoms in the reactive part, which is the most important information in the analysis of a crystalline-state reaction, would be clarified. In this work, we demonstrate that the distribution of H and D atoms in organic molecule can be clarified by powder neutron diffraction.

As a target compound, we choose an unsaturated thioamide derivative which is the reactant of the crystalline-state photo-cyclization to form a b-thiolactam[2]. For the PND measurements, we prepared a partly deuterated derivative (Fig. 1). The crystal system is monoclinic, the cell parameter is a=8.654Å, b=10.156Å, c=10.102Å, b=98.76 , and the space group is $P2_1$. Though the two phenyl groups are not the reactive part, the hydrogen atoms of those phenyl groups were replaced with deuterium atoms to reduce the background. PND patterns were measured by Vega and Sirius TOF powder neutron diffractometers at KENS with 15K. Rietveld analyses were carried out with RIETAN-2001T. The structure of non-hydrogen atoms determined by single crystal X-ray diffraction was adopted as an initial model structure and the ratio of H and D atoms at each hydrogen/deuterium sites in the reactive part were refined. The ratio of H and D obtained by PND was consistent with the known structure. This suggests that PND would be a powerful tool such as SND for analyses of crystalline-state reactions.

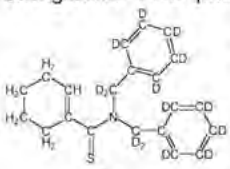

Fig.

References

1 Ohhara, T., Ikeda, S., Imura, H., Uekusa, H., Ohashi, Y., Tanaka, I., Niimura, N. (2002) *J. Am. Chem. Soc.*, 124, 14736-14740.

2 Hosoya, T., Ohhara, T., Uekusa, H., Ohashi., Y. (2002) *Bull. Chem. Soc. Jpn.*, 75, 2147-2151.

PHASE TRANSITION OF DEHYDRATED CALCINED $AlPO_4$-5 INVESTIGATED BY IN-SITU SYNCHROTRON XRD

Hwo-Shuenn Sheu,[a] Jey-Jau Lee,[a] Khin Win Phyu,[a] and Kuei-Jung Chao[b]

[a]National Synchrotron Radiation Research Center, Hsinchu 300, Taiwan;
[b]Department of Chemistry, National Tsinghua University, Hsinchu 300, Taiwan
(hsheu@srrc.gov.tw)

$AlPO_4$-5 (IUPAC structure type AFI) was reported to consist of 4, 6, 12-membered rings and forms a hexagonal arrangement of parallel and one-dimensional channels. A commensurate modulated structure along c axis was observed in the dehydrated, calcined $AlPO_4$-5. The commensurate modulated structure is reversible during hydration and dehydration at room temperature. The modulation structure of dehydrated $AlPO_4$-5 was determined to give the wave vector q being one-dimensional and a value of 3/8c*. *In-situ* synchrotron XRD studied found that modulation peaks disappear at the temperature above 70°C. This phase transition is reversible during heating and cooling between room temperature and 90°C (Fig. 1). No further phase transition was found up to 400°C. The crystal structure at 90°C was refined by Rietveld method with space group P6cc. This crystal structure is similar to that of hydration form at room temperature.

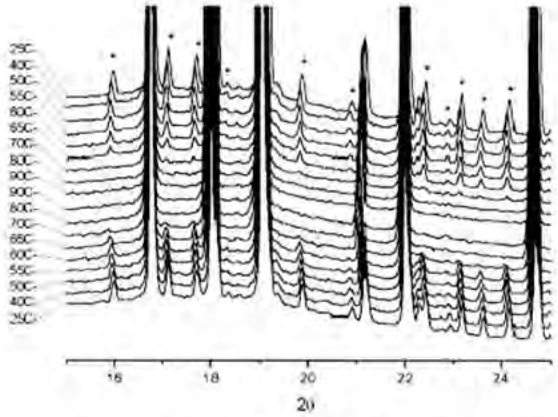

Fig. 1. Variable temperature synchrotron XRD of dehydrated $AlPO_4$-5. The modulation peaks are marked (*). Baseline of each pattern was shifted for clarity.

COMPLEXES OF SIMPLE ALKALI METAL SALTS WITH N,N'-AROMATIC BIDENTATE LIGANDS

Allan H. White, Jarrod N. Buttery, Effendy, George A. Koutsantonis, Siti Mutrofin, Neil C. Plackett, Brian W. Skelton, and Claire R. Whitaker

Chemistry, University of Western Australia, Crawley WA 6009, Australia (ahw@crystal.uwa.edu.au)

A wide variety of adducts has been obtained between alkali metal salts MX, M = Li, Na, K, Rb, (but not, as yet, Cs); X = Cl, Br, I, NCS, NO_3, ClO_4, PF_6, F_3CSO_3 (= 'tfs'), and *N,N'*- aromatic bidentate ligands, 'L' = 2,2'-bipyridyl ('bpy'), 1,10-phenanthroline ('phen'), and 2,9-dimethylphenanthroline ('dmp') MX:L (1:n), n predominantly 1,2,3 from non-aqueous solvent, S, the form of the complex being strongly influenced by the packing of the aromatic ligand planes. The 1:1 X = oxyanion adducts are infinite one-dimensional anion-bridged polymers, the unsolvated halide adducts binuclear (one only: [(dmp)Li(μ-Cl)$_2$(dmp)]), while the solvated adducts commonly have the form [LMSX] or [LMS$_2$]X (M = Li), Na, or more complex arrays for larger M. For n = 2, the adducts are predominantly of the mononuclear forms[XML$_2$], M = Li, Na, or [ML$_2$]X ; for M = Li, L = dmp, an isomorphous array is found with discrete cations, but for L = phen, *quasi*-square-planar [ML$_2$]$^+$ cations form stacks with the anions in between, with $NaPF_6$:phen (6:13) an unusual variant. In the limited number of 1:3 complexes, the complexes predominantly take unusual forms.

A number of complexes are found with unusual stoichiometries: KI:dmp:MeOH (6:8:3) is [K_6I_4(dmp)$_8$]I_2 .3MeOH, while Ktfs:dmp (4:3) is a double-stranded polymer. $KClO_4$:phen:H_2O (1:5:6) is [(phen)$_3$K(μ-OH_2)$_2$(phen)$_3$](ClO_4)$_2$. 4phen. 4H_2O.

CADB: CONFORMATION ANGLES DATABASE OF PROTEINS

K. Sekar, G. Ramya Bhargavi, P. Ananthalakshmi and S.S. Sheik

Bioinformatics Centre and Supercomputer Education and Research Centre, Indian Institute of Science, Bangalore 560 012, India (sekar@physics.iisc.ernet.in)

CADB (Conformation Angles DataBase) provides an online resource for access to data on conformation angles (both main-chain and side-chain) of protein structures in two data sets corresponding to 25% and 90% non-redundant protein chains available in the Protein Data Bank. In addition, the database contains the necessary crystallographic parameters. Also, the package has several flexible options and a display facility to visualize the main-chain and the side-chain conformation angles for a particular amino acid type. The package can also be used to study the interrelationship between the main-chain and the side-chain angles. A web based JAVA graphics interface has been deployed to display the user interested information on the client machine. The database is being updated at regular intervals and can be accessed over the World Wide Web Interface at the following URL: http://cluster.physics.iisc.ernet.in/cadb or http:// 144.16.71.148/cadb/. The details and the newly added options will be discussed.

Reference

1 Sheik, S.S., Ananthalakshmi, P., Ramya Bhargavi, G., Sekar., K. (2003) *Nucl. Acids. Res.* **31(1)**, 448-451.

USING STRUCTURAL INFORMATION IN FUNCTIONAL GENOMICS: IDENTIFICATION OF PROTEIN KINASE SUBSTRATES

Bostjan Kobe, Robert A. Breinl and Ross I. Brinkworth

Department of Biochemistry and Molecular Biology, University of Queensland, Brisbane, Qld 4072, Australia (b.kobe@mailbox.uq.edu.au).

Protein structure determines its function. Structural genomics initiatives take advantage of this relationship, aiming to contribute to the global "functional genomics" effort to functionally annotate every gene product. We hypothesized that for certain large families of proteins, structural information available for some members of the family can be used in a comprehensive fashion to identify the functions of all members of the family. We tested this hypothesis on the protein Ser/Thr kinase family.

Protein kinases are responsible for protein phosphorylation, a post-translational modification that regulates essentially every cellular process including metabolism, growth, differentiation, motility, membrane transport, learning and memory. To ensure the signalling fidelity, protein kinases must be specific and act only on a defined subset of cellular targets. Understanding the substrate specificity of a protein kinase therefore defines its cellular role.

The large number of protein kinases makes it impractical to determine their specificities and substrates experimentally. Based primarily on three-dimensional structural information on protein kinases, we developed a web-interfaced bioinformatic tool Predikin that predicts an optimal substrate sequence for any Ser/Thr kinase, and this optimal sequence can then be used to search for substrate proteins [1]. First, we developed a set of rules governing the binding of a heptapeptide substrate motif (surrounding the phosphorylation site) to the kinase, using the available crystal structures, molecular modelling and sequence analyses of kinases and substrates. We then implemented these rules in a web-interfaced program for automated prediction of optimal substrate motifs, taking only the amino acid sequence of a protein kinase as input. We adapted the available algorithms (e.g., Ref. [2]) to search protein databases (using the heptapeptide motif) for putative substrate proteins.

We show the utility of the method by analyzing yeast signal transduction pathways. Our tool also allows us to assign likely kinases to all the phosphorylation sites identified by the yeast phosphoproteome analysis via mass spectrometry [2].

Our method is the only available predictive method generally applicable for identifying possible substrate proteins for protein kinases, and helps *in silico* construction of signalling pathways. The accuracy of prediction is comparable to the accuracy of data obtained from systematic large-scale experimental functional genomics approaches.

References

1 Brinkworth, R.I, Breinl, R.A. and Kobe, B. (2003) *Proc. Natl. Acad. Sci. USA.* **100**, 74-79.

2 Yaffe, M.B., Leparc G.G., Lai, J., Obata, T., Volinia, S. and Cantley, L.C. (2001) *Nature Biotech.* **19**, 348-353.

3 Ficarro, S.B., McCleland, M.L., Stukenberg, P.T., Burke, D.J., Ross, M.M., Shabanowitz, J., Hunt, D.F. and White, F.M. (2002) *Nature Biotech.* **20**, 301-305.

CAN YOU PREDICT WHETHER A PROTEIN WILL CRYSTALLISE FROM THE PRIMARY SEQUENCE ?

Adrian H. Batchelor

University of Maryland, School of Pharmacy, Baltimore, USA
(abatchel@rx.umaryland.edu)

I'll be presenting a simple 'back of an envelope' approach to looking at a protein sequence and deciding whether it is likely to crystallise. One example in which this approach proved to be useful was the crystallisation of Apical Membrane Antigen 1 from Plasmodium falciparum. Work in progress towards solving this structure will also be discussed.

CYSTEINE DISTRIBUTION AND THE EVOLUTION OF SHORT CHAIN OXIDOREDUCTASE ENZYMES: COVARIANCE AND DISULFIDE BOND POTENTIAL

W. L. Duax,[a,c] V. Pletnev,[b] and R. Huether[a]

[a]Hauptman-Woodward Institute, Buffalo, NY 14203, USA; [b]Shemyakin Institute, Moscow, Russia; [c]SUNY@Buffalo, Buffalo, NY, (duax@hwi.buffalo.edu)

The short chain oxidoreductase (SCOR) family of enzymes includes over 5000 members, extending from bacteria and archaea to humans, for which 36 have known crystal structures. The superfamily has at most one fully conserved residue. One major subgroup of 1651 known and hypothetical proteins has a highly conserved TGxxxGIG pattern in the first $\beta\alpha$ turn of the Rossmann fold. Approximately 20% of these enzymes have no cysteines, 20% have two, three and four cysteines each and the remaining 20% have from five to eight cysteines. The majority of enzymes having no cysteines are from prokaryotes. Many of the enzymes having 5 to 8 cysteines are found in plants. None of the PDB crystal structures contain disulfide bridges. There are 10 sites with 7% or more Cys occupancy. Covariance analysis reveals that 96 members of the TGxxxGIG subfamily have Cys in more than one of the ten Cys-rich sites. Of particular interest is the frequency of covariance of Cys in position 36 and 59, 119 and 177, and 181 and 238 (3α,20β-HSD sequence numbering). A model of 1HDC in which C36-C59, C117-C179, and C181-C238 pairs have replaced the corresponding residues in the observed structure reveals that the distances between the hypothetical pairs of sulfur atoms are 1.9Å, 2.7 Å, and 4.4 Å, respectively. These distances suggest that little or no change in backbone conformation would be required for disulfide bridges to form. The 22 SCOR proteins containing C36 **and** C59 residues include 14 known or putative tropinone reductases from plants. One of these is PDB structure 2AE2. The sulfurs of the two cysteines in this crystal structure are within 5 Å of one another. Permissible rotations about the C_α-C(S) bonds would reduce the separation to 2 Å. The presence of 1mM dithiothreitol in the crystallization media may have reduced a disulfide bond in the native structure. Research supported in part by NIH Grant No. DK26546.

THREE NOVEL POLYMERIC NETWORK OF CUPPER(II) CONSTRUCTED WITH SUCCINATO LIGAND AND THE INFLUENCES OF WEAK INTERACTIONS ON THEIR CRYSTAL PACKING

Tian-Huey Lu,[a] G. Mostafa,[a] and N. Ray Chaudhuri[b]

[a]Department of Physics, National Tsing Hua University, Taiwan, R.O.C.;
[b]Department of Inorganic Chemistry, IACS, W.B., India (thlu@phys.nthu.edu.tw)

The crystal engineering of metal organic coordination network is now a growing field. The key objective of the advanced crystal engineering is the control on manipulation of weak interactions in order to tune the properties of the bulk material to design and prepare of new functional materials, such as molecular-based magnets etc. Thus, to synthesize new solid phases with predictable stoichiometry and architecture for specific applications, one has to understand the underlying factors such as hydrogen bonding, π-π, C-H...π interactions *etc.* that determine crystal packing. Till date, an accurate prediction of the overall crystal structure currently is almost impossible but it may be achieved in the near future.

With this background, the carboxylate group is one of the most widely used bridging ligands for designing polynuclear complexes with interesting magentic properties. The versatility of a carboxylate group can be illustrated by the variety of bridging conformations, the most important being (a)syn-syn, (b)syn-anti and (c)anti-anti.

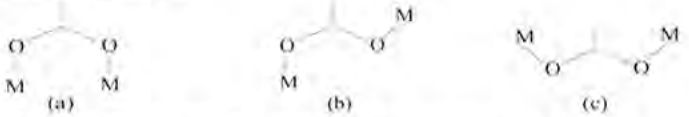

Of the carboxylato groups, major studies have been done on oxalato bridged metal complexes with a few examples of terepthalate, fumarate, maleate, malonate, adipate etc but the reports on succinate and glutarate as superexchange pathways are scanty in literature. These carboxylates showed wide varieties of the superexchange phenomenon and are closely related to the bridging conformations adopted by the carboxylate group in polynuclear systems. To design a carboxylato bridged pre-assigned functional material, hence to achieve a particular bridging conformation, a systematic study and more examples of carboxylato bridged complexes are needed.

Here, we wish to report the relevance of the weak interactions for the construction of novel succinato bridged network structure of Cu(II) and their exchange pathway.

Crystal Data:

(1) $[Cu_2(\mu\text{-}OH_2)_2(\mu\text{-succinate})(bipy)(NO_3)_2]_n$, Triclinic, $P\bar{1}$, a=7.0641(6), b=9.8410(8), c=10.4885(9) Å, α=72.079(2)^0, β=73.176(2)^0, γ=74.6290(10)^0

(2) $[Cu_2(\mu\text{-}OH_2)_2(\mu\text{-succinate})(phen)(NO_3)_2]_n$, Triclinic,$P\bar{1}$, a=6.9386(8), b=10.3463(14), c=10.8572(17) Å, α =69.734(11)^0, β=81.354(11)^0, γ =75.687(10)^0

(3) $[\{Cu_8(\mu\text{-succinate})_4(phen)_{12}\}(BF_4)_4]_n$, Triclinic,$P\bar{1}$, a=12.5769(10), b= 19.3034(15), c=19.3348(16) Å, α =60.187(2)^0, β=86.864(2)^0, γ =80.538(2)^0

NEW BOROPHOSPHATES IN MAIN GROUP ELEMENT AL, GA AND IN SYSTEMS : SYNTHESES AND STRUCTURES

J.-T. Zhao,[a] J.-X. Mi,[b] Y.-X. Huang,[bc] M.-R. Li,[ac] S.-Y. Mao[b] and R. Kniep[c]
[a]State Key Laboratory of High Performance Ceramics and Superfine Structures, Shanghai Institute of Ceramics, Chinese Academy of Sciences, Shanghai 200050, P.R. China; [b]College of Chemistry and Chemical Engineering, Xiamen University, Xiamen 361005, P.R. China; [c]Max-Planck Institute for Chemical Physics of Solids, Dresden 01187, Germany (jtzhao@mail.sic.ac.cn)

Borophosphates, as potential microporous materials, have drawn much attention in recent years and shown rich structural chemistry[1]. Although many compounds with transition metal elements have been reported, compounds with the p-block main group elements participating in the framework are rare. During our systematic investigations of borophosphate compounds in systems containing Al, Ga and In elements, more than ten new phases have been synthesized by mild hydrothermal methods and structurally characterized by X-ray diffraction methods [2].

Although the molar ratio of the main non-oxygen elements (or cations), A^{I} : M^{III} : B : P, are all the same in different compounds, they form four different structures belonging to four types. The preferences of the type seem largely governed by the ratio of the cation sizes of A^{I} and M^{III}. These four structure types contain different anion complex of borophosphates. These different anion complexes have different connectivity to the octahedral $M^{III}O_6$ units, which lead to different porosities in these structures. A^{I} cations reside inside the channels with 6- or 8-membered rings of polyhedral units as cross sections.

$A^{I}M^{III}[BP_2O_7(OH)_3]$, A^{I} = Na, K; M^{III} = Ga, In; monoclinic, C2/c, $NaFe[BP_2O_7(OH)_3]$ type [3]. The structure contain isolated anion units $[(OH)O_2PO_{1/2}\text{-}O_{1/2}B(OH)_2O_{1/2}\text{-}O_{1/2}PO_3]^{4-}$.**NaIn[$BP_2O_8$(OH)]** [4], triclinic, P-1, new type. The structure contains dimeric $[O_{1/2}O_3P\text{-}B(OH)O_{3/2}\text{-}O_{2/2}PO_2]^{4-}$ units.

A^{I}In[BP_2O_8(OH)] , A^{I} = K, NH_4, Rb; triclinic, P-1, $KFe[BP_2O_8(OH)]$ type [3]. The structures also contain dimeric $[O_{1/2}O_3P\text{-}B(OH)O_{3/2}\text{-}O_{2/2}PO_2]^{4-}$ units. It is an intergrowth structure with the above type.**$A^{I}M^{III}[BP_2O_8(OH)]$** , A^{I} = NH_4, Rb, Cs; M^{III} = Al, Ga; monoclinic, $P2_1/c$, $RbFe[BP_2O_8(OH)]$ type [5]. The structures contain connected $[O_2PO_{2/2}\text{-}O_{3/2}B(OH)\text{-}O_{1/2}PO_3]^{4-}$ units.**References**

1 Kniep, R., Engelhardt, H. and Hauf, C. (1998) *Chem. Mater.* **10**, 2930-2934.
2 Zhao, J.-T., Mi, J.-X., Huang, Y.-X., Li, M.-R., Mao, S.-Y., Kniep, R. et al. (2001) *Z. Kristallogr. NCS* **216**, 15-16; (2002) *Z. Kristallogr. NCS* **217**, 3-8; 163-172; 305-306.
3 Boy, I., Cordier, G., Eisenmann, B. and Kniep, R. (1998) *Z. Naturforsch.* **53B**, 165-170.
4 Li, M.R., Master Thesis, Xiamen University, (2002), p.60.
5 Kniep, R., Boy, I. and Engelhardt, H. (1999) *Z. Anorg. Allg. Chem.* **625**, 1512-1516.

IN-SITU SINGLE CRYSTAL X-RAY DIFFRACTION STUDIES OF GUEST-EXCHANGE IN NANOPOROUS FRAMEWORK MATERIALS

Gregory J. Halder,[a] Cameron J. Kepert,[a] Boujemaa Moubaraki,[b] Keith S. Murray,[b] and John D. Cahsion[c]

[a]Department of Chemistry, University of Sydney, NSW 2006, Australia; [b]School of Chemistry, Monash University, Clayton, VIC 3800, Australia; [c]School of Physics and Materials Engineering, Monash University, Clayton, VIC 3800, Australia (g.halder@chem.usyd.edu.au)

Recently there has been much speculation that molecular framework materials, like coordination frameworks, may have the potential to emulate industrially important porous materials such as zeolites. However, to date there have been few conclusive structural reports, and the question as to what happens to the frameworks during desolvation and resolvation remains unanswered. Here we report the first complete crystallographic study of reversible guest-exchange in one such material, utilising a new type of single crystal x-ray diffraction experiment.

The robustness of the material $M_2(bpy)_3(NO_3)_4.2(guest)$ (M = Ni^{II} or Co^{II}, bpy = 4,4'-bipyridine) to guest-exchange has been well documented [1,2], including the first single-crystal structural refinement of the fully desolvated system. Presently we have extended this work with *in-situ* single-crystal x-ray diffraction experiments, monitoring the uptake and release of a range of guest molecules into the host framework (Figure 1). These results represent the first of their kind and have yielded very unique information on the structural consequences guest-exchange.

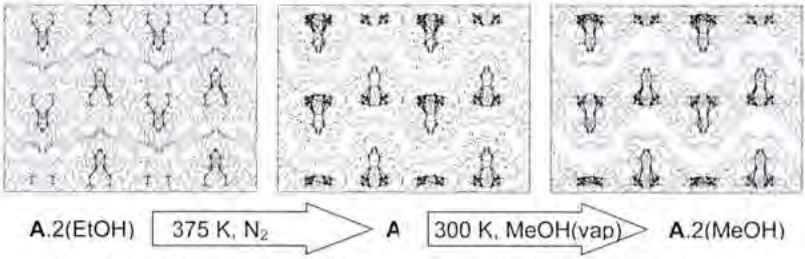

Figure 1: Electron density difference maps (platon) illustrating the desorption and resorption of guest species in the framework material $M_2(bpy)_3(NO_3)_4$ (**A**).

This technique has been further implemented to study a range of nanoporous framework materials, including a system that exhibits guest-dependent spin-state switching [3].

References

1 Kepert, C.J. and Rosseinsky, M.J. (1999) *Chem. Commun.*, 375-376.
2 Fletcher, A.J., Cussen, E.J., Prior, T.J., Rosseinsky, M.J., Kepert, C.J. and Thomas, K.M. (2001) *J. Am. Chem. Soc.* **123**, 10001-10011.
3 Halder, G.J., Kepert, C.J., Moubaraki, B., Murray, K.S. and Cashion, J.D., (2002) *Science* **298**, 1762-1765.

CHANNELS IN 3-DIMENSIONAL COORDINATION POLYMERS: ZINC SACCHARATE AND LANTHANUM MUCATE

Michael Moylan, Brendan Abrahams, Simon Orchard, and Richard Robson

School of Chemistry, University of Melbourne, Victoria, 3010, Australia
(m.moylan@pgrad.unimelb.edu.au)

Reaction of monopotassium saccharate (figure 1) with zinc acetate produces a three-dimensional coordination polymer of composition $ZnC_6H_8O_8.2H_2O$ consisting of pillars of zinc linked by saccharate ligands (figure 2). Channels with square cross-section are formed with metals occupying the corners and ligands generating the edges.

There are two types of channels in the structure, and they provide remarkably different chemical environments. The channels alternate like the black and white squares on a chessboard. The hydroxy groups attached to the two central carbons of the ligands surrounding the first channel are directed into that channel. The neighbouring channel is lined with the carbons and hydrogens from the ligand. This arrangement renders the first channel hydrophilic and the second hydrophobic in character[1].

Crystals of lanthanum mucate (figure 3) form from hot aqueous mixtures of lanthanum nitrate and monopotassium mucate (figure 4). The resulting coordination arrangement generates channels with hexagonal cross section. The structure of the two polymers and the successful introduction and crystallographic detection of several small non-polar guests such as I_2, azobenzene, and cyclooctatetraene into the hydrophobic channel of zinc saccharate is described.

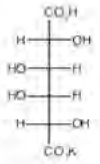

Figure 1: potassium saccharate

Figure 2: zinc saccharate viewed down the channel axis

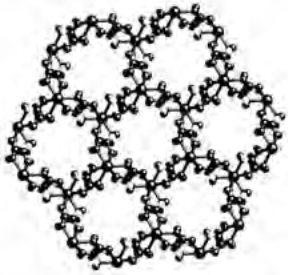

Figure 3: lanthanum mucate viewed down the channel axis

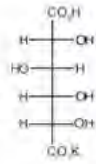

Figure 4: potassium mucate

Reference

1 Abrahams, B., Moylan, M., Orchard, S. and Robson, R. *Angew. Chem.* In press.

Monday August 11

AsCA'03/Crystal-23

ABSTRACTS

POSTER SESSIONS

EXPERIMENTAL CHARGE DENSITIES IN STRONGLY HYDROGEN-BONDED AROMATICS

Ross O. Piltz,[a] David E. Hibbs,[b] Jacob Overgaard[b] and Peter Williams[c]

[a]Bragg Institute, ANSTO, Lucas Heights, NSW 2234, Australia; [b]School of Chemistry, University of Sydney, Sydney, NSW 2006, Australia; [c]Biostructural and Biomolecular Research Group, University of Western Sydney, Parramatta, NSW 2150, Australia (rop@ansto.gov.au)

Conventional strong hydrogen bonds such as O – H ...O, N – H ...O and O – H ...N are clearly important in the areas of supramolecular chemistry, crystal engineering and the study of biological activity. Unfortunately the position of such hydrogen atoms cannot be located unambiguously in conventional charge density work using X-ray diffraction techniques. To overcome this limitation combined X-ray/neutron diffraction studies have been performed using the facilities of ANSTO, Lucas Heights and the University of Sydney on a set of hydrogen-bonded aromatics, including (Z)-N-methyl-C-phenylnitrone and 1-(2-hydroxy-5-nitro-phenyl)-ethanone. The results of these, and other more recent studies, will be presented.

A WAVEFUNCTION CONSTRAINED JOINTLY TO X-RAY AND POLARISED NEUTRON DIFFRACTION DATA FOR THE Cs_3CoCl_5 CRYSTAL

Dylan Jayatilaka

Department of Chemistry, University of Western Australia, Crawley, WA 6009, Australia (dylan@theochem.uwa.edu.au)

The experimental wavefunction technique [1,2] is extended, to implement the joint refinement of X-ray and Polarised Neutron Diffraction (PND) data. Results are presented for the $CoCl_4^{2-}$ ion in the Cs_3CoCl_5 crystal.

References

1 See, e.g., Grimwood, D., Bytheway, I. and Jayatilaka, D., (2003) *J. Comp. Chem.* **24**, 470-483.

2 Grimwood, D. and Jayatilaka, D., *TONTO: A System for Computational Chemistry*, www.theochem.uwa.edu.au/tonto/index.html.

USING THE HIRSHFELD SURFACE TO INVESTIGATE CRYSTAL PACKING IN POLYMORPHS AND CRYSTALS WITH $Z' > 1$

Joshua McKinnon, and Mark Spackman

Chemistry, School of Biological, Biomedical and Molecular Sciences, University of New England, Armidale, NSW 2351, Australia (jmckinn4@une.edu.au)

Understanding the differences in the crystal packing of molecules in polymorphic structures, or differences in the crystalline environment of the unique molecules in crystals with $Z' > 1.0$ can be extremely difficult, particularly when packing differences are subtle.

We have previously shown that the Hirshfeld surface of a molecular crystal offers a remarkable new way of exploring packing modes and intermolecular interactions in molecular crystals using a novel partitioning of crystal space[1]. Because these surfaces are most effectively utilised in the laboratory where access to interactive molecular graphics is available, we have also devised a two-dimensional mapping, called a 2D fingerprint plot, which quantitatively summarises the nature and type of intermolecular interaction and presents this information in a convenient colour graph[2].

We have found that the combination of the Hirshfeld surface and 2D fingerprint plot for a molecule in a crystal provides a particularly powerful tool when attempting to investigate subtle differences where a molecule exists in different crystallographic environments. Here we present two detailed examples - three polymorphs of *p*-dichlorobenzene, and two polymorphs of tetrathiafulvalene (TTF), one of which contains four unique molecules.

References

1 McKinnon, J. J., Mitchell, A. S., Spackman, M. A. (1998) *Chem. Eur. J.* **4**, 2136-2141; McKinnon, J. J., Mitchell, A. S., Spackman, M. A. (1998) *Chem. Commun.* 2071-2072

2 Spackman, M. A., McKinnon, J. J. (2002) *CrystEngComm*, **4**, 378-392

A NEW HYBRID MATERIAL WITH THREE DIMENSIONAL Na-O-Cu CONNECTIVITY AND ITS NANOSTRUCTURES BY ANNEALING

G. Mostafa,[a] Tian-Huey Lu,[a] and N. Ray Chaudhuri[b]

[a]Department of Physics, National Tsing Hua University, Taiwan, R.O.C.;
[b]Department of Inorganic Chemistry, IACS, W.B., India
(mostafa@phys.nthu.edu.tw)

There has been considerable interest in recent years in ordered arrays of magnetically coupled novel inorganic-organic hybrid framework, both from a technological and a fundamental point of view. Incorporation of metal ions into organic systems, functionality can be, introduced either through the inorganic species or the organic linker molecules. Therefore, rational design and construction of new materials with specific networks has become a particularly important and topical subject. We wish to report here, a new molecular magnetic system of a heterometallic structure of general formula $[Na_2Cu(malonate)_2(H_2O)_2]_n$ obtained from a one pot synthesis which consists of interlocked anionic $[Cu(malonate)_2]_n$ and cationic $[Na(H_2O)_2]_n$ chains to form 3D coordination-polymeric network where the malonate dianion functions as a hexadentate ligand. To the best of our knowledge this is the first molecular system in which malonate functions as hexadentate ligand. The low temperature magnetic study reveals that the compound is ferromagnetically coupled. The high temperature annealing of the 3D array leads to a mixed metal oxide $NaCuO_2$ which shows nanowire (Figure) and nanodisks depending upon annealing temperatures.

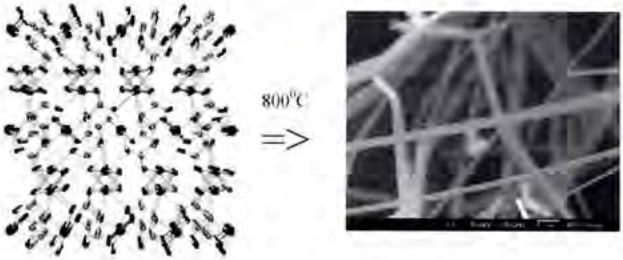

PROTEIN CRYSTALLIZATION IN SPACE USING COUNTER-DIFFUSION TECHNIQUE

Hiroaki Tanaka,[a,b] Koji Inaka,[c] Sachiko Takahashi,[b] Satoshi Sano,[a] Masaru Sato,[a] and Susumu Yoshitomi[a]

[a]Space Utilization Research Center, National Space Development Agency of Japan (NASDA), Ibaraki 305-8505, Japan; [b]Japan Space Utilization Promotion Center, Tokyo 169-8624, Japan; [c]Maruwa Food Industries, Inc., Nara 639-1123, Japan (PXW01674@nifty.ne.jp)

Microgravity environment is known to provide ideal diffusive conditions for protein crystallization such as reducing convective fluid motions and sedimentations. However it is not widely utilized because flight opportunities had been limited and irregular. To overcome these problems and to promote the utilization of microgravity environment, NASDA performs the protein crystallization experiments twice a year for three years from February 2003 using Russian Service Module. At the first three flights, we use the facilities, Granada Crystallization Box(GCB), which is designed as a passive, light, inexpensive and high-density experimental device for protein crystallization inside capillaries by counter-diffusion technique, developed by Garcia-Ruiz (http://lec.ugr.es/).

To perform this project effectively, we developed two ingenious methods as follows. Since most of the protein samples are crystallized by vapour-diffusion technique, we have to optimise the crystallization conditions of each sample especially for counter-diffusion technique. To carry out this preliminary study efficiently, we developed a new crystallization device using shorter capillary and the simple gel in the silicone tube in the test tube (figure 1), which requires less time and less amount of samples. A single capillary can correspond to a lot of vapour-diffusion drops because it scans a wide area of crystallization conditions. We also developed the simulation program using the empirically estimated diffusion constant values of the protein solution and the precipitant solution to prospect the position and the timing of crystallization in the capillary. Hereby, we can easily find out the suitable condition of the crystallization for each sample.

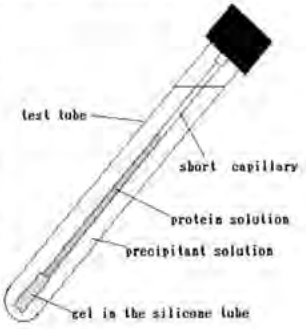

Figure 1

Our first 46 protein samples are now in ISS(International Space Station). As far as the results of the preliminary crystallization experiments on the ground, combination of the preliminary experiment and the simulation program worked very effectively. We have convinced that the crystallization in space will contribute to the determination of the protein structure more effectively using this technique in the very near future. The standardization of the crystallization conditions is now under consideration.

PROTEIN CRYSTAL GROWTH WITH STIRRING SOLUTION

Hiroaki Adachi,[a] Kazufumi Takano,[b] Masashi Yoshimura,[a] Yusuke Mori,[a] and Takatomo Sasaki[a]

[a]Department of Electrical Engineering and Venture Business Laboratory, Osaka University, 2-1 Yamadaoka, Suita, Osaka 565-0871, Japan; [b]Department of Material and Life Science, Osaka University, and PRESTO, JST, 2-1 Yamadaoka, Suita, Osaka 565-0871, Japan (adachi@ssk.pwr.eng.osaka-u.ac.jp)

The production of protein crystals with suitable diffraction quality and size is a rate-limiting step for determining the three-dimensional structure of proteins at atomic resolution. We propose a protein crystal growth with stirring the solution, which is entirely different approach compared with the conventional method, leading to an effective growth of protein crystals. Crystallographers believe that protein crystal growth must be under a still condition, and it is ultimately performed under a microgravity condition due to reducing convective flow. It is important that the protein solution must be stirred gently in protein crystal growth because directly stirring a protein solution causes problems such as spontaneous nucleation, protein denaturation and damaged crystals. We developed two methods for growing large, high-quality protein crystals. One is *FAST* (*f*loating *a*nd *s*tirring *t*echnique) using the *Two-Liquid System*[1] and a magnetic stirrer. The other is *Micro-Stirring* technique using a rotary shaker.

FAST realizes mild stirring suitable for protein crystal growth by stirring the liquid of the lower layer, which is primarily an indirect stirring method. The stirring intensity is changed to optimize the growth conditions for a specific rotation rate, shape of stirring bar, and volume of lower liquid. Using this method together with slow cooling, we obtained a 3.0 mm-long lysozyme crystal in 20 days from a seed crystal[2]. This is larger than the 2.0 mm-long crystal grown without stirring. When the protein solution is kept still, protein concentration gradually increases in the lower part of the solution. Consequently, excess protein solute that is not supplied to the seed crystal leads to additional spontaneous nucleation. Stirring the protein solution accelerates the growth of the protein crystal and prevents additional spontaneous nucleation.

On the other hand, Micro-Stirring enables to stir multiple micro-scale samples in the growth of protein crystals by the sitting-drop and *floating-drop*[3] vapor diffusion techniques. This is also effective in reducing the number of crystals and in growing large crystals compared to the conventional vapor diffusion technique[4]. We also expect that stirring the solution will improve crystallinity.

References

1 Adachi, H., Watanabe, T., Yoshimura, M., Mori, Y. and Sasaki, T. (2002) *Jpn. J. Appl. Phys.* **41**, L726-L728.
2 Adachi, H., Takano, K., Yoshimura, M., Mori, Y. and Sasaki, T. (2002) *Jpn. J. Appl. Phys.* **41**, L1025-L1027.
3 Adachi, H., Takano, K., Morikawa, M., Kanaya, S., Yoshimura, M., Mori, Y. and Sasaki, T. (2003) *Acta. Cryst.* **D59**, 194-196.
4 Adachi, H., Takano, K., Yoshimura, M., Mori, Y. and Sasaki, T. (2003) *Jpn. J. Appl. Phys.* **42**, L314-L315.

A STRUCTURAL STUDY ON THE POLYMORPH OF ICOSANE-1,20-DIOL

K. Uno,[a] N. Nakamura,[a] and Y. Ogawa[b]

[a]Integrated Science and Engineering Major, Graduate School of Science and Engineering, Ritsumeikan University, 1-1-1, Nojihigashi, Kusatsu, Shiga 525-8577, Japan; [b]Department of Chemistry, Faculty of Science, Kumamoto University, 2-39-1, Kurokami, Kumamoto 860-8555, Japan (nakamura@se.ritsumei.ac.jp)

The two different crystal structures of icosane-1,20-diol, $HO–(CH_2)_{20}–OH$, which were obtained under the control of the crystallizing condition, were analyzed by single crystal X-ray diffraction method. All measurements were made on a Rigaku AFC-5*R* diffractometer with graphite monochromatized Cu $K\alpha$ radiation. All calculations were performed using *CrystalStructure*[1] crystal structure analysis package.

One of the crystal structures was a monoclinic system (a=9.697(3)Å, b=5.231(2)Å, c=39.674(3)Å, β=91.75(1) , Z=4) with a space group $C2/c$. The structure was solved by direct methods with *SIR*92[2]. The non-H atoms were refined anisotropically. The H atoms were located from a difference Fourier map and the positional parameters were allowed to refine for the final refinements. The isotropic displacement parameters were set at $1.2U_{eq}$ of the parent atom. The $R(F^2>2\sigma(F^2))$ value was converged to 0.065 by the final refinement. In the molecular structure, the hydrocarbon skeleton included both terminal hydroxy groups had an all-*trans* conformation. The long axis of the molecule was inclined to the *ab* plane, and the molecules formed layers in a herring-bone arrangement, just as in the tilt-smectic phase of liquid crystals.

Another crystal structure was a monoclinic system (a=5.058(3)Å, b=7.219(4)Å, c=27.746(2)Å, β=93.47(2) , Z=2) with a space group $P2_1$. The structure was solved by direct methods with *SIR*92[2]. The non-H atoms were refined anisotropically. The methylene H atoms were located from a difference Fourier map, and were allowed to ride on the parent C atoms. The hydroxy H atoms were located from a difference Fourier map and the positional parameters were allowed to refine for the final refinements. All H-atom isotropic displacement parameters were set at $1.2U_{eq}$ of the parent atom. The $R(F^2>2\sigma(F^2))$ value was converged to 0.040 by the final refinement. In the molecular structure, one of the hydroxy groups adopted a *gauche* conformation with respect to the hydrocarbon skeleton, whereas the other adopted a *trans* conformation. The long axis of the molecule was normal to the *ab* plane, and the molecules formed layers which were similar to those of the smectic A liquid crystal. In this study, the crystal structures of icosane-1,20-diol are compared with those of other homologues, alkane-α,ω-diols. Moreover, we discuss a correlation between the polymorphism and the phase-transition phenomena in alkane-α,ω-diols.

References

1 Rigaku/MSC and Rigaku Corporation. (2001) *CrystalStructure Version* 3.10., Rigaku/MSC, 9009 New Trails Drive, The Woodlands, TX 77381, USA. Rigaku, 3-9-12 Akishima, Tokyo 196-8666, Japan.

2 Altomare, A., Cascarano, G., Giacovazzo, C., Guagliardi, A., Burla, M., Polidori, G. and Camalli, M. (1994) *J. Appl. Cryst.*, **27**, 435.

HYDROTHERMAL SYNTHESIS OF SINGLE-PHASE HYDROXYAPATITE WHISKERS AND CRYSTAL STRUCTURE CHARACTERISATION BY HRTEM AND IMAGE SIMULATION

Z.L. Dong and T.J.White

Centre for Advance Research of Ecomaterials, Institute of Environmental Science and Engineering, Innovation Centre, Blk 2, Unit 237, Nanyang Technological University, Singapore 637723 (zldong@ntu.edu.sg)

This study reports the crystallographic characterisation of synthetic hydroxyapatite (HA) whiskers suitable for both environmental (e.g. toxic metal capture) and biomedical (e.g. hard tissue replacement) applications. In both cases, an excellent understanding of HA crystal structure and microstructure is critical to ensure good chemical durability. In this study, hydroxyapatite whiskers were synthesised through soft chemical reaction followed by hydrothermal and heat treatments. Powder X-Ray diffraction (XRD) and high resolution transmission electron microscopy (HRTEM) confirmed that either HA or HA plus tricalcium phosphate (TCP) composite were obtained, depending on the treatment conditions. Pure HA crystallised after hydrothermal reaction at 200 C. Rietveld refinement was used to determine the hexagonal lattice parameters and atom positions of $P6_3/m$ HA. Microstructures were investigated by HRTEM (with cooling holder) and interpreted via multislice image simulation (with JEMS). Further study is needed to control the particle size, morphologies and HA/TCP ratios, which will subsequently influence the properties of fabricated HA coatings or bulk materials, as well as their capacity for heavy metal removal from waste effluents and *in vivo* longevity.

THE EFFECT OF MIXED Mn VALENCES ON Li MIGRATION IN $LiMn_2O_4$: MOLECULAR DYNAMICS SIMULATIONS

Kenji Tateishi, Douglas du Boulay, and Nobuo Ishizawa

Materials and Structures Laboratory, Tokyo Institute of Technology, 4259 Nagatsuta Midori Yokohama 226-8503, Japan (tateishi@r3401.msl.titech.ac.jp)

Lithium manganese spinels are attractive candidates for cathode materials of rechargeable lithium ion batteries and have been studied extensively. $LiMn_2O_4$ presents a first order structural phase transition at 290 K. Rodriquez-Carvajal et al [1] solved the structure at 230 K and concluded that the transition results from partial charge ordering on the Mn sites. Verhoeven et al [2] showed that lithium ions exist at both 8*a* and 16*c* interstices of the *Fd*-3*m* structure and that lithium exchange between those sites begins at around 285K and correlates with the Mn charge ordering. In our previous x-ray study, it was revealed that lithium and oxygen atoms are distributed statistically about their ideal positions at room temperature, an effect which we attributed primarily to mixed Mn valences.

Here, molecular dynamics simulations were undertaken to study the correlation between local structural disorder and lithium ion migration in stoichiometric $LiMn_2O_4$. The displacements of oxygen atoms from ideal positions were strongly governed by the arrangement of neighboring Mn^{3+} and Mn^{4+} valences. Consequently, changes of Mn valences with respect to time directly involve time-dependent LiO_4 tetrahedral distortions. Simulations were made assuming two distinct models: a) a model in which the arrangement of Mn valences do not change with respect to time and, b) a model in which the arrangement of Mn valences change in time keeping but preserving overall charge neutrality. In the model a), although lithium atoms occupy both 8*a* and 16*c* interstices, continuous lithium ion migrations were not observed. On the other hand using model b), continuous lithium migrations were observed. If we adopt the charge ordering viewpoint, then these results are quite consistent with Verhoeven's report because the lithium exchange commenced near the reported phase transition temperature. That is, we have strong evidence that lithium migration is indirectly associated with the hopping of 3*d* electron between Mn^{3+} and Mn^{4+} ions via the displacements of the coordinated oxygen atoms.

References

1 Rodriquez-Carvajal, J., et al (1998) *Physical Review Letters* **81**, 4660-4663.

2 Verhoeven, V. W. J., et al (2001) *Physical Review Letters* **86**, 4314-4317.

MECHANISM FOR PIEZOELECTRICITY OF LANGASITE CRYSTAL UNDER HIGH PRESSURE

N. Araki,[a] T. Iwataki,[a] K. Kakimoto,[a] H. Ohsato,[a] T. Kuribayashi,[b] Y. Kudoh,[b] and H. Morikoshi[c]

[a]Nagoya Institute of Technology, Nagoya, Japan; [b]Tohoku University, Sendai, Japan; [c]Materials Research Centre, TDK Co., Chiba, Japan
(araki@zymail.mse.nitech.ac.jp)

Langasite ($La_3Ga_5SiO_{14}$) is expected to be one of the new materials for surface acoustic wave (SAW) device, because of its excellent piezoelectric properties. Langsite belongs to trigonal system with space group *P*321 and lattice parameter of a_1=8.1674(4) and c=5.0964(8)Å. Figure 1 shows the crystal structure (a_1-c plane) of langasite. *A* site containing La^{3+} forms decahedron, *B* and *C* sites containing Ga^{3+} form octahedron and tetrahedron, respectively. *D* site containing Ga^{3+} and Si^{4+} with 1:1 ratio forms tetrahedron. We reported that the change in the piezoelectric properties of langasite by substitution of the cation shows a close relation to the crystal structure at atmospheric pressure [1].

In this work, we investigated the mechanism for piezoelectricity of langasite by single-crystal X-ray analysis under high pressure to confirm the mechanism proposed in the previous report.

Langasite crystal was prepared by the Czokralski method. The grown crystal was formed into sphere. Diffraction intensity data were collected with a four-circle diffractometer. Diamond anvil cell (DAC) was used under high pressure (3.3, 4.8 and 6.1GPa) measurement. Refinement of the crystal structure was performed by the full-matrix least-squares program RADY [2]. The difference of the crystal structure observed at atmospheric, 3.3 and 6.1 GPa were investigated.

The a_1-axis is preferentially shrunk compared to the c-axis and their change depended the applied pressure and followed liner functions. The cause of preferential shrinkage observed in a_1-axis is shrinkage of open space surrounded *A*, *B* and *C* sites under high pressure. The mechanism for piezoelectricity of langasite is explained, as follows. Under high pressure, *A* site is shrunk in the [100] direction accompanied with shrinkage of the open space. Polarization in *A* site was enhanced by applied pressure. This resulted in large piezoelectricity.

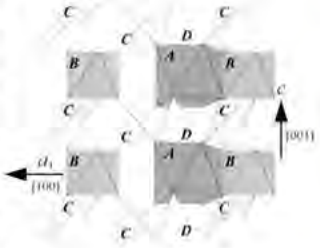

Fig. 1 Crystal structure of langasite (a_1-c plane)

References

1 Iwataki, T., Ohsato, H., Tanaka, K., Morikoshi, H., Sato, J., and Kawasaki, K. (2001) *Journal of the European Ceramic Society* **21**, 1409-1412.

2 Sasaki, S. (1982) *XL Report, ESS*, State University of New York, 1-17.

IMIDE-AMIDE BETWEEN KEMP'S ACID AND L-PROLINOL AND THE HYDROGEN BONDING

M. Kawaminami,[a] Y. Odo,[b] T. Shimo,[b] and K. Somekawa[b]

[a]Dept. of Physics, Faculty of Science; [b]Dept. of Applied Chemistry and Chemical Engineering, Faculty of Engineering, Kagoshima University, Korimoto, Kagoshima-shi 890-0065 Japan (kawamina@sci.kagoshima-u.ac.jp)

Kemp's acid imide and L-prolinols each has an interesting hydrogen bonding ability. The two molecules were combined to study chiral host-guest phenomena, and the hydrogen bonding in the new molecule, an imide-amide were characterized by X-ray crystallography. The synthesis is as follows.

The imide acid chloride (**1**) derived from Kemp's triacid was reacted with equimolar L-prolinol (**2**) in the presence of pyridine in CH_2Cl_2 to give the chiral imide-amide (**3**) (mp. 237-9°C) $[\alpha]_D$=-47.2°(MeCN) after recrystallization with MeCN.

X-ray crystal structure analysis of the compound has been determined using Enraf-Nonius CAD-4 diffractometer with Mo$K\alpha$ radiation. The compound crystallizes in tetragonal space group $P4_12_12$, with cell parameters a = 11.892Å, c = 23.749(1) Å, z = 8 and V = 3358.3Å^3, the calculated density is 1.28 g/cm^3. The structure was solved by direct methods (SIR) and refined with anisotropic thermal parameters using full-matrix least-squares using Molen for all non-hydrogen atoms to a final R-value of 0.051 for 1898 reflections at $Fo>3\sigma(Fo)$.

From the X-ray data one imide carbonyl seems to connect with the hydroxyl group in the L-prolinol moiety by a hydrogen bond to make the imide group asymmetric. The C=O···HO distance is 1.65Å.

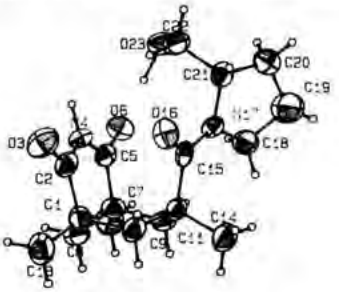

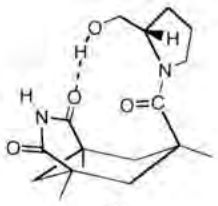

3

Reference

1 Bach et al. (2002) *J. Am. Chem. Soc.* **124**, 7982.

STRUCTURE ANALYSIS BEFORE AND AFTER ACCELERATED EXAMINATION FOR DETERIORATION OF BAM, BLUE PHOSPHOR

H. Imura,[a] T. Honma,[b] I. Hirosawa,[b] Y. Shimomura,[c,d] and N. Kijima[d]

[a]Center for Analytical Chemistry and Science, Inc., 1000 Kamoshida-cho, Aoba-ku Yokohama, 227-0033, Japan; [b]Japan Synchrotron Radiation Research Institute (JASRI), 1-1-1 Koto, Mikazuki-tyo, Sayo-gun, Hyogo, 679-5198, Japan; [c]Kasei Optonix, Ltd., 1060 Naruta Odawara, 250-0862, Japan; [d]Mitsubishi Chemical Corporation, 1000 Kamoshida-cho, Aoba-ku Yokohama, 227-8502, Japan. (imura.hiroyuki@mp.m-kagaku.co.jp).

Barium magnesium aluminate doped bivalent europium ions (Eu^{2+}), $BaMgAl_{10}O_{17}:Eu^{2+}$ (BAM) is known as one kinds of Blue Phosphor that is used in plasma display panel (PDP). The luminescence intensity derived from 5d-4f transition of activator ion (Eu^{2+}), however, was gradually underlying in repeated emission. The site-shift of activator ions from the Beevers-Ross(BR) site to the anti-Beevers-Ross(a-BR) site or to the mid-oxygen(m-O) site in intermediate plane[1], and the partial valence-changes of the activated ion (Eu^{2+}) to Eu^{3+}[2], were suggested as the reasons of deteriorated mechanism, but the mechanism has not been shown clearly yet. So, in order to observe the structural alternations in the deteriorated BAM, the accelerated examination for deterioration of BAM was carried out. X-ray diffraction patterns of the BAM were measured and the structures before and after the accelerated examination were analysed by Rietveld method and Maximum Entropy Method (MEM).

The specimen was prepared from a commercial standard BAM (KX-501A/Kasei Optonix, Ltd.). Accelerative examination was carried out under the following procedure: the capillary stuffed with BAM was exposed to white x-ray beam at SPring-8 BL28B2 for a day. X-ray diffraction data was measured at SPring-8 BL19B2 installed with Debye-Scherrer camera. The XRD pattern of **BAM-2** (After exposure) was compared carefully with that of **BAM-1** (Before exposure). The specific peak-shifts to higher-angle were observed, that is the position of the 00l peaks corresponding to c-axis was selectively shifted. The lattice parameters of **BAM-1** and **BAM-2** were refined (Table 1.), respectively. It was observed that the c-axis of **BAM-2** was shorter than the one of **BAM-1**.

Table 1. Lattice parameters of **BAM-1** and **BAM-2**

Specimens	*A*	*C*	V
BAM-1	5.630(0)	22.644(0)	621.62(1)
BAM-2	5.630(0)	22.628(0)	621.12(1)

In order to reveal the reason of the positional shifts of 00l peak, Rietveld analysis and MEM analysis were carried out. The increase of the electron density around a-BR and m-O sites was not observed in **BAM-2** as a result of MEM analysis. It means that Eu ions were mostly located on initial BR site after the accelerated examination. Furthermore it was observed that the atomic coordinates and the atomic displacement factors (temperature factor) of each element were slightly changed as a result of Rietveld Analysis. The relationship between the changes of lattice parameters and atomic parameters will be discussed in detail.

References

1 Carrillo-Cabrera, W., et al. (1986) *Solid State Ionics* **18&19**, 645.

2 Oshio, S., et al. (1998) *J. Electrochem. Soc.* **145**, 3903

CRYSTAL STRUCTURE OF A STREPTOCOCCAL SUPERANTIGEN, SPE-J

Heather M. Baker,[a] Vickery L. Arcus,[a] Thomas Proft,[b] Melissa Nicholson,[b] John D. Fraser,[b] and Edward N. Baker[a]

[a]School of Biological Sciences; [b]Department of Molecular Medicine, University of Auckland, Auckland, New Zealand (h.baker@auckland.ac.nz).

Superantigens (SAgs) are potent protein toxins that target the human immune system. The best known examples are those secreted by two significant human pathogens, *Staphylococcus aureus* and *Streptococcus pyogenes*, which are responsible for conditions that range from minor food poisoning to severe invasive disease. These SAgs disrupt the cellular immune response by simultaneously binding to both MHC class II molecules and T-cell receptors. More than 20 are known, characterised by a highly conserved fold but relatively weak sequence conservation and much allelic variation. Intriguingly, their modes of binding are surprisingly diverse [1]; some have two MHC-II binding sites, others only one, some form dimers that can cross-link MHC-II, and different sites on MHC-II can also be targeted.

SPE-J (streptococcal pyrogenic exotoxin J) was identified as a potential SAg from the *S. pyogenes* genome sequence, cloned, expressed and shown to have potent SAg activity. It appears to have only one binding site for MHC-II, binding to its β-chain in a zinc-dependent mode, yet it can also cross-link MHC-II [2]. Dynamic light scattering suggests it forms dimers, and this may explain its cross-linking activity.

Monoclinic crystals of SPE-J were obtained: C2, a=165.6, b=46.3, c=72.2 Å, β=90.6°, with two molecules of 209 residues each in the asymmetric unit. Although very tiny (maximum dimension 0.03 Å), these crystals gave a synchrotron data set to 1.7 Å resolution. The structure has been solved by molecular replacement, using the related SPE-C structure as search model, followed by model-building with wARP. Intriguingly, SPE-J appears to form quite a different dimer from that found for SPE-C [3], suggesting the likelihood of a different mode of MHC-II and TCR binding. Structure refinement is in progress, and the details of the structure and its implications for superantigen activity will be presented.

References

1 Arcus, V.L., Proft, T., Sigrell, J.A., Baker, H.M., Fraser, J.D. and Baker, E.N. (2000) *J. Mol. Biol.* **299**, 157-168.

2 Proft, T., Arcus, V.L., Handley, V., Baker, E.N. and Fraser, J.D. (2001) *J.Immunol.* **166**, 6711-6719.

3 Roussel, A., Anderson, B.F., Baker, H.M., Fraser, J.D. and Baker, E.N. (1997) Nature Struct. Biol. 4, 635-643.

STRUCTURAL GENOMICS OF MOUSE MACROPHAGE PROTEINS

Nathan Cowieson,[a] Pawel Listwan,[b] Christine Wells,[a] Thomas Huber,[c] Timothy Ravasi,[a] Anna Aagaard,[a] Bostjan Kobe,[b] David Hume[a] and Jenny Martin[a]

[a]IMB, University of Queensland, Brisbane, QLD, Australia; [b]Biochemistry and Molecular Biology, University of Queensland, Brisbane, QLD, Australia; [c]Advanced Computational Modelling Center, University of Queensland, Brisbane, QLD, Australia (n.cowieson@imb.uq.edu.au)

Microarray experiments conducted in the laboratory of David Hume (IMB, UQ) have identified large numbers of genes that are transcriptionally up-regulated when mouse macrophages are challenged with various antigens. The gene products of many of these are uncharacterised. In an attempt to functionally annotate these, several structural biology groups at the University of Queensland are collaborating in a structural genomics initiative.

By gradually implementing high throughput or automated techniques to time consuming steps in the structure determination process the group aims to solve the structures, by x-ray crystallography, of as many of these novel proteins as possible. In this poster I present preliminary results on a number of these structural genomics target proteins.

CRYSTALLOGRAPHIC STUDIES ON HEN SERUM TRANSFERRIN

Piyali Guha Thakurta, Debi Choudhury, Rakhi Dasgupta and J. K. Dattagupta

Crystallography and Molecular Biology Division,Saha Institute of Nuclear Physics, 1/AF Bidhanagar, Kolkata-700064, India (piyali@cmb2.saha.ernet.in)

Serum transferrin is the major iron-transport protein in vertebrates having molecular mass ~80 kDa. Its function depends on its ability to bind iron with very high affinity, yet to release this bound iron at the low intracellular pH. The three dimensional structure of diferric hen serum transferrin (hST) has been determined by X-ray crystallography at 2.8 Å resolution. The overall fold of the polypeptide chain of hST is similar to those of hen ovo transferrin (hOT), rabit serum transferrin (rST) and human lactoferrin (hLF), being delineated into two homologous lobes, each containing two dissimilar domains with one Fe^{3+} and one CO_3^{2-} ion bound at a specific site in each interdomain cleft. However, the relative orientations of the two lobes, which may be related to the class specificity of transferrins to recepters, is different in hST from that of hOT, rST and hLF. A number of additional hydrogen bonds between the two domains in the N- and C- lobes have been identified in this structure that might indicate a more compact structure of hST than that of hOT and hence may be correlated with its iron transport function. A pair of hydrogen bonded lysine residues, Lys209 and Lys301, close to the N-lobe iron binding site in the serum and ovo transferrins is termed as a "dilysine trigger". The NZ atoms of two lysine residues in hST are 2.45 Å apart which is comparable to other serum transferrins but is different from that of hOT. One carbohydrate binding site has been identified in the N- lobe at Asn52 of hST which is different from the carbohydrate binding site Asn473 of hOT present in the C- lobe. A fucose molecule has been modelled at this site. We also have a 3.45 Å diffraction data set of apo- form of hST, the $C\alpha$ chain trace of which has already been completed. The apo- and the holo- forms of chicken serum transferrins have been compared with each other as also with other proteins of the same family.

TOWARDS THE STRUCTURE OF THE GRB7-SH2 DOMAIN

Corrine J. Porter,[a] Peter J. Leedman,[b] Matthew C. J. Wilce,[a,c] and Jackie A. Wilce[a]

[a]School of Biomedical and Chemical Sciences, University of Western Australia, Nedlands, WA 6009, Australia; [b]Laboratory for Cancer Medicine, University Department of Medicine, Royal Perth Hospital, University of Western Australia, Perth, WA, 6000; [c]Department of Pharmacology, University of Western Australia, Crawley, WA, 6009. (cporter@chem.uwa.edu.au).

Growth factor receptor bound protein-7 (Grb7) is a member of a family of SH2 domain containing adaptor proteins. SH2 domains are present in a diverse group of proteins which are implicated in tyrosine kinase signalling. The SH2 domain of Grb7 binds to phosphorylated tyrosine residues located in the cytoplasmic domain of several growth factor receptors including the epidermal growth factor receptor (EGF-R). Grb7 is co-amplified with EGF-R in a number of human breast cancers. As it has been shown that breast tumours that overexpress EGF-R are generally estrogen-receptor negative and have a poor prognosis, the Grb7-EGF-R complex provides an attractive target for the development of novel therapeutics in the treatment of breast cancer.

The aim of this research is to structurally characterise the Grb7 SH2 domain. Milligram quantities of the Grb7 SH2 domain has been prepared and used in crystallisation trials. Small crystals have been produced which diffract to 3Å and we will present a preliminary analysis of this data.

DETAILED STRUCTURE OF L-METHIONINE γ–LYASE FROM PSEUDOMONAS PUTIDA BASED ON THE RESULT OF 1.8 Å RESOLUTION X-RAY CRYSTAL STRUCTURE DETERMINATION

Shintaro Misaki,[a] Tomoaki Takakura,[b] Takayuki Yoshioka,[c] Robert M Hofman,[d] Shigeo Yagi,[d] Kenji Inagaki,[e] and Akio Takimoto[b]

[a]Pharmaceutical Research & Development Division, SHIONOGI & CO., LTD. 12-4 Sagisu 5-chome, Fukushima-ku, Osaka 553-0002, Japan; [b]Discovery Research Laboratories, SHIONOGI & Co., LTD. 1-3, Kuise Terajima 2-chome, Amagasaki, Hyogo 660-0813, Japan; [c]Strategic Development Department, SHIONOGI & CO., LTD. 12-4 Sagisu 5-chome, Fukushima-ku, Osaka 553-0002, Japan; [d]AntiCancer Inc., 7917 Ostrow Street, San Diego, CA 92111, USA; [e]Department of Bioresources Chemistry, Faculty of Agriculture, Okayama University, Okayama, Okayama 700-8530, Japan (shintaro.misaki@shionogi.co.jp)

L-Methionine γ-lyase from *Pseudomonas putida* (MGLpp) has received much attention as an effective anti-tumor agent to various type of the cancer, such as lung cancer, colon cancer, kidney cancer and fibre sarcoma [1,2]. Therefore the application of MGLpp to the medicine has been desired. However, the stability of MGLpp in the plasma could be poor for its use of a protein-drug. To resolve this problem, Tan et al investigated the modification of this enzyme with polyethylene glycol [3]. In alternative idea, any site mutation using protein engineering would be useful. However, information about crystal structure of MGLpp, especially, regions concerned with stability, is few [4]. To increase the stability, information about N-terminal, C-terminal and active centre would be necessary. In this study, detailed structure, recognition and reaction mechanism of MGLpp would be discussed. Present R-value is 22.4 %. Geometries of the active site are obtained very clearly.

References

1 Yoshioka, T., Wada, T., Uchida, N., Maki, H., Yoshida, H., Ide, N., Kasai, H., Hojo, K., Shono, K., Maekawa, R., Yagi, S., Hoffman, R. M., and Sugita, K. (1998) Anticancer efficacy *in vivo* and *in vitro*, synergy with 5-fluorouracil, and safety of recombinant methioninase, *Cancer Res.* **58**, 2583-2587.

2 Tan, Y., Sun, X., Xu, M., Tan, X., Sasson, A., Rashidi, B., Han, Q., Tan, X., Wang, X., An, Z., Sun, F. X. and Hoffman, R. M. (1999) Efficacy of recombinant methioninase in combination with cisplatin on human colon tumors in nude mice, *Clin Cancer Res.* **5**, 2157-63.

3 Tan, Y., Sun, X., Xu, M., An, Z., Tan, X., Tan, X., Han, Q., Miljkovic, D. A., Yang, M. and Hoffman, R. M. (1998) Polyethylene glycol conjugation of recombinant methioninase for cancer therapy, *Protein Expression Purif.* **12**, 45-52.

4 Motoshima, H., Inagaki, K., Kumasaka, T., Furuichi, M., Inoue, H., Tamura, T., Esaki, N., Soda, K., Tanaka, N., Yamamoto, M. and Tanaka, H. (2000) Crystal structure of the pyridoxal 5'-phosphate dependent L-methionine γ-lyase from *Pseudomonas putida*, *J. Biochem.* **128**, 349-354.

THE EAFP CRYSTAL GROWTH OBSERVED BY ATOMIC FORCE MICROSCOPY

Sheng Wang,[a,b] Ye Xiang,[b] Genpei Li,[b] and Dacheng Wang[b]

[a]Bioengineering Institute of Chongqing University, Chongqing, 400044, P.R. China; [b]Institute of Biophysics and National Microgravity Lab., CAS, 100101, P.R. China (wtscrystal@sina.com)

Eucommia antifungal protein(EAFP) is one kind of antifungal protein[1]. EAFP has 41 residues and crystals of EAFP belong to space group $P2_1$ with unit-cell parameters a=19.085, b=23.225, c=30.854, β=98.64 [2]. EAFP crystals grew in only 4-5 hours much faster than most of other macromolecular crystals. It is noteworthy that the EAFP crystals diffract to almost the limiting resolution (~0.8 Å). The 3D structure was determined by direct methods with SnB[3,4] and refined with Shelx-97 [5].

The EAFP crystals were grown according to the method of Mr. Xiang[2]. The target crystals grown directly on a glass cover glass were moved onto the AFM sample stage for the acquisition of AFM images. All the AFM images were collected on the {100} faces of the EAFP crystals in a fluid cell filled with mother liquor by both the contact and non-contact modes.

Nucleation and dynamic growth were studied by *in situ* Atomic Force Microscopy (Autoprobe CP-Research, Park Scientific Instruments). We found that EAFP had special aggregates, ring-shaped clusters in original solution. The diameter varied from about 180nm to 350nm. During AFM experiments we also found that many linear aggregates sedimented on the surface of EAFP and then incorporated into the lattice of the crystals. So the ring-shaped aggregates might be split by precipitator and absorbed on the surface directly or be connected with each other into longer linear aggregates.

At higher supersaturation we found that the EAFP crystals grew very fast with macro steps by two-dimensional nucleation. The growing steps developed by groups which consisted of about 5-6 steps. The step height was about 1.9 nm corresponding well with the length of one axis. At low-to-moderate supersaturation, one type of apparently anisotropic single-double-like spiral dislocations was found on the {100} faces of EAFP crystals. After 8-9 screw steps all of them would automatically grow into a series of whole intact elliptic layers. Thus we concluded that during the process of growth EAFP molecules had strong ability to adjust themselves to fit the lattice which perhaps was related to the special character of EAFP molecules.

This work intended to understand the nucleation of EAFP crystal growth and kinetic mechanisms. This will help and maybe guide us to choose crystal conditions for obtaining good quality crystals to give higher diffraction ability, and shed light on our knowledge concerning protein crystallization.

References

1 Huang, R.-H., Xiang, Y., Liu, X.-Zh., et al. (2002) *FEBS Letters*, 521: 87-90.
2 Xiang, Y., Huang, R.-H., Liu W., et al. (2002) *Acta Cryst.D58*, 1838-1840.
3 Weeks, C.M. & Miller, R. (1999) *J. Appl. Cryst.* 32, 120-124.
4 Blessing, R.H., & Smith, G.D. (1999) *J. Appl. Cryst.* 32, 664-670.
5 Sheldrick, G.M.(1997)*SHELX97*, University of Göttingen, Germany.

CRYSTAL STRUCTURE OF ESCHERICHIA COLI ATASE N-TERMINAL DOMAIN

Yibin Xu,[a] Rongguang Zhang,[b] Paul D. Carr,[c] David L. Ollis,[c] and Subhash G.Vasudevan[a,d]

[a]Department of Biochemistry & Molecular Biology, James Cook University, Townsville, QLD 4811; [b]Structural Biology Centre, Argonne National Laboratory, USA; [c]Research School of Chemistry, Australian National Univeristy, Canberra, ACT 2601; [d]Present address: Novartis Institute for Tropical Diseases, 1 Science Park Road, #04-14 The Capricorn, Singapore (yibin.xu@jcu.edu.au)

E.coli glutamine synthetase adenylyltransferase (ATase, EC 2.7.7.42) catalyses the adenylylation and deadenylylation of glutamine synthetase (GS). The two activities of ATase are mechanistically distinct, but are functionally the reverse of one another and must be carefully controlled by the organism in order to prevent futile cycling. Growth will occur in a low ammonia environment if GS is active with the deadenylylation activity of ATase switched on and the adenylylation activity switched off. Conversely, in a high ammonia environment, GS activity can be tuned down progressively by adenylylation until it is completely switched off when all 12 subunits are converted to the inactive GS-AMP form. It has been shown that two activities of ATase reside on separate domains. AT-N consisted of residues 1 through to 423 and was found to have the deadenylylation activity but only partially soluble [1]. However ATN440 (residues 1 to 440) is soluble and here we report the purification, crystallization and 3D structure determination of AT-N 440.

The crystals of ATN-440 belong to space group $P3_221$ with a=b= 116.6 Å, c=67.6 Å, $\alpha=\beta=90°$ and $\gamma=120°$. Its crystal structure has been determined by the MAD method and refined up to a resolution of 2.0 Å. The structure reveals a conserved protein motif present also in kanamycin nucleotidylyltransferase and human DNA polymerase β.

References

1 Jaggi, R., van Heeswijk, W. C., Westerhoff, H.V., Ollis, D.L. and Vasudevan, S.G. (1997). *EMBOJ* **16**, 5562-5571.

1.7Å AND 2.1Å X-RAY STRUCTURES OF HEMOGLOBIN E AND HEMOGLOBIN A_2, ISOLATED FROM THE BLOOD SAMPLES OF β-THALASSEMIC PATIENTS

J. K. Dattagupta, Udayaditya Sen, Debi Choudhury and Jhimli Dasgupta

Crystallography and Molecular Biology Division, Saha Institute of Nuclear Physics, 1/AF Bidhan Nagar, Kolkata 700 064, India
(jiban@cmb2.saha.ernet.in)

Hemoglobin A_2 ($\alpha_2\delta_2$), a minor (2-3%) component of circulating red blood cells, acts as an anti-sickling agent [1] and its elevated concentration in β-thalassemia is a useful clinical diagnostic. In β-thalassemia major, where there is a failure of β-chain production, HbA_2 acts as the predominant oxygen deliverer. Hemoglobin E, another common abnormal hemoglobin caused by splice site mutation in exon 1 of β globin gene, when combined with β-thalassemia causes severe microcytic anemia. The purification, crystallization and the structural studies of HbA_2 and HbE are reported here. HbA_2 and HbE are purified by cation exchange column chromatography in presence of KCN from the blood samples of individuals suffering from β-thalassemia minor and Eβ-thalassemia. X-ray diffraction data of HbA_2 and HbE were collected upto 2.1Å and 1.73Å respectively. HbA_2 crystallized in space group $P2_1$ with unit cell parameters a=54.33Å, b=83.73Å, c=62.87Å, β=99.80 whereas HbE crystallized in space group $P2_12_12_1$ with unit cell parameters a=60.89Å, b=95.81Å, c=99.08Å [2]. Asymmetric unit in each case contains one Hb tetramer in R_2 state. The structure of HbA_2 and HbE were refined to an R factor of 18.3% (R_{free} 21.9%; PDB CODE 1NX5) and 19.1% (R_{free} 21.1%; PDB CODE 1NQP) respectively.

References

1 Nagel, R. L., Bookchin, R. M., Johnson, J., Labie, D., Wajcman, H., Isaac-Sodeye, W. A., Honig, G. R., Schiliro, G., Crookston, J. H., Matsutomo, K. (1979) *Proc. Natl. Acad. Sci.* **76(2),** 670-672.

2 Dasgupta, J., Sen, U., Choudhury, D., Datta, P., Chakrabarti, A., Basu Chakrabarty, S., Chakrabarty, A. and Dattagupta, J. K. (2003) *Biochem Biophys Res Commun.* **303,** 619-623.

STRUCTURAL AND KINETIC IMPLICATIONS OF SUBSTRATE INHIBITION IN THE HUMAN SULFOTRANSFERASE 1A1 ENZYME

Niranjali U. Gamage,[a,c] Ronald G.Duggleby,[b] Amanda C. Barnett,[a] Michael Tresillian,[a] Catherine F. Latham,[a,c] Nancy E. Liyou,[a] Michael E. McManus,[a] and Jennifer L. Martin[c]

[a]Department of Physiology and Pharmacology, School of Biomedical Sciences, University of Queensland, Brisbane, Queensland, 4072, Australia; [b]Department of Biochemistry and Molecular Biology, School of Molecular and Microbial Sciences, University of Queensland, Brisbane, Queensland, 4072, Australia; [c]Institute for Molecular Bioscience, University of Queensland, Brisbane, Queensland, 4072, Australia (n.gamage1@mailbox.uq.edu.au)

Sulfonation catalyzed by sulfotransferases is an important pathway in detoxification of a broad range of endobiotics and xenobotics, but evidence has emerged in recent years that sulfonation can lead to bioactivation of carcinogens. A major human sulfotransferase, SULT1A1, has been shown to play a significant role in metabolizing many endogenous compounds and is implicated in a range of cancers due to its ability to bioactivate carcinogenic and mutagenic xenobiotic compounds. The crystal structure that we report here is that of SULT1A1 complexed with PAP and the xenobiotic substrate p-nitrophenol (pNP) [1]. This is the first sulfotransferase structure complexed with a xenobiotic substrate and unexpectedly it reveals two molecules of pNP in the active site. The kinetics of SULT1A1with pNP shows slight non-hyperbolic behaviour at low concentrations and substrate inhibition at higher pNP concentrations. These kinetic features are fully consistent with the SULT1A1 structure. The extended active site of SULT1A1 revealed by the crystal structure is also in agreement with binding of the endogenous ligand di-iodothyronine but it cannot accommodate its other substrate β-estradiol as easily. This therefore suggests that the binding site is flexible to accept diverse hydrophobic molecules of varying sizes and shapes. Therefore, the SULT1A1 structure provides the structural basis for substrate inhibition and reveals the first clues as to how this enzyme sulfonates various liphophlic compounds.

References

1 Gamage NU, Duggleby RG, Barnett AC, Tresillian M, Latham CF, Liyou NE, McManus ME, Martin J (2003). Structure of a human carcinogen converting enzyme, SULT1A1: structural and kinetic implications of substrate inhibition. *J Biol Chem.* **278**, 7655-7662.

SERA PROTEINS: ARE THEY CYSTEINE OR SERINE PROTEASES?

Robyn L. Malby,[a] Anthony N. Hodder,[a] Vidana C. Epa,[b] and Brendan S. Crabb[a]

[a]Walter and Eliza Hall Institute of Medical Research, Melbourne VIC 3050, Australia; [b]CSIRO Division of Health Sciences and Nutrition, Parkville VIC 3052, Australia (rmalby@wehi.edu.au)

The serine repeat antigen (SERA) of *Plasmodium* is a candidate for inclusion in a malaria vaccine. The full-length protein of ~120 kDa is processed into several smaller fragments, one of which (P50) has significant homology to the papain-like cysteine proteases [1, 2]. Various members of the SERA family exhibit intriguing differences in putative enzyme active site residues; for example, the dominantly expressed member of the *P. falciparum* gene family, SERA-5, has serine substituted for the active site cysteine. A three-dimensional model of the enzyme domain of SERA-5 has been constructed [3], by comparison with crystal structures of several cysteine proteases.

The enzyme domain of SERA-5 was produced as a recombinant protein in *E. coli*, and purified by affinity and ion exchange chromatography. Small crystals (*ca.* 80 μm × 40 μm × 20 μm) were grown, and were found to diffract to ~3Å. Diffraction data were collected [4] from a single cryo-cooled crystal on a Rigaku R-AXIS IV image plate detector, using a Rigaku RU-300 generator equipped with monocapillary optics [5]. We are currently attempting to solve the crystal structure by molecular replacement, with the SERA-5 model and related crystal structures as search models. We are also continuing to investigate both site-directed mutagenesis and altered crystallization conditions with the aim of optimizing crystal growth.

References

1 Eakin, A.E., Higaki, J.N., McKerrow, J.H. and Craik, C.S. (1989) *Nature* **342**, 132.
2 Higgins, D.G., McConnell, D.J. and Sharp, P.M. (1989) *Nature* **340**, 604.
3 Hodder, A.N. *et al.*, manuscript in preparation.
4 We thank Bert van Donkelaar (CSIRO Division of Health Sciences and Nutrition) for assistance with data collection.
5 Balaic, D.X., Barnea, Z., Nugent, K.A., Garrett, R.F., Varghese, J.N. and Wilkins, S.W. (1996) *J. Synchrotron Rad.* **3**, 289-295.

STRUCTURAL FEATURES OF MORACEAE LECTINS

K. Sekar,[a] J.V.Pratap,[b] A.A. Jeyaprakash,[b] A. Surolia,[b] and M. Vijayan[b]

[a]Bioinformatics Centre and Supercomputer Education and Research Centre; [b]Molecular Biophysics Unit, Indian Institute of Science, Bangalore 560 012, India (sekar@physics.iisc.ernet.in)

Lectins are carbohydrate-binding proteins, which mediate various biological processes. The β-prism fold was first discovered in the galactose specific lectin jacalin from jackfruit seeds. Structural studies on the lectin, carried out in this laboratory, also established post translational modification as a strategy for generating carbohydrate specificity. The homologous artocarpin, a second lectin from jackfruit seeds, also assumes a β-prism fold. The absence of post translational modification and the replacement of aromatic residues in the binding site, make it mannose specific. Similar structures determined in other laboratories include *Maclura fomifera* agglutinin (MPA), *Helianthus tuberosus* lectin (heltuba), domain II of δ-endotoxin and the vittelline membrane outer layer protein. These structures among them, define the structural features of the β-prism fold as indeed those of *Moraceae* lectins. Among the proteins of the structural family, the structures belonging to the lectin family (jacalin, MPA and heltuba) have much more similarity amongst themselves than those belonging to other types of proteins. In addition, among the lectins, the similarity is higher with the *Moraceae* family (with jacalin and MPA), even when their carbohydrate specificities are different. The details will be presented.

THE CRYSTAL STRUCTURE OF A NOVEL CALCIUM BINDING PROTEIN ATCBL2 FROM ARABIDOPSIS THALIANA

Masamichi Nagae,[a] Akira Nozawa,[b] Nozomu Koizumi,[b] Hiroshi Sano,[b] Mamoru Sato,[a] and Toshiyuki Shimizu[b]

[a]Graduate School of Integrated Science, Yokohama City University, 1-7-29 Suehiro-cho, Tsurumi-ku, Yokoham, Kanagawa, Japan; [b]Laboratory of Plant Molecular Breeding, Research and Education Center for Genetic Information, Nara Institute of Science and Technology, Ikoma, Nara, Japan (nagae@tsurumi.yokohama-cu.ac.jp).

AtCBL2 is a member of a new family of calcineurin B-like calcium binding proteins that has recently been identified in *Arabidopsis thaliana*. These proteins have been shown to interact with novel family of serine-threonine protein kinases (AtCIPKs) in a calcium dependent manner. The signal pathway of AtCBL/AtCIPK plays critical roles in stress response such as salt, drought, light. Despite the great importance of intracellular signaling pathways in plants, no structural information has been obtained for AtCBL/AtCIPK system. Here, we report the crystal structure of AtCBL2 and propose a unique target recognition mecanizm of AtCBL/AtCIPK. Crystal of calcium bound AtCBL2 was obtained in space group $C222_1$ with unit-cell parameters a=83.9 Å, b=118.1 Å, c=49.1 Å. Using a synchrotron-radiation source, the crystal diffracts to 2.1 Å, with an overall R_{merge} of 6.0 % and a completeness of 98.8 %. One independent molecule was estimated to be present in the asymmetric unit, with a solvent content of 48 %. Phase to 2.5 Å was determined by conventional multiple isomorphous replacement with anomalous scattering method (MIRAS). The final model refined to an R value of 20.4 % and free R value of 24.8 % at 2.1 Å resolution. The three-dimensional structure of AtCBL2 reveals a compact _-helical structure with two pairs of EF-hands and the overall fold resembles that of calcineurin B and neuronal calcium sensor 1, but significant structural differences are observed. The first and fourth EF-hands differ from the canonical sequence, but calcium ions are coordinated in the EF-hand. The rest of the EF-hands are maintained in the open form by internal hydrogen bonds despite lacking calcium ions. A possible site for the target binding based on the three-dimensional structure is discussed.

EXPRESSION, PURIFICATION AND CRYSTALLIZATION OF DEUTERATED PROTEINS FOR NEUTRON DIFFRACTION

Kyoko Suto,[a] Noritake Yasuoka,[b] Masaya Kitamura,[c] and Hiroshi Mizuno[a]

[a]National Institute of Agrobiological Sciences, Tsukuba, Ibaraki 305-8602, Japan; [b]Faculty of Science, Himeji Institute of Technology, Hyogo, 678-1297, Japan; [c]Faculty of Engineering, Osaka City University, Osaka 558-8585, Japan (ksuto@affrc.go.jp)

In cases of most proteins, it is not easy to obtain crystals larger than $2mm^3$ necessary for neutron diffraction measurement. Instead of preparation of such large crystals, we tried to prepare and crystallize deuterated proteins. Replacement of hydrogen atoms by deuterium atoms reduces the background noise and increases the scattering power in neutron diffraction. In this case, such large crystals may not be required. We'll show expression, deuteration and crystallization FMN-binding protein (FMN-bp) using *E. Coli* system.

FMN-bp from *Desulfovibrio vulgaris* Miyazaki F is composed of 122 amino acids and a FMN, which is the smallest among known flavoproteins[1]. The function of FMN-bp *in vivo* is unclear at present, however it might take part in the electron-transfer pathway. Structural studies have been already carried out by X-ray crystallography[2].

Crystals of FMN-bp were grown to 2mm x 0.5mm x 0.7mm and diffracted up to 0.84 Å resolution at 100K, and to 1.10 Å at room temperature using X-ray. In the density maps, assignments of the atom species have been easily carried out, judging from the peak height in electron density map. The O, N, C atoms were identified even at side chain of aspartic acid and / or threonine. Some peaks in the difference Fourier map could be assigned for hydrogen atoms when they were involved in the hydrogen bonding, but plurality of hydrogen atoms bonding to oxygen atoms could not be clearly assigned. It was difficult to find hydrogen atoms particularly bonding to electronegative atoms or high temperature factor atoms[3]. Neutron crystallography may provide to determine above hydrogen atoms positions. Deuteration of FMN-bp was carried out using E. Coli-OD2 D medium made by Silantes. Hi level expression system suitable to the medium was prepared using pET-20b(+) vector with *E. Coli* strain BL21(DE3). The deuterated FMN-bp expressed without any tags and purified by ion-exchange column and gel filtration. Purified 5mg holo FMN-bp and 3mg apo FMN-bp were obtained from 1L medium. The molecular weights of deuterated FMN-bp and non-labeled FMN-bp were measured by TOFF-MASS spectrum and deuterium ratio was estimated to 73%. Firstly crystallization of the deuterated FMN-bp was tried with conditions similar to the case of non-labeled FMN-bp. Although some crystals appeared, good crystals could not be obtained. When suitable crystallization condition was dramatically changed, the unit cell of the crystal changed from non-labeled FMN-bp. The crystals obtained in D_2O solution grew up to 1mm x 0.5mm x 0.3mm. The X-ray diffraction data was measured up to 1.35Å resolution. Preparation of larger size of crystals is now in progress for neutron diffraction study.

References

1 Kitamura, M., et al. (1994) *J. Biol. Chem.* **269**, 5566-5573.
2 Suto, K., et al. (2000) *Acta Crystallogr.*, **D56**, 368-371
3 Suto, K., et al. (2001) *J. Phys. Soc. Jpn.*, **70**, Supplement A, 406-407

CRYSTAL STRUCTURE OF FLINC4, AN INTRAMOLECULAR LMO4:LDB1 COMPLEX

Janet E. Deane, Megan Maher, J. Mitchell Guss, and Jacqueline M. Matthews

School of Molecular and Microbial Biosciences, University of Sydney, NSW 2006, Australia (J.Deane@mmb.usyd.edu.au)

LMO4 is a member of a small family of nuclear transcriptional regulators that is important for both normal development and disease processes. The LMO family comprises four members, LMO1–4 of which two, LMO1 and LMO2, are known oncogenes. LMO4 was originally identified as a breast cancer autoantigen [1] and has recently been shown to be overexpressed in over 50% of primary breast cancers [2]. LMO4 is comprised primarily of two tandemly repeated LIM domains. These domains each contain two structural zinc ions and have been identified as important motifs that mediate specific protein:protein interactions. In particular, LMO4 has been shown to interact directly and simultaneously with BRCA1, CtIP and the ubiquitous nuclear adaptor protein LIM domain binding protein 1 (ldb1) to form a stable complex *in vivo* [3]. LMO4 interacts with ldb1 via a 39-residue region towards the C-terminus known as the LIM interaction domain (LID). Ldb1 is of particular interest as it binds LMOs and related LIM homeodomain (LHX) proteins with high affinity, and contains an N-terminal homodimerization domain that may allow the formation of higher order functional complexes [4].

An intramolecular complex consisting of the two LIM domains from LMO4 linked to the LID domain of ldb1 has been engineered; FLINC4 (fusion of the LID domain of ldb1 and the N- and C-terminal LIM domains of LMO4). FLINC4 was purified and crystals belonging to space group $P312$ with unit-cell parameters a = 61.3 Å and c = 93.2 Å were grown. There is one molecule of FLINC4 per asymmetric unit (ASU). Native and multiple-wavelength anomalous dispersion (MAD) data at the zinc edge have been recorded to resolutions of 1.3 Å and 1.7 Å, respectively. Anomalous Patterson maps calculated from data collected at the peak wavelength and showed strong peaks sufficient to determine the positions of the four zinc atoms per ASU. Initial phases calculated to a resolution of 1.7 Å allowed 154 out of 188 residues of FLINC4 to be traced. Refinement of this structure to 1.3 Å resolution is underway with current values of R = 20.4 % and R_{free} = 23.8 %. Analysis of the structure of FLINC4 suggests a mechanism by which ldb1 can bind LMO4 specifically, and LIM domains from LMO and LHX proteins in general. Important residues at the interaction interface have been identified and may help in the design of specific inhibitors of this interaction as potential treatments for some forms of breast cancer.

References

1 Racevskis, J., Dill, A., Sparano, J.A. and Ruan, H. (1999) *Biochim. Biophys. Acta*, **1445**, 148-53.

2 Visvader, J.E., Venter, D., Hahm, K., Santamaria, M., Sum, E.Y., O'Reilly, L., White, D., Williams, R., Armes, J. and Lindeman, G.J. (2001) *Proc. Natl Acad. Sci. USA*, **98**, 14452-7.

3 Sum, E.Y., Peng, B., Yu, X., Chen, J., Byrne, J., Lindeman, G.J. and Visvader, J.E. (2002) *J. Biol. Chem.*, **277**, 7849-7856.

4 Jurata, L.W., Kenny, D.A. and Gill, G.N. (1996) *Proc. Natl Acad. Sci. USA*, **93**, 11693-8.

CATCHING CATALYSIS IN THE ACT: USING SINGLE CRYSTAL KINETICS TO TRAP METHYLAMINE DEHYDROGENASE REACTION INTERMEDIATES FOR STRUCTURAL STUDIES.

Arwen R. Pearson, Teresa De la Mora Rey, Kevin T. Watts, Ed Hoeffner, and Carrie M. Wilmot

University of Minnesota, Department of Biochemistry, Molecular Biology & Biophysics, Minneapolis, MN 55455, U.S.A. (pears079@umn.edu)

Methylamine dehydrogenase (MADH) is an $\alpha_2\beta_2$ heterotetramer containing a novel quinone cofactor, TTQ, derived from two modified tryptophan residues. It is expressed in response to methylamine, allowing certain bacteria to utilise methylamine as their sole carbon source. MADH catalyses the conversion of methylamine to formaldehyde and ammonia, leaving the TTQ cofactor in a 2e- reduced state. To complete the catalytic cycle, MADH is reoxidised via two successive electron transfer (ET) events.

In the case of the *Paracoccus denitrificans* enzyme (PD-MADH) the physiologic ET chain involves the protein redox partners amicyanin (a blue-copper protein) and cytochrome *c*551i. Stable binary (PD-MADH/amicyanin) and ternary (PD-MADH/amicyanin/cytochrome *c*551i) catalytically competent complexes can be formed and crystallized, and their structures have been solved to better than 2.0Å resolution in the laboratory of F. Scott Mathews (Washington University Medical School, St. Louis).

MADH (TTQ), amicyanin (Cu) and cytochrome *c*551i (Fe) have spectral features in the visible region that change during catalytic turnover, thus defining spectrally distinct intermediates that reflect the electron distribution in the complex.

Through a novel combination of single crystal visible microspectrophotometry, X-ray crystallography and freeze trapping, reaction intermediates of MADH in complex with the physiological redox partners in the crystalline state have been trapped.

This poster will present the methods used to monitor and trap reaction intermediates in the crystalline state, as well as some preliminary X-ray structural data.

AURACYANIN B STRUCTURE IN SPACE GROUP $P6_5$

Mihwa Lee,[a] Megan J. Maher,[a] Robert E. Blankenship,[b] Hans C. Freeman,[a] and J. Mitchell Guss[a]

[a]School of Molecular and Microbial Biosciences, University of Sydney, NSW 2006, Australia; [b]Department of Chemistry and Biochemistry, Arizona State University, Tempe, Arizona 85287-1604, USA (m.lee@mmb.usyd.edu.au)

Auracyanin B is one of two similar blue copper proteins produced by the thermophilic green photosynthetic bacterium *Chloroflexus aurantiacus* [1]. It is likely to be involved in photosynthetic electron transfer in this organism. The structure of auracyanin B has previously been solved and refined in the hexagonal space group $P6_422$ with a single molecule in the asymmetric unit (unit cell parameters $a = b = 115.7$, $c = 54.5$ Å) [2].

The protein has now been crystallized in a new crystal form, $P6_5$ with unit cell parameters, $a = b = 115.9$, $c = 108.2$ Å. In the new crystal form the asymmetric unit contains four protein molecules. The structure has been solved by molecular replacement and refined at 1.9 Å resolution. In relation to the earlier crystal structure, the c-axis of unit cell is doubled and the number of molecules is increased from one to four. The main-chain structure of auracyanin B in $P6_5$ is very similar to that in $P6_422$ but some residues including those involved in the crystal contacts have slightly different side chain conformations. The other interesting feature of this structure in $P6_5$ is that the operation which relates two pairs of molecules in the asymmetric unit is very close to a formal crystallographic two-fold axis, which could yield space group $P6_522$. Yet the structure could be refined only in the lower symmetry space group $P6_5$. The final residuals are $R = 19.2\%$ and $R_{free} = 22.0\%$.

References

1 McManus, J. D., Brune, D. C., Han, J., Sanders-Loehr, J., Meyer, T. E., Cusanovich, M. A., Tollin, G., and Blankenship, R. E. (1992) *J. Biol. Chem.* **267**, 6531-40.

2 Bond, C. S., Blankenship, R. E., Freeman, H. C., Guss, J. M., Maher, M. J., Selvaraj, F. M., Wilce, M. C. J., and Willingham, K. M. (2001) *J. Mol. Biol.* **306**, 47-67.

THE STRUCTURE OF THE LYSYL OXIDASE FROM PICHIA PASTORIS - A COPPER-CONTAINING AMINE OXIDASE THAT CAN OXIDISE LYSINE-CONTAINING PEPTIDES

Anthony P. Duff,[a] Paul J. Ellis,[b] Aina E. Cohen,[b] Jason A. Kuchar,[c] David Langley,[a] David M. Dooley,[c] Hans C. Freeman,[a] and J. Mitchell Guss[a]

[a]School of Molecular and Microbial Biosciences, The University of Sydney, Sydney Australia; [b]The Stanford Synchrotron Research Laboratory, Menlo Park, California, USA; [c]Department of Chemistry & Biochemistry, Montana State University, Bozeman, Montana, USA (A.Duff@usyd.edu.au)

We have determined the structure of the lysyl oxidase from *Pichia pastoris* (PPLO) at 1.65Å resolution with R=16.0% and R_{Free}=18.7%. Crystals belong to space group *C*2, with *a*=249Å *b*=120Å *c*=152Å and β=125° [1]. The asymmetric unit contains two dimers, thus providing four-fold non-crystallographic symmetry. The structure was solved by molecular replacement, despite the search model having only a 25% identity match to 66% of the sequence.

PPLO is a copper amine oxidase (CuAO) [2]. CuAOs catalyse the oxidative deamination of a primary amine to produce an aldehyde, ammonia and hydrogen peroxide ($R\text{-}CH_2\text{-}NH_2 + O_2 + H_2O \rightarrow R\text{-}CHO + NH_3 + HOOH$). They contain Cu(II) and utilise a side chain derived cofactor that is autocatalytically generated in the presence of Cu(II) and O_2.

PPLO is the fifth CuAO to be structurally characterised, after the CuAOs from the bacteria *Escherichia coli* and *Arthrobacter globiformis*, the yeast *Hansenula polymorpha*, and a higher plant *Pisum sativum*. It is like the previous four in overall architecture, but has some substantially different features consistent with its unique ability to oxidise the side chains of lysine residues in peptides - the initial step in the reactions for the cross-linking of collagen and elastin. This functional activity (*in vitro*) relates PPLO to another class of CuAOs, having a different size, sequence and cofactor, known as the lysyl oxidases. No bona fide lysyl oxidases have been structurally characterised to date.

The structure of PPLO explains its unusual substrate specificity. Other CuAOs can oxidase only small organic amines, such as methylamine or benzylamine, but are unable to oxidise lysyl peptides since they have buried active sites and narrow substrate channels. PPLO on the other hand has a broad open funnel leading from the solvent to the active-site cofactor. We have modelled putative peptide substrates into this site.

A solvent lake lies between the otherwise tightly associated subunits in the dimers. This lake is larger in PPLO and borders the ligands of the active site copper ion. This supports the proposal that the smaller reactants and products (O_2, H_2O, NH_3, HOOH and H^+) may enter or leave the active site via this lake.

References

1 Lee M, Willingham K, Langley D, Maher MJ, Cohen AE, Ellis PJ, Kuchar JA, Dooley DM, Freeman HC, Guss JM. (2002) *Acta Crystallogr D.* **58,** 2177-9 "Crystallization of *Pichia pastoris* lysyl oxidase"

2 Dove JE, Smith AJ, Kuchar J, Brown DE, Dooley DM, Klinman JP.(1996) *FEBS Lett.* **398**, 231-4. "Identification of the quinone cofactor in a lysyl oxidase from *Pichia pastoris*"

INSECT CELL EXPRESSION OF A PLANT DISEASE RESISTANCE PROTEIN Cf-9 FOR STRUCTURAL STUDIES

T. Teh,[a] S. Lang,[b] D. A. Jones,[b] and B. Kobe [a]

[a]Department of Biochemistry and Molecular Biology, University of Queensland, St. Lucia, Qld 4072, Australia; [b]Plant Cell Biology, Research School of Biological Sciences, Australian National University, Canberra, ACT 2601, Australia (t.teh@mailbox.uq.edu.au).

Plants have evolved specific mechanisms to recognise individual pathogens and activate defence systems. The induction of plant defence responses, which often include a hypersensitive response leading to rapid localised cell death at the site of infection, requires the interaction of a plant-derived resistance protein (R protein) with a specific pathogen-derived avirulence protein (Avr protein) [1]. The molecular and structural basis of the recognition events involving most R and Avr protein combinations remains unknown. It has been postulated that R proteins are receptors for Avr components [2,3] and that R and Avr proteins participate in a complex with other proteins to initiate signal transmission and activate host defence responses [4,5].

One well established model in which to study molecular aspects of host resistance and pathogen avirulence is that of the tomato Cf-9 protein which confers resistance to the leaf mould fungus *Cladosporium fulvum* through recognition of the fungus encoded Avr9 peptide [6]. Cf-9 is a mainly extracytoplasmic membrane-anchored glycoprotein, composed predominantly of leucine rich repeats (LRRs). LRRs are sequence motifs present in a variety of proteins involved in protein-protein interactions, including many plant R proteins; however, their role in disease resistance is unknown. In an effort to provide the first structural view of a plant R protein and to extend the present knowledge of the molecular basis of plant disease resistance, the Cf-9 protein is being expressed in insect cells. Through optimisation of expression conditions, it is hoped to produce adequate quantities of protein for crystallisation trials.

References

1 Flor, H. (1971) *Annu. Rev.Phytopthol.* **9,** 275-296.
2 Staskawicz, B.J., Ausubel, F.M., Baker, B.J., Ellis, J.G., and Jones, J.D.G. (1995) *Science* **268,** 661-667.
3 Ellis, J., Dodds, P. and Pryor, T. (2000) *Curr. Opin.Plant Biol* **3,** 278-284.
4 Dixon, M.S., Golstein, C., Thomas, C.M., van Der Biezen, E.A., and Jones, J.D.G. (2000) *Proc. Natl. Acad. Sci. USA* **97,** 8807-8814.
5 Dangl, J.L., and Jones, J.D.G. (2001) *Nature* **411,** 826-833.
6 Joosten, M.H.A.J., and De Wit, P.J.G.M. (1999) *Annu. Rev.Phytopthol.* **37,** 335-367.

THE COMPARISON OF THE LOOP STRUCTURES OF MEMBRANE BINDING SITES BETWEEN HUMAN AND BOVINE ANNEXINS IV

Michiko Konno, Yae Kanzaki, Kayoko Mochizuki, Nahomi Fushinobu, Ayano Sato, Kyoko Aikawa, and Isamu Matsumoto

Department of Chemistry, Ochanomizu University, 2-1-1 Otsuka, Bunkyo-ku, Tokyo 112-8610 Japan (konno@cc.ocha.ac.jp)

Annexins are a ubiquitous family of structurally related eukaryotic proteins capable of binding phospholipid membranes in calcium-dependent manner [1]. Membrane binding properties of these proteins have suggested that they are involved in numerous processes such as exocytosis, endocytosis, vesicular trafficking, membrane fusion, and ion-channel formation. It has been reported that annexin I, II and IV proteins aggregate synthetic phospholipid vesicles and chromaffin granules. The mRNA of human annexin IV is highly expressed in normal pancreas, lung and kidney and also in various adenocarcinoma cell lines. On the basis of idea that a little structural difference between the loops of annexins, which interact with membranes, should reflect a little difference of circumstances within vesicles, in order to compare in detail with loop structures of membrane binding sites of reported bovine annexins IV, we have determined the crystal structure of recombinant human annexin IV.

Recombinant human annexin IV was crystallized at 20 °C by a hanging drop vapor diffusion method. Crystals were grown from a drop of 6mg/ml protein, 6 % PEG 6000, 1.5mM $CaCl_2$, 3 % dioxane, and 50mM tris-HCl (pH 7.5) equilibrated against a reservoir of 20 % PEG 6000, 20 mM $CaCl_2$, 6 % dioxane, and 100 mM tris-HCl (pH7.5). X-ray data were collected at 100 K at Photon Factory (Tsukuba). Crystals adopt the space group $P2_1$ with lattice distances of a = 44.223 Å, b = 55.132 Å, c = 127.147 Å, and β = 91.45°. The structure was solved by molecular replacement and refined to R_{factor} = 23.3 %, R_{free} = 31.1 % at 2.0 Å resolution using XPLOR.

In recombinant human annexin a C-terminal core has four domains each which fold into five α-helices and an N-terminal "tail region" of fifteen residues (MAMATKGGTVKAASG) lies across the concave protein surface. One calcium ion is bound in domain II, two in domain III and one in domain IV. Three Ca^{2+} ions are bound in type II-binding sites of AB loop and one in type III-binding site of DE loop. The calcium binding groups of AB loop of domain I coordinate ε-amino group of Lys99 of adjacent molecule. On the other hand, in bovine annexin IV two Ca^{2+} ions are bound in the AB loops of domains I and IV [2]. The conformation of the AB loop of 184GEKKWGTDEV193 of domain III bound Ca^{2+} ion of human annexin IV is different largely from that of the corresponding loop of the same residues without Ca^{2+} ion in bovine annexin IV. In the former the side chain of Trp188 is intruded out, while in the latter that of Trp185 adopts a buried conformation. In human annexin IV the AB loop of domain II is ordered and binds Ca^{2+} ion, while in bovine annexin IV that is totally disordered and does not any binds Ca^{2+} ion.

References

1 Gerke, V. and Moss, S. E. (2001) *Physiol Rev.* **82**, 331-371.

2 Sutton, R.B., and Sprang, S.R. (1996) *in Annexin: molecular structure to cellular function* (Seaton, B., Ed) pp 31-42, R.G.Landes Co., Austin, TX.

THE CRYSTAL STRUCTURE OF 9-AMINO-[N-(2-DIMETHYL-AMINO)PROPYL]ACRIDINE-4-CARBOXAMIDE BOUND TO D(CGTACG)$_2$: A COMPARISON OF STRUCTURES OF D(CGTACG)$_2$ COMPLEXED WITH INTERCALATORS IN THE PRESENCE OF COBALT

Adrienne Adams,[a] J. Mitchell Guss,[a] William A. Denny,[b] and Laurence P.G. Wakelin[c]

[a]School of Molecular & Microbial Biosciences, University of Sydney, NSW 2006, Australia; [b]Auckland Cancer Society Research Centre, Faculty of Medicine and Health Science, University of Auckland, Private Bag 92019, Auckland, New Zealand; [c]School of Medical Sciences, University of New South Wales, NSW 2052, Australia (a.adams@mmb.usyd.edu.au)

The structure of the complex formed between an inactive derivative of the clinical trial anti-cancer drug and topoisomerase II poison DACA (9-amino-[N-(2-dimethyl-amino)propyl]acridine-4-carboxamide) and d(CGTACG)$_2$ has been solved and refined to a resolution of 1.55 Å. The complex crystallised in space group C222. An asymmetric unit comprises 2 strands of DNA, one disordered drug molecule, 2 cobalt (II) ions, 2 disordered magnesium ions and 32 water molecules. The DNA helices stack in continuous columns with their central 4 base pairs adopting a B-like motif. The terminal GC base pairs engage in different interactions. At one end of the duplex there is a CpG dinucleotide overlap modified by ligand intercalation and terminal cytosine exchange between symmetry-related duplexes. An intercalation complex is formed involving four DNA duplexes, four disordered ligand molecules, and two pairs of base tetrads. The other end of the DNA is frayed with the terminal guanine lying in the minor groove of the next duplex in the column. The structure is stabilised by guanine N7/cobalt (II) coordination. We compare our structure with the six published structures of d(CGTACG)$_2$ complexed with intercalators in the presence of cobalt [1-4] and find them all to be very similar. The seven structures appear to be independent of biological activity and sidechain configuration and dependent mainly on the presence of an intercalator and cobalt ions. It is likely that many different intercalators, besides those discussed here, would be capable of forming a similar structure with d(CGTACG)$_2$ in the presence of cobalt. Intercalators appear to destabilise B-DNA in the presence of cobalt ions and promote formation of multistranded DNA structures. Although we find no evidence for biological significance of this structure in terms of topoisomerase activity, this does not exclude the possibility that this is an important property of intercalators which may have an effect on other biological processes.

References

1 Adams, A., Guss, J. M., Collyer, C. A., Denny, W. A., Prakash, A. S., and Wakelin, L. P. G. (2000) *Mol. Pharmacol.* **58,** 649-58.

2 Thorpe, J. H., Hobbs, J. R., Todd, A. K., Denny, W. A., Charlton, P., and Cardin, C. J. (2000) *Biochemistry* **39,** 15055-61.

3 Yang, X.-l., Robinson, H., Gao, Y.-G., and Wang, A. H. J. (2000) *Biochemistry* **39,** 10950-57.

4 Teixeira, S. C. M., Thorpe, J. H., Todd, A. K., Powell, H. R., Adams, A., Wakelin, L. P. G., Denny, W. A., and Cardin, C. J. (2002) *J. Mol. Biol.* **323,** 167-71.

STRUCTURAL GENOMICS STUDIES OF MENAQUINONE BIOSYNTHESIS PROTEINS FROM MYCOBACTERIUM TUBERCULOSIS: INSGHTS FROM THE STRUCTURES OF MENG AND MENB

J. M. Johnston, V. Arcus, and E. N. Baker

Laboratory of Structural Biology, School of Biological Sciences, University of Auckland, Auckland, New Zealand (jm.johnson@auckland.ac.nz)

Menaquinone plays an important role in anaerobic electron transport in a range of bacteria. Homologs for the menaquinone biosynthesis pathway genes can be identified in the genome sequence of *Mycobacterium tuberculosis* H37Rv strain. Due to the significance of this pathway in anaerobic conditions, combined with the fact that the menaquinone biosynthesis pathway is not present in humans, means these genes may be possible drug targets. Six of the seven homologs of menaquinone biosynthesis genes identified in the *Mycobacterium tuberculosis* H37Rv strain genome sequence were chosen for study. Cloning, expression tests and refolding experiments resulted in three soluble proteins. Two of these proteins have been crystallized and their structures solved. The 1.9 Å trimeric structure of refolded protein Rv3853, annotated as the S-adenosylmethionine (SAM) dependent methyltransferase MenG, revealed no structural similarity to other SAM dependent methyltranferases and posed questions about the validity of its functional annotation. The discovery of two small molecules bound in this structure highlight regions of this protein that may be significant for its function. Unlike Rv3853, the structure of Napthoate synthase (MenB) solved to 2.15 Å, supports the suggested annotation and confirms its place as part of the crotonase superfamily.

CRYSTAL STRUCTURES OF RESTRICTION ENDONUCLEASE ECOO109I

Hiroshi Hashimoto,[a] Tsuyoshi Imasaki,[a] Matsuri Kato,[a] Toshiyuki Shimuzu,[a] Mamoru Sato,[a] and Keiko Kita[b]

[a]Graduate School of Integrated Science, Yokohama City University, Yokohama, Kanagawa 230-0045, Japan; [b]Graduate School of Agriculture, Kyoto University, Uji, Kyoto 611-0011, Japan (hash@tsurumi.yokohama-cu.ac.jp)

Restriction endonucleases in bacteria recognize and cleave foreign DNA that is unmethylated. Most of the > 3,000 restriction endonucleases discovered to date belong to the type II class. The orthodox type II restriction endonuclease is homodimer, which recognize short and usually palindoromic sequences of 4~8 base pairs, and in the presence of Mg^{2+} cleaves the DNA within or immediately adjacent to the recognition site to give a 5'-phospahte and a 3'-OH end. Although type II restriction endonucleases are widely spread within bacteria, there is generally no sequence similarity among them. Type II restriction endonucleases comprise the largest family of functionally related enzymes, but less known about how their specificity.

The restriction endonuclease, *Eco*O109I from *Escherichia coli* forms functional homodimer and its molecular weight is 62 kDa. The *Eco*O109I monomer is made up with 272 amino acids. *Eco*O109I recognizes and cleaves the interrupted DNA sequence of 5'-RG|GNCCY-3' and produces 5'-overhang DNA. To understand the molecular basis of DNA recognition and hydrolysis of phosphodiester bond, we have studied crystallographic analysis of *Eco*O109I.

Crystal of *Eco*O109I (DNA free) was obtained by hanging drop vapour diffusion method using polyethylene glycol as a precipitant at 277 K. Crystal of *Eco*O109I (DNA free) belongs to space group of *I*4 with the unit cell parameters of $a = b = 175.5$ Å, $c = 44.6$ Å. X-ray diffraction experiments for native data collection of *Eco*O109I DNA free crystals were performed with ACSC Quantum 4R CCD deterctor at BL38B1, SPring-8. The intensity data consists of 307,433 measurements of 26,765 unique reflections with an overall $R_{merge} = 4.2\%$ and 99.1% of theoretically observable reflections at 2.4 Å resolution. Crystal structure of *Eco*O109I was determined by MAD method with mercury derivative crystal using programs *SOLVE/RESOLVE*. The three-wavelength MAD data were collected by Rigaku MSC Jupiter 210 CCD detector at BL45PX, SPring-8.

Crystal of *Eco*O109I DNA complex was obtained by hanging drop vapour diffusion method using polyethylene glycol as a precipitant at 293 K. Crystal of *Eco*O109I DNA complex belongs to space group of $P2_12_12_1$ with the unit cell parameters of $a = 71.8$ Å, $b = 203.2$ Å, and $c = 49.1$ Å. Diffraction intensities of native and mercury derivative crystals of DNA complex were collected by Rigaku R-AXIS IV^{++} imaging plate detector on Rigaku FR-D rotating anode X-ray generator. The native diffraction data consists of 202,201 measurements of 55,952 unique reflections with an overall $R_{merge} = 8.8\%$ and 93.5% of theoretically observable reflections at 1.9 Å resolution. Crystal structure of the DNA complex was determined by SIRAS method using programs *SOLVE/RESOLVE*.

Crystallographic structure refinement of *Eco*O109I and DNA complex are now in progress.

CRYSTAL STRUCTURE OF THERMOSTABLE ENDO-1,5-α-L-ARABINASE FROM BACILLUS THERMODENITRIFICANS TS-3

Asako Yamaguchi,[a] Toshiji Tada,[a] Tetsuko Nakaniwa,[a] Makoto Takao,[b] Takuo Sakai,[b] and Keiichiro Nishimura[a]

[a]Research Institute for Advanced Science and Technology, Osaka Prefecture University, Sakai, Osaka 599-8570, Japan; [b]IGA Bioresearch, Amagasaki, Hyogo 660-0805, Japan (asako-y@biochem.osakafu-u.ac.jp)

Arabinan is a common structural component of plant cell walls. It consists of a backbone of α-1,5-linked L-arabinofuranosyl residues, some of which are substituted with α-1,3- and α-1,2-linked L-arabinosyl side-chains in the furanose conformation. End-1,5-α-L-arabinase (ABN) hydorolyzes the α-1,5-L-arabinofuranoside linkage of arabinan. Thermostable ABN (ABN-TS) from *Bacillus thermodenitrificans* TS-3 showed optimal activity at 343 K, and its thermostability was characterized by a half-life of 4 h at 348 K. We have initiated an analysis for the crystal structure of ABN-TS to clarify the structural features participating in thermostability of ABN.

The recombinant ABN-TS was overexpressed in *B. subtilis* MI112. The purified enzyme was crystallized by using sodium citrate as a precipitant. The crystals were soaked in a cryo-protectant solution containing 40% sucrose and frozen in a nitrogen-gas stream at 100 K. A native data set was collected to 1.9 Å resolution from a frozen crystal using synchrotron radiation of wavelength 0.9 Å at SPring-8. A total of 88876 observed reflections were scaled and reduced to yield a data set containing 22751 unique reflections with an R_{merge} of 8.6%. The data set was 99.2% complete. The crystals belong to the orthorhombic space group $P2_12_12_1$ with unit-cell parameters a = 40.2, b = 77.8 and c = 89.2 Å. Molecular-replacement calculations were carried out with the program *AmoRe* using the structure of α-L-arabinase 43A from *Cellvibrio japonicus* as a search model (46% homology). A clear peak was found with a correlation coefficient of 35.2 and R-factor of 47.3% after translation-function calculations in the space group $P2_12_12_1$. Refinement of the model was performed, resulting in an R-factor of 36.7% and an R_{free} of 42.1%. Manual modifications of the model structure are currently in progress.

STRUCTURAL BASIS OF LIPID BINDING IN RICE NON-SPECIFIC LIPID TRANSFER PROTEIN COMPLEXES

Yuh-Ju Sun, Cheng Pei-Tsung, Hui-Chun Cheng, Peiyu Peng, and Ping-Chiang Lyu

Institute of Bioinformatics and Structural Biology, National Tsing Hua University, Hsinchu, Taiwan 300, ROC (yjsun@life.nthu.edu.tw)

Non-specific lipid transfer proteins (nsLTPs) bind to a variety of lipid molecules and catalyze their transfer across membranes [1]. Other biological functions for nsLTPs also have been proposed such as transfer phospholipids from liposomes or microsomes to mitochondria [2], transport cuticular components for the biosynthesis of surface wax [3], regulate fatty acid beta-oxidation in glyoxysomes [4] and exhibit resistance to avirulent and virulent pathogens in the plant defense system [5]. NsLTPs have been isolated from many plants including wheat, rice, barley, maize, peach, and apricot. NsLTPs are basic proteins (PI 8-10), disulfide-rich, with molecular weight 9 and 7 kDa (nsLTP1 & nsLTP2) [1]. We report here the crystal structures of rice nsLTP1 and fatty acid complexes have been determined by X-ray crystallography. We suggest that the structural plasticity of nsLTP1 manages the lipid binding in the rice nsLTP1 lipid complexes. The tunnel-like hydrophobic cavity inside nsLTP1 provides a space large enough to accommodate a long fatty acyl chain. The hydrophobic and hydrophilic interactions from three key residues, Arg44, Try79 and Ile81, were contributed in the lipid binding.

References

1 Kader, J.C., (1996) *Annu. Rev. Plant Physiol. Plant Mol. Biol.* **47**, 627–654.

2 Breu, V., Guerbette, F., Kader, J. C., Kannangara, C. G., Svensson, B. & Wettstein-Knowles, P. (1989). *Carlsberg. Res. Commun.* **54**, 81-84.

3 Sterk, P., Booij, H., Schellekens, G. A., Van Kammen, A. & De Vries, S. C. (1991). *The Plant Cell* **3**, 907-921.

4 Tsuboi, S., Osafune, T., Nishimura, M. & Yamada, M. (1992). *J. Biochem.* **111**, 500-508.

5 Maldonado, A. M., Doerner, P., Dixonk, R. A., Lamb, C. J. & Cameron, R. K., *Nature* (2002) **419**, 399-403.

REFINEMENT OF THE 7/2-AND 10/3-HELICAL STRUCTURES BASED ON THE FIBER DIFFRACTION PATTERN FROM NATIVE COLLAGEN

K. Okuyama, X. Xu, and K. Noguchi

Faculty of Technology, Tokyo University of Agriculture and Technology, Koganei, Tokyo 184-8588, Japan (okuyamak@cc.tuat.ac.jp)

After fifty years since the first proposal of a triple helical structure, there are still two models for collagen with different helical symmetry and different fiber repeating period. One is the Rich and Crick model in which three strands form a left-handed 10/3-helix with an axial repeat of 28.6Å [1]. The other is our model in which three strands form a left-handed 7/2-helix with an axial repeat of 20Å [2]. The latter model was strongly supported by single crystal analyses of several collagen model peptides reported so far. On the other hand, the former model has no such supporting data other than the fiber diffraction analyses of poly(Pro-Gly-Pro) [3] and native collagen [4]. Since the quality of fiber diffraction pattern from poly(Pro-Gly-Pro) was very poor compared with that from native collagen, the former analysis is not a powerful supporting evidence for the 10/3-helical model. On the other hand, in the latter analysis, only the 10/3-helical structure was refined by using continuous layer intensities. In this study, we refined both 7/2- and 10/3-helical structures by using continuous X-ray diffraction intensities on the layer lines corresponding to their axial repeat.

The fiber diffraction pattern from kangaroo tail tendon was taken by using synchrotron radiation (BL40B2, SPring-8) and recorded on an imaging plate (RAXISIV^{++}, Rigaku). The background subtraction and acquisition of continuous X-ray intensities on the corresponding layer lines were performed by using CCP13 softwares. According to the recent single crystal analyses of collagen model peptides at high resolution, in most of the cases, there are water molecules bound to the carbonyl oxygen of Gly and Pro, and those to the hydroxyl oxygen of Hyp. Therefore, some of these water molecules were also included in the triple helical structures. Refinement calculation was performed by WinLALS, Windows version of Linked-Atom Least-Squares (LALS) program for fiber diffraction analyses.

In both models, triple-helical structures with no bound water molecules gave fairly high discrepancy (R-) factor (~0.40) compared with that (0.27) of the previous analysis [4]. Although Pro-Hyp-Gly triplet was taken as a helical asymmetric unit, occupancies of $C\gamma$, $C\delta$ and $O\delta$ atoms of imino acids were reduced to 1/3 according to the imino acid occurrences in the amino acid sequence of tendon collagen, which decreased R-factors by several percent. Furthermore, addition of water molecules decreased R-factors to 0.25 (7/2-helix) and 0.30 (10/3-helix). This fairly large improvement of the discrepancy factor by addition of water molecules was also experienced in many single crystal analyses of collagen model peptides. The obtained result showed that the 7/2-helical model can explain fiber diffraction patterns from native collagen better than, or at least as well as, the 10/3-helical model can do.

References

1 Rich, A. and Crick, F.H.C. (1961) *J. Mol. Biol.* **3**, 483-506.
2 Okuyama, K., Takayanagi, M., Ashida, T. and Kakudo, M. (1977) *Polymer J.* **9**, 341-343.
3 Yonath, A. and Traub, W. (1969) *J. Mol. Biol.* **43**, 461-477.
4 Fraser, R.D.B., MacRae, T.P. and Suzuki, E. (1979) *J. Mol. Biol.* **129**, 463-481

INTERSUBUNIT SALT BRIDGES AND OLIGOMERIZATION DO NOT CONTRIBUTE TO THE HIGH THERMAL STABILITY OF A HYPERTHERMOPHILIC PROTEIN FROM PYROCOCCUS FURIOSUS

Jai K. Kaushik,[a] Yuriko Yamagata,[b] Kyoko Ogasahara,[c] and Katsuhide Yutani[d]

[a]Molecular Biology Unit, National Dairy Research Institute, Karnal 132001, India; [b]Graduate School of Pharmaceutical Sciences, Kumamoto University, Kumamoto, Japan; [c]Institute for Protein Research, Osaka University, Japan; [d]Kwansei Gakuin University, Sanda City, Hyogo, Japan (jaik@ndri.hry.nic.in)

Electrostatic interactions play an important role in the extraordinary high stability of proteins from hyperthermophilic organisms. These proteins contain large number of ion pairs forming complex networks. However, due to large desolvation penalty involved in formation of salt bridges and consequent burial in between the interfaces, their contribution to extraordinary high stability of hyperthermophilic proteins has been controversial. There are numerous experimental results in support as well as opposing the significant role of salt bridges in protein stability.

Pyrrolidone carboxyl peptidase (PCP) from *Pyrococcus furiosus* is a homotetramer and considered to be stabilized by several salt bridges at the interface of subunits which could eventually be responsible for oligomerization. Its melting temperature is above 107°C at pH 7. To elucidate the role of inter-subunit salt bridges in the stabilization mechanism of proteins, the following mutants were generated and expressed in *E. coli*: R80A/K118A (IM2), D87A/E99A/D100A (IM3), and R80A/K118A/D87A/E99A/ D100A (IM5). Subunits A and B, and subunits C and D are located diagonally opposite. The salt bridges in PCP are located at interfaces between subunits A and D and subunits B and C; whereas, the interfaces between A and C, and B and D are strengthened mainly by hydrophobic interactions and some salt bridges. The sedimentation analyses showed that disruption of salt bridges affect the molecular assembly of the mutants. At pH 3 and 3.8, PCP exists in dimeric and tetrameric forms, respectively, whereas the ionic mutants are close to monomeric form at both the pH values. It indicates that alteration of electrostatic interactions at one interface also affects the interactions at the other interfaces. There seems a cooperativity of interactions forming at two different interfaces. The formation of dimer and tetramer in ionic mutants takes place at pH 4.4 and above 5, respectively. DSC results indicated that disruption of salt bridges led to changes in thermal stability. The stability of IM2 (basic residues replaced) decreased in the acidic as well in the neutral zones, whereas it increased for IM3 (acidic groups replaced) in these regions; the stability of IM5 seemed to be resulting from the additive effect of removal of basic and acidic groups. In the region near pH 4, all these mutants were more stable than PCP. X-ray structure analyses indicated that Asp87, Glu99 and Asp100 on one subunit are located very closely causing considerable repulsion among themselves and thus offsetting the contributory effect due to pairing with Arg80 and Lys118 on the adjacent subunit. Whereas Arg80 and Lys118 are well separated and removal of these residues leads to a decrease in stability due to not only breaking of salt bridges but also because it leaves the acidic residues at position 87, 99 and 100 unpaired and hence more repulsive. Results indicate that assembly form does not have a direct relation with the stability of PCP. This could be because the positive effect of oligomerization is offset by negative effect of desolvation of charged groups due to burying in between the interfaces.

STRUCTURAL CHARACTERISATION OF THE INI OPERON OF MYCOBACTERIUM TUBERCULOSIS

J. Shaun Lott,[a] Moyra M. Komen,[a] Tet Verne Lee,[a] Clare Scott,[a] Joel McKay,[b] Edward N. Baker,[a] and Vickery L. Arcus[a]

[a]Laboratory of Structural Biology, School of Biological Sciences, University of Auckland, Private Bag 92-019, Auckland 1020, New Zealand; [b]School of Molecular and Microbial Biosciences, University of Sydney, NSW 2006, Australia (s.lott@auckland.ac.nz)

Isoniazid (INH) is the primary antibiotic used in the treatment of *M. tuberculosis* infection. INH asserts its toxic activity on the bacterium by inhibiting the biosynthesis of cell wall mycolic acids, rendering it susceptible to reactive oxygen radicals and other environmental factors [1].

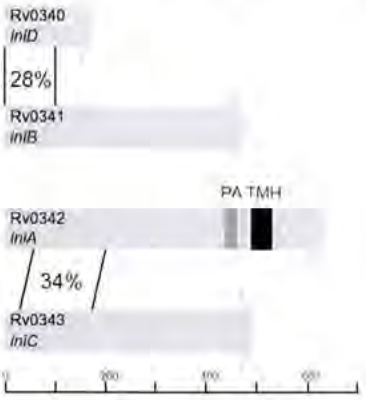

ORFs from the *ini* operon have been identified by DNA microarray [2] and differential mRNA expression studies as being strongly upregulated by INH and to a lesser extent by ethambutol (EMB), another antibiotic that also inhibits cell wall biosynthesis. These observations imply that this gene cluster may be important for bacterial cell viability when membrane integrity is compromised by cell wall biosynthesis inhibitors. None of the ORFs in this cluster show informative amino acid sequence similarity to any other proteins, and their biochemical functions remain unknown. However, they show clear conservation with each other in particular segments of their sequences (see figure), which implies that they share conserved structural domains.

We have defined structural domains in iniA, iniC and iniD using a combination of sequence analysis, limited proteolysis, mass spectrometry and amino acid sequencing. The structure of the folded domain from iniD is currently being pursued using high-field heteronuclear NMR spectroscopy, and diffracting crystals have been obtained of the conserved domain shared by iniA and iniC. Results of these structural analyses will be presented, which may enable biochemical functions to be assigned to these proteins to explain their physiological roles in antibiotic response.

References

1 Rattan, A., Kalia, A. and Ahmad, N. (1998) "Multidrug-resistant *Mycobacterium tuberculosis*: Molecular Perspectives." *Emerging Infectious Diseases* **4,** 195-209.

2 Wilson, M. *et al.* (1999) "Exploring drug-induced alterations in gene expression in *Mycobacterium tuberculosis* by microarray hybridization." *PNAS* **96,** 12833-12838.

STUDIES OF PROTEINS OF THE FOLATE BIOSYNTHESIS PATHWAY

Jacqueline F. Satchell, Brian J. Smith, Jonathan Baell, and Peter M. Colman

The Walter and Eliza Hall Institute, Structural Biology Division. 1G Royal Parade, Parkville, Victoria, 3050, Australia (satchell@wehi.edu.au).

Organisms parasitic upon humans, such as *Plasmodium* and *Pneumocystis*, are responsible for some of the world's major health problems. These infections have commonly been treated with a class of compounds known as antifolates[1]. These inhibitors block the enzymes of the folate biosynthesis pathway causing decreased pyrimidine synthesis resulting in reduced DNA, serine and methionine formation, ultimately resulting in growth inhibition[2].

The structures of several prokaryotic folate biosynthesis enzymes are available, and allow for preliminary hypotheses to be drawn regarding likely inhibitors of this pathway. Docking experiments have been conducted in order to determine whether DHP-analogues, previously shown in *E. coli* to be formed by the consensation of the substrate DHPP with sulfa drugs (shown in figure 1), are capable of inhibiting this pathway. These compounds have been chemically synthesised and have shown to have activity against dihydrofolate reductase (DHFR) in yeast[3].

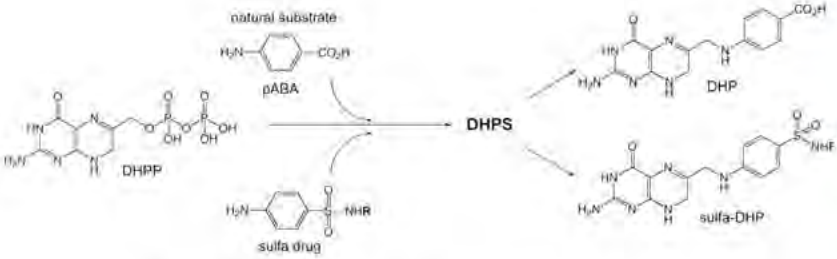

Figure 1 – Formation of DHP-analogues *in vivo*.

Pneumocystis carinii combines enzymes of this pathway in a more elaborate protein complex, the FAS protein, which incorporates hydroxymethyldihydropterin pyrophosphokinase (PPPK), dihydroneopterin aldolase (DHNA) and DHPS. Existing prokaryotic structures have also provided useful information with regards to the design of constructs for expression of this protein in insect cells. The structure of this protein will provide useful information from which drugs can be designed to target parasitic organisms.

References

1 Olliaro,P., Cattani, J. and Wirth, D. *JAMA*. **1996**, 275, 230-234.
2 Volpe, F., Ballantine, S.P. and Delves, C.J. *Eur. J. Biochem.* **1993**, 216, 449-458.
3 Patel O., Satchell J.F., Coloe P., Baell J. and Macreadie I. *Microbial Drug Resistance*. Accepted for publication in 2003.

IDENTIFYING ANTAGONISTS TOWARDS A G-PROTEIN COUPLED RECEPTOR USING THE STRUCTURE OF A HORMONE COMPLEXED TO A NEUTRALISING MONOCLONAL ANTIBODY

Galina Polekhina,[a*] William J. McKinstry,[a*] Hannelore Diefenbach-Jagger,[a] Patricia W. M. Ho,[a] Craig J. Morton,[a] Koh Sato,[b] Etsuro Onuma,[b] Matthew T. Gillespie,[a] T. John Martin,[a] and Michael W. Parker[a]

[a]St. Vincent's Institute of Medical Research, 9 Princes Street, Fitzroy, VIC 3065, Australia; [b]Pharmaceutical Research Laboratory, Chugai Pharmaceutical, 1-135 Komakado, Gotemba, Shizuoka, 412-8513 Japan
(galinap@medstv.unimelb.edu.au)

[*]Both authors contributed equally to the work

G-protein coupled receptors (GPCR) are the most common receptor class in humans controlling critical cell functions and are thus an important class of drug targets. They are notoriously difficult to over-express and crystallize, and to date only one high resolution structure (bacterial rhodopsin) is available. We present a promising new method for discovering GPCR agonists and antagonists using structures of GPCR ligands bound to antibodies.

Parathyroid hormone related protein (PTHrP) was discovered as a hypercalcemia-causing factor of malignancy [1]Under normal circumstances PTHrP plays a key role in regulating embryonic development of the skeleton and other tissuesPTHrP as well as parathyroid hormone (PTH) act upon the same GPCR, parathyroid hormone receptor (PTH-R). PTHrP has also been shown to be one of the main culprits of metastasis into bone of human breast cancer cells causing bone breakdown.We have crystallized and determined the structure of the complex between PTHrP and a neutralizing monoclonal antibody. The humanised version of this antibody is currently in clinical trials (Phase II) in Japan for treatment hypercalcemia, bone metastasis and cachexia [2]. The structure revealed that the residues of PTHrP involved in the interaction with the antibody are either strictly conserved among PTH and PTHrP sequences or have been implicated in the binding to the receptor. We therefore predicted that the binding pocket on the antibody resembles the receptor's. Using the structural data, we will screen the large library of small "drug-like" molecules for the best fit into the PTHrP binding pocket of the antibody. The top hits will be screened in cellular assays for inhibition towards action of PTHrP on PTH-R. The structural biology results and those from the computational screen and cellular assays will be presented.

References

1 Martin, T. J. (2002) *The Journal of Clinical Investigations.* **10**, 1399-1401.
2 Sato, K. (1999) *The Seventh International Forum on Calcified Tissue and Bone Metabolism.* 32-37.

RECENT DEVELOPMENTS AT ASRP X-RAY DIFFRACTION FACILITIES

James R Hester, and David Cookson

ANSTO, PMB 1, Menai, NSW 2234, Australia (jrh@anbf2.kek.jp)

The Australian Synchrotron Research Program (ASRP) has been operating a high throughput Debye-Scherrer powder diffractometer at the Australian National Beamline Facility (ANBF) in Tsukuba, Japan, for almost 10 years. The unique design of the instrument enables rapid collection of multiple datasets in which one or more experimental parameters are varied, for example, wavelength or temperature. The ANBF has offered as standard a modular furnace giving a temperature-controlled environment in the 400-1000K range, with user-constructed furnaces reaching almost 1400K. Recently, a commercial Joule-Thompson refrigerator has been acquired for flat plate/capillary experiments in the 80-500K range. Early results from this device are presented together with information on availability for general use in the upcoming (October) beamtime cycle.

The ChemMatCARS project at the APS in Chicago, of which the ASRP is a member, offers micro-crystal single-crystal diffraction using a Bruker CCD area detector with cryostream cooling and a turnkey data collection and processing system. Publishable structures are routinely obtained from crystals with average dimension < 50 microns and data collection times of around 6-8 hours. Typical results from this system are presented [1].

Access to the ANBF is normally by peer-reviewed proposal [2]; users with a small number of powder samples may submit them for 'ad-hoc' data collection by beamline staff [3]. The ASRP offers the SCrAPS service for microcrystal data collection at the APS [4].

References

1 Smyth, D. R., Hester, J., Young, V. G. and Tiekink, E. R. (2002) *CrystEngComm*, 517-521.
2 http://www.ansto.gov.au/natfac/asrp1001.html
3 http://www.ansto.gov.au/natfac/ANBF/adhoc_final.html
4 http://www.ansto.gov.au/natfac/scraps.html

COMPARISON OF THE FR-E AND RU-H2R X-RAY SOURCES FOR PROTEIN CRYSTALLOGRAPHY APPLICATIONS

Karl A. Byriel[a], Anna Aagaard[a], Christine L. Gee[a], Nirajali Gamage,[b] and Jennifer L. Martin[a]

[a]Institute for Molecular Bioscience, The University of Queensland, QLD 4072 Australia; [b]Department of Physiology and Pharmacology, The University of Queensland, QLD 4072 Australia (k.byriel@imb.uq.edu.au)

The FR-E Superbright rotating anode generator was designed as a successor to the FR-D generator. It provides a high brilliance focal spot, 2.0 kW at 0.07 x 0.07 mm compared to the traditional home source RU-H2R or RU-H3R focal spot 5.0 kW at 0.3 x 3 mm or the FR-D focal spot 3.5 kW at 0.1 x 0.1 mm or 5.0 kW at 0.15 x 0.15 mm. The FR-E has the advantage of lower maintenance and easier handling than the FR-D.

Preliminary data will be presented for the comparison of the RU-H2R rotating anode generator and MSC Confocal Blue-3 optic against the FR-E Superbright generator with both MSC Confocal HiRes^2 and MaxScreen optics. Data in both cases are measured on an R-AXIS IV++ detector and the cryocooling apparatus is the same in each case, the CryoIndustries Cryocool NFC 1259 XRD.

We will present the results of characterization of the physical properties of the X-ray beam and data sets collected on the same small frozen lysozyme crystal from these systems. Results will also be presented for other protein crystal samples as they become available.

EVALUATION OF MICROSTRUCTURE PARAMETERS FROM POWDER X-RAY DIFFRACTION DATA

Takashi Ida, and Hideo Toraya

Ceramics Research Laboratory, Nagoya Institute of Technology, Asahigaoka, Gifu 507-0071, Japan (ida@crl.nitech.ac.jp)

Recently, we have developed a new method to deconvolute instrumental aberrations from powder X-ray diffraction data [1]. The effects of spectroscopic distribution of the source X-ray, axial divergence, flat specimen and sample transparency are all eliminated by a fast Fourier transform calculations. As compared with the conventional method of Stokes [2], our method is advantageous at the following points: (i) no measurement of reference sample is needed, (ii) integrated peak intensity is strictly conserved or properly corrected after the deconvolution, (iii) the systematic peak shifts are automatically corrected, (iv) the whole diffraction data are simultaneously treated no matter how complicated the peak pattern may be, and (v) the propagation of statistical errors is properly evaluated. Those features are particularly useful for evaluation of microstructure parameters, the finite crystallite size and amount of structural defects in crystallites.

We have also developed an advanced algorithm for numerically evaluating the theoretical diffraction peak profile from spherical crystallites with log-normal size distribution (SLN profile) [3]. The algorithm efficiently evaluates the precise model profiles even for extremely broad size distribution, while the method originally proposed by Langford *et al.* [4] and a modified version of Popa and Balzar [5] are only applicable to restricted widths of distribution. Curve fitting analysis based on the SLN profile model provides a simple way to estimate both mean and width of crystallite size distribution from each of experimental diffraction peak profiles.

Our original methods are applied to estimate microstructure parameters of a fine SiC powder sample (JFCC, RP-2). The deconvolution of the instrumental aberration from experimental powder X-ray diffraction data has revealed the intrinsic 'super-Lorentzian' line shape [6], which is characteristic of the SLN profile for broad size distribution. The logarithmic standard deviation of the distribution is estimated at 0.93(3), which is in good agreement with the value 0.97 estimated by a laser diffraction method. It is also shown that the anisotropic features in shifts of the peak positions and also variation of the peak widths dependent upon the Miller indices indicate the existence of deformation-type stacking fault along 111-direction, the frequency of which is estimated at about 0.005(1) based on the Paterson's model for stacking faults [7].

References

1 Ida, T. and Toraya, H. (2002). *J. Appl. Cryst.* **35**, 58-68.
2 Stokes, A. R.. (1948). *Proc. Phys. Soc. London* **61**, 382-393.
3 Ida, T., Shimazaki, S., Hibino, H. and Toraya, H. *J. Appl. Cryst.* (submitted).
4 Langford, J. I., Louër, D. and Scardi, P. (2000). *J. Appl. Cryst.* **33**, 964-974.
5 Popa, N. C. and Balzar, D. (2002). *J. Appl. Cryst.* **35**, 338-346.
6 Wertheim, G. K., Butler, M. A., West, K. W. and Buchanan, D. N. E. (1974). *Rev. Sci. Instrum.*. **11**, 1369-1371.
7 Paterson, M. S. (1952). *J. Appl. Phys.* **23**, 805-811.

THEORETICAL AND EXPERIMENTAL STUDY OF THE NEWEST HIGH BRILLIANCE ROTATING ANODE GENERATORS AND CMF OPTICS

K. F. Tesh,[a] A. R. Criswell,[a] C. Yang,[a] D. A. Courville,[a] J. D. Ferrara,[a] M. Kuribayashi,[b]
B. Verman,[c] and L Jiang[c]

[a]Rigaku/MSC, Inc., 9009 New Trails Drive, The Woodlands, TX 77381, USA; [b]Rigaku Corp., 3-9-12 Matsubara-Cho, Adisima-Shi, Tokyo 196, Japan; [c]Osmic, Inc., 1900 Taylor Rd., Auburn Hills, MI 48326 USA (kft@RigakuMSC.com)

The synergistic match of microfocus cathode technology, state of the art anode development, and confocal optics has produced a new generation of X-ray sources unequalled in performance. But, does all this extra flux, now available in the home lab, really add to the capabilities previously only accessible at synchrotron sources?

A careful study of the added flux benefit for a series of new generators and optics will be presented. It will be shown that recent data improvements have led to consideration of collecting high resolution data sets at home, and with more ease. Flux measurements and real datasets support these revolutionary advances. Data sets from smaller and more poorly diffracting crystals can now be attained without a trip to the synchrotron.

PHASE TRANSITION OF LANTHANUM TITANATE PEROVSKITES

Masatomo Yashima,[a] Mizuki Mori,[a] Koh Saitoh,[a] Kenji Tsuda,[b] Takashi Kamiyama,[c] Ken-ichi Oikawa,[c] Akinori Hoshikawa,[c] Shuki Torii,[d] Masahiko Tanaka,[c] Takeharu Mori,[c] Ken-ichi Kato,[e] Shinobu Aoyagi,[e] Masaki Takata,[f] and Eiji Nishibori[f]

[a]Department of Materials Science and Engineering, Interdisciplinary Graduate School of Science and Engineering, Tokyo Institute of Technology, 4259 Nagatsuta-cho, Midori-ku, Yokohama, 226-8502, Japan; [b]Institute of Multidisciplinary Research for Advanced Materials, Tohoku University, Sendai 980-8577, Japan; [c]Institute of Materials Structure Science, High Energy Accelerator Research Organization, 1-1 Oho, Tsukuba, Ibaraki, 305-0801, Japan; [d]Satellite Venture Business Laboratory, Ibaraki University, 4-12-1, Naka-Narusawa-cho, Hitachi, Ibaraki, 316-8511, Japan; [e]SPring-8, JASRI, 1-1-1 Kouto, Mikazuki-cho, Sayo-gun, Hyogo 679-5198, Japan; [f]Department of Applied Physics Graduate School of Engineering, Nagoya University Chikusa-ku, Nagoya, 464-8603, Japan (yashima@materia.titech.ac.jp)

$La_{2/3}TiO_3$-based compounds with an *A*-site deficient perovskite-type structure ABO_3 are attractive materials with high ionic conductivity at high temperatures and dielectric constants where A=$La_{2/3\pm y}$, B=(Ti_{1-x},M_x) and M is dopant cation. Despite of the importance of many perovskite-related oxides at high temperatures, only a limited number of accurate high-temperature structural studies have been performed. The $La_{0.64}(Ti_{0.92},Nb_{0.08})O_3$ and $La_{0.68}(Ti_{0.95},Al_{0.05})O_3$ compounds were reported to exhibit a structural phase transition between the orthorhombic (*Pmmm*) and tetragonal (*P4/mmm*) phases at 623 K and 643 K, respectively [1,2]. However, the Rietveld analysis of the low-temperature phase has been carried out by an invalid space group *Pmmm*, ignoring small diffraction peaks as shown in the present paper. Furthermore, the previous $La_{0.64}(Ti_{0.92},Nb_{0.08})O_3$ sample included a small amount of impurity phases of $LaTiNbO_6$ and $La_2Ti_2O_7$. The present paper reports new data on the evolution of the crystal structure of high-purity $La_{0.64}(Ti_{0.92},Nb_{0.08})O_3$ at high temperatures. High-resolution neutron and synchrotron powder diffraction measurements are carried out to determine the temperature dependence of positional parameters. Neutron, synchrotron and electron diffraction analyses indicate that $La_{0.64}(Ti_{0.92},Nb_{0.08})O_3$ compound has *Cmmm* space group at room temperature. We report for the first time that the tetragonal (*P4/mmm*)-to-orthorhombic (*Cmmm*) phase transition in $La_{0.64}(Ti_{0.92},Nb_{0.08})O_3$ is induced by the tilt of oxygen octahedron around Ti and Nb atoms. The angle of the tilt and the *b/a* ratio of cell parameters decrease with an increase of temperature and become 0 deg. and unity, respectively, at a transition temperature between 534 and 637 K.

References

1 Ali, R., Yashima, M., Tanaka, M., Yoshioka, H., Mori, T. and Sasaki, S. (2002) *J. Solid State Chem.* **163**, 51-59.

2 Yashima, M., Ali, R., Tanaka, M. and Mori, T. (2002) *Chem. Phys. Lett.* **363**, 129-133.

PRECISE MEASUREMENT OF THE LATTICE SPACING OF LaB_6 STANDARD BY POWDER DIFFRACTION AND THE X-RAY EXTENDED RANGE TECHNIQUE USING SYNCHROTRON RADIATION

C. T. Chantler,[a] Z. Barnea,[a] C. Q. Tran,[a] and D. J. Cookson[b]

[a]School of Physics, University of Melbourne, Parkville, Vic 3010, Australia; [b]ANSTO, Private Mail Bag 1, Menai, NSW 2234 and Chem-Mat-CARS-CAT (Sector 15, Bldg 434D), Argonne National Laboratory, 9700 S. Cass. Avenue, Argonne, IL 6043 (chantler@ph.unimelb.edu.au)

Some 20% of Australian synchrotron usage involves powder diffraction, particularly of micro-crystalline organic and inorganic samples for biomedical and chemical structure determination. A similar percentage applies to world synchrotron usage. While structures can often be reliably determined directly from the diffraction patterns using Rietveld and other methods, resulting errors often depend upon the errors of calibrating standards which should be used in the measurement.

We used the X-ray Extended-Range Technique [1] to measure the lattice spacing of LaB_6 standard powder samples relative to silicon standard powder samples with an accuracy of 0.4 eV. Measurements were carried out over a 5 keV - 20 keV energy range [2]. Hence the determination was not constrained to one energy. These measurements used powder diffraction to determine the synchrotron beam energy; to determine beam divergence; and to correct the nominal calibrated beam energies. Discrepancies in nominal beam energies often create difficulties in interpretating aspects of the structural evaluation, and can involve corrections of 100 eV or more. This technique provides a result independent of certain energy-dependent systematics and yields the most accurate determination of the lattice spacing of LaB_6 so far undertaken.

References

1 Chantler, C. T., Tran, C. Q. , Paterson, D., Cookson, D. and Barnea, Z. (2001) *Phys. Lett.* **A286,** 338-346.

2 Chantler, C. T., Tran, C. Q., Barnea, Z., Paterson, D., Cookson, D. and Balaic, D.X. (2001) *Phys. Rev.* **A64,** 062506-1 – 15

ANALYSIS OF THE DEPTH DEPENDENCE ON THE POLY-CRYSTAL STRACTURE NEAR THE SURFACE BY THE USE OF SCATTERED X-RAY AT SMALL GLANCING ANGLE INCIDENCE

Y. Fujii,[a] A. Tao,[a] T. Komai,[a] and K. Ikeda[b]

[a]Faculty of Engineering, Kobe University, Rokkodai, Nada, Kobe 657-8501, Japan; [b]Materials Research Laboratory, Kobe Steel, Ltd., Nishiku, Kobe 651, Japan (fujiiyos@kobe-u.ac.jp)

New analyzing method for evaluating the poly-crystal structure near the surface using X-rays at small glancing angle incidence was studied. When X-rays are applied to the material surface at a grazing angle of incidence, the intensity of X-rays scattered on the surface is the sum of the X-rays that scattered by the atoms only on the surface, ca. several ten atomic layers deep, and the contribution of the atoms of each depth to the X-rays intensity varies on the incidence angles. Since the penetration depth of X-rays changes by changing an incidence angle, a structural change of the depth direction of a material surface layer can be known in analyzing incidence angle dependence of the information that the scattered X-rays have. So the intensities of the scattered X-rays were measured continuously at the various incidence angles, and the dependency of the incidence angles was analyzed. The small glancing angle X-rays scattering on polycrystalline iron surface were measured by using synchrotron radiation at Hyogo Prefecture beam line BL24 of SPring-8. The polycrystalline surface of pure iron (ferrite, 3nines purity) was mechanically polished and annealed at 400 degrees for 5 minutes. The pre-heating forms a thin amorphous oxide layer on the iron surface. Angular distributions of the scattered X-rays intensities were measured at several glancing angle incidences of 10keV X-rays. X-rays diffraction patterns in the direction parallel to the surface at the several incident angles of the X-rays show that the peak intensity corresponding to Fe_2O_3 is large at an incident angle of 3.5mrad and decreases at a larger incident angle, and show that the peak intensity corresponding to Fe_3O_4 is large at an incident angle of 5.1mrad and decreases at a larger incident angle, and show that the peak intensity corresponding to Fe increases at a larger incident angle. Analyzing these intensity profiles as the function of the incident angle leads to the contribution of the atoms of each depth under the surface. The result of this experiment was analyzed with some surface structure models. Based on these results, we propose a new method of surface characterization; a depth profile of the surface structure can be detectable by this measurement technique.

References

1 Fujii, Y., Tao, A., Ikeda, K., Kusumi, Y., Yanase, E. and Nishio, K. (2001) *Proc. ALC01*, 267-270.

THE USE OF PARENT SYMMETRY TO IDENTIFY SPACE GROUP OPTIONS FOR TWINNED/DISORDERED PSEUDO SYMMETRIC CRYSTAL STRUCTURES

A. David Rae

Research School of Chemistry, The Australian National University, Canberra, ACT 0200, Australia (rae@rsc.anu.edu.au)

Reflections of many modulated structures can be described as **H** = **G** + *m***q** where **G** is a subset of reflections that are strong and can be described by a particular index condition. A parent structure description based on the Fourier transform of these reflections alone is necessarily disordered, but may be approximated using a space group with a higher point symmetry than the true structure. The identification of this symmetry allows a logical assessment of the possible twinnings, stacking faults, site symmetries and space groups that may be initiated by different orderings of this parent structure. The symmetry of coherent substructures can be identified, reducing the range of possibilities. Algebra for the combination of structure factors for ordered substructures can be used for constrained refinement.

Alternative stackings of substructures allows the possibility of polytypes and indeed crystals containing coherent blocks of structure of different space groups and different orientations [1].

Twinning allows the overlay of systematic absences and presences. The true symmetry may induce displacements from the idealised parent symmetry and corrupt the absences and diffraction symmetry of the idealised parent structure. However the use of symmetrised components derived using irreducible representation theory can identify a hierarchy for model development. An example [2] is the low temperature structure obtained by a non destructive phase transition from a *P4/ncc* room temperature structure. The cell volume doubles and *P4/mmm* diffraction symmetry is maintained. A knowledge of the options allowed a twinned *Pnca/Pcnb* structure to be determined.

Absences allowed a twinned *Pcna/Pncb* option imposing different site symmetries but indistinguishable absences. Stacking faults would lower the symmetry and the intensity of the extra reflections. A description of the various options will be given.

References

1 Rae, A. D, and Willis, A. C. (2003) *Z. Krist.* **218**, 221-230.

2 Sugiyarto, K. H., McHale, W. A., Craig, D. C., Rae, A. D., Scudder, M. L., and Goodwin, H. G. (2003) *Inorg Chem.* accepted.

PHASE TRANSITION AND STRUCTURE OF $C_8H_{20}NX \cdot nCH_4N_2S$ (X=I, Br, Cl, n=2, 4, 5)

H. Ishigami,[a] M. Sumita,[a] Y. Tsunashima,[a] S. Sato,[a] M. Shiro,[b] and T. Hikita[c]

[a]Faculty of Engineering, Shibaura Institute of Technology, Minuma, Saitama 330-8570, Japan; [b]X-ray Research Laboratory, Rigaku Corporation, Akishima, Tokyo 196-8666, Japan; [c]School of Engineering, Tohoku University, Aoba, Sendai, Miyagi 981-8579, Japan (ishigami@sic.shibaura-it.ac.jp)

The title compounds $C_8H_{20}NX \cdot 2CH_4N_2S$ (X=I, Br, Cl) were prepared by addition of thiourea to tetraethylammonium salts. The crystal $C_8H_{20}NI \cdot 2CH_4N_2S$ undergoes a phase transition at 288K. The structure at room temperature belongs to orthorhombic system with the space group *Ibca*; the low temperature phase is orthorhombic *Pccb*. Both phase are centric. Large differences of the cell dimensions were not found between both phases. The structure consists of the tetraethylammonium cations, iodide anions and thiourea molecules. No short contacts other than van der Waals ones are observed. The main difference between both structures is that the cations show a disordered arrangement at room temperature whereas they are ordered in the low-temperature phase. The disordered cation statistically occupies two sites relating the two-fold rotation axis with one-half occupancies each. Very recently we have determined the crystal structure of $C_8H_{20}NI \cdot 2CH_4N_2S$ at 300K. The dimensions are a=11.5447(5) Å, b=22.605(1) Å, c=15.1038(6) Å, V=3941.6(3) Å^3, Z=8, R=0.090. Next, intensity of low temperature phase was measured at 153K. The cell dimensions are a=11.5252(5) Å, b=22.3020(9) Å, c=14.7548(6) Å, V=3792.5(5) Å^3, Z=8, R=0.035. $C_8H_{20}NBr \cdot 2CH_4N_2S$ and $C_8H_{20}NCl \cdot 2CH_4N_2S$ undergo the phase transitions at 338K and 265K, respectively.

Previous structure determination have been carried out on $C_8H_{20}NBr \cdot 4CH_4N_2S$ and $C_8H_{20}NCl \cdot 5CH_4N_2S$. The structure of $C_8H_{20}NBr \cdot 4CH_4N_2S$ and $C_8H_{20}NCl \cdot 5CH_4N_2S$ found to be orthorhombic, space group $Pna2_1$, and monoclinic, space group $P2_1$, respectively.

TRANSMISSION ELECTRON MICROSCOPE STUDY OF $RuSr_2Gd_{1.5}Ce_{0.5}Cu_2O_{10-\delta}$ MAGNETO-SUPERCONDUCTOR

Yoshio Matsui,[a] Tadahiro Yokosawa,[a] Veer Pal Singh Awana,[a] Koji Kimoto,[a] Eiji Takayama-Muromachi,[a] Maarit Karppinen,[b] and Hisao Yamauchi[b]

[a]National Institute for Materials Science, 1-1 Namiki, Tsukuba, 305-0044, Japan; [b]Materials and Structures Laboratory, Tokyo Institute of Technology, Yokohama, 226-8503, Japan (MATSUI.Yoshio@nims.go.jp)

Coexistence of superconductivity and magnetism in $RuSr_2(Gd,Sm,Eu)_{1.5}Ce_{0.5}Cu_2O_{10-\delta}$ (Ru-1222) (1) and $RuSr_2GdCu_2O_8$ (Ru-1212) (2) have been of tremendous interest. In this study, we have investigated the microstructure of $RuSr_2Gd_{1.5}Ce_{0.5}Cu_2O_{10-\delta}$ (Ru-1222) (3), by SAED, dark-field electron microscopy, convergent-beam electron diffraction (CBED) and high-resolution TEM (4). The $RuSr_2Gd_{1.5}Ce_{0.5}Cu_2O_{10-\delta}$ (Ru-1222) sample was synthesized through a solid-state reaction route from RuO_2, SrO_2, Gd_2O_3, CeO_2 and CuO. The block of specimen was crushed and dispersed on a carbon thin film on a Cu grid for transmission electron microscopy. The SAED and CBED patterns and conventional dark-field images were taken at room temperature using transmission electron microscopes (Hitachi: HF-3000S and HF-3000L) operated at an accelerating voltage of 300 kV. The SAED and CBED patterns were taken from specimen areas of about 100 and 8 nm, respectively. The HRTEM images were taken by high-resolution high-voltage TEM (H-1500), with 0.14nm resolution at 800kV. Figure 1(a) shows a CBED pattern taken with [310] incidence. Sharp superlattice reflections without diffuse streaks are observed at $l = 2n$ as indicated by a white arrowhead. Figure 1 (b) shows a [310] CBED pattern taken from a different illumination area than that of Fig. 1(a). It should be noted that sharp superlattice reflections without diffuse streaks are observed at $l = 2n+1$ as indicated by a white arrowhead. Figures 2(a) and 2(b) show dark-field images by using the superlattice reflections at $l = 2n = 4$ and $l = 2n+1 = 3$, respectively as indicated by the white arrowheads in Figs. 1(a) and 1(b). The superlattice domains are clearly seen as many bright striated areas of about 10 nm in width as indicated by white arrowheads. We constructed a model, on the basis of ordering of rotated RuO_6 octahedra about the *c* axis, with *A*- and *B*-centered orthorhombic superlattices (A and B superlattices) that correspond to those of the observed superlattice domains.

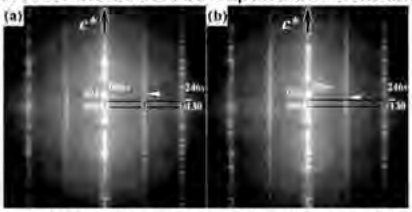

Fig.1: [310] CBED patterns of Ru-1222 taken from (a)one illumination area, (b)a different illumination area compared with that of (a).

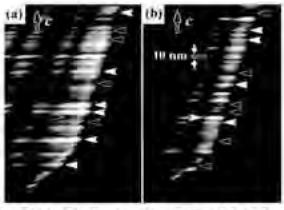

Fig.2: Dark-field images of Ru-1222 by using the superlattice reflections at (a)*l*=4 and (b)*l*=3 in Figs.1(a) and 1(b), respectively.

References

1 Felner, I. *et al.*(1997) *Phys. Rev. B* **55**, R3374.
2 Bernhard, C. *et al.*(1999) *Phys. Rev. B* **59**, 14099.
3 Awana, V. P. S. *et al.* (2002) *Physica C* **249-254,** 378.
4 Yokosawa, T. *et al.*, *Ultramicroscopy* In press.

X-RAY DIFFRACTION STUDY ON THE PHASE TRANSITIONS OF $BaTiO_3$ SINGLE CRYSTAL

Yukio Yoshimura,[a] Naotoshi Tokunaga,[a] Hiroshi Iwasaki,[a] Akira Kojima,[b] Hiroshi Sasou,[b] and Ken-ichi Tozaki[c]

[a]Faculty of Science and Engineering, Ritsumeikan University, Kusatsu, Shiga 525-8577, Japan; [b]Department of Materials Science, The University of Shiga Prefecture, Hikone, Shiga 522-8533, Japan; [c]Department of Physics, Faculty of Education, Chiba University, Chiba 263-8522, Japan (yukio@se.ritsumei.ac.jp)

It is well known that the $BaTiO_3$ crystal undergoes three phase transitions at 408 K, 278 K and 183 K. Recently we have made precise measurements of physical properties such as heat flow, dielectric constants and displacement currents at each phase transition on both heating and cooling using the "mK-stabilized cell" having fine temperature stability[1]. Samples used are single crystals from three different sources grown by the top-seeded solution growth method. Measurements of the heat flow and other physical properties have revealed that both the 408 K and 183 K transitions are accompanied by complicated multi-step anomaly, whereas the 278 K transition showed a single step.

In order to get structural information related to the results of the physical properties mentioned above, the phase transitions in $BaTiO_3$ have been reexamined by X-ray single crystal precession method in the temperature range between 420 K and 90 K. As a temperature is lowered from 420 K, the crystal transforms at 408 K from the perovskite cubic phase into a room temperature phase, where a tetragonal and a monoclinic_forms coexist. The crystal further transforms its structure at 278 K and 183 K. At 278 K transition, the monoclinic_form, one of the coexistence structure, vanishes and the tetragonal lattice changes into another monoclinic_ form with twinned crystal suffering a shear distortion in the low temperature phase. The lowest temperature phase below 183 K is an orthorhombic lattice as a single domain with lattice constants a=0.401 nm, b=0.400 nm, and c=0.402 nm.

Reference

1 Kojima, Y. Kawakatsu, H. Sasou, Y.Yoshimura, N. Tokunaga, H. Iwasaki and K. Tozaki, Ferroelectrics, In press.

ALKALI METAL COMPLEXES OF AROMATIC POLYCARBOXYLATES - A BALANCE OF π-STACKING AND COORDINATE BONDING INTERACTIONS?

George A. Koutsantonis, Stephen Burnet, Annegret K. Hall, Jack M. Harrowfield, Vanessa Sanford, Daan Sauter, Brian W. Skelton, and Allan H. White

Chemistry, School of Chemical and Biomedical Sciences, University of Western Australia, Crawley, WA 6009, Australia (gak@chem.uwa.edu.au)

Crystal structure determinations of, in most cases, hydrated alkali metal derivatives of the dicarboxylic acids, 2,2'-bipyridine-3,3'-dicarboxylic acid (H_2BDC) and chelidamic acid (4-hydroxypyridine-2,6-dicarboxylic acid, H_2CHEL) show numerous similarities, such as in the predominance of *O*-coordination in generating solid state polymers in which parallel arrays of the essentially planar ligand ring units are apparent, though not necessarily indicative of conventional -stacking interactions, and some unanticipated differences. In particular, all species derived from chelidamic acid, including its diammonium compound, appear to be complexes of the partially deprotonated pyridone form of this ligand. In both systems, close contacts between atoms constituting the aromatic entities take a variety of forms depending upon the associated metal.

COMPLEX COINAGE METAL(I) THIOSULFATES

E. J. Chan, B.W. Skelton, and A.H. White

University of Western Australia, School of Biomedical and Chemical Sciences, 35 Stirling Hwy, Crawley, W.A. 6009, Australia (eric@crystal.uwa.edu.au)

Materials crystallized from aqueous solutions of thiosulfates (i.e. Na, K, and NH_4) and coinage metal halides, may be relevant to photographic 'fixation'. Previously known members of the isomorphous, tetragonal *I*-42*d* $M^1_9M^2_2X_2(S_2O_3)_2$, M^1 = group 1 cation, M^2 = (Cu, Ag), series, together with further new members, have been isolated as eight complexes, the nitrates and the potassium/copper adduct all new, containing the complex anion $[M^2(SSO_3)_4]^{7-}$ with quasi tetrahedral S-M-S geometry. Salts of the form $M^1_{(2n-1)}M^2(S_2O_3)_n.xH_2O$, n = 1-3, have also been defined: For n = 3, M^2 = Cu, M^1/x = K/2.25 or 1 5/6, NH_4/6, (and also for the $(NH_4)_4Na/4H_2O$.MeOH adduct) the arrays take the form $M^1_5[Cu(SSO_3)_3].xS$ with distorted trigonal planar CuS_3 coordination environments; the silver counterparts take the form $M^1_{10}[(O_3SS)_2Ag(\mu\text{-}SSO_3)_2Ag(SSO_3)_2]$ for M^1 = K, NH_4. For n = 2 adducts have only been defined for M^2 = Ag, the anions of the M = Na, K adducts being dimeric and polymeric: $Na_6[(O_3SS)_2Ag(\mu\text{-}SSO_3)_2Ag(SSO_3)].3H_2O$, $K_3[Ag(\mu\text{-}SSO_3)_2].H_2O$; a polymeric copper 1 counterpart of the latter is found in $Na_5Cu(NO_3)_2(S_2O_3)_2$ = $2NaNO_3.Na_3[Cu(\mu\text{-}SSO_3)_2]$. For n = 1, $NaAgS_2O_3$, isolated as both the known mono and a new anhydrate, exhibit a two dimensional polymeric complex anion in both forms but with different contributing motifs, 6- and 4- membered rings respectively. $(NH_4)_{13}Ag_3(S_2O_3)_8.2H_2O$ takes the form $(NH_4)_{13}[\{(O_3SS)Ag(\mu\text{-}SSO_3)_2\}_2Ag]$, a linear central silver atom linking a pair of $[Ag(SSO_3)_4]^{7-}$ entities. In $Na_6[(O_3SS)Ag(\mu\text{-}SSO_3)_2Ag(SSO_3)].3H_2O$, two binuclear anions are present as single clusters, the associated oxygen atoms disposed to one side, sandwiching layers of sodium ions.

STRUCTURE DETERMINATION OF ADDUCTS OF LEAD(II) IODIDE WITH N-METHYL SUBSTITUTED ETHYLENEDIAMINE AT LOW AND ROOM TEMPERATURES (123, 209 AND 295 K)

Hiroshi Miyamae, Kouichirou Enomoto, Youhei Maruyama, and Goro Hihara

Department of Chemistry, Josai University, Saitama 350-0295, Japan
(miya@josai. ac.jp)

We have reported that a series of *N*-methyl substituted ethylenediamines forms 1:1 adducts with lead(II) halides [1]. Among them *N,N'*-dimethyl- and *N,N,N'*- trimethyl-ethylendiamine (*N,N'*-en and *N,N,N'*-en) with PbI_2 crystallize in tetragonal forming 4_1 spiral with bridging two of iodides. We examined which part contributes mainly volume contraction upon cooling.

X-ray data were taken at three different temperatures, 296, 209 and 123K. The variation in cell volume and axes are gathered in Table 1. The cell parameters do not vary linearly on cooling, especially for *N,N,N'*-en. However, the contraction could relate to reduction of the nonbonding contacts between the spirals or period of a spiral (Fig. 1). Thus it appears that the ordinal bonds are quite rigid for temperature variation.

Table 1. Cell parameters at different temperatures.

PbI_2-*NNN'*en	123K	209K	296K
a(pm)	848.16(6)	853.96(3)	855.98(3)
b(pm)	1651.4(2)	1669.15(8)	1659.73(7)
V(x10^{6}pm^3)	1188.0(2)	1217.22(8)	1216.09(8)
PbI_2-*NN'*en	123K	209K	296K
a(pm)	879.34(4)	879.43(7)	880.26(5)
b(pm)	1499.04(6)	1509.89(9)	1521.20(7)
V(x10^{6}pm^3)	1159.12(8)	1167.7(1)	1178.7(1)

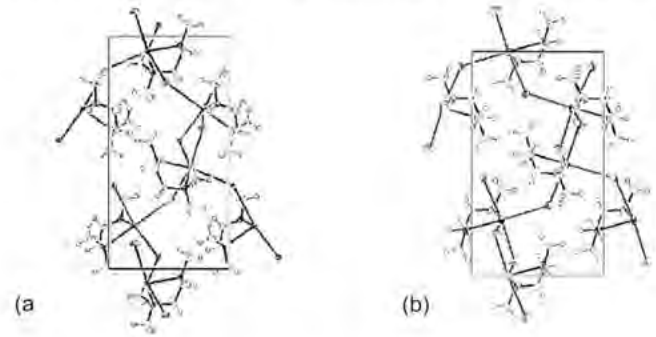

Fig. 1. Crystal packings viewed along ***a*** for PbI_2- *NNN'*en (a) and PbI_2-*NN'*en (b) at 123K.

References

1 Miyamae, H., Hatanaka, Y., Iijima, Y., Hihara, G. and Nagata, M. (1992) *AsCA Program Abstracts*, 16S 44.

UNEXPECTED PIPERAZINE DERIVATIVE LIGANDS FROM A MIXTURE OF $CuCl_2.2H_2O$, Na_2CO_3, AND TRIETHYLENETETRAMINE TETRAHYDRO-CHLORIDE

Norihiro Tamura,[a] Masato Sakai,[b] Katsuya Kudoh,[b] Goro Hihara,[b] and Hiroshi Miyamae[b]

[a]School of Dentistry, Meikai University, Saitama 350-0283, Japan; [b]Department of Chemistry, Josai University, Saitama 350-0295, Japan (miya@josai.ac.jp)

We have already reported that $PbCl_2$ can remove contaminated 2,2',2"-triaminotriethylamine (tren) from commercially available triethylenetetramine (trien) [1]. There are another stories of impurities in trien.

One of us mixed $CuCl_2.2H_2O$ with trien in water, the mixture gave a complex cation as shown in Fig. 1(**1**) with $[CuCl_3]^{2-}$ anion. There is a ligand, 1-(6,3-diaza- hexyl)piperazine, which act as a tridentate with the terminal N of the piperidine ring being protonated. The starting Cu compound contains Cu(II) ion, but in the anion the Cu atom should be oxidation state of +1. The result indicates that the reaction must contain a redox step which might has relation to form a new ligand. The other trial to produce compound **1** gave us two nuclear Cu complex as shown in Fig. 2(**2**), when we had used excess of Na_2CO_3. The ligand is 1,4-bis(2-aminoethyl)piperazine which act as bidentate to each Cu and make bridging. There is no indication for redox process, but the excess of CO_3^{2-} ion seems to compensate the positive charge of the Cu(II) ions.

It is uncertain whether the organics come originally from impurities or from reaction products of the complex formation. However it is one of the good procedures to get the ligands, which are not commercially available.

Fig. 1. The structure of **1**.

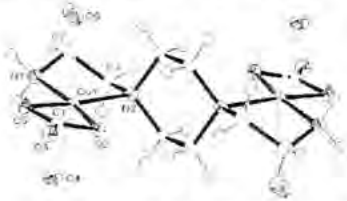

Fig. 2. The structure of **2**.

References

1 Miyamae, H., Yoshinari, K., Hihara, G. and Nagata, M. (1988) *Acta Cryst.* **C44**, 1528-1530.

ANALYSIS OF PHASE TRANSITION MECHANISM OF ACYLUREA DERIVATIVE CRYSTAL BY A DETAILED TEMPERATURE RESOLVED MEASUREMENT OF POWDER X-RAY DIFFRACTION

Daisuke Hashizume,[a,b] Masaru Ogawa,[b] Yasuhiro Iimura,[a] Masanori Yasui,[b] Eiji Nishibori,[c] Masaki Takata,[d] and Fujiko Iwasaki[b]

[a]Advanced D & S Center, RIKEN, Wako, Saitama 351-0198, Japan; [b]Department of Applied Physics and Chemistry, The University of Electro-Communications, Chofu, Tokyo 182-8585, Japan; [c]Department of Applied Physics, Nagoya University, Chikusa, Nagoya 464-8603, Japan; [d]Materials Science Division, JASRI/SPring-8, Mikazuki, Hyogo 679-5198, Japan (hashi@postman.riken.go.jp)

Crystal of 1-(2-chloroacetyl)-3-pentylurea shows a solid-to-solid first order phase transition at 347K with heat absorption of 17 kJ mol^{-1}. During the phase transition, the single crystalline form of the crystal is collapsed. To elucidate mechanism of the transition, we performed powder diffraction analysis to obtain the structures at high temperature phase.

Diffraction data were collected with large Debye-Scherrer camera installed on BL02B2 beam line at SPring-8 using X-rays of 12.398 keV (1.0 Å) at 15 temperature points in the range of 300 to 350K, especially the data from 340 to 350K were collected at every 1K. The phase transition was started from 340K and completed at 346K. Both phases were coexisted at the temperature range. Space group was changed from $P2_1/a$ to P-1 and periodicity along the a axis became a half with the transition.

1-(2-chloroacetyl)-3-pentylurea

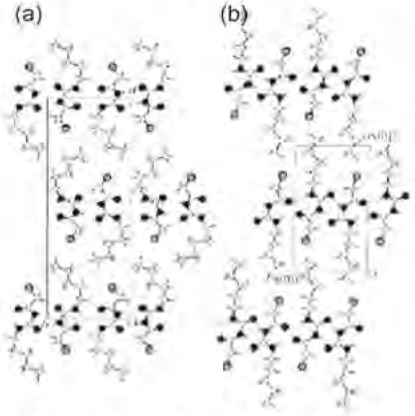

Fig. Crystal Structures of (a) LTP and (b) HTP

The structure at high temperature phase was solved by a simulated annealing method following Pawley refinements. At low temperature phase, carbonylurea moieties form one-dimensional hydrogen bonding ribbon structure and the pentyl group at the N-terminal of the carboxyurea moiety sticks out from the ribbon. After the transition, the ribbon structure is maintained but relative positions of the ribbons are changed with rotation of whole the ribbon structures. Conformation of the pentyl group is drastically changed. The conformational variations may be coupled with the change of relative position between the ribbon structures.

OBSERVATION OF THE PHOTO-EXCITED STRUCTURE OF PLATINUM COMPLEXES

Nobuhiro Yasuda, Hidehiro Uekusa, and Yuji Ohashi

Department of Chemistry and Materials Science, Tokyo Institute of Technology, Ookayama, Meguro-ku, Tokyo 152-8551, Japan (nyasuda@chem.titech.ac.jp)

It was reported that the crystal lattice of the platinum complex, $[Bu_4N]_4[Pt_2(pop)_4]$ (pop = $[P_2O_5H_2]^{2-}$), contracted on exposure to visible light and back to the original cell dimensions when the irradiation was stopped [1]. The contraction was assumed to be due to the formation of the excited state by photo irradiation. In order to examine the photo-excited structure of the platinum complex anion, the structures of several related platinum complex crystals during the irradiation were analyzed by X-ray diffraction method at low temperatures [2]. The crystals have tetrabutylammonium(I), tetrapentylammonium(II), benzyl(triethyl)ammonium(III), benzyl(tributyl)ammonium (IV) and benzyl(dimethylphenyl)ammonium(V) as cation. In some crystals, solvent molecules are included and polymorph structures were found.

The preliminary structure analysis by X-rays revealed that the chemical formula of the platinum complex (I-IV) is not $[Pt_2(pop)_4]$ but $[Pt_2H_2(pop)_4]$, as shown in Figure 1. This means that two protons are attached to the phosphate groups, which are clearly assigned by the differential density map or the P-O distances.

Each crystal was irradiated with the filtered xenon light (λ_{max}=470nm) at low temperatures (173 and 103 K) and the three dimensional crystal structures were analyzed before and during the irradiation. The unit-cell volume decreased, ΔV=20.33(24) and 13.86(23) Å^3 for II and III, respectively (Table 1). Comparing the structures between on and off, the Pt-Pt and Pt-P distances decreased significantly by the light irradiation (Table 2). These results clearly indicate that photo-excited structures were observed by laboratory X-ray analysis.

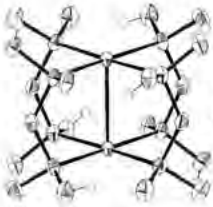

Figure 1
$[Pt_2H_2(pop)_4]^{2-}$ anion

Table 1 Unit-cell volume before and during the irradiation

	Light OFF (Å^3)	Light ON (Å^3)	Δ(ON-OFF)
I	1320.18(3)	1312.16(5)	-8.02(8)
II	3046.45(7)	3026.12(17)	-20.33(24)
III	2108.78(12)	2094.92(11)	-13.86(23)
IV	2696.42(16)	2691.27(12)	-5.15(28)
V	3613.30(6)	3607.44(6)	-5.86(12)

Table 2 The difference of averaged bond distance (Δ(on-off))

	Pt-Pt (Å)	Pt-P (Å)	P-O(-H) (Å)	P-O(-P) (Å)	P=O (Å)
I	-0.0038(3)	-0.0060(10)	-0.003(3)	-0.003(3)	-0.003(3)
II	-0.0082(3)	-0.0053(11)	-0.003(4)	-0.003(3)	0.002(3)
III	-0.0127(5)	-0.0085(16)	-0.007(5)	-0.009(5)	-0.002(5)
IV	-0.0030(3)	-0.0019(12)	0.001(4)	-0.001(4)	-0.005(4)
V	-0.0019(2)	-0.0033(8)	-0.003(3)	-0.002(3)	-0.001(3)

References

1 Ikagawa, T., Okumura, T., Otsuka, T. and Kaizu, Y. (1997) *Chem. Lett.* **26**, 829-830.

2 Yasuda, N., Kanazawa, M., Uekusa, H. and Ohashi, Y. (2002) *Chem. Lett.* **31**, 1132-1133.

DISORDER IN STRUCTURAL CRYSTALLOGRAPHY

S. Banerjee, and A. K. Mukherjee

Department of Physics, Jadavpur University, Calcutta – 700 032, India
(surajit@juphys.ernet.in)

Structural disorder is a long standing problem in X-ray crystallography and the accuracy and reliability of final results of structure analysis depend largely on the degree of disorder present in the system. A disorder in a crystal is often associated with poor quality of diffraction data leading to an apparently high final R factor. But certain types of disorder are potentially informative about the bonding and the chemistry of the compounds in which they occur. A disorder usually occurs when there are more sites available to a set of atoms in a particular structure than the number of atoms to fill them. Three common types of disorder encountered in structural crystallography are (i) solvent disorder (ii) positional disorder (iii) orientational disorder. Here we present the positional disorder of three oxo-peroxo tungsten complexes which are important for their catalytic activity as a part of our ongoing study of molybdenum/tungsten complexes of organic ligands. All complexes crystallize in same monoclinic system with different space groups having disorder in the oxo-peroxo sites with occupancies (66%, 34%), (53%, 47%) and (51%, 49%), respectively. The geometry around the W atom can be best described as distorted pentagonal bipyramidal with the axial sites being occupied by one oxo and one ligand oxygen atoms[1,2]. All the structures are stabilized by Van der Waals forces.

References

1 Gresley, N. M., Griffith, W. P., White, A. J. P. and Williums, D. J. (1997), *J. Chem. Soc., Dalton Trans.*, 89-92.

2 Griffith, W. P., Parkin, B. C., White, A. J. P. and Williums, D. J. (1995), *J. Chem. Soc., Chem. Commun.*, 2183-2184.

NOVEL CRYSTAL STRUCTURES OF VANADYL GALLOPHOSPHATES

Sue-Lein Wang

Department of Chemistry, National Tsing Hua University, Hsinchu, Taiwan 300 (slwang@mx.nthu.edu.tw)

Substitution of the first-raw transition metal (TM) ions for Al^{3+} in the frameworks of aluminum phosphates is of particular interest for the enhancement of catalytic activity and the design of novel catalysts. The location and environment of the TM ion site is of considerable importance for understanding the catalytic and adsorptive properties of molecular sieves. As only few single-crystal data available for most of the MAlPO-*n* samples, actual incorporation of TM ions into the tetrahedral frameworks is difficult to prove [1] Owing to the similarity in the framework topology, the search for gallium phosphates adopting microporous structures has attracted much attention [2,3] By employing hydrothermal crystallization, we have prepared a series of novel open frameworks including the first 24-ring containing gallium phosphate phase [4] which exhibits large channels with a measured pore diameter of ~11.2 Å. In this presentation, the crystal structures and magnetic properties of several large-channel containing VGaPO frameworks shall be described and discussed.

References

1 Hartmann, M., Kevan, L., (1999) *Chem. Rev.* **99**, 635, and references therein.
2 Cheetham, A. K., Ferey, G., Loiseau, T. (1999) *Angew. Chem. Int. Ed.* **38**, 3268.
3 Lin, C. H., Wang, S. L. (2000) *Chem. Mater.* **12**, 3617, and references therein.
4 Lin, C. H., Wang, S. L., Lii, K. H. (2001) *J. Amer. Chem. Soc.* **123**, 4649.

ON THE DIELECTRIC CONSTANT OF $Ba_{6-3x}R_{8+2x}Ti_{18}O_{54}$(R=Sm,Nd) SOLID SOLUTIONS: CRYSTAL STRUCTURAL ANALYSIS

H. Sakashita, H. Ohsato, N. Araki, and K. Kakimoto

Nagoya Institute of Technology, Nagoya 466-8555, Japan
(ohsato@mse.nitech.ac.jp)

Recently, microwave telecommunication technology, for example portable telephones and satellite broadcasting, has been developing rapidly. In the developmental process, microwave dielectric ceramics with high dielectric constant have contributed to the miniaturization of the resonators. Especially, tungstenbronze type-like $Ba_{6-3x}R_{8+2x}Ti_{18}O_{54}$ solid solutions have large permittivity in addition to the high quality factor and nearly zero temperature coefficient of resonant frequency. We have reported the results of the extensive crystal structural investigations on tungstenbronze type-like solid solutions formed with many rare-earth ions. Presently, we report the structural correlations with the dielectric constant in the tungstenbronze type-like solid solutions formed with Sm and Nd. Single crystals of solid solutions were grown by self-flux method. Structural data were deduced by performing crystal structure analysis on the raw data obtained from x-ray 4-circle goniometer (ω-2θ scan and λ=0.71073).

The structural network of this solid solutions are composed of squares (*A*1-site: Sm/Nd), pentagons (*A*2-site: Ba & Sm / Ba & Nd) and octahedrons (Ti). Individual site-volumes and the octahedral tilting angles are calculated from the precision structural data. It is found that there is an explicit correlation between the site-volumes and dielectric constant in the series of solid solutions synthesized and analyzed. The volume of *A*1-site and octahedron at x= 0.5 is higher than that of at x= 0.71 with an exception only for *A*1(4)-site for Sm solid solutions. Also, the tilting angle of TiO_6 along the *c*-axis is smaller at x=0.5 in comparison to that of at x=0.71. A similar trend is also observed in solid solutions prepared with Nd. These structural correlations with dielectric constant of solid solutions will be presented in detail.

DEUTERIUM TRANSFER MECHANISM IN CHIRAL THIOLACTAM FORMATION BY NEUTRON DIFFRACTION MEASUREMENT USING BIX-III DIFFRACTOMETER

Takaaki Hosoya,[a] Hidehiro Uekusa,[a] Yuji Ohashi,[a] Takashi Ohhara,[b] Ichiro Tanaka,[c] and Nobuo Niimura[c]

[a]Department of Chemistry and Materials Science, Tokyo Institute of Technology, O-okayama, Meguro, Tokyo 152-8550, Japan; [b]Institute of Materials Structure Science, High Energy Accelerator Research Organization, Oho, Tsukuba, Ibaraki 305-801, Japan; [c]Neutron Structural Biology, Advanced Science Research Center, Japan Atomic Energy Research Institute, Tokai-mura, Naka-gun, Ibaraki 319-1195, Japan (thosoya@chem.titech.ac.jp)

It has been found that *N,N*-dibenzyl-1-cyclohexenecarbothioamide **1a** is photo-isomerized to optically active β-thiolactam **2a** in high optical yield in the solid state [1]. Although X-Ray diffraction study of crystalline-state photoreaction from **1a** to **2a** revealed the mechanism of chiral β-thiolactam formation, the hydrogen transfer process remained unsolved. In order to make clear the mechanism, the neutron diffraction technique was applied to a new compound **2a** with all benzyl hydrogen atoms of **1a** were replaced with deuterium atoms. The photo-product **2b** from **2a** has a methylene carbon atom with a hydrogen and a deuterium atoms, "chiral methylene". The absolute configuration of this "chiral methylene" indicates the direction of deuterium transfer, *i.e.*, via intramolecular or intermolecular. We used neutron-IP diffractometer BIX-III to determine the absolute configuration of this chiral methylene. The difference Fourier map clearly showed negative and positive peak around the chiral methylene, corresponding to a hydrogen and a deuterium, respectively. This result revealed that a deuterium atom bonded to the benzyl carbon atom was transferred to the intramolecular cyclohexene carbon to occupy the equatorial position of the produced cyclohexyl ring.

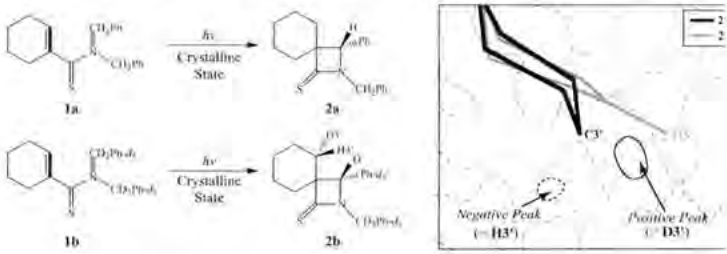

Because the deuterium should occupy the axial position if it was transferred from the neighboring benzyl carbon.

References

1 Sakamoto, M., Takahashi, M., Kamiya, K., Yamaguchi, K., Fujita, T. and Watanabe, S. (1996) *J. Am. Chem. Jpn.* **118**, 10664.

2 Hosoya, T., Ohhara, T., Uekusa, H. and Ohashi, Y. (2002) *Bull. Chem. Soc. Jpn.* **75**, 2147.

STRUCTURE OF THE PSEUDORHOMBOHEDRAL $InFe_{1-x}Ti_xO_{3+x/2}$ COMPOSITE CRYSTAL

Yuichi Michiue,[a] Mitsuko Onoda,[a] Francisco Brown,[b] Noboru Kimizuka,[c] and Mamoru Watanabe[a]

[a]Advanced Materials Laboratory, National Institute for Materials Science, 1-1 Namiki, Tsukuba, Ibaraki, 305-0044, Japan; [b]Departamento de Investigaciones en Polimeros y Materiales, Universidad de Sonora, Rosales s/n Hermosillo, Sonora, C.P.83000, Mexico; [c]Ceramic Materials Research Institute, Hanyang University, 17 Haengdang-dong, Seongdong-gu, Seoul 133-791, Korea (MICHIUE.Yuichi@nims.go.jp)

In pseudobinary systems $InAO_3$-$In_2Ti_2O_7$ (A:Fe, Ga, Al, Cr), composite crystals $InA_{1-x}Ti_xO_{3+x/2}$ with two types of layered structures were found [1]. The one obtained in the Ti-rich region has the pseudorhombohedral (p-R) structure and the other in the A-rich region does the pseudohexagonal (p-H). The incommensurately modulated structure of the p-H $InFe_{1-x}Ti_xO_{3+x/2}$ was clarified by the 4-dimensional superspace group analysis for diffraction data of a single crystal [2]. In this paper the structure of the p-R form is discussed on the basis of the profile fitting of X-ray diffraction patterns.

The structure of a commensurate (x=2/3) p-R form for A=Fe is shown in Fig. 1. In analogy with the p-H form, the p-R phases are also described as the composite crystal consisting of the two subsystems with different periods along the b-axis. The first subsystem is constructed by InO_6 octahedral sheets and the Fe/Ti atoms in a slab at z=0.5, while the second one is made only by the O atoms in the slab containing the Fe/Ti atoms. Atomic arrangement in the slab is given in Fig. 2, which is similar to that seen in a part of the p-H structure [2].

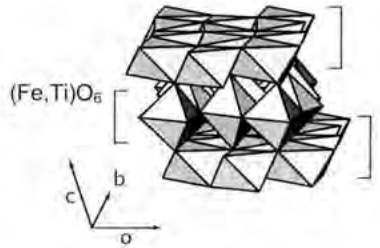

Fig.1 Structure of psuedorhombohedral

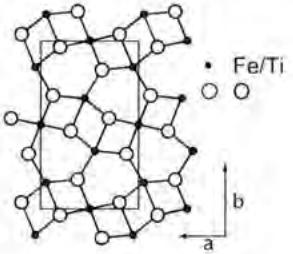

Fig.2 Atomic arrangement in the slab at z=0.5 .

References

1 Brown, F., Flores, M. J. R., Kimizuka, N., Michiue, Y., Onoda, M., Mohri, T., Nakamura, M. and Ishizawa, N. (1999) *J. Solid State Chem.* **144**, 91-99.

2 Michiue, Y., Onoda, M., Watanabe, M., Brown, F. and Kimizuka, N. (2001) *Acta Crystallogr.* **B57**, 458-465.

USING THE HREM TO STUDY MORPHOLOGY AND STRUCTURE OF NANOMATERIAL Ta AND TaN_x

Vo Vong,[a] Luu tien Hung,[b] Steffen Schulze,[c] and Michael Hietschold[c]

[a]Laboratory of Electron Microscopy - National Centre for Natural Science and Technology, 18 Hoangquocviet Str., Caugiay Hanoi, Vietnam; [b]Department of Physics, Vinh University, Vinh City, Nghean, Vietnam; [c]Institute of Physics, Chemnitz University of Technology, D-09107 Germany (vvemlab@ncst.ac.vn)

The grain sizes, phases, structures and morphology of Ta and TaN_x thin films on Si and SiO_2 substrates, which belong to the most promising barrier materials for copper in interconnect systems of semiconductor devices were determined by using high resolution electron microscopy (HREM).

In this work, we present the sample preparation of these films for TEM plan-view investigations. Special efforts had to be made in order to reach electron transparency despite of the high internal stress in the thin films. In detail, we discuss the grain sizes, phases and structures of the films and alloys as deduced from bright-field and dark-field images and selected area electron diffraction patterns.

STRUCTURE–BASED DESIGN OF ANTI-INFLAMMATORY AGENTS: CRYSTAL STRUCTURE OF A COMPLEX FORMED BETWEEN COBRA VENOM PHOSPHOLIPASE A2 AND A DESIGNED POTENT PEPTIDE INHIBITOR VAL-ALA-PHE-ARG-SER- (VAFRS) AT 1.9 Å RESOLUTION.

R. K. Singh, J. Makker, P. Vikram, M. Paramsivam, T. Jabeen, S. Sharma, S. Dey, P. Kaur, A. Srinivasan and T. P. Singh

Department of Biophysics, All India Institute of Medical Sciences, New Delhi-110029, India (rajendra84@hotmail.com)

Phospholipase A_2 (PLA_2) is a key enzyme involved in the production of prostaglandins and other related compounds collectively known as eicosanoids. These substances mediate inflammatory response in humans. Among several structure-based designed peptide molecules, a pentapeptide VAFRS showed an inhibition of PLA_2 with a binding constant of 10^{-11}M. In order to understand the mechanism of binding and evaluate the interactions between PLA_2 and peptide VAFRS, a complex between PLA_2 and VAFRS was prepared. The complex was crystallized using 35% ethanol as a precipitant. The crystals belong to space group $P4_1$ with a = b = 42.8 Å, and c = 65.9 Å. The crystals diffracted to 1.9 Å resolution. The structure was determined by molecular replacement method and refined to an R-value of 0.182. The peptide was located at the binding site of PLA_2. It formed several hydrogen bonds and van der Waals interactions. The most notable interactions were observed with the Arg of peptide molecule. The side chain of arginine formed multiple interactions with Asp49, His 48, Cys 45, Gly 30, Tyr 28 indicating the significance of its substitution at polar end of the peptide. The VAF part of the peptide was involved in a number of van der Waals interactions in the hydrophobic channel. The prominent conformational differences between the native cobra PLA_2 and the PLA_2 in the complex were restricted to ß-wing and the C- terminal regions of the enzyme. Indeed, the structure provided an excellent model based on the method of structure based drug design.

Tuesday August 12

AsCA'03/Crystal-23

ABSTRACTS

ORAL SESSIONS

ULTRA-HIGH SPEED NEUTRON DIFFRACTION STUDIES: COMBUSTION SYNTHESIS OF Ti_3SiC_2 AND RELATED COMPOUNDS

Erich H. Kisi, and Daniel P. Riley

School of Engineering, The University of Newcastle, Callaghan NSW 2308, Australia (meehk@cc.newcastle.edu.au)

Ti_3SiC_2 is an exciting new material that combines the attractive properties of both metals and ceramics. Combustion synthesis (or Self-propagating High-temperature Synthesis, SHS) has received considerable attention as a low cost alternative to synthesising materials such as Ti_3SiC_2. The process is attractive because, after an initial input of heat to initiate the reaction, the heat of formation of the product phases supplies all of the remaining energy requirement. A quantitative understanding of SHS has been hampered by the rapid reaction rates and high temperatures involved.

In-situ neutron diffraction patterns (0-160°) at 0.9s and 0.38s time resolution were used to capture the reaction mechanism during SHS of Ti_3SiC_2 from furnace ignited stoichiometric Ti/SiC/C, Ti/Si/C and $Ti/Al_4C_3/C$ mixtures. As shown in Fig 1, the diffraction patterns are rich in detail. They indicate five stages: (i) pre-heating of reactants, (ii) *hcp*→*bcc* phase transformation in Ti, (iii) pre-ignition reactions, (iv) formation of a single solid intermediate phase in ~0.5s and (v) rapid precipitation of Ti_3SiC_2 after a short incubation period. The intermediate phase is believed to be a solid solution of Si in TiC which preserves the overall stoichiometry, (3Ti:1Si:2C). The results are quite general, applying to all of the reactants studied and independent (apart from the ignition temperature) of the physical state of the reactant powders.

Lattice parameters and known thermal expansion data were used to estimate the ignition and combustion temperatures eg, in the system 3Ti+SiC+C, these were 923(10) °C and 2320(50) °C respectively. An anomaly in the cooling curve measured in this way was used to propose a diffraction-based thermal analysis technique capable of supplying estimates of phase transition enthalpies.

Fig. 1. Three dimensional plot of a portion of the diffraction patterns during SHS of Ti_3SiC_2. Time is on the y-axis, two theta on the x-axis and diffracted intensity on the z-axis. The labels refer to peaks from (a) α-Ti, (b) α-Ti (decreasing) and β-Ti (increasing), (c) SiC, (d) the intermediate phase and (e) Ti_3SiC_2.

ELECTRON MICROSCOPY TECHNIQUES - MICROSCOPY, DIFFRACTION AND SPECTROSCOPY

Michiyoshi Tanaka

Institute of Multidisciplinary Research for Advanced Materials, Tohoku University
Katahira 2-1-1 Aoba-ku, Sendai Japan (tanakam@tagen.tohoku.ac.jp)

The electron microscope has three functions for the characterization of materials, 1) microscopy, 2) diffraction and 3) spectroscopy.

1) The spatial resolution of the standard electron microscope has been a little less than 0.2 nm. Recently, owing to the development of the correction techniques of the spherical aberration of the objective lens, the resolution is reaching 0.1nm. It is, however, noted that the resolution is far from the wavelength of the electrons, namely 0.0025nm at 200kV, because the convergence angle of the electron beam allowed is only about 10^{-2} rad. Further development of electron optics is strongly expected for the improvement of the spatial resolution.

2) Electron diffraction is divided into two techniques. The first is selected area diffraction (SAD), which has been long time used as the standard technique. The second is convergent beam electron diffraction (CBED), which uses a convergent beam instead of a parallel beam used in SAD. CBED can determine all the 32 crystal point groups using dynamical diffraction effect, while X-ray diffraction can determine 11 Laue groups. Dynamical extinctions allow us to distinguish between mirror planes and glide planes, and rotation axes and screw axes. As a result, CBED can determine most space groups using the dynamical extinctions. A nanometer-scale crystal structure refinement can be performed by fitting the reflection intensities of CBED patterns with simulation patterns, where the phase problem does not appear because the reflected intensities contain phase information due to multiple reflections in the materials. The defocus technique or the large angle technique (LACBED), by which both the information from the real and reciprocal spaces can be obtained, can determine unambiguously the quantitative feature of crystal defects, while the traditional electron microscope method uses only limited information from the defects.

3) Electron spectroscopy is increasing its importance, because it can obtain spectra from nanometer-scale areas and can cover a very wide energy range, namely from 1 to 1000eV. Electron energy loss spectroscopy (EELS) and wave dispersive spectroscopy (WDS) with an about 0.2eV energy resolution are very effective for the analysis of electronic structures of materials. CBED is the major subject to be reported in this talk.

CATALYSIS AND ALLOSTERIC REGULATION IN PHOSPHORIBOSYL DIPHOSPHATE SYNTHASE; THE ROLE OF TWO MAGNESIUM IONS

Sine Larsen, and Frank B. Nygaard

Centre for Crystallographic Studies, University of Copenhagen, Universitetsparken 5, 2100 Copenhagen, Denmark (sine@ccs.ki.ku.dk)

5-Phospho-D-ribosyl "-1-diphosphate (PRPP) provides exclusively the ribose moiety present in all purine, pyrimidine and pyridine nucleotides. The essential metabolite PRPP is prepared in a reaction between ATP and ribose-5 phosphate, catalysed by enzyme PRPP synthase (PRPPase). The key position of PPRP in the metabolism of the cell explains why the activity of PRPPase is highly regulated. Most PRPPases are regulated in an allosteric manner, in which purine nucleotides especially ADP acts as the most potent inhibitor. Inorganic phosphate (P_i) is an activator of bacterial and mammal PRPPases. MgATP is the true substrate for PRPPases, but in addition the enzyme requires a free Mg^{2+} ion as an activator. The structure of the PRPPase from *Bacillus subtilis* has been determined complexed with sulfate (mimicking P_i), ADP and Cd^{2+}. All structures reveal the same hexameric arrangement of the PRPPase subunits in which crystallographic threefold symmetry relates two independent subunits related by non-crystallographic twofold symmetry. Furthermore the structures made it possible to identify the binding sites for substrates, activators, allosteric inhibitors and divalent metal ions [1,2]. However it could not be ascertained which state of the enzyme the different complexes represented, as neither of them contained structural information about the supposedly active site loop rich in conserved residues.

The structures have been determined for six additional complexes of the PRPPase from *B. subtilis* determined from crystals grown under different experimental conditions making use of the kinetic data for the enzyme [3]. It was possible to trace the active site loop in the structure, which had the transition state analogue AlF_3 bound. The complex with the allosteric inhibitor GDP gave similar information about the allosteric regulation. The new structural results have enabled us to propose detailed reaction models for both catalytic function and allosteric regulation of the enzyme, that can explain the abundant kinetic data available for the enzyme. The two Mg^{2+} ion play a crucial role in catalysis, and the allosteric regulation can be rationalized in terms of domain movements in the subunits and subunit movements within the hexamer, that can explain why single point mutations in the *prs* gene causes severe illness.

References

1 Eriksen, T. A., Bentsen, A. -K., Kadziola, A., Harlow, K. W. and Larsen, S. (2000) *Nature Struc. Biol.* **7,** 303-308.

2 Eriksen, T. A., Kadziola, A. and Larsen. S. (2000) *Protein Science* **11,** 271-279.

3 Willemoës, M, Hove-Jensen, B. and Larsen, S (2000) *J. Biol. Chem.* **275,** 35409-35412.

ENZYMES OF RIBOSE METABOLISM: STRUCTURE AND MECHANISM

Sherry L. Mowbray,[a] C. Evalena Andersson,[b] Annette Roos,[b] Torsten Unge[b] and T. Alwyn Jones[b]
[a]Department of Molecular Biosciences, Division of Structural Biology, Swedish University of Agricultural Sciences, BMC, Box 590, SE-751 24 Uppsala, Sweden; [b]Department of Cell and Molecular Biology, Uppsala University, BMC, Box 596, S-751 24 Uppsala, Sweden (mowbray@xray.bmc.uu.se)

Although it is well established that ribose is a crucial sugar, its metabolism has only recently been investigated from a structural and mechanistic point of view. Our studies have explored the ribokinase and ribose-5-phosphate isomerases essential for using (and re-cycling) ribose, as well as in its interconversion with other sugars.

Ribokinase was the first example of a new fold since found in related enzymes such as adenosine kinase. Conformational changes associated with ribose binding also are typical of the family[1]. Ribokinase's activation by a monovalent cation was linked to the formation an anion hole in the active site, the first documented case of allosteric activation of a carbohydrate kinase by an ion[2] Site-directed mutagenesis successfully created an ion-independent version of ribokinase[3].

Ribose-5-phosphate isomerase interconverts ribose-5-phosphate and ribulose-5-phosphate, and is thus an essential enzyme in the pentose phosphate pathway and the Calvin cycle of plants. Two types of unrelated enzyme exist, often within the same organism. The structure of RpiA from *E. coli* was studied together with the groups of Savchenko (Toronto), Edwards (Toronto) and Joachimiak (Argonne)[4]. This was again a new fold; the structure showed how the ribose ring could be opened to provide the linear form necessary for isomerizaton, as well as identifying the groups needed for binding and catalysis. A second, unrelated type of ribose-5-phosphate isomerase from *E. coli* (RpiB) was found to have a completely different fold and catalytic mechanism[5]. The enzyme from *Mycobacterium tuberculosis* has a structure closely related to RpiB, but with a different catalytic mechanism[6]. The three Rpis thus present interesting examples of convergent and divergent evolution.

References

1 Sigrell, J.A., Cameron, A.D., Jones, T.A. & Mowbray, S.L. (1998) *Structure* **6**, 183-193; Sigrell, J.A., Cameron, A.D. and Mowbray, S.L. (1999) *J. Mol. Biol.* **290**, 1009-1018.
2 Andersson, C.E. and Mowbray, S.L. (2002) *J. Mol. Biol.* **315**, 409-19.
3 Andersson, C.E., Roos, A. Unge, T. and Mowbray, S.L. (2003) *in preparation.*
4 Zhang, R., Andersson, C.E., Savchenko, A., Skarina, T., Evdokimova, E., Beasley, S., Arrowsmith, C.H., Edwards, A.M., Joachimiak, A. and Mowbray, S.L. (2003) *Structure* **11**, 31-42.
5 Zhang, R.-g., Andersson, C.E., Skarina, T., Evdokimova, E., Edwards, A.M., Joachimiak, A., Savchenko, A. & Mowbray, S. L. (2003) *J. Mol. Biol.* submitted.
6 Roos, A., Andersson, C.E., Joachimiak, A., Unge,, T., Jones, T.A, and Mowbray, S.L. (2003) *in preparation.*

CRYSTAL STRUCTURE OF TWO KNOTTED PROTEINS: ACETOHYDROXY ACID ISOMEROREDUCTASE AND tRNA(m^1G37)METHYLTRANSFERASE

Se Won Suh, Hyung Jun Ahn, Jin Kuk Yang, Byung Il Lee, and Hye-Jin Yoon

Department of Chemistry, Seoul National University, Seoul 151-742, Korea (sewonsuh@snu.ac.kr)

Acetohydroxy acid isomeroreductase (AHIR) is a key enzyme in biosynthesis of branched chain amino acids. We have determined the first crystal structure of a class I AHIR from *Pseudomonas aeruginosa*. Its dodecameric architecture of 23 point group symmetry is assembled of six dimeric units and dimerization is essential for the formation of the active site. The dimeric unit of *P. aeruginosa* AHIR partially superimposes with a three-domain monomer of spinach AHIR, a class II enzyme, thus demonstrating that (i) the so-called 'plant-specific' insert in the middle of spinach AHIR is structurally and functionally equivalent to the C-terminal α-helical domain of *P. aeruginosa* AHIR, and (ii) the C-terminal α-helical domain was duplicated during evolution from the shorter, class I AHIRs to the longer, class II AHIRs. The dimeric unit of *P. aeruginosa* AHIR possesses a deep figure-of-eight knot, essentially identical to that in the spinach AHIR monomer.

tRNA(m^1G37)methyltransferase (TrmD) catalyzes the transfer of a methyl group from S-adenosyl-L-methionine (AdoMet) to G^{37} within a subset of bacterial tRNA species, which have a residue G at 36^{th} position. The modified guanosine is adjacent to and 3' of the anticodon and is essential for the maintenance of the correct reading frame during translation. We have determined the first crystal structure of TrmD from *Haemophilus influenzae*, as a binary complex with either AdoMet or S-adenosyl-L-homocysteine (AdoHcy), as a ternary complex with AdoHcy/phosphate, and as an apo form. The structure indicates that TrmD functions as a dimer. It also suggests the binding mode of $G^{36}G^{37}$ in the active site of TrmD and catalytic mechanism. The N-terminal domain has a trefoil knot, in which AdoMet or AdoHcy is bound in a novel, bent conformation.

References

1 Ahn, H. J., Eom, S. J., Yoon, H. J., Lee, B. I. and Suh, S. W. (2003) *J. Mol. Biol.* **329**, 000-000. (in press)

2 Ahn, H. J., Kim, H. W., Yoon, H. J., Lee, B. I., Suh, S. W. and Yang, J. K. (2003) *EMBO J.* **22**, 000-000. (submitted)

SUPEROXIDE DISMUTASES FROM HYPERTHERMOPHILES

Geoffrey B. Jameson,[a] Julian J. Adams,[a] Paul D. Hempstead,[a] Irene Morgenstern-Badarau,[b] James W. Whittaker,[c] Edward N. Baker,[d] and Bryan F. Anderson[a]

[a]Centre for Structural Biology, Institutes of Fundamental Sciences and Molecular BioSciences, Massey University, Palmerston North, New Zealand; [b]Institut de Chimie Moleculaire d'Orsay, Bat. 420 Université Paris-Sud XI, 91405 Orsay, France; [c]School of Biological Sciences, University of Auckland, Auckland, New Zealand, [d]Department of Biochemistry and Molecular Biology, Oregon Graduate Institute School of Science and Engineering, Beaverton, Oregon 97006, USA (G.B.Jameson@massey.ac.nz)

The structures of the apo, Fe and Mn forms of the manganese-preferring superoxide dismutase from the hyperthermophilic microaerobic archaeon *Pyrobaculum aerophilum* (*Pa*-SOD) have been determined at 2.0, 2.2 and 1.9 Å, respectively, and the structure of the Fe-specific superoxide dismutase from the thermophilic methanogenic anerobic archaeon *Methanobacterium thermoautotrophicum* (*Mt*-FeSOD) has been determined at 2.6 Å. Corresponding values for R (R_{free}) are, presently, 0.16 (0.20), 0.19 (0.24), 0.17 (0.20), and 0.22 (0.24); the asymmetric unit is a dimer for *Pa*-SODs and a tetramer and half-tetramer for *Mt*-FeSOD.

The extreme thermal stability of Pa-SOD, which survives the autoclaving necessary to insert metal ions into the *E. coli*-expressed apo-protein, appears to arise from a combination of previously identified structural determinants for thermal stability. In particular, both the *Pa*-SODs and the *Mt*-FeSOD form extremely compact tetramers.

In common with all other structurally characterised Mn- and FeSODs, the central metal ions of *Pa*-FeSOD, *Pa*-MnSOD and *Mt*-FeSOD have an identical primary coordination sphere. Three histidines, a monodentate aspartate and a solvent-derived ligand (OH^- in oxidised M^{III} forms) coordinate in a trigonal bipyramidal manner, in which the solvent-derived ligand and a histidine ligand are *trans* to each other. No differences exist in the second coordination sphere – for both species a histidine C-H moiety hydrogen bonds to the solvent-derived ligand, although in many other SODs this aprotic C-H moiety is substituted by a glutamine NH_2 moiety. It is only in the third coordination sphere, involving the hydrogen-bonding network to the amine moiety of the coordinated axial histidine that significant differences can be found not only for these SODs but also for other SODs that have been well-characterised both structurally and functionally. A methionine thioether moiety appears to direct a different hydrogen-bonding network to the axial histidine for Mn-specific SODs, in contrast to Fe-specific SODs where an aliphatic residue is found at this location, position n on the helix supporting the axial histidine at position n+3.

X-RAY ANALYSES OF FAMILY 8 CHITOSANASE FROM *BACILLUS* SP. K17

Wataru Adachi, Shinji Shimizu, Tomoko Sunami, Tesuya Fukazawa, Mamie Suzuki, Rie Yatsunami, Satoshi Nakamura, and Akio Takénaka

Graduate School of Bioscience and Biotechnology, Tokyo Institute of Technology, Nagatsuta, Midori-ku, Yokohama 226-8501, Japan (wadachi@bio.titech.ac.jp)

Glycosylases are classified into 86 families according to the characteristics of their amino acid sequences. Chitosanase from *Bacillus* sp. K-17 (C-K17) belongs to the family 8 and differs from other chitosanases in cleavage site specificity. The family 8 also includes cellulase, xylanase and lichenase. Sequence comparison was difficult to distinguish the difference of their catalytic site. The active site of C-K17 must, however, have some difference in their three-dimensional structures. To understand the structural evolution of the enzymes in the family 8, X-ray analyses of C-K17 have been performed at different pH.

The two structures of the active (pH 6.4) and inactive (pH3.7) forms are almost the same except the Glu74 residue that have two conformations at pH3.7, suggesting its inactiveness. The architecture of the enzyme is composed of a double-α6-barrel structure, the protruded loops from the β-sheets making a large cleft for binding the substrate.

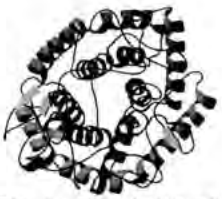

Fig. 1. The double-α6-barrel structure of C-K17.

A structural comparison between cellulase from *Clostridium thermocellum* (CelA) and C-K17 shows that their overall structures are similar, but different in the cleft regions with insertions of additional β-sheets and loops. The Asp residue, which acts as a proton acceptor in CelA, is changed to Asn271 in C-K17. Instead, the inserted Glu261 residue is located close the catalytic site as a proton acceptor.

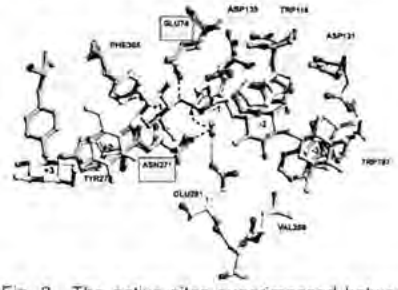

Fig. 2. The active sites superimposed between C-K17(CPK color in gray scale) and CelA(gray). The inserted loop is circled.

Sequence alignment based on the above structural feature shows that proteins in the family 8 are classified into the three subfamilies (A, B and C) according to the proton acceptor, chitosanases and lichenases being in the subfamily A, whereas cellulases and xylanases in the subfamily B. It is thus concluded that the common ancestor of proteins in the family 8 is diverged into three subfamilies by inserting a loop to change the specificity of catalytic reactions.

EXPERIMENTAL SYSTEM FOR X-RAY MAGNETIC DIFFRACTION UNDER EXTREME CONDITIONS

Etsuo Arakawa,[a] Masahisa Ito,[b] Naoki Ishimatsu,[c] Motohiro Suzuki,[d] Naomi Kawamura,[d] Hiroshi Sakurai,[b] Fumitake Itoh,[b] Yoshiya Honma,[e] Akira Ochiai,[f] Yuichi Akahama,[g] Kazuyuki Matsuda,[g] Yoh Kohori,[h] Shunji Kishimoto,[i] Keiichi Hirano,[i] Hiroshi Maruyama,[c] Kazumichi Namikawa,[a] and Osamu Shimomura[j]

[a]Department of Physics, Tokyo Gakugei University, Koganei, Tokyo, 184-8501, Japan; [b]Gunma University, Japan; [c]Hiroshima University, Japan; [d]JASRI/SPring-8, Japan; [e]Inst. of Metal Res., Tohoku University, Japan; [f]Tohoku University, Japan; [g]Himeji Inst. of Tech., Japan; [h]Chiba University, Japan; [i]PF/KEK, Japan; [j]JAERI/SPring-8, Japan (arakawae@u-gakugei.ac.jp)

Experimental system of an x-ray magnetic diffraction with a phase plate under extreme conditions at BL39XU/SPring-8 is reported. The main parts of this system are a superconducting magnet and a diamond anvil cell (DAC). This experimental system is made to study magnetic phenomena under conditions of low temperature (5 K), high magnetic field (6 T) and high pressure (20 GPa).

A method of switching the magnetic field direction has been used so far to measure magnetic signals in the measurement. It is however not suitable for measuring magnetic signals with a superconducting magnet. On the contrary, polarization modulation method which reverses the helicity of the elliptical polarization has been developed to observe magnetic signals in XMCD[1] and resonant x-ray magnetic scattering experiment[2]. The polarization modulation method is suitable for measuring the magnetic signals with a superconducting magnet. Principally, both methods give same magnetic signals.

The experimental system contains four parts; (1) a phase plate of diamond crystal, (2) the superconducting magnet of 6 T, (3) two axis manipulator for adjusting sample orientation in a DAC, (4) five axis goniometer for the magnet. Small single crystal of UTe (0.3 mm x 0.2 mm x 0.1 mm) was mounted in the DAC. Incident x-ray beam of small size (0.1 mm x 0.1 mm) was irradiated on the sample, and the diffracted x-rays were detected at sample temperature of 5 K. Instrumental details of the present system are to be presented.

References

1 Suzuki, M., Kawamura, N., Mizumaki, M., Urata, A., Maruyama, H., Goto, S. and Ishikawa, T. (1999) *J. Synchrotron Radiation* **6**, 190-192.

2 Hashizume, H., Ishimatsu, N., Sakata, O. and Hosoito, N., *et al.*, (1997) *Jpn. J. Appl. Phys.* **36**, 4252.

ELECTRONIC DIPOLE-MOMENT OF HYDROGEN ATOM IN A HYDROGEN-BOND STUDIED BY X-RAY AND NEUTRON

Yukio Noda,[a] Ryoji Kiyanagi,[a] Masashi Watanabe,[a] Hiroyuki Kimura,[a] Akiko Kojima,[b] Tomoyuki Mochida,[c] and Tadashi Sugawara[d]

[a]Institute of Multidisciplinary Research for Advanced Materials, Tohoku University, 2-1-1 Katahira, Aoba-ku, Sendai 980-8577, Japan; [b]Graduate School of Science and Technology, Faculty of Science, Chiba University, Yayoi, Chiba 263-8522, Japan; [c]Department of Chemistry, Faculty of Science, Toho University, Miyama, Funabashi-shi, Chiba 274-8510, Japan; [d]Department of Basic Sciences, Graduate School of Arts and Sciences, The University of Tokyo, Komaba, Meguro-ku, Tokyo 153-8902, Japan (ynoda@tagen.tohoku.ac.jp).

We have performed detailed structure analyses of an isolated hydrogen-bond material MeHPLN ($C_{14}O_2H_{14}$, 5-methyl-9hydroxy-phenalenone)[1] by X-ray and neutron scattering experiments. Since neutrons look nuclei and X-rays look electron cloud, we can get slightly different information from each technique. For neutron experiments, we used a newly developed four-circle diffractometer FONDER installed at JRR3M Tokai[2]. Maximum Entropy method[3] is used to get image of distribution of nuclei and electron cloud.

Both structure analyses gave reasonably good R-factors, and essentially the positional parameters of skeleton atoms are identical. By comparing the distribution of electrons and nuclei of hydrogen atoms participating in the hydrogen bond, we have found peculiar difference of the center of mass of electrons and nuclei. Such displacement of electrons introduces a local dipole moment, which may play an important role in the phase transition of this hydrogen-bonded material. The magnitude of the local dipole moment is about the one seen in the ordinal ferroelectric materials. We also investigated the temperature dependence of the structure down to 8K through the phase transition temperature 34K. Ordering of hydrogen atoms in the hydrogen-bond and methyl-molecule as well as the rotational ordering of molecules were revealed. The transition scheme became clear on this structure analysis. The complimentary usage of neutron and X-ray will open the field of the structural physics.

References

1 Mochida, T., Izuoka, A., Sugawara, T., Moritomo, Y. and Tokura, Y. (1994) *J. Chem Phys.* **101**, 7491.
2 Noda, Y., Kimura, H., Kiyanagi, R., Kojima, A., Morii, Y., Minakawa, N. and Takesue, N. (2001) *J. Phys. Soc. Jpn.* **70**, S456.
3 Sakata, M. and Takata, M. (1990) *Acta Cryst.* **A46**, 263.

THREE-BEAM DIFFRACTION ANOMALOUS FINE STRUCTURE OF GALLIUM ARSENIDE

Shih-Lin Chang,[a] Yen-Ru Lee,[a] Yu. P. Stetsko,[b] Sen-Yuan Cheng,[a] Guin-Gi Lin,[a] Shih-Chang Wong[a] and Wen-Shien Sun[a]

[a]Department of Physics, National Tsing Hua University; [b]National Synchrotron Radiation Research Center, Hsinchu, Taiwan, 300, R.O.C. (slchang@phys.nthu.edu.tw).

The coherent interaction in three-beam diffraction provides information about crystallographic phase [1] and resonance phase shift due to electronic transition [2]. This phase information may be useful in understanding the atomic and electronic structures of the constituent atoms of a crystal. Following this idea a three-beam diffraction anomalous fine structure (DAFS) technique is developed, where three-beam diffraction intensity as a function of x-ray photon energy in the vicinity of an absorption edge is measured.

A [111] cut GaAs single crystal is used as a sample crystal. The diffracted intensity of the three-beam (222/113) case, as well as fluorescence yield are measured for the photon energies covering the GaK and AsK edges. The phase information is used to link the real and imaginary parts of the atomic scattering factors considered. Analysis based on the dynamical diffraction theory and XAFS gives fine structures of DAFS spectra. The details about the experimental aspects and the analysis procedures this technique will be presented and discussed.

References

1 Chang, S.-L., King, H. E., Huang, M.-T., and Gao, Y. (1991) *Phys. Rev. Lett.* **67**, 3113-3116.

2 Stetsko, Yu. P., Lin, Huang, Y.-S., Chao, C.-H., and Chang, S.-L. (2001) *Phys. Rev. Lett.* **86**, 2026-2029.

THE NEW QUASI-LAUE DIFFRACTOMETER AT THE REPLACEMENT RESEARCH REACTOR

Wim T. Klooster

Bragg Institute, ANSTO, PMB 1, Menai, NSW 2234, Australia
(wim@ansto.gov.au)

The new single-crystal diffractometer for the Replacement Research Reactor will be a quasi-Laue diffractometer, similar to VIVALDI at ILL, France. It will be competitive with the best instruments currently available. Data collection times for a normal structure determination will be less than a day, a considerable improvement on current data collection times, typically a few weeks at HIFAR. Also, the crystal size needed for an experiment can as small as about 0.1 mm^3, opening up new research areas where it has proved difficult to grow crystals sufficiently big (several mm^3) which are currently needed. Another area of research opening up will be multiple temperature and/or pressure measurements.

This new instrument will be a useful tool to obtain structural information in a timely fashion, where x-rays do not provide enough detail.

The instrument will be on the end of a thermal supermirror guide, and we are exploring the possibility of enhancing the flux further by using a converging guide section immediately before the instrument itself.
More detailed information on the instrument will be presented.

VALENCE AND STRUCTURAL PHASE TRANSITIONS IN THE SERIES $Ba_2PrRu_{1-x}Ir_xO_6$

Brendan J. Kennedy,[a] Leqing Li,[a] Christopher J. Howard[b] and Brett A. Hunter[b]

[a]The School of Chemistry, the University of Sydney, Sydney, NSW 2006, Australia; [b]ANSTO, PMB1 Menai NSW 2234, Australia; (b.kennedy@chem.usyd.edu.au)

There is considerable interest in the magnetic and electronic properties of the 4d and 5d oxides. The double perovskites Ba_2PrRuO_6 and Ba_2PrIrO_6 both exhibit rocksalt ordering of the B-type cations (Pr and Ru(Ir)). Previous studies have demonstrated that in the Ru compound the oxidation states are Pr(III) and Ru(V) whereas in the Ir compound they are Pr(IV) and Ir(IV). The series of oxides $Ba_2PrRu_{1-x}Ir_xO_6$ might therefore be expected to show interesting properties and structures.

High-resolution powder synchrotron diffraction studies of 15 members in the series $Ba_2PrRu_{1-x}Ir_xO_6$ have been undertaken at the ANBF. These studies have confirmed that the structure of Ba_2PrRuO_6 is best described in the monoclinic space group $P2_1/n$, however we find that Ba_2PrIrO_6 is in fact tetragonal and can be adequately described in $P4/mnc$. The transition between these two structural types is related to the relative size of the B-cations involved and occurs near x = 0.3. That is the Pr exists in the +3 oxidation state in the Ru rich compounds and this stabilizes a $a^+b^-b^-$ tilt patterns so that the structure is monoclinic. In the Ir rich compounds the Pr is present in the +4 oxidation state and the reduction in size of the Pr cation alters the tilt system is $a^0a^0c^+$. Interestingly although a continuous $P4/mnc$ to $P2_1/n$ transition is allowed, in the present compounds this is observed to be first order and there is a two-phase region between x = 0.4 and 0.5.

The temperature dependence of the $P2_1/n$ to $P4/mnc$ transition in two members of this series have been also investigated using both synchrotron and powder neutron diffraction methods. These measurements confirm the first order nature of the monoclinic to tetragonal transition. In both cases the volume of the tetragonal structure is noticeably smaller than the monoclinic structure as a consequence of the change in the Pr valency.

STRUCTURE OF THE PUTATIVE ANTITERMINATOR PROTEIN Rv1626 FROM MYCOBACTERIUM TUBERCULOSIS

J. P. Morth,[a] V. Feng,[b] L. J. Perry,[b] and P. A. Tucker[a]

[a]EMBL c/o DESY Hamburg Outstation, D-22603 Hamburg, Germany; [b]Molecular Biology Institute, UCLA, CA 90095, USA (premo@embl-hamburg.de)

The project is a part of the *Mycobacterium tuberculosis* structural genomics project. Rv1626 was initially identified by sequence comparison as a response regulator of a two component system without an apparent histidine kinase associated with it. Just recently a new domain type was discovered by sequence comparison, the domain was found in (A)miR and (N)asR (T)ranscription (A)ntitermination (R)egulators (ANTAR) [1]. Rv1626 contain a C-terminal ANTAR domain in addition to the N-terminal receiver domain, common to response regulators.

The untagged Rv1626 was purified from an *E. coli* expression strain, and crystallised using the microbatch method. Heavy atom derivitation was done by a quick soak using sodium iodide. The structure was solved by single anomalous scattering (SAS) from the anomoluos signal of iodide. The structure shows high structural similarity to an antiterminator protein AmiR, except for a kink region in the linker helix between the N- and C- terminal domains of Rv1626, which breaks up the proposed coiled coil found present in the AmiR dimer.

References

1 Shu, C. J. and Zhulin, I. B. (2002) *TRENDS in Biochemical Science* **27**, 3-5.

STRUCTURAL STUDIES OF LATEXIN, A NOVEL CARBOXYPEPTIDASE INHIBITOR

Anna Aagaard,[a] Pawel Listwan,[b] Nathan Cowieson,[a] Thomas Huber,[c] Christine Wells,[a] Timothy Ravasi,[a] Bostjan Kobe,[a,b] David Hume,[a] and Jennifer Martin[a]

[a]Institute for Molecular Bioscience, The University of Queensland, Brisbane, QLD 4072, Australia; [b]Department of Biochemistry and Molecular Biology, The University of Queensland, Brisbane, QLD 4072, Australia; [c]Advanced Computational Modelling Centre, The University of Queensland, Brisbane, QLD 4072, Australia (a.aagaard@imb.uq.edu.au)

Latexin is a 222 amino acid protein possessing inhibitory activity against carboxypeptidase A1 (CPA1) and CPA2 as well as mast-cell CPA[1]. It is unusual in the sense that it is by far the largest proteinaceous carboxypeptidase inhibitor so far reported[2]and it shows no sequence similarity to any of the other known carboxypeptidase inhibitors. Furthermore, it is the only known CPA protein inhibitor of mammalian origin[1]. Studies on rat and human latexin showed that it is expressed in many different tissues including heart, prostate, ovary and kidney[3].

We found that latexin is also expressed at high levels in mouse macrophages and is further inducible in these cells by lipopolysaccharide. Based on these results, latexin was selected as a target for structural studies as part of a focused high throughput crystallography project at The University of Queensland. The gene was cloned and the protein expressed in *E. coli*. We used an autoinduction method to produce tens of milligrams of native and selenomethionine labelled protein from 500 ml cultures. Crystals of both the native and labelled protein were obtained by means of hanging-drop vapour diffusion using a 96-well format crystallisation tray. Conditions for freezing crystals have been identified and frozen crystals diffract to 2.2 Å on our in-house X-ray equipment. Beamtime has been allocated for both MAD and native data collection at the Advanced Light Source in Berkeley early in 2003. We expect that the structure of the protein will be solved from the MAD data. Results from these experiments will be presented at the conference.

References

1 Normant, E., et al., Proceedings of the National Academy of Sciences of the United States of America, 1995. **92**(26): p. 12225-12229.

2 Vendrell, J., E. Querol, and F.X. Aviles.Biochimica Et Biophysica Acta-Protein Structure and Molecular Enzymology, 2000. **1477**(1-2): p. 284-298.

3 Liu, Q., et al. Molecular Biology Reports, 2000. **27**(4): p. 241-246.

CRYSTAL STRUCTURE OF AN ANCIENT CONSERVED DOMAIN

J. Shaun Lott,[a] Mark J. Banfield,[b] Jill Sigrell,[c] and Edward N. Baker[a]

[a]Laboratory of Structural Biology, School of Biological Sciences, University of Auckland, Private Bag 92-019, Auckland 1020, New Zealand; [b]Department of Biochemistry, University of Bristol, University Walk, Bristol, BS8 1TD, UK; [c]Amersham Pharmacia Biotech, Research and Development, Bjorkgatan 30, Uppsala Se-751 84, Sweden (s.lott@auckland.ac.nz)

As a pilot exercise in structural genomics, we selected a small set of open reading frames (ORFs) from the hyperthermophilic archaeon *Pyrobaculum aerophilum* [1], which were annotated as unknowns and for which no functional or structural predictions could be made based on amino acid sequence. We set out to determine the three-dimensional structures of the proteins encoded by these ORFs in order to establish if they indeed represent new protein folds, and to attempt to identify their functions.

Here we report the structure of one of these functionally uncharacterised proteins, PAE2307, which is a representative of a conserved family of proteins found in both archaeal and bacterial species. As such, it represents an 'ancient conserved domain', which presumably has an evolutionarily distant origin, prior to the divergence of the bacteria and the archaea.

PAE2307 was expressed in *E. coli* and purified by immobilised metal affinity and size exclusion chromatography. It crystallised readily in two crystal forms. The prevalent form appeared twinned and diffracted to 3 Å, but the rarer form diffracted to 1.45 Å resolution. The non-twinned crystals proved difficult to reproduce, so screening of potential heavy atom derivatives by native polyacrylamide gel electrophoresis was used to establish suitable derivatization conditions. The structure was solved by SAD using data collected from a single crystal soaked in $K_2Pt(NO_2)_4$.

PAE2307 exists as a tightly associated hexamer. The monomer is composed of two domains. The main domain consists of a five-stranded anti-parallel β-sheet with two α-helices packed against one face and a third helix packed against the other. The second domain domain consists of a three-stranded β-sheet and a C-terminal helix, which makes extensive contacts with an adjacent subunit in the hexamer. A histidine residue at the start of the β5 strand is modified, possibly by phosphorylation, indicating a putative active site. The fold of the protein is similar but not identical to a number of other proteins, the most similar being a thermostable DNA polymerase.

The structure of PAE2307 and the information that it gives towards a functional assignment for this protein family will be discussed.

References

1 Fitz-Gibbon, S. T., Ladner, H., Kim, U. J., Stetter, K. O., Simon, M. I., and Miller, J. H. (2002) "Genome sequence of the hyperthermophilic crenarchaeon *Pyrobaculum aerophilum*." *PNAS* (2002) **99**, 984-989.

RIKEN STRUCTURAL GENOMICS/PROTEOMICS INITIATIVE

Shigeyuki Yokoyama

RIKEN Genomic Sciences Center, RIKEN Harima Institute at SPring-8, and Department of Biophysics and Biochemistry, Graduate School of Science, The University of Tokyo (yokohama@biochem.s.u-tokyo.ac.jp)

The RIKEN Institute has started the Structural Genomics/Proteomics Initiative (RSGI) (http://www.rsgi.riken.go.jp) at the Genomic Sciences Center (GSC) and the Harima Institute at SPring-8. RSGI is now integrated into the Japanese national project, National Project on Protein Structural and Functional Analyses, which studies both structures and functions of proteins in selected biological systems. We have been determining the three-dimensional structures of proteins of sequence families and analyzing molecular and cellular functions of these proteins in order to establish the structure-function relationships.

RSGI has two main components. One is genome-driven structural genomics to analyze the structures and functions of proteins encoded by the genome of an organism. The other is to study structures and functions of medically/biologically important proteins from higher eukaryotes in collaboration with pharmaceutical and chemical companies. For the genome-driven structural genomics, a eubacterial extreme thermophile, *Thermus thermophilus* HB8, and an archaeal hyperthermophile, *Pyrococcus horikoshii* OT3 have been selected as the target organisms. The other component of targets are higher enkaryotes, human, mouse, and *Arabidopsis thaliana*. Mouse and *Arabidopsis* full-length cDNA clones have been collected and analyzed by H. Hayashizaki and K. Shinozaki, respectively. Human cDNAs collected by the Kazusa DNA Institute and others are also used. The target proteins are selected by bioinformatics of both sequence clustering with respect to domains and functional (interaction) proteomes of biological and medical interest. Protein-protein interactions are analyzed mainly by mass spectrometry, while natural and non-natural ligands are screened *in silico* and examined by wet experiments. For protein sample preparation, the cell-free protein synthesis method is routinely used in addition to authentic recombinant methods. After the screening step of solubility, structural stability, feasibility of large-scale expression and crystallizability, large-scale sample preparation is conducted. Selenomethionine substituted proteins for X-ray crystallography are prepared by cell-free method. Robotic techniques are introduced and large protein preparation facilities are established.

We use both X-ray crystallography and NMR spectroscopy to the same extent. For X-ray crystallography, in addition to other structural biology beamlines, two beamlines at SPring-8 in Harima, dedicated to structural genomics are in use. The NMR methods can be applied for proteins that do not crystallize.

DETERMINATION AND REFINEMENT OF A DISORDERED HOST-GUEST CRYSTAL STRUCTURE USING AN EVOLUTIONARY ALGORITHM IN COMBINATION WITH MONTE CARLO METHODS

H.-B. Bürgi,[a] and T. Weber[b]

[a]Laboratory of Crystallography, University of Berne, Freiestr. 3, CH-3012 Bern; [b]Laboratory of Crystallography, ETH Zentrum, CH-8092 Zurich, Switzerland (hans-beat.buergi@krist.unibe.ch)

The complex diffraction pattern of a heavily disordered host-guest compound [perhydro-triphenylene with 1-(4-nitrophenyl)piperazine ($5C_{18}H_{30}{\cdot}C_{10}H_{13}N_3O_2$)] has been investigated with synchrotron radiation and an area detector. A complete, three-dimensional data set collected at 120 K revealed a rich variety of features including one-, two- and three-dimensional diffuse scattering, as well as incommensurate satellites. Most of the scattering could be assigned to *R*/*S* occupational disorder of the chiral host molecules, to positional disorder of the guest molecules or to local distortions of the average structure. Assignments are based on the disorder deduced from the average structure and the molecular form factors of host and guest molecules both of which show characteristic patterns in reciprocal space. Two smaller, orthorhombic twin fragments and an additional phase with hexagonal symmetry have also been found [1].

An evolutionary algorithm called 'differential evolution' is combined with Monte Carlo simulation to determine and optimise models of the disordered crystal structure. Requirements for successfully finding the parameters describing disorder from diffuse scattering data are discussed. The algorithm is applied to resolving the racemic and associated displacive disorder of the perhydrotriphenylene host substructure. Refinement results in a very good visual agreement between observed and calculated intensities and in a relatively low value of $R_{diffuse}$ = 0.148(3). Initially the computations for determining and refining the structure took 29 d with five to ten workstations running in parallel. Improved computing power and more efficient programs have reduced this time to 3-4 days. Analysis of the progress of the structure determination shows that the essential information can be obtained within a few hours. Limits of the technique and strategies to further optimise the procedure are discussed. Nearest neighbour correlations are –0.15 along x, –0.28 along y and 0.86 along z [2].

ReferencesWeber, Th., Estermann, M. A. and Bürgi, H. –B. (2001) *Acta Cryst.* **B57,** 579-590.

2 Weber, Th. and Bürgi, H. –B. (2002) *Acta Cryst.* **A58**, 526-540.

THE IMPORTANCE OF MULTISITE CORRELATIONS IN DISORDERED STRUCTURES

T.R. Welberry and R.L. Withers

Research School of Chemistry, Australian National University, Canberra, ACT 0200, Australia (welberry@rsc.anu.edu.au)

Conventional crystal structure determination using Bragg reflections reveals only *single-site* properties of a structure (average atomic positions mean-square atomic displacement amplitudes, site occupancies). Diffuse scattering, on the other hand, being the Fourier transform of the pair correlation function contains information about *two-site* properties and gives direct information about the mutual behaviour of (neighbouring) pairs of atoms. Since many theories of how atoms and molecules interact involve pair interactions (e.g. Lennard Jones potential, Buckingham potential etc.) it might be supposed that there will be a direct correspondence between the observed diffuse scattering and the pair-interactions that may be considered to be the fundamental parameters of the system. It should be noted, however, that without any direct phase information the diffraction experiment does not contain any information about multi-site correlations.

If a system has properties which stem from multi-site interactions then, although diffuse scattering effects may be observed, these arise only from the indirectly generated pair correlations. In such circumstances there is no direct link between the observed pair correlations and the fundamental inter-atomic interactions and little purpose is served by trying to interpret the scattering in terms of a model formulated in terms of pair-interactions. In this paper we describe examples of real systems in which complex diffraction patterns can be explained by extremely simple models involving multi-site atomic interactions.

The first of these examples involves O/F ordering and associated Mo ion shifts in the system $K_3MoO_3F_3$. Monte Carlo modelling is used to show how the latter, when coupled with an appropriate local crystal chemical constraint (a multi-site interaction), can give rise to the observed highly structured diffuse scattering patterns. Examples of different sections of the calculated diffraction pattern are shown in Fig.1.

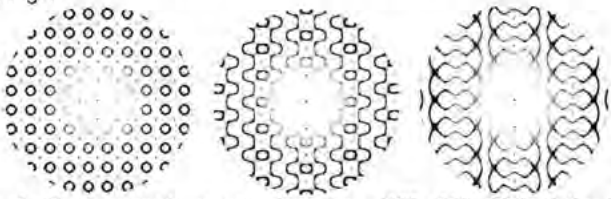

Fig. 1. Three example reciprocal sections (100, 113, 331) of the $K_3MoO_3F_3$ system, calculated from a Monte Carlo model based on a simple chemical constraint.

A second example involves Bi/Zn cation ordering in the cubic pyrochlore $(Bi_{1.5}Zn_{0.5})(Zn_{0.5}Nb_{1.5})O_7$. Here too a multi-site interaction based on a simple chemical constraint is required to explain the observed diffraction patterns.

STRUCTURE SOLUTION AND REFINEMENT OF $KNbOB_2O_5$ – A COMMENSURATE MODULATED STRUCTURE

Siegbert Schmid

School of Chemistry, The University of Sydney, NSW 2006, Australia (siegbert@chem.usyd.edu.au)

Non-centrosymmetric oxo pyroborates, $AMOB_2O_5$ (A = K, Rb, Cs, Tl; *M* = Nb, Ta) [1-5], have attracted considerable interest owing to their potential use as non-linear optical materials. All members of the family possess a common underlying average structure. In addition most exhibit superstructures of varying multiplicities (2, 5 and 8) along the *b* axis (corresponding to the $Pmn2_1$ setting of $CsNbOB_2O_5$ [4]). Despite the availability of single crystals for all compounds, single-crystal structure refinements have only been reported for $TlNbOB_2O_5$ [1], $RbNbOB_2O_5$ [3], $CsNbOB_2O_5$ [4-5] and $CsTaOB_2O_5$ [5]. The Cs compounds are reported without superstructure, *i.e.* to be of the basic structure type, while the Tl compound displays a two-fold superstructure and the Rb compound a five-fold superstructure, however, the structure wasn't truly refined as a superstructure.

An electron diffraction and single-crystal X-ray diffraction investigation of $RbNbOB_2O_5$ verified the existence of an exact five-fold superlattice along *b* [6]. A characteristic hierarchical intensity distribution among the satellite reflections was strongly suggestive of a modulated structure in that the $\mathbf{G}_p \pm {}^2/_5\mathbf{b}_p^*$ (p for parent) satellite reflections were clearly much stronger than the $\mathbf{G}_p \pm {}^1/_5\mathbf{b}_p^*$ satellite reflections). For $KNbOB_2O_5$ the single-crystal X-ray diffraction patterns were very similar to the patterns for $RbNbOB_2O_5$. The superlattice along *b* was exactly eight-fold, with the $\mathbf{G}_p \pm {}^3/_8\mathbf{b}_p^*$ (p for parent) satellite reflections clearly the strongest satellite reflections. While the Rb compound was best refined as an incommensurate modulated structure, solution and refinement of $KNbOB_2O_5$ showed, that this structure was best described as a commensurate modulated structure.

In both refined structures apparent valence calculations show, that rubidium and potassium, respectively, are satisfactorily bonded. While caesium, the largest *A* ion in this family realises an unmodulated structure, the modulation in the other compounds provides the *A* ions with an adequate bonding environment. If Rb, Tl and K were to form the same structure as Cs, they would be significantly underbonded. A calculation of bond valence sums after simply substituting these cations for Cs gives values of 0.59, 0.46 and 0.42, respectively.

References

1 Gasperin, M. (1974), *Acta Crysta.* B**30**, 1181 - 1183.
2 Baucher, A. and Gasperin, M. (1975), *Mat. Res. Bull.* **10**, 469 - 472.
3 Baucher, A., Gasperin, M. and Cervelle, B. (1976), *Acta Crysta.* B**32**, 2211 - 2215.
4 Becker, P., Bohaty, L. and Fröhlich, R. (1995), *Acta Crysta.* C**51**, 1721 - 1723.
5 Akella, A. and Keszler, D. A. (1995), *J. Solid State Chem.* **120**, 74 - 79.
6 Schmid, S., Withers, R. L., Corker, D. and Baules, P. (2000), *Acta Crysta.* B**54**, 558 - 564.

APPLICATION OF A SIX-DIMENSIONAL TWIN REFINEMENT TECHNIQUE TO MULTIPLE-TWINNED CRYSTALS OF Cu_2SnS_3, Cu_8GeS_6 and Ag_7TaS_6

M. Onoda, H. Wada, X. -a. Chen, A. Sato, and M. Ishii
Advanced Materials Laboratory, National Institute for Material Science, Namiki 1-1, Tsukuba, Ibaraki, 305-0044, Japan (ONODA.Mitsuko@nims.go.jp)

The twinned structure could be described by a six-dimensional formalism and refined using the multi-dimensional refinement program FMLSM [1,2]. When the reflections can be indexed based on two sets of basic vectors, **a**, **b**, **c** and **a'**, **b'**, **c'**, each reflection is expressed by $\mathbf{q}=h\mathbf{a}^*+k\mathbf{b}^*+l\mathbf{c}^*+h'\mathbf{a}'^*+k'\mathbf{b}'^*+l'\mathbf{c}'^*$. Symmetry operations are also expressed in the (3+3)-dimensional formalism [2]. Those for the major domains (**a**, **b**, **c**) are given by the scheme $\mathbf{g}=((\mathbf{R}\ \mathbf{0}\ |\ \mathbf{0}\ \mathbf{R})\ |\ (\mathbf{v}|\mathbf{v}))$, where **R** and **v** are the matrix and the vector of the corresponding three-dimensional symmetry operations. The symmetry operations for the minor domains (**a'**, **b'**, **c'**) are obtained by multiplying the six-dimensional twinning operation $\mathbf{t}=\{\mathbf{T}\ |\ \mathbf{0}\}$ into the major domain symmetry operations **g** where **T** is the matrix (000100 | 000010 | 000001 | 100000 | 010000 | 001000) [2].

The X-ray diffraction data of low-symmetry Cu_2SnS_3 were obtained from a twinned monoclinic crystal (a=6.653, b=11.537, c=6.665 Å, β=109.39!) [3]. The reflections were indexed on the basis of **a**, **b**, **c** and **a'**, **b'**, **c'**, where $\mathbf{a}'^*=-\mathbf{a}^*$, $\mathbf{b}'^*=\mathbf{b}^*$, $\mathbf{c}'^*=-(2/3)\mathbf{a}^*+\mathbf{c}^*$. The reflections are of three groups, the first is assigned by both of $hkl000$ and $000h'k'l'$ and considered to be common to two twin domains, while the second ($hkl000$) comes from the major domain and the third ($000h'k'l'$) comes from the minor domain. The structure was described based on **a**, **b**, and **c** with space group Cc. Refinement was performed using all reflections through FMLSM. The agreement was satisfactory with 52 structural parameters and 2 scale factors; R_F=0.036 and wR_F=0.038. Observed reflections of Cu_8GeS_6 [4] seemed to be from a twinned rhombohedral crystal (a~9.9 Å and α~90!), the major ones based on **a**, **b**, **c** and minor ones based on **a'**=-**a**, **b'**=-**b**, **c'**=-**c**. The model proposed using powder data was that with A=7.0445, B=6.9661, C=9.8699Å and $Pmn2_1$. After selecting new bases $\boldsymbol{a}=\boldsymbol{A}+\boldsymbol{B}$, $\boldsymbol{b}=\boldsymbol{B}-\boldsymbol{A}$, $\boldsymbol{c}=\boldsymbol{C}$, the lattice constants were a=b= 9.9073, c=9.8703Å, α=β=90!, γ=90.642!. Symmetry operations were also converted into the formula based on C-lattice: generator sets are 1/2+x,1/2+y, z; y,x,z; 3/4-y,1/4-x,1/2+z. The major group reflections and six major domains with the twin operations x,y,z, y,z,x, z,x,y, x,-y,-z, -y,-z,x, and -z,x,-y were considered. Then the minor group reflections and six minor domains were added. Besides structural parameters, 12 scale factors were considered as parameters in refinement. The agreement was satisfactory for 1804 reflections; R_F=0.083 and wR_F=0.091.

In a similar manner, the structure of the monoclinic low-temperature phase of Ag_7TaS_6 was examined on the basis of X-ray diffraction data from a 24-fold twinned crystal with 12 major domains and 12 minor domains.

References

1 Kato, K. (1994) *Acta Cryst.* **A50**, 351-357.
2 Kato, K. (1997) *Z. Kristallogr.* **212**, 423-427.
3 Onoda, M., Chen X.-a., Sato, A. and Wada, H., (2000) *Mat. Res. Bull.* **35**, 1563-1570.
4 Onoda, M., Chen X.-a., Kato, K., Sato, A. and Wada, H., (1999) *Acta Cryst.* **B55**, 721-5.

Tuesday August 12

AsCA'03/Crystal-23

ABSTRACTS

POSTER SESSIONS

ELECTRON MOMENTUM DENSITY STUDY OF ICOSAHEDRAL $Cd_{84}Yb_{16}$

Y. Sakurai,[a] J. T. Okada,[b] Y. Watanabe,[b] S. Nanao,[b] R. Tamura,[c] S. Takeuchi,[c]
Y. Yokoyama,[d] N. Hiraoka,[e] and M. Itou[a]
[a]Japan Synchrotron Radiation Research Institute (JASRI), SPring-8, 1-1-1 Kouto, Mikazuki, Sayo, Hyogo 679-5198, Japan; [b]Institute of Industrial Science, University of Tokyo, 4-6-1 Komaba, Meguro, Tokyo 153-8505, Japan; [c]Science University of Tokyo, Noda, Chiba 278-8510, Japan; [d]Hineji Institute of Technology, 2167 Himeji, Hyogo 671-2201, Japan; [e]European Synchrotron Radiation Facility (ESRF), BP 220, F-38043 Grenoble Cedex, France (sakurai@spring8.or.jp)

Quasicrystal is a new form of solids that differs from crystalline and amorphous materials since it possesses quasi-periodicity and non-crystallographic rotational orders. The presence of a pseudogap is one of the characteristics in quasicrystals and is of great importance to understanding the cohesion mechanism of the unconventional compounds. The pseudogap opens in the density of states across the Fermi level, possibly by two scenarios; one is the quasi-Brillouin zone – Fermi surface interaction (called Hume-Rothery mechanism) and the other is the sp-d hybridization.

Icosahedral $Cd_{84}Yb_{16}$ is a stable binary quasicrystal that has been recently discovered by Tsai *et al.*[1]. A pseudogap signature has been observed in the high-resolution photoemission spectra [2]. Theoretically, Ishii and Fujiwara have carried out computations on the 1/1 cubic approximant Cd_6Yb and concluded that the hybridization of the d states of Yb with a wide sp band plays a major role in the pseudogap formation while the Hume-Rothery mechanism is minor [3].

In this conference, we present the electron momentum density distribution (Compton profile) of icosahedral $Cd_{84}Yb_{16}$ obtained using the high-resolution Compton scattering spectrometer [4] at SPring-8. The energy of the incident x rays was 116 keV and the scattering angle was 165 degrees. The overall momentum resolution was 0.16 atomic units.

The experimental valence-electron Compton profile is decomposed into two partial profiles: an inverted parabola-like profile and a broad Gaussian-like profile. It is found that the Fermi sphere, whose radius is estimated from the number of electrons under the inverted parabola-like profile, is just inscribed in the quasi-Brillouin zones defined by the strong (211111) and (221001) diffraction planes. The broad Gaussian-like profile is accounted for by the Yb-5d states which are lowered below the Fermi level by hybridization with the sp bands. These results show that the Hume-Rothery mechanism and the sp-d hybridization effects work cooperatively for forming the deep pseudogap and thus stabilizing the icosahedral phase of $Cd_{84}Yb_{16}$.

References

1 Tsai, A., P., Guo, J., Q., Abe, E., Takakura, H. and Sato, T., J. (2000) *Nature (London)* **408**, 537.
2 Tamura, R., Murao, Y., Takeuchi, S., Kiss, T., Yokoya, T. and Shin, S. (2002) *Phys. Rev. B* **65**, 224207.
3 Ishii, Y. and Fujiwara, T. (2001) *Phys. Rev. Lett.* **87**, 206408.
4 Hiraoka, N., Itou, M., Ohata, T., Mizumaki, M., Sakurai, Y. and Sakai, N. (2001) *J. Synchrotron Rad.* **8**, 26-32.

CHARGE DENSITY STUDIES OF Z' = 2 MOLECULES. POSSIBILITIES AND LIMITATIONS

Dai Hibbs, Mark P. Waller and Jacob Overgaard

School of Chemistry, University of Sydney, NSW 2006, Australia
(hibbs_d@chem.usyd.edu.au)

Experimental X-ray charge density (CD) studies of molecules with more than one molecule in the asymmetric unit are relatively rare [1]. On the contrary, such occurrences are abundant in structural chemistry, evidenced by the 22015 hits of Z'≥2 in CCDC, corresponding to 8% of all published structures [2]. Thus, it is apparent that such compounds have been avoided by the CD community. This is due to several factors. Firstly, the increase in the number of parameters is a significant drawback, since a successful multipole model in most cases requires more than 300 reflections per non-hydrogen atom. Secondly, one of the molecules often experiences a rather weak crystal field; hence the thermal motion of this molecule can be severe and the molecule may even be disordered. Thirdly, there can exist significant correlations between multipole parameters from different molecules. All in all, CD studies of this type of crystal structures offer a range of problems that need to be addressed.

There are, however, large potential benefits of studying the CD in such molecules. In the case of rigid molecules, it allows the determination of multipole parameters of identical atoms in slightly different environments without the presence of systematic errors intrinsic in a comparison of different experiments. Hence, it is important in the evaluation of transferability of atomic multipole parameters [3].

This presentation will outline the details of experimental and theoretical charge density studies of three organic molecules all having two molecules in the asymmetric unit (see Figure). Besides a discussion of the prospects of giving an independent description of the two molecules in the same study, each of the three systems represents interesting chemical and theoretical issues that will be addressed.

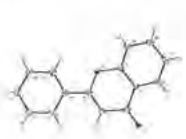

FLAVONE

FLUORENOL

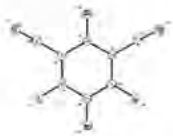

TFIPN

References

1 Gatti, C., May, E., Destro, R. and Cargnoni, F. (2002) *J. Phys. Chem. A.* **106**, 2707; van Reeuwijk, S. J., van Beek, K. G. and Feil, D. (2000) *J. Phys. Chem. A.* **104**, 10901.

2 CCDC search 13/3/03 gave 22015 hits equalling Z'≥2 out of 272066.

3 Pichon-Pesme, V., Lecomte, C. and Lachekar, H. (1995) *J. Phys. Chem.* **99**, 6242.

CRYSTAL EXPLORER: A GRAPHICAL USER INTERFACE FOR DISPLAYING AND MANIPULATING HIRSHFELD SURFACES AND FINGERPRINTS FOR CRYSTAL ENGINEERING APPLICATIONS

Dylan Jayatilaka, Daniel Grimwood, and Stephen Wolff

Department of Chemistry, University of Western Australia, Crawley, WA 6009, Australia (dylan@theochem.uwa.edu.au)

The Hirshfeld surface is a region enclosing a moeity in a crystal, within which more than 50% of the electron density comes from that moeity. The surface can be coloured in a number of ways, to highlight local packing interactions in the crystal. In addition, a fingerprint of the surface can be made which quickly displays in a 2D format inter-moeity interactions - thus making comparison of crystalline interactions in different crystal structures straightforward [1].

Crystal Explorer is a graphical user interface (GUI) for manipulating Hirshfeld surfaces [2]. Examples of the GUI and its uses will be presented.

References

1 See, e.g., McKinnon, J. J., Mitchell, A. S., and Spackman, M. A. (1998) *Chem. Eur. J.* **4**, 2136-2141.

2 *Crystal Explorer: A GUI for manipulating Hirshfeld Surfaces*, www.theochem.uwa.edu.au/hirshview.

CRYSTALLIZATION OF SECRETED PROTEIN BY COMPLEXATION WITH AN ANTIBODY FRAGMENT

Taro Tamada,[a] Keiko Kurosawa,[a] Uichi Nishiyama,[b] Tomoaki Kuwaki,[b] and Ryota Kuroki[a]

[a]Pharmaceutical Research Laboratories, Pharmaceutical Division, Kirin Brewery Co., Ltd., 1-13-5 Fukuura, Kanazawa-ku, Yokohama, Kanagawa 236-0004, Japan; [b]Pharmaceutical Development Laboratory, Pharmaceutical Division, Kirin Brewery Co., Ltd., 3 Miyahara-cho, Takasaki 370-1295, Japan (ttamada@kirin.co.jp)

It is known that secreted glycoproteins, such as cytokines, are hard to crystallize in spite of their industrial importance. Our approach for crystallization of these proteins is the use of antibody fragment (Fab). The first example was the crystallization of thrombopoietin (TPO). TPO is a cytokine which primarily stimulates megakaryocytopoiesis and thrombopoiesis. TPO was crystallized by complexation with Fab derived from a neutralizing monoclonal antibody [1]. The tertiary structure of TPO was also successfully determined only by molecular replacement technique using the known coordinates of Fab as a search model. It was confirmed that the use of Fab was effective not only for protein crystallization, but also for phase determination.

The second example is the crystallization of soluble receptors. The extracellular domain of receptors is the entrance of signals induced by ligand binding. The interaction of the receptors with several drug candidates is widely investigated. To elucidate activation mechanism of TPO receptor by ligand binding, we aim to determine the complex structure of TPO and its receptor by complexation with Fab. The extracellular region of human TPOR expressed using by the animal cell was used for crystallization. Several Fab fragments derived from a monoclonal antibody that recognize the extracellular domain of TPOR were used for the search of crystallization condition. After various screening for crystallization condition, TPO/TPOR/Fab complex, and TPOR/Fab complex, were successfully obtained with the use of one of the Fab fragments. Although further optimization of crystallization condition is needed, the use of Fab was effective approach for TPOR crystallization. The structure information of TPOR will give the useful information for pharmaceutical development of TPO.

References

1 Kuroki, R., Hirose, M., Kato, Y., Feese, M. D., Tamada, T., Shigematsu, H., Watarai, H., Maeda, Y., Tahara, T., Kato, T., & Miyazaki, H. (2002) *Acta Cryst.* **D58**, 856-858.

CRYSTALLIZATION OF ALPHA-AMYLASE AS A MODEL PROTEIN FOR DEMONSTRATING THE EFFICACY OF THE COUNTER-DIFFUSION TECHNIQUE UNDER MICROGRAVITY CONDITIONS

Masaru Sato,[a] Hiroaki Tanaka,[a,b] Koji Inaka,[c] Sachiko Takahashi,[b] Satoshi Sano,[a] Susumu Yoshitomi,[a] and Hiroshi Komatsu[d]
[a]Space Utilization Research Center, National Space Development Agency of Japan (NASDA), Ibaraki 305-8505, Japan; [b]Japan Space Utilization Promotion Center, Tokyo 169-8624, Japan; [c]Maruwa Food Industries, Inc., Nara 639-1123, Japan; [d]Iwate Prefectural University, Iwate 020-0193, Japan (PXW01674@nifty.ne.jp)

It is necessary to work for a well characterized model protein for demonstrating the efficacy of the new protein crystallization method. Therefore we chose alpha-Amylase as a representative of many significant proteins for its molecular weight and biochemical characteristics. Alpha-Amylase is a glycoprotein derived from *Aspergillus oryzae*, which catalyze the hydrolysis of the alpha-1,4 glycosidic linkage in starch. The major problems of the crystallization of alpha-Amylase on the ground using PEG as precipitant are the incorporation of isozyme and the highly clustered morphology, which cause difficulties to obtain monocrystal on the ground experiment. We expect that the microgravity effects can provide the optimal diffusive environment to overcome these problems.

Crystallization of alpha-Amylase was carried out by counter-diffusion method using Granada Crystallization Box (GCB)[1] with the condition of 90 mg/ml protein, 40%(w/v) PEG 8000, 2mM $CaCl_2$, and 50mM Tris-HCl pH 7.5 at 20C under microgravity for 10 weeks in Odissea mission in 2002. On the ground, crystals were appeared within 10 days as highly clustered crystals at the acupunctured-end of the capillary. Each crystal belonged to the orthorhombic space group $P2_12_12_1$ with unit cell dimensions a=50.2 b=65.7 c=130.8, and diffracted beyond 1.6 Å resolution. In space, however, crystals were obtained as a single crystal. They belonged to the tetragonal space group $P4_32_12$ with unit cell dimensions a=b=67.4, c=268.0 Å, which had the same space group as reported previously [2]. Preliminary diffraction experiments at ambient temperature at SPring-8, BL12b2 indicated that diffraction pattern extends beyond 1.6 Å resolution. Three crystals were grown only in one capillary. There were no crystal observed in other five capillaries, however, the clustered orthorhombic crystals had started to grow within 24 hours after landing.

These results suggest that the mechanism of nucleation and/or growth of protein crystal under microgravity is quite different from those under gravity. Characterization of crystals obtained with and without gravity will be reported in detail.

Acknowledgements: The flight opportunity of Odissea mission was donated by favour of ESA and Dr. Garcia-Ruiz in University of Granada, Spain.

References

1 Garcia-Ruiz, J.M. and Moreno, A. (2002) *Acta Cryst.* **D58**, 1638-1642.
2 Ninomiya, K., Yamamoto, T., Oheda, T., Sato, K., Sazaki, G. and Matsuura, Y. (2001) *J. Crystal Growth* **222**, 311-316.

INVESTIGATION OF CRYOPROTECTANT CONDITION FOR PROTEIN STRUCTURE ANALYSIS USING CRYOPROTECTANT DATABASE

Sachiko Takahashi,[a] Takashi Yoshimine,[a] Masaru Sato,[b] Hiroaki Tanaka,[a,b] Kensaku Hamada,[c] and Susumu Yoshitomi[b]
[a]Japan Space Utilization Promotion Center, Tokyo 169-8624, Japan; [b]Space Utilization Research Center, National Space Development Agency of Japan (NASDA), Ibaraki 305-8505, Japan; [c]Shimane University, Shimane 690-8504, Japan (PXW01674@nifty.ne.jp)

To perform X-ray diffraction experiment properly and obtain the complete data sets, it is essential to protect protein crystals from the serious damages caused by synchrotron X-ray beam. It is well known that freezing crystals reduces radiation-induced damages on crystals, however, inadequate cryoprotectants and operational techniques frequently deteriorate valuable crystals. Therefore it is very important to decide appropriate conditions for freezing each protein crystal. Since NASDA has promoted protein crystallization experiments in space twice a year since 2003, it is necessary to improve the cryoprotective technique for crystals grown in space, which is the main purpose to construct this database.

We picked up 279 cryo-data mainly from articles in *Acta Crystallographica D* 2000 and 2002. The information we extracted were the name of the protein, origin, PDB reference, precipitant, crystallization method, cryoprotectant, freezing method and freezing temperature. The database is available free in the following address: http://idb.exst.nasda.go.jp/. We will continue to update (200 more data this year) and analyze these data sequentially.

According to the investigation from the database, 54% of the crystals were flash-frozen and glycerol was most commonly used as cryoprotectant in 48% of the flash-frozen crystals. In case of flash-frozen crystals, the relationship between PEG 4K % and glycerol % in cryoprotectant is shown in Fig. 1. This figure indicates that composition of glycerol as cryoprotectant for flash-freezing can be preliminary optimized according to the concentration of PEG used as precipitant. We will also show the relationships between glycerol % and other precipitants in detail.

The crystallization occurs in capillaries using counter-diffusion technique for NASDA's experiment in space. Taking advantage of it, we came up with the idea of the simple method for soaking the crystals in glycerol as cryoprot-ectant mildly within the capillaries. We will report this method in detail. We will apply these techniques for freezing the crystals which will return from the International Space Station in May 2003.

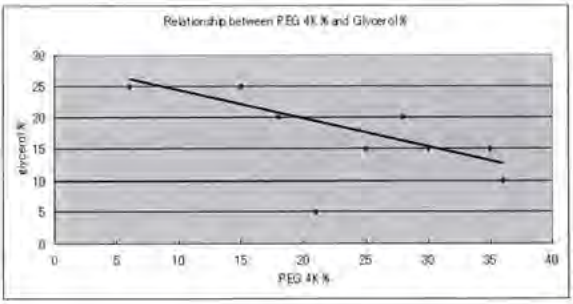

CRYSTAL STRUCTURE OF NONADECANE-1,19-DITHIOL

H. Shimizu,[a] K. Uno,[a] Y. Ogawa,[b] and N. Nakamura[a]
[a]Material-Energy Science and Engineering Major, Graduate School of Science and Engineering, Ritsumeikan University, 1-1-1, Nojihigashi, Kusatsu, Shiga 525-8577, Japan; [b]Department of Chemistry, Faculty of Science, Kumamoto University, 2-39-1, Kurokami, Kumamoto 860-8555, Japan (rc005999@se.ritsumei.ac.jp)

It has been well known that long-chain aliphatic compounds with a terminal mercapto group form a self-assembled monolayer on a surface of gold[1]. In this study, the crystal structure of nonadecane-1,19-dithiol, HS–$(CH_2)_{19}$–SH, was analyzed.

The single crystal of the title compound was obtained from a solution with a mixed solvent of ethyl acetate and ethanol (2:1) by the slow evaporation method. All measurements were made on a Rigaku AFC-5*R* diffractometer with graphite monochromatized Cu-$K\alpha$ radiation. The crystal structure was a triclinic system (a=4.7628(6)Å, b=5.5741(7)Å, c=40.927(5)Å, α=92.51(1)°, β=92.02(1)°, γ=102.57(1)°, Z=2) with a space group $P\bar{1}$. All calculations were performed using the *CrystalStructure* crystallographic software package. The structure was solved by direct methods with *SIR*92. The non-H atoms were refined anisotropically. The methylene H atoms were located at idealized positions, and were allowed to ride on the parent C atoms (C–H=0.95Å). The isotropic displacement parameters were set at $1.2U_{eq}$ of the parent atom. However, the position of mercapto H atoms could not be determined from a difference Fourier map. The final refinement was made by full-matrix least-squares based on 3809 observed reflections (F^2>-3σ(F^2)). The refinement was concluded with final reliability factors $R(F^2>2\sigma(F^2))$=0.060, $wR(F^2)$=0.135.

As is shown in Fig.1, the hydrocarbon skeleton included both terminal mercapto groups had an all-*trans* conformation. In the crystal structure, the long axis of the molecule is inclined to the *ab* plane.

In this study, a feature of the crystal structure of nonadecane-1,19-dithiol will be discussed with those of other alkane-α,ω-dithiols[2-4].

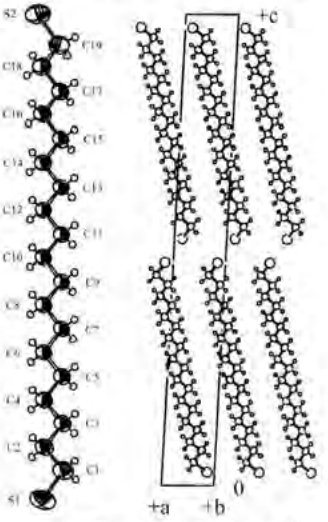

Fig.1 The molecular and crystal structure of nonadecane-1,19-dithiol.

References

1 Drawhorn, R.A. and Abbott. N.L. (1995) *J. Phys. Chem.*, **99**, 16511.
2 Thalladi, V.R., Boese, R. and Weiss, H.C. (2000) *J. Am. Chem. Soc.*, **122**, 1186.
3 Nakamura, N., Uno, K. and Ogawa, Y. (2001) *Acta Cryst.*, **E57**, o508.
4 Nakamura, N., Uno, K. and Ogawa, Y. (2001) *Acta Cryst.*, **E57**, o505.

A STRUCTURAL STUDY ON THE MONOSUBSTITUTED FERROCENE DERIVATIVES

Y. Kawamura, Y. Okada, K. Uno and N. Nakamura

Material-Energy Science and Engineering Major, Graduate School of Science and Engineering, Ritsumeikan University, 1-1-1, Nojihigashi, Kusatsu, Shiga 525-8577, Japan (rc004983@se.ritsumei.ac.jp)

The crystal structures of *o*-nitrophenylferrocene, *m*-nitrophenylferrocene and *p*-nitrophenylferrocene were already analyzed by other workers[1]. In this study, the crystal structures of *o*-acetylphenylferrocene and *p*-acetylphenylferrocene were determined by the X-ray diffraction method in order to discuss an influence of the substituent over the crystal structures. All measurements were made on a Rigaku AFC-5*R* diffractometer with graphite monochromatized Cu $K\alpha$ radiation. All calculations were performed using *CrystalStructure*[2] crystal structure analysis package. The single crystals of *o*-acetylphenylferrocene and *p*-acetylphenylferrocene were obtained from a solution with a mixed solvent of benzene : ethanol (1:3) and ethyl acetate : ethanol (1:4) by the slow evaporation method, respectively.

The crystal structure of *o*-acetylphenylferrocene was a orthorhombic system (a=7.552(2)Å, b=31.114(2)Å, c=5.901(3)Å, Z=4) with a space group $P2_12_12_1$. The structure was solved by direct methods with *SIR*92[3] and expanded using the Fourier Technique. All non-H atoms were refined anisotropically. The H atoms were located from a difference Fourier map, and were allowed to ride on the parent C atoms to which they are attached. The H-atom isotropic displacement parameters were set at $1.2U_{eq}$ of the parent atom. The final refinement was made by full-matrix least-squares based on 1560 observed reflections (F^2>-3σ (F^2)). The $R(F^2>2\sigma(F^2))$ value was converged to 0.034 by the final refinement.

The crystal structure of *p*-acetylphenylferrocene was a orthorhombic system (a=10.544(5)Å, b=33.998(4)Å, c=7.725(5)Å, Z=8) with a space group *Pbca*. The structure was solved by direct methods with *SIR*92[3] and expanded using the Fourier Technique. All non-H atoms were refined anisotropically. The H atoms were introduced at their theoretical positions and allowed to ride on the C atoms to which they are attached. The H-atom isotropic displacement parameters were set at $1.2U_{eq}$ of the parent atom. The final refinement was made by full-matrix least-squares based on 2532 observed reflections (F^2>-3σ (F^2)). The $R(F^2>2\sigma(F^2))$ value was converged to 0.096 by the final refinement.

References

1. Roberts, R.M.G., Silver, J., Yamin, B.M., Drew, M.G.B. and Eberhardt, U. (1988) *J. Chem. Soc., Dalton Trans.*, **6**, 1549.
2. Rigaku/MSC and Rigaku Corporation. (2001) *CrystalStructure Version* 3.10., Rigaku/MSC, 9009 New Trails Drive, The Woodlands, TX 77381, USA. Rigaku, 3-9-12 Akishima, Tokyo 196-8666, Japan.
3. Altomare, A., Cascarano, G., Giacovazzo, C., Guagliardi, A., Burla, M., Polidori, G. and Camalli, M. (1994) *J. Appl. Cryst.*, **27**, 435.

CRYSTAL STRUCTURE of $Te_{0.4}Se_{0.6}$

Yuji Soejima,[a] Akie Hoshiko,[a] Hirotoshi Hayashida,[a] Yoshinori Ohmasa,[b] Hirohisa Endo,[c] and Masaru Kawaminami[d]
[a]Department of Physics, Kyushu Univ., Hakozaki 6-10-1, Fukuoka 812-8581, Japan; [b]Department of Physics, Kyoto Univ., Sakyo-ku, Kyoto 606-8502, Japan; [c]Faculty of Engineering, Fukui Univ. of Technology, Gakuen 3-6-1, Fukui 910-8505, Japan; [d]Department of physics, Kagoshima University, 890-0065 Kagoshima, Japan; (oko6scp@mbox.nc.kyushu-u.ac.jp)

At the atmospheric pressure, the most stable form of tellurium and selenium is trigonal. Under pressure, they show several structural transitions and semiconductor-to-metal transition. It has been well known that Te-Se mixture also shows interesting electronic properties under high pressure, and recently, it was found that the crystal structure of Te_xSe_{1-x} is quenched to the atmospheric circumstance only in the case of x = 0.4 [1]. In the present work we have carried out the structure determination of $Te_{0.4}Se_{0.6}$, with short wave length of synchrotron radiation.

The X-ray diffraction measurements were made on BL-10A at Photon Factory, KEK. The incident X-ray was tuned at 0.4 A by 311 diffraction with silicon flat-plate monochromator. One specimen crystal was chosen for intensity measurement after being examined, in particular, in connection with crystalline quality by rotational photography. The size of the specimen was 230x130x150 μm^3. The linear absorption coefficient μ=15.76 mm^{-1} thus absorption collection is not required for the present case. The orientation matrix was determined using thirteen strong reflections within θ=15°. The lattice constants were determined *a*=8.164, *b*=27.856, *c*=13.852 A and β=108°, and the space group *Cc* was assigned. The intensities of the higher harmonics of the monochromated beam were very weak, but further reduced by a discriminator of the detector circuit. The intensity data of the unique region of the reciprocal space were collected in the range $\sin\theta/\lambda$! 0.5 by assuming no extinction rule: to collect additional reflections which have non-integer indices due to longer periodicity of the real lattice; namely ax9bx2c , the lattice parameter were defined as *a*=8.164, *b*=250.70, *c*=27.704 Å. 1630 unique diffractions were measured and the integrated intensity was determined by summing up the intensity measured stepwise in the ω–scan and by subtracting background. After correction for incident of synchrotron beam, a set of structure factor was obtained.

At first, the least-square refinement (SHELX-97 coded by G. M. Sheldric) was carried out assuming monotonic occupancy of 0.4 Te and 0.6 Se atoms at all atomic site. After reaching a minimal R factor of 0.124, the refinement was continued introducing occupation parameter r of Te fraction at 27 unique sites. Finally we obtained the structure with R=0.098 using isotropic temperature factors. The results indicate that the discrepancy of two facts that Te and Se atoms tend to align alternatively and that the composition of Te and Se is 0.4:0.6 leads to the ax9bx2c structure.

References

1 Ohmasa, Y., et al. (1995) *J. Phy. Soc. Jpn*, **64**, 4766.

CRYSTAL STRUCTURES OF A BISAZOMETHINE DYE FORMING J-AGGREGATES

Shinya Matsumoto,[a] Kazuko Shirai,[a] Kimiko Kobayashi,[b] Tatsuo Wada,[c] and Motoo Shiro[d]
[a]Faculty of Education and Human Sciences, Yokohama National University, Yokohama 240-8501 Japan; [b]Molecular Characterization Division; and [c]Supramolecular Science Laboratory, RIKEN (The Institute of Physical and Chemical Research), Saitama 351-0198 Japan; [d]X-ray Research Laboratory, Rigaku Corporation, Tokyo 196-8666 Japan (smatsu@edhs.ynu.ac.jp)

The title dye 1 synthesized from diaminomaleonitrile together with 4-diethylaminobenzaldehyde has attracted attention as a material for organic electroluminescent devices because of its red fluorescence in solution as well as in the solid state [1,2]. This dye was also found to form J-aggregates in a vacuum deposited film as shown in Fig. 1. X-ray structure analysis of 1 was carried out to elucidate the solid state structure. The result indicates that the molecules are arranged in a characteristic stacking fashion that reminds us of molecular arrangement in J-aggregates, as depicted in Fig. 2. The J-aggregates films were characterized by the almost same phase as that of the single crystals: Crystal data (298 K), a = 9.225 (2), b = 11.290 (3), c = 18.182 (6) Å, α = 79.94 (3), β = 76.09 (2), γ = 89.69 (2) °, triclinic, P-1 (Z=3). Bond lengths of the terminal amino moieties were found to be unusual. Then several attempts were made to separate disordered groups. The phase in which there are six molecules in the unit cell was found at around 93 K: Crystal data (93 K), a = 11.040 (1), b = 18.097 (1), c = 18.255 (1) Å, α = 103.76 (1), β = 90.33 (1), γ = 100.32 (1) °, triclinic, P-1 (Z=6). However, the ethyl groups are still partially disordered. Theoretical investigation of the electronic states of the aggregates on the basis of the present crystal structure will also be discussed.

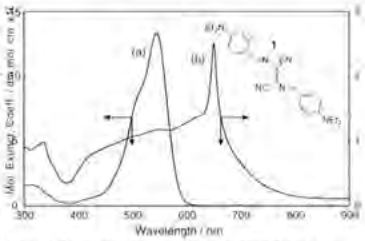

Fig. 1 Absorption spectra of dye **1** (a) in $CHCl_3$ and (b) in a deposited film (1500 Å).

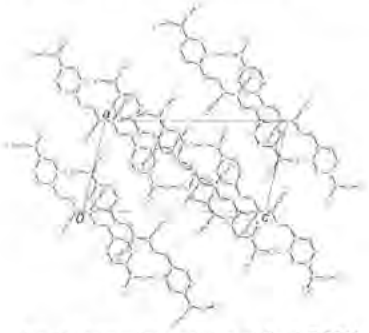
Fig. 2 Molecular packing of **1** at 298K.

References

1 Shirai, K. et al. (2000) *Dyes Pigm.* 47, 107-115.
2 Yu, J. et al. (2001) *Jpn. J. Appl. Phys.* 40, 3201-3205.

STRUCTURAL STUDY OF STRESS-INDUCED LUMINESCENT PARTICLE $SrAl_2O_4$:Eu

Hiroshi Yamada,[a] Hajime Kusaba,[a] Weng-Shen Shi,[b] Keiko Nishikubo,[b] and Chao-Nan Xu[b]

[a]PRESTO, Japan Science and Technology Corporation (JST), Honcho, Kawaguchi, Saitama 332-0012, Japan; [b]National Institute of Advanced Industrial Science and Technology (AIST), Shuku, Tosu, Saga 841-0052, Japan (cn-xu@aist.go.jp)

$SrAl_2O_4$ doped with Eu^{2+} shows an intense green luminescence induced by mechanical stress so-called the mechanoluminescence. A lot of interest has been paid in the relation to the crystal structure and the luminescent mechanism because the atomic configurations around Eu^{2+} strongly affect the luminescent properties.

The crystal structure of $SrAl_2O_4$ is a family of the stuffed tridymite structure and possesses polymorphism of α- and β-phase as shown in figure, where $SrAl_2O_4$ usually transforms to β-phase above 650°C. Recently we successfully synthesized spherical fine particles with pure α-phase, pure β-phase, and the mix phase by the spray pyrolysis method but only the particle with pure β-phase shows no photoluminescence [1, 2]. In this work, we have investigated the relation to the stabilization of β-phase and the disappearance of the luminescence. The structural characterization of these samples have been carried out by the Rietveld analysis with high-resolved powder X-ray diffraction data, which were measured by using a synchrotron radiation with wavelength 0.775 Å. Furthermore, in order to determine the distribution of doped Eu ion, the electron density distribution is derived by the maximum entropy method, demonstrating that the Eu ions partially occupy the Sr ion sites. We will discuss the additional structural features at the conference.

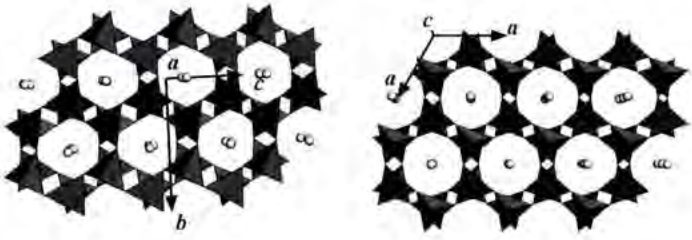

α -phase *β -phase*

References

1 Shi, W. S., Yamada, H., Nishikubo, K., Kusaba, H., and Xu, C. N. *Chem. Mater.* (submitted).

2 Yamada, H., Kusaba, H., Shi, W. S., Nishikubo, K. and Xu, C. N. (2003) *J. Electrochem. Soc.* **150** (4) (to be published).

POSITIONS OF La AND Ba OF $BaLa_4Ti_4O_{15}$ HOMOLOGOUS COMPOUND

H. Ohsato,[a] Y. Tohdo,[a] K. Kakimoto,[a] T. Okawa,[b] and H. Okabe[b]

[a]Department of Materials Science and Engineering, Nagoya Institute of Technology, Gokiso-cho, Showa-ku, Nagoya 466-8555, Japan; [b]Daiken Chemical Co., Ltd., Japan, 2-7-9 Hanaten-Nishi, Joto-ku, Osaka 536-0011, Japan; (ohsato.hitoshi@nitech.ac.jp)

Homologous compound $Ba_nLa_4Ti_{3+n}O_{12+3n}$ (n=1, 2, and 4) series are one of candidate materials for base station of mobile telecommunications. The compound with n=1 has good microwave dielectric properties: ε_r =46, $Q \cdot f$ = 46,000 GHz and τ_f = -11[1]. Moreover, temperature coefficient of resonant frequency was improved to near zero: 1.3 ppm/°C with high ε_r of 44 and $Q \cdot f$ of 47,000 GHz[1].

These homologous compounds were reported by Saltykova *et al.* [2], which have three kinds of compound on the $La_4Ti_3O_{12}$-$BaTiO_3$ tie line near the tungsten bronze-type like $Ba_{6-3x}R_{8+2x}Ti_{18}O_{54}$ (R = rare earth) solid solutions in the BaO-La_2O_3-TiO_2 ternary system. The homologous compounds $Ba_nLa_4Ti_{3+n}O_{12+3n}$ with n=0, 1, 2, and 4, have been composed by means of adding n-times of $BaTiO_3$ on $La_4Ti_3O_{12}$ as following:

$$La_4Ti_3O_{12} + n(BaTiO_3) \rightarrow Ba_nLa_4Ti_{3+n}O_{12+3n}.$$

These crystal structures are presented by Harri[3], which have a layer perovskite structure so called hexagonal perovskite. The crystal data are as follows: trigonal system, P-3c1, a=5.571(1), c=22.488(2) Å, Z=2, Dx=6.178 g/cm^3.

In this study, we determined the positions of Ba and La (denoted as A ion) of homologous compound $BaLa_4Ti_4O_{15}$ based on the radius of Ba and La ions, which have never been reported up to now to our knowledge because of the inherent difficulty due to similarity of the atomic scatter factors. These A ions: 2Ba and 8 La in one unit-cell are considered to locate in the $A$1:4d, $A$2:4d and $A$3:2a sites with 12 coordination numbers in the close packing layer of oxygen and A ions. Here, 4d and 2d are multiplicity and Wyckoff letter of positions. The Ba occupation was finally confirmed by X-ray single crystal structural refinements with the least square method with constraint of site occupancies. $A$1 sites locate near the empty cation octahedra, but other $A$2 and $A$3 sites locate near the TiO_6 octahedra. $A$1 sites are displaced upward on the packing layer toward the empty octahedra side.

References

1 Okawa, T., Kiuchi, K., Okabe, H. and Ohsato, H. (2001) *Jpn. J. Appl. Phys.* **40,** 5779-5782.

2 Saltykova, V. A., Mel'nikova, O. V., Leonova, N. V. and Fedorov, N. F. (1985) *Russ. J. Inorg. Chem.*, **30,** 105-107.

3 Harre, N., Mercurio, D., Trolliard, G. and Frit, B. (1998) *Material Research Bulletin,* **33**[10], 1537-1548.

RELATIONSHIPS BETWEEN RUTILE STRUCTURES

Christopher J. Howard,[a,b] Zhaoming Zhang,[a] and Brendan J. Kennedy[c]

[a]Australian Nuclear Science and Technology Organisation, PMB 1Menai, NSW 2234, Australia; [b]School of Physics, The University of Sydney, Sydney, NSW 2006, Australia; [c]School of Chemistry, The University of Sydney, Sydney, NSW 2006, Australia (B.Kennedy@chem.usyd.edu.au)

The structure of rutile, TiO_2, can best be viewed as an edge sharing and corner sharing arrangement of nearly regular TiO_6 octahedra. Specifically the structure consists of chains of edge-sharing octahedra corner linked to neighboring chains.

The tetragonal rutile structure permits some flexibility in the octahedral co-ordination, through variation of the anion position parameter along with the lattice parameters *a* and *c*. A greater flexibility, and the ability to accommodate a wider range of cations is achieved in distorted variants. In this work, we review these structures using group theory as implemented in the computer program ISOTROPY.

Typical distortions are (i) the distortion of the AX_6 octahedron for example due to Jahn-Tellar effects; (ii) off-centre displacements of the cations (several different displacement patterns are possible) (iii) tilting relative to one another of the corner-linked chains. Each of these distortions can be associated with irreducible representations of the parent space group $P4_2/mnm$, and ISOTROPY details structures produced by these different distortions acting separately or in combination. We have included a consideration of cation ordering in double rutiles ABX_4 and trirutiles A_2BX_6. Structures from the literature have been checked against the structures we have derived.

STRUCTURAL STUDIES ON JACALIN – CARBOHYDRATE COMPLEXES

K. Sekar,[a] A. A. Jeyaprakash,[b] P. G. Rani,[b] S. Katiyar,[b] A. Surolia,[b] and M. Vijayan[b]

[a]Bioinformatics Centre and Supercomputer Education and Research Centre; [b]Molecular Biophysics Unit, Indian Institute of Science, Bangalore 560 012, India (sekar@physics.iisc.ernet.in)

Jacalin is a 66kDa tetrameric lectin from the seeds of jackfruit (*Artocarpus integrifolia*). Each subunit consists of two chains, a long α chain and a short β chain, produced by post-translational proteolysis. The structure of the lectin-bound to Me-α-galactose was earlier solved in this laboratory. The structure revealed a novel lectin fold and the use of post-translational modification as a strategy for generating specificity for galactose at the primary binding site. At the disaccharide level, it is specific to tumour-related Galβ1-3GalNAc, known as T-antigen. We have now prepared and solved the structures of the complexes of the lectin with Gal, Me-α-GalNAc, T-antigen, Me-α-T-antigen and GalNAcβ1-3Gal-O-Me. In the complexes with T-antigen and Me-α-T-antigen, the primary site is occupied by the GalNac residue. The interactions of the Gal residue with the protein are confined to water bridges. The methyl group in Me-α-T-antigen has favourable interaction with an aromatic residue, accounting for its increased affinity to the lectin. In the complex with GalNAcβ1-3Gal-O-Me, however, the primary site is occupied by the Gal residue presumably on account of the favourable interaction of the methyl group with the residue. The structures of the complexes provide a reasonable explanation for the available thermodynamic data of jacalin-carbohydrate interactions. The details will be presented.

PRESENT STATUS OF PHARMACEUTICAL INDUSTRY BEAMLINE AT SPRING-8

Shintaro Misaki,[a] Kenji Suzuki,[b] Yoshio Katsuya,[c] Kazumi Nishijima,[d] and Yukiteru Katsube[c,e]

[a]Shionogi & Co., Ltd., Sagisu 5-chome, Fukushima-ku, Osaka, 553-0002, Japan; [b]Dainippon Pharmaceutical Co., Ltd., Enoki, Suita, Osaka, 564-0053, Japan; [c]Pharmaceutical Consortium for Protein Structure Analysis, Kouto, Mikazuki, Sayo, Hyogo, 679-5198, Japan; [d]Mochida Pharmaceutical Co., Ltd., Yotsuya 1-chome, Shinjuku-ku, Tokyo, 160-0004, Japan; [e]RIKEN Harima Institute, Kouto, Mikazuki, Sayo, Hyogo, 679-5148, Japan (shintaro.misaki@shionogi.co.jp)

The Pharmaceutical Consortium for Protein Structure Analysis (PCProt) was established in April 2001. This consortium is composed of 22 pharmaceutical companies affiliating with the Japan Pharmaceutical Manufacturers Association (JPMA). The Pharmaceutical Industry Beamline is constructed at SPring-8 for exclusive use by members of PCProt. The full-time operation of this beamline was started last September.

The specification of the Pharmaceutical Industry Beamline is almost same as that of RIKEN Structural Genomics Beamline I & II. The Pharmaceutical Industry Beamline is technically supported by RIKEN and the Japan Synchrotron Radiation Research Institute (JASRI). It is expected that the beamline will contribute to both pharmaceutical protein crystallography for drug design and structural genomics carried out in RIKEN.

The Pharmaceutical Industry Beamline has the SPring-8 standard transport channel and optics for bending magnet. Energy of monochromatic X-rays is tuneable from 7 to 17 keV using a double crystal monochromator and is focused at sample using a bent cylindrical mirror. The authors will report on MAD experiments and some others carried out in the beamline.

REFINEMENT OF THE CRYSTALLIZATION CONDITIONS OF CONGER EEL GALECTIN, CONGERIN I AND II

Takashi Yamane,[a] Atsuo Suzuki,[a] Yumiko Miyabe,[a] Clara Shionyu-Mitsuyama,[a] Yuusuke Niwa,[a] Tomohisa Ogawa,[b] Koji Muramoto,[b] and Mitsuo Ataka[c]
[a]Graduate School of Engineering, Nagoya University, Nagoya 464-8603, Japan; [b]Graduate School of Agricultural Science, Tohoku University, Sendai 981-8555, Japan; [c]National Institute of Advanced Industrial Science and Technology (AIST), Ikeda 563-8577, Japan (yamane@hix.nagoya-u.ac.jp)

The skin of conger eel (*Conger myriaster*) secrets mucus containing the galectin family proteins, congerin I and II. To understand the carbohydrate recognition mechanism of congerins, the crystal structure of congerin I was determined at 1.5 Å resolution[1]. Recently the crystal structure of congerin II with lactose and 2-(*N*-morphorino)ethansulfonic acid (Mes) was determined at 1.45 Å resolution[2]. In order to obtain further insights into the structure-function relation between congerins, the refinement of the crystallization conditions has been carried out as a part of the efforts to conduct microgravity experiments using High Density Protein Crystal Growth (HDPCG) cell[3].

Congerin I: *original conditions*; A 5 µl of protein solution (2.0% (w/v) protein in 0.01 M Tris-HCl buffer (pH 7.0)) was mixed with 5 µl reservoir solution (25% (w/v) PEG6000 in 0.1 M Tris-HCl buffer (pH 9.0)). Crystals were grown within one month to max. dimensions of 0.5 x 0.4 x 0.2 mm^3; *refined conditions*; 40 µl droplet of protein solution (1.75-2.0% (w/v) protein in 0.1 M Tris-HCl buffer (pH 8.5) with 17.5-20% (w/v) PEG6000) and 560 µl reservoir solution (35% (w/v) PEG6000 in 0.1 M Tris-HCl buffer (pH 8.5)). Crystals were grown within two weeks to max. dimensions of 0.2 x 0.2 x 0.2 mm^3. **Congerin II**: *original conditions*; 8 µl droplet of protein solution (1% (w/v) protein in 0.5 M Mes buffer (pH 6.5) with 1 mM lactose and 0.8 M $MgSO_4$) and 1 ml reservoir solution (1.6 M $MgSO_4$ in 1.0 M Mes buffer (pH 6.5)). Crystals were grown in one month to max. dimensions of 0.5 x 0.5 x 0.5 mm^3; *refined conditions*; 40 µl droplet of protein solution (1.0-1.75% (w/v) protein in 0.1 M Mes buffer (pH 6.5) with 1.2-1.3 M $MgSO_4$) and 560 µl reservoir solution (1.6-1.75 M $MgSO_4$ in 0.1 M Mes buffer (pH 6.5)). Crystals were grown within two weeks to max. dimensions of 0.4 x 0.4 x 0.2 mm^3.

The synchrotron radiation experiments were performed at SPring-8 (Proposal No. J03A12B2-0500N). For congerin I, 1.3 Å resolution data were collected from new crystals. It is interesting that two morphologically different crystals were grown. One belongs to orthorhombic system, with a=40.7, b=93.7 and c=113 Å. The other is isomorphous to that of congerin II. On the other hand, both new and original crystals of congerin II are isomorphous, and the new crystals diffracted to 1.0 Å resolution. Structure determination of congerin I and II using these data is currently under way.

This study is funded in part by "Science Research Program Experiment Themes for Protein Crystal Growth Experiment in Space using STS-107 " by NASDA and Japan Space Forum.

References

1 Shirai, T. *et al.*, (1999) *Structure* **7**, 1223-1233.
2 Shirai, T. *et al.* (2002) *J. Mol. Biol.*, **321**, 879-889.
3 DeLucas, L. J. *et al* (2002) *J. Crystal Growth* **237-239**,1646-1650.

NEUTRON PROTEIN CRYSTALLOGRAPHY OF CUBIC INSULIN

M. Maeda,[a] T. Chatake,[a] I. Tanaka,[a] A. Ostermann,[a,b] and N. Niimura[a]

[a]Advanced Science Research Center, Japan Atomic Energy Research Institute (JAERI), 2-4 Sirakata Shirane, Tokai-mura, Naka-Gun, Ibaraki, 319-1195, Japan; [b]Physik-Department E 17 der TUM, James Frank Str., 85747 Garching, Germany (mmaeda@neutrons.tokai.jaeri.go.jp)

Hydrogen atoms and water molecules surrounding protein play important roles in many physiological functions. However, it is difficult to determine hydrogen atoms in protein molecules in X-ray protein crystallography. On the other hand, neutron protein crystallography has become a powerful method for locating position of hydrogen (deuterium) atoms bound waters of proteins [1]. In order to elucidate hydration structure in cubic insulin crystals, large single crystals of cubic insulin for neutron protein crystallography have been grown in D_2O by a dialysis method. The size of the grown largest crystal of cubic insulin is 4.0 x 4.0 x 1.25 mm^3 in volume.

The neutron diffraction experiment has been carried out with single crystal diffractometer BIX-3 installed of JRR-3M reactor in JAERI. The structure analysis has been investigated, and important information has been extracted from the structural result.

This study is supported by a grant from the Organized Research Combination System (ORCS).

References

1 Niimura, N., Minezaki, Y., Nonaka, T., Castanga, J-C., Cipriani, F., Hoghoj. P., Lehmann., M. S., & Wilkinson. C. (1997). *Nat. Struct. Biol.* **4**, 909-914.

PREPARATION, CHALACTERIZATION AND CRYSTALLIZATION OF THE COMPLEX COMPOSED OF GRANULOCYTO COLONY-STIMULATING FACTOR AND ITS RECEPTOR

Eijiro Honjo,[a] Shouhei Mine,[a] Takumi Koshiba,[b] Tomoyuki Okamoto,[a] Taro Tamada,[a] Yoshitake Maeda,[a] Yasuko Matsukura,[a] Akane Horie,[a] Matsujiro Ishibashi,[c] Miharu Sato,[a] Mizue Azuma,[a] Masao Tokunaga,[c] Katsutoshi Nitta,[b] and Ryota Kuroki[a]

[a]Protein Engineering Group, Pharmaceutical Research Laboratories, Kirin Brewery Co. Ltd., 1-13-5 Fukuura, Kanazawa-ku, Yokohama 236-0004, Japan; [b]Division of Biological Sciences, Graduate School of Science, Hokkaido University, Kita-ku, Sapporo 060-0810, Japan; [c]Laboratory of Applied Microbiology, Faculty of Agriculture, Kagoshima University, 1-21-24 Korimoto, Kagoshima 890-0065, Japan (Eijirou_Honjo@beer.kirin.co.jp)

Granulocyte colony-stimulating factor (G-CSF) is a cytokine that regulates the proliferation and differentiation of neutrophils. These responses are initiated by interaction with a specific receptor (G-CSFR). G-CSFR has a composite structure consisting of an immunoglobulin (Ig)-like domain, a cytokine receptor homologous (CRH) domain and three fibronectin type III domains in the extracellular region. G-CSF forms a tetrameric complex with G-CSFR, comprising two G-CSF and two receptor molecules. The tetrameric structure of the complex is unknown, but it is indicated that the Ig domain and the CRH domain of G-CSFR are involved in G-CSF binding.

To attempt to determine the tertiary structure of G-CSF/G-CSFR complex by X-ray crystallography, we first prepared G-CSFR (Ig-CRH) insect cell culture, in which G-CSFR was expressed as fusion protein with Fc region of mouse IgG. After digestion of G-CSFR-Fc by thrombin to remove Fc region, the G-CSFR was prepared by gel filtration. The isothermal titration of G-CSFR with G-CSF showed that the ligand-receptor affinity was ~10^8 M^{-1}. The light scattering experiment equipped with gel filtration column showed that the average molecular weight of G-CSF/G-CSFR complex was 132000 daltons indicating a 2:2 ligand-receptor complex. The G-CSF/G-CSFR complex thus characterized was used for crystallization screening. The complex was crystallized to a space group $P4_12_12$ with unit cell dimensions of a = b = 110.1Å, c = 331.8 Å at a condition containing 0.1 M Na formate and 1.0 M Na acetate (pH 4.6). The preliminary diffraction experiment indicated that the crystal diffracts only upto 4 Å resolution. We are now attempting to obtain the different form of G-CSF/G-CSFR complex by removing the N-linked sugar chains located in G-CSFR using several glycosidases.

CRYSTAL STRUCTURE OF DSBG A DISULFIDE BOND ISOMERASE FROM ESCHERICHIA COLI

Begoña Heras,[a] Melissa A. Edeling,[a] Jennifer L. Martin,[a] and Satish Raina[b]

[a]Institute for Molecular Bioscience. University of Queensland, Brisbane QLD 4072 Australia; [b]Centre Médical Universitaire, Département de Biochimie Médicale, 1 Rue Michel-Servet, 1211 Genève 4, Switzerland (b.heras@imb.uq.edu.au)

The correct formation of disulfide bonds is important for the folding and function of many secretory and membrane proteins. In bacteria, disulfide bond formation occurs in the periplasmic space and is catalysed by the Dsb (**dis**ulfide **b**ond formation) family of proteins (DsbA, DsbB, DsbC, DsbD, DsbE, and DsbG) [1]. These proteins form two distinct pathways for disulfide formation and rearrangement. The DsbA-DsbB pathway [2] rapidly introduces disulfide bonds into target proteins, sometimes resulting in the formation of nonnative disulfide bonds, the DsbC/DsbG-DsbD pathway [3] catalyzes the rearrangement of incorrect disulfide bonds, allowing proteins to fold correctly.

Crystal structures of three Dsb proteins have been determined, DsbA, DsbC and DsbE [4-6]. Here we present the crystal structure of the last soluble member of the Dsb family, DsbG, a disulfide bond isomerase from *E. coli* that also functions as a molecular chaperone [7]. DsbG crystal structure determination required dehydration of crystals prior to data collection. This post-growth treatment dramatically improved the diffraction resolution of DsbG crystals from 10 to 2 Å (1.7 Å at a synchrotron source) [8]. The crystal structure of DsbG was determined by multiwavelength anomalous diffraction (MAD) methods and refined to an R free of 20.5% (R factor 18.8%) at 1.7 Å.

The overall structure of DsbG resembles that of DsbC [5]. Both are V-shaped homodimers in which each monomer incorporates an N-terminal dimerisation domain and a thioredoxin like catalytic domain separated by a linker α-helix. However, a striking difference between the two is the length of the linker helix located between the dimerisation and catalytic domain in each monomer, which is 2.5 turns longer in DsbG.

References

1. Kadokura, H., Katzen, F. and Beckwith, J. (2003) *Annu. Rev. Biochem.* **72**, 111-135.
2. Bardwell, J. C., Lee, J. O., Jander, G., Martin, N., Belin, D. and Beckwith, J. (1993) *Proc. Natl. Acad. Sci. USA* **90**, 1038-1042.
3. Rietsch, A., Belin, D. Martin, N. and Beckwith, J. (1996) *Proc. Natl. Acad. Sci. USA* **93**, 13048-13053.
4. Martin, J. L., Bardwell, J. C. and Kuriyan, J. (1993) *Nature* **365**, 464-468.
5. McCarthy, A. A., Haebel, P. W., Torronen, A., Rybin, V., Baker, E. N. and Metcalf, P. (2000) *Nature Struct. Biol.* **7**, 196–199.
6. Edeling, M. A., Guddat, L. W., Fabianek, R. A., Thöny-Meyer, L. and Martin, J. L. (2002) *Structure* **10**, 973-979.
7. Shao, F., Bader, M. W., Jakob, U. and Bardwell, J. C. (2000) *J. Biol. Chem.* **275**, 13349-13352.
8. Heras, B., Edeling, M. A., Byriel, K. A., Jones, A., Raina, S. and Martin, J. L. (2003) *Structure* **11**, 139-145.

PROTEIN MODEL BUILDING USING IMAGE PROCESSING TECHNIQUE AND OPTIMIZATION ALGORITHMS

Osamu Takahashi,[a,b] and Shigenobu Kobayashi[b]
[a]NEDO Fellow, New Energy and Industrial Technology Development Organization; [b]Department of Computational Intelligence and Systems Science, Tokyo Institute of Technology, 4259 Nagatsuta Midoriku Yokohama 226-8502 Japan (osamu@fe.dis.titech.ac.jp).

To reveal protein structures becomes important more and more at the period of post sequence genomics. X-ray crystallography is one of effective methods to do that, but it often requires much time and effort at some processes that include tracing and building model from an electron density map. And, an automated iterative model building method was proposed by Perrakis et al. [1].

We presented a new basic concept using three-dimensional image processing technique to obtain rough protein molecular model at the last ICCBM9 [2]. We extended *thinning* technique, which is one of normal image processing techniques for two-dimensional images, to for three-dimensional images like electron density maps. Thinned electron density map shows its skeletal structure. Trunk of the skeleton corresponds to main chain of the protein, and branches correspond to the side chains. And the branching points on it roughly correspond with C-alpha atoms.

Here, we present the latest work after the image processing. Referring to rough positions of branching points, we refine C-alpha atom positions using real number optimization algorithm with peptide bond template. To form the template, we use Gaussian density distribution as a pseudo electron density distribution from an atom in real space. After the process, incremental atom position optimizing search forms tables of amino residue fitting value into each side chain positions. At the last we can build a molecule model from the value table and given amino acid sequence. Using the image processing technique and the optimization algorithm, we can robustly build protein molecule model from X-ray crystallography data.

Fig 1. Obtained Skeleton in a Density Map

Fig 2. Branching Points in the Skeleton

References

1 Perrakis, A., Morris, R. J. and Lamzin, V. S. (1999) *Nature Structural Biology* **6**, 458-463.

2 Takahashi, O. and Kobayashi, S. (2002) *9th International Conference on the Crystallization of Biological Macromolecules* O-A5.5(Oral Presentation).

CRYSTAL STRUCTURE OF TBP-INTERACTING PROTEIN (*TK*-TIP26) FROM HYPERTHERMOPHILIC ARCHAEON THERMOCOCCUS KODAKARAENSIS STRAIN KOD1

T. Yamamoto,[a] T. Matsuda,[b] H. Matsumura,[a] T. Inoue,[a] M. Morikawa,[b] S. Kanaya,[b] and Y. Kai[a]

[a]Department of Materials Chemistry, Graduate School of Engineering, Osaka University, 2-1 Yamada-oka, Suita, Osaka 565-0871, Japan; [b]Department of Material and Life Science, Graduate School of Engineering, Osaka University, 2-1 Yamada-oka, Suita, Osaka 565-0871, Japan (taka@chem.eng.osaka-u.ac.jp)

The 26 kD TBP-interacting protein from hyperthermophilic archaeon *Thermococcus kodakaraensis* KOD1 (*Tk*-TIP26) is a possible transcriptional regulatory protein in *Thermococcales*. It was isolated from cell lysates of this strain by affinity chromatography with TBP-agarose. Cloning of the gene encoding this protein showed that *Tk*-TIP26 is composed of 224 amino acid residues (molecular weight of 25,558) and exists in a dimeric form. The recombinant *Tk*-TIP26 and *Tk*-TBP interact with each other with an equilibrium dissociation constant, K_D of 1.24-1.46 μM. In the presence of *Tk*-TFB, *Tk*-TIP26 does not inhibit the formation of TFB/TBP/DNA ternary complex, but interact with this complex to form TIP26/TFB/TBP/DNA quaternary complex. On the other hand, in the absence of *Tk*-TFB, *Tk*-TIP26 prevents *Tk*-TBP from binding to TATA-DNA. These results suggest that TIP26 plays an important role in transcriptional regulation in *Thermococcales*. We have determined 3rd-dimensional structure of *Tk*-TIP26 by the multiwavelength anomalous dispersion method at 2.3 Å. The monomer structure had the shape of a 'foot', containing two domains (N-terminal domain, and C-terminal domain). N-terminal domain formed β-sandwich structure comprising 4 α-helixes and 6 β-strands, and its topology resembled Holiday junction resolvase (Hjc) from *Pyrococcus furiosus*. The dimer structure of *Tk*-TIP26 was composed of two monomers related by the crystallographic 2-fold axis. Dimeric *Tk*-TIP26 had a few clefts that might accommodate TBP. The minute discussion on the interaction between *Tk*-TIP26 and *Tk*-TBP is in progress.

TOWARDS A MORE USABLE PROTEIN STRUCTURE DATABASE

W. Bret Church,[a,b] Hong Wing Lee,[b] William M. Shui,[c] Stephen C. Graham,[b] Lawrence K. Lee,[b] and Raymond K. Wong[c]

[a]Molecular Biotechnology Program; [b]School of Molecular and Microbial Biosciences G08, University of Sydney, NSW 2006, Australia; [c]School of Computer Science and Engineering, University of New South Wales, NSW 2052, Australia (b.church@biotech.usyd.edu.au)

In recent years several structural genomics initiatives have been started with the aim of determining the structures of a large number of proteins, and it has been suggested that the PDB may hold 35,000 entries by the end of 2005.

We are using a database management system to provide a consistent XML database interface for data storage and retrieval of PDB data. This system employs the Semi-structured Object Database (SODA) [1]. A SODA specific translation language is responsible for mapping external, non-XML data sources to XML so that they can be queried by SODA. The entire contents of PDB files can be made available. While the ATOM (and HETATM) records are critical to a protein structure database, significant additional annotation records such as CAVEAT and SITE records could also be made available to query.

Data derived from the PDB entries, such as accessible surface calculations, can easily be housed within the database. Based on the given and derived meta-data, whenever the source data layer is changed a trigger system invokes modules to recalculate and update the meta-data layer. SODA gives users the choice of triggers at either the source data layer or the meta-data layer. The latter option makes for a rate limiting initial step but it uses fewer resources overall. An extended form of the XML query language XQuery providing support for updates is available in SODA [1].

The wider context of this work allows for integration of existing repositories of data and information created with tools for biological analysis. Populating and querying these databases can be conducted according to the whims of the researcher.

We will report our progress on the installation and use of this database.

References

1 Wong, R.K., In *Proceedings of the ACM Symposium on Document Engineering*, Eds. Ethan Munson, Atlanta USA, 9-10 Nov. 2001, ACM, USA, pp95-104. http://www.sodatech.com

DATA BASE OF HYDROGEN AND HYDRATION IN PROTEINS

N. Niimura

Advanced Science Research Center, Japan Atomic Energy Research Institute, Tokai-mura, Ibaraki-ken, 319-1195, Japan (niimura@kotai3.tokai.jaeri.go.jp)

Neutron diffraction provides an experimental method of directly locating hydrogen atoms in proteins, and the development of the neutron imaging plate (NIP) became a breakthrough event in neutron protein crystallography. Several high resolution neutron diffractometers dedicated to biological macromolecules (BIX-2, BIX-3 and BIX-4) with the NIP have been constructed at the Japan Atomic Energy Research Institute and these have enabled high resolution (such as from 1.5Å to 2.0Å) structural analyses of several proteins to have been carried out. The crystal structures of myoglobin, rubredoxin (wild & mutant), hen egg-white lysozyme (at pH4.9 and 7.0) and, human lysozyme, cubic insulin, DsrD and oligomer DNA have been determined using BIX. From these studies, all the hydrogen and hydration in these proteins have been summarized as data base, and by using them, very interesting topics relevant to hydrogen and hydration in proteins, such as hydrogen bonds, H/D exchange, acidic hydrogen atom, the role of hydrogen atoms in enzymology, the identification of methyl hydrogen atoms and dynamical behaviors of hydration structures including hydrogen have been extracted from the structural results.

E. COLI DIHYDROOROTASE: STRUCTURE OF THE ENZYME CRYSTALLISED IN THE PRESENCE OF DIHYDROOROTATE. THE POSSIBILITY OF COOPERATIVITY BETWEEN SUBUNITS?

Mihwa Lee, J. Mitchell Guss, Richard I. Christopherson, and Megan J. Maher

School of Molecular and Microbial Biosciences, University of Sydney, NSW 2006, Australia (m.lee@mmb.usyd.edu.au)

Dihydroorotase (DHOase) is a zinc metalloenzyme that catalyses the reversible cyclisation of *N*-carbamyl-L-aspartate (CA-asp) to dihydroorotate (DHO) in the third step of the *de novo* pyrimidine biosynthetic pathway. In prokaryotes DHOase is a homodimeric and monofunctional enzyme of approximate molecular weight 40 kDa [1]. In higher eukaryotes, DHOase activity is associated with a trifunctional enzyme (CAD) which catalyses the first three steps of the pathway [2].

The first structure of a DHOase (from *E. coli*) has been reported to a resolution of 1.7 Å with one homodimer per asymmetric unit [3]. In agreement with sequence-based predictions, the overall architecture of the enzyme resembles that of urease. The protein folds into a TIM-barrel motif, with eight strands of parallel β-sheet flanked on the outer surface by α-helices. The active site was shown to contain a binuclear Zn site with bridging water/hydroxide and carboxylated lysine ligands. The crystals of DHOase were grown in the presence of the substrate CA-asp and interestingly the structure showed DHO bound at the active site of one subunit (molecule A) with CA-asp at the active site of the other subunit (molecule B). Importantly, a loop flanking the active site of molecule B (CA-asp-bound) including residues 109-112 was not observed in the published structure.

We have been working on crystallizing hamster DHOase for some time with limited success [4]. Since the ultimate aim of the work is that of inhibitor design, we decided to direct our attention to the structure of inhibitor complexes of *E. coli* DHOase. As a preliminary study, we have collected data from crystals of the enzyme grown in the presence of DHO (rather than CA-asp as in the original report [3]) and refined the structure to 1.9 Å resolution. Again, we find the product DHO bound in the active site of one subunit and CA-asp in the active site of the other subunit. Importantly, we have been able to resolve the conformations of the formerly missing residues 109-112. These residues comprise a loop which takes on very different orientations in the two subunits, depending on whether DHO or CA-asp is present in the active site. This raises the possibility of cooperation/communication between the subunits and may have important implications for both mechanism and inhibitor design.

References

1 Washabaugh, M. W. and Collins, K. D. (1984) *J. Biol. Chem.* **259**, 3293.
2 Coleman, P. F., Suttle, D. P. and Starck, G. R. (1977) *J. Biol. Chem.* **252**, 6379.
3 Thoden, J. B., Phillips, G. N. J., Neal, T. M., Raushel, F. M. and Holden H. M. (2001) *Biochemistry* **40**, 6989.
4 Maher, M. J., Huang, D. T. C., Guss, J. M., Collyer, C. A. and Christopherson, R. I. (2003) *Acta Cryst.* **D59**, 381.

THE CRYSTAL STRUCTURE OF RUBREDOXIN FROM DESULFOVIBRIO GIGAS AT ULTRA-HIGH 0.68 Å RESOLUTION

Chun-Jung Chen,[a,c] Yi-Ting Chen,[a] Ming-Yih Liu,[b] and Jean Le Gall[b]

[a]X-ray Structural Biology Group, National Synchrotron Radiation Research Center, Hsinchu 30077, Taiwan; [b]Department of Biochemistry & Molecular Biology, University of Georgia, Athens, GA 15260, U. S. A.; [c]Department of Physics, National Tsing-Hua University, Hsinchu 30077, Taiwan (cjchen@srrc.gov.tw)

More and more examples of phasing macromolecular crystal structures based on single-wavelength anomalous dispersion (SAD) show that this method is more powerful and may have more general application in structural biology. Advanced data-collection facilities and cryogenic techniques, coupled with powerful programs for data processing, phasing, density modification and automatic model building, have made the SAD approach gain wider use because of its simplicity and faster data collection and phasing than the multi-wavelength (MAD) method or other methods. It can be performed at any wavelength where anomalous scattering can be observed in synchrotron. For those proteins containing metal ions, metal clusters or heavier atoms with sufficiently large Df", such as Fe, Ni, Cu and S, the SAD experiment can be carried out directly on the native crystals without the need of seleno-derivatives. The SAD method combines the use of SAD data and solvent flattening to resolve phase ambiguity.

We have recently determined the *ab initio* structure of rubredoxin at ultra-high resolution, 0.68 Å, using the single-wavelength iron anomalous dispersion signal at SPring-8 BL12B2 and NSRRC BL17B2 Taiwan beamline. Rubredoxin from anaerobic sulfide reducing bacteria *Desulfovibrio gigas* is a small redox protein composed of 52 amino acids. It contains with single iron atom bound in a tetrahedral coordination by the sulfur atoms of four cysteinyl residues. The protein is often purified from anaerobic bacteria where it is thought to be involved in electron transfer or exchange processes. The crystal belongs to the space group $P2_1$ with unit cell of a = 19.44 Å, b = 41.24 Å, c = 24.10 Å, and β = 108.46°. The electron density at 0.68 Å ultra-high resolution can help determining very accurate atomic position, especially for the coordination of [Fe-4S] cluster, which reveals detailed information of biological function. In this study, we will demonstrate the power of Fe-SAD combining solvent flattening as the demanding phasing method for metal or sulfur-containing proteins, and report the ultra-high resolution crystal structures.

TUMOUR PEPTIDE PRESENTATION BY MHC CLASS I

Michelle A. Dunstone,[a] Andrew Z. Webb,[b] Anthony W. Purcell,[b] and Jamie Rossjohn[a]

[a]The Protein Crystallography Unit, Department of Biochemistry and Molecular Biology, Monash University, Clayton, VIC 3800, Australia; [b]Department of Microbiology and Immunology, University of Melbourne, VIC 3010, Australia (michelle.dunstone@med.monash.edu.au)

The role of Class I Major Histocompatibility Complex (MHC) is to capture, transport and present intracellular peptides to the cell surface. These peptides are derived by the proteolytic processing of both endogenous host cell proteins and viral proteins. Discrimination of whether these peptides are foreign is performed by circulating T lymphocytes, where recognition of a foreign peptide results in activation of an immune response.

Tumourogenesis can result in expression of proteins that are silent in normal cell types resulting in peptides presented specifically by tumour cells. These peptides have also been found to be immunogenic opening up the prospect of stimulating the immune system to target tumours using peptide vaccination. One such candidate is the region 155-167 of NY-ESO, called NY-ESO-1 (sequence SLLMWITQCFL). Peptides of this region have been found to be presented by the HLA-A2 MHC in melanoma, breast, lung and bladder cancers.

Research into development of a vaccine to this region so far has identified a need to improve the resistance to peptidases and to modification of the cysteine and methionine residues without compromising immunogenicity of the peptide. The aim of this research is to develop a peptide analogue which addresses these aspects. The structure NY-ESO-$1_{157\text{-}165}$ (SLLMWITQC), in complex with the HLA-A2 molecule, has been solved to a resolution of 2.1 Å and is presented here. Effects on the structure by the substitution with peptide analogues are analysed together with the results of functional assays of these peptide analogues.

THE CRYSTAL STRUCTURE OF A CORAL POCILLOPORIN

Pascal G. Wilmann,[a,b] Travis Beddoe,[a,b] Mark Prescott,[b] Michael Ling,[b] Aaron J. Oakley,[c] Sophie Dove,[d] Ove Hoegh-Guldberg,[d] Rodney J. Devenish,[b] and Jamie Rossjohn[a,b]
[a]The Protein Crystallography Unit; [b]Department of Biochemistry and Molecular Biology, School of Biomedical Sciences, Monash University, Clayton, Victoria 3800, Australia; [c]Department of Pharmacology/ Crystallography Centre, University of Western Australia, Crawley, Western Australia 6009, Australia; [d]Centre for Marine Studies, University of Queensland, St. Lucia, Queensland 4072, Australia (pascal.wilmann@med.monash.edu.au)

Reef building corals contain fluorescent pigments, termed pocilloporins that function by regulating the light environment of coral. These act as photoprotectants to the excessive sunlight that is related to the photo bleaching phenomenon in corals. Rtms5 is a blue non fluorescent pocilloporin from the reef-building coral *Montipora efflorescens* which has strong sequence and structural homology to both green fluorescent protein from *Aqueorea victoria* (GFP) and a red fluorescent protein from *Discosoma* coral (DsRed).

To date no pocilloporin structure has been published, however the information gained from elucidating the structure of a pocilloporin would provide detailed insights into the mechanism of coral photoprotection. Rtms5 has been cloned, expressed, purified and crystallized resulting in intensely blue crystals (0.3 x 0.2 x 0.3 mm) with an octahedral appearance [1]. Directed mutagenesis of residues surrounding the chromophore have been performed resulting in a fluorescent variant termed Rtms5His^{146}Ser. Fluorescence analysis has revealed Rtms5His^{146}Ser is currently the most red-shifted fluorescent mutant, with an emission maximum of 636nm. Rtms5His^{146}Ser has also been purified and crystallized. The structures of both Rtms5 and Rtms5His^{146}Ser have been determined through molecular replacement using DsRed as the probe [2].

Structural analysis of Rtms5 showed the chromophore to be in a unique trans configuration and it was believed that Rtms5His^{146}Ser structure should have a cis chromphore conformation due to its fluorescent nature. However the trans conformation was also observed in Rtms5His^{146}Ser. Subsequently it is hypothesized that only a small population of Rtms5His^{146}Ser molecules adopt the cis chromophore conformation and it is these molecules that are responsible for the observed fluorescence. Under some conditions the fluorescence intensity of Rtms5His^{146}Ser is markedly increased. It is proposed that the increase in fluorescence is due to an increased proportion of the molecule in the cis conformation. This observation may be related to a documented "kindling phenomenon" [3] of another pocilloporin. Efforts are being made to determine the structures of Rtms5 under the conditions that increase fluorescence.

References

1 Beddoe, T., Ling, M., Dove, S., Hoegh-Guldberg, O., Devenish, R., Prescott, M. and Rossjohn, J. (2003) *Acta Cryst* **D59**, 597-599.
2 Prescott, M., Ling, M., Beddoe, T., Oakley, A., Dove, S., Hoegh-Guldberg, O., Devenish, R. and Rossjohn, J. (2003) *Structure* **11**:(3), 275-284.
3 Chudakov, D., Belousov, V., Zaraisky, A., Novoselov, V., Staroverov, D., Zorov, D., Lukyanov, S. and Lukyanov, K. (2003) *Nat Biotechnol* **21**:(2), 191-194.

STRUCTURAL CHARACTRISATION OF MITOCHONDRIAL IMPORT RECEPTORS

Travis Beddoe,[a,b] Pascal Wilmann,[a,b] Simon Bushell,[a,b] Judy Scoble,[c] Diana Macasev,[c] Trevor Lithgow,[c] and Jamie Rossjohn[a,b]

[a]The Protein Crystallography Unit; [b]Department of Biochemistry and Molecular Biology School of Biomedical Sciences Monash University Clayton, Victoria, 3168, Australia; [c]Department of Biochemistry and Molecular Biology, University of Melbourne, Victoria, 3010, Australia (travis.beddoe@med.monash.edu.au)

Nuclear genes encode the majority of mitochondrial proteins therefore the proteins are synthesised by cytosolic ribosomes and are then imported by the mitochondria. Preproteins are targeted to the mitochondria by specific sequences, either at their N-terminus, C-terminus or internal sequences. They are recognised at the surface of the mitochondria by the TOM (translocase of the outer membrane) complex. In yeast, the receptor subunits of the TOM complex are Tom70-Tom37 and Tom20-Tom22, and are involved in initial binding of all precursors. The Tom70 receptor is especially important in binding precursors with internal targeting sequences, whereas the Tom20-Tom22 receptor complex binds N- and C-terminal targeting sequences. Once a precursor has bound to the Tom70 receptor it is passed to the Tom20-Tom22 complex via an interaction between Tom70 and Tom20. After binding to Tom20-Tom22, the precursor proteins are transferred to the translocation pore, consisting of Tom40 and its associated subunits Tom5, Tom6 and Tom7. Once through the Tom40 pore, the precursor is sorted into the correct submitochondrial compartment, often with a requirement for membrane potential, where it will be folded and assembled by the TIM (translocase of the inner membrane) complex.

To determine how this complex recognises preproteins and imports them, several of the individual proteins have been expressed and purified from *E.coli*. Data will be presented on the progress towards their structural determination.

MHC CLASS I PEPTIDE PRESENTATION – A STRUCTURAL INSIGHT

L. K. Ely,[a] W. A. MacDonald,[b] L. Kjer-Nielsen,[b] C. S. Clements,[a] A. G. Brooks,[b] A. Purcell,[b] J. McCluskey,[b] and J. Rossjohn[a]

[a]The Protein Crystallography Unit, Department of Biochemistry and Molecular Biology, Monash University, Clayton, VIC 3800, Australia; [b]Department of Microbiology and Immunology, The University of Melbourne, Parkville, VIC 3052, Australia (lauren.ely@med.monash.edu.au)

The ability for T lymphocytes to selectively recognise peptide-MHC complexes is critical for cell-mediated immunity. Antigen presenting cells digest both endogenous and viral antigenic protein to produce peptide fragments; these peptides are transported to the plasma membrane by MHC molecules. Passing T lymphocytes recognise specific peptide-MHC complexes through their T cell antigen receptors (TCRs) and selectively kill virally infected cells. The ability for self-TCRs to recognise foreign MHC complexes is termed allorecognition. This cross reactivity has significant clinical implications as it is the basis for T cell mediated transplant rejection.

To understand the structural basis of T-cell allorecognition we are studying the immune response to Epstien Barr Virus (EBV). EBV is a ubiquitous human pathogen that infects approximately 90% of the population. In individuals that express the MHC allele HLA B8, TCRs are produced to specifically recognise the EBV peptide in complex with the B8 allele. Previous work in our laboratories has resolved the crystal structure of the HLA B8 with the EBV peptide in complex with this TCR [1]. These TCRs are alloreactive binding an endogenous peptide in complex with the MHC alleles HLA B4402 and B4405 however not with the closely related HLA B4403. Historically, transplants between HLA B4402 and B4403 patients have been associated with organ rejection and thus considered taboo. These two alleles are extremely abundant, making up 10-15% of Caucasian HLA B alleles, and thus this mismatch represents a significant transplant barrier.

The endogenous peptide or "allopeptide" that is recognised by this TCR in the cleft of the HLA B44 alleles is unknown. Little is understood about how the peptide sequence influences the presentation in the MHC cleft and the effect this has on TCR recognition. To address this question I have solved a series of high-resolution HLA B44 structures with varying peptide ligands. Here I will present a structural analysis of this alloreactive system.

References

1 Kjer-Neilsen, L., Clements, C. S., Purcell, A. W., Brooks, A. G., Whisstock, J. C., Burrows, S. R., McCluskey, J. and Rossjohn, J. (2003) *Immunity* **18**, 53-64.

THE CRYSTALLIZATION AND X-RAY DIFFRACTION OF THE HALOACID DEHALOGENASE DEHIVA FROM THE SOIL BORNE BACTERIUM BURKHOLDARIA CEPACIA MBA4

Jason W. Schmidberger, Matthew C. J. Wilce, Aaron J. Oakley, and Colin A. Thompson

[a]Structural Biology Group, Department of Pharmacology, University of Western Australia, Nedlands, WA 6009 (jwschmidberger@yahoo.com.au).

DehIVa is a dehalogenase enzyme with a hydrolytic activity found in *Burkholdaria cepacia* MBA4. It belongs to a group of dehalogenating enzymes that degrade halogenated aliphatic acids and exhibit a broad range of substrate specificities. Although a significant amount of biochemical information about DehIVa is already known, its tertiary structure is not. Furthermore, only two related enzymes from this group have had their structures solved. This study aimed at solving the tertiary structure of DehIVa. Protein was purified to ~98% through a series of mostly chromatographic methods, and then screened against JB Screens 2 and 3. Bipyramidal crystals with largely hexagonal shape were successfully grown in less than 24 hours in JB Screen 3, conditions A6, B1 and B4. A succession of screens around these growing conditions (15% PEG_{4000}, 0.2M ammonium sulfate, and 0.1M sodium acetate buffer pH 4.4) produced larger crystals, which were found to diffract to 3.4 angstroms. Five crystal forms have since been identified growing in a variety of conditions.

TRYPTOPHAN BIOSYNTHESIS IN MYCOBACTERIUM TUBERCULOSIS

J. Shaun Lott,[a] Anthony J. Harrison,[a] Emily Parker,[b] Rochelle J. Ramsay,[a] and Edward N. Baker[a]

[a]Laboratory of Structural Biology, School of Biological Sciences, University of Auckland, Private Bag 92-019, Auckland, New Zealand; [b]Institute of Fundamental Sciences, Massey University, Private Bag 11-222, Palmerston North, New Zealand (s.lott@auckland.ac.nz)

Mycobacterium tuberculosis is the most successful pathogen of mankind. More people are killed by *M. tuberculosis* infection than by infection with any other bacterium. Recent estimates of the worldwide problem indicate that more than 1000 new cases of tuberculosis (TB) occur every hour, resulting in the death of more than 7000 people per day. Although TB is readily treated with antibiotic therapy, the treatment is slow (6-9 months) and incomplete therapy has given rise to TB strains which are resistant to one or all of the preferred antibiotics [1,2]. The rise of multiple drug resistant (MDR) TB strains has contributed to the increase in the incidence of TB in the major industrialised nations throughout the 1990s, reversing the steady decline of previous decades [3] and has precipitated the search for new therapies and antibiotics.

Tryptophan biosynthesis makes an attractive target for the design of new anti-TB drugs, as auxotrophic mutants of *M. tuberculosis* are essentially avirulent [4] and the biosynthetic pathway is not present in humans. The first step in tryptophan biosynthesis is carried out by the anthranilate synthase (AS) complex, made up of two polypeptides, trpE and trpG. There are two candidates trpE ORFs in *M. tuberculosis* (Rv1609 and Rv2386c) but no clear candidate for trpG. The second step in tryptophan biosynthesis is carried out by anthranilate phosphoribosyltransferase, trpD (Rv2192c).

We have expressed in *E. coli* and purified trpD, trpE and trpE2 from *M. tuberculosis* as either GST fusion proteins or histidine-tagged proteins. TrpD has been crystallised and data has been collected from these crystals to a resolution of 2.3Å. TrpE2 has also been crystallised and these crystals diffract to a resolution of ~3.5Å. We are currently working to improve the quality of these crystals and to prepare selenomethionine-substituted protein for MAD phasing.

References

1 Rattan, A., Kalia, A. and Ahmad, N. (1998) "Multidrug-resistant *Mycobacterium tuberculosis*: Molecular Perspectives." *Emerging Infectious Diseases* **4**, 195-209.

2 World Health Organisation (2000) *Drug-resistant strains of TB increasing worldwide*.

3 Stokstad, E. (2000) "Drug-Resistant TB on The Rise." *Science*, **287**, 2391.

4 Smith, D.A., Parish, T., Stoker, N.G. and Bancroft, G.J. (2001) "Characterization of auxotrophic mutants of *Mycobacterium tuberculosis* and their potential as vaccine candidates." *Infection & Immunity* **69**, 1142-1150.

UNDERSTANDING THE FUNCTIONING OF THE COPPER BINDING DOMAIN OF THE AMYLOID PRECURSOR PROTEIN

G. K. W. Kong,[a,b] W. J. McKinstry,[a] J. J. Adams,[a] G. Polekhina,[a] N. A. Williamson,[b] D. Cappai,[b] K. J. Barnham,[b] R. Cappai,[b] and M. W. Parker [a]

[a]Biota Structural Biology Laboratory, St. Vincent's Institute of Medical Research, Fitzroy, Victoria 3065, Australia; [b]Department of Pathology, The University of Melbourne, Victoria 3010, Australia (g.kong1@pgrad.unimelb.edu.au)

Redox active metal ions, like copper (Cu), are abundant in human brains and may contribute to the pathogenesis of various neurodegenerative diseases [1]. In Alzheimer's Disease (AD), the amyloid plaques, the pathological hallmark of the disease formed by the over-production and aggregation of peptides called Aβ, bind and thus concentrate Cu ions in the vicinity of brain neurones. As Cu(II) ions are highly oxidising and can react with oxygen to produce reactive oxygen species, they can inflict oxidative damage to the neurones [1]. The clearance of metal ions from Aβ and/or plaques thus represents an important means of intervention in AD.

The Aβ peptide is derived from the cleavage of the amyloid precursor protein (APP), a single transmembrane protein found on the surface of brain neurones, by enzymes called secretases. The APP contains, near the N-terminus, a copper binding domain (CuBD) which binds Cu(II) with high affinity [2]. The binding of Cu(II) to APP helps to clear the ion from the extracellular environment [3] and influences APP metabolism so as to lower Aβ secretion [4]. Cu(II)-binding also causes changes to the structure of the CuBD and may subsequently modulate APP-APP interactions [5]. Structural studies of the CuBD will help to understand the Cu(II)-binding process and may enable the development of CuBD agonists that disfavour the production of Aβ.

Well-diffracting crystal forms of the CuBD have been grown in a few conditions and attempts to solve the phase problem involved using an existing NMR model for molecular replacement (MR) [6]. With a large number of molecules per asymmetric unit in the initial crystal forms (between 6 to 12), MR was further complicated by errors in the NMR model. Eventually a crystal form was found containing only one molecule in the asymmetric unit and a 2 Å resolution data set collected. After trying various MR programs, a solution was obtained by AMoRe [7]. The current, preliminary crystal structure is free of any metal ions, and like the NMR model, the fold is based on a helix packed against a β sheet of 3 strands. The focus is now on defining the Cu binding site through obtaining a Cu-bound structure of the CuBD.

References

1 Bush, A.I. (2000) *Curr. Opin. Chem. Biol.* **4**, 184-191.
2 Multhaup, G. *et al.* (1997) *Biochem. Pharmacol.* **54**, 533-539.
3 White et al (1999) *Brain Res.* **84**, 439-444.
4 Borchadt, T. *et al.* (1999) *Biochem. J.* **344**, 461-467.
5 Beher, D. *et al.* (1996) *J. Biol. Chem.* **271**, 1613-1620.
6 Barnham, K.J. *et al.* (2002), submitted.
7 Navaza, J. (1994) *Acta Cryst. A* **50**, 157-163.

CRYSTALLOGRAPHIC STUDIES OF THE MITOCHONDRIAL FISSION PROTEIN FIS1

Michael A. Gorman,[a] Diana Stojanovski,[b] Michael T.Ryan,[b] and Jacqueline M. Gulbis[a]

[a]Department of Structural Biology, The Walter and Eliza Hall Institute, 1G Royal Parade, Parkville, Victoria, 3050, Australia; [b]Department of Biochemistry, La Trobe University, Victoria, 3086, Australia (gorman@wehi.edu.au)

The vital role of mitochondria for ATP production, Ca2+ homeostasis and initiation of apoptosis has been apparent for some time. Mitochondria are not singular organelles but are dynamic structures that divide and fuse continually throughout the life of the cell. Since mitochondria are not created *de novo*, they must proliferate and segregate into daughter cells during cell division so that each one maintains a full complement. Most of the work has been done in the model system of *S. cerevisiae* in which two conserved GTPases regulate mitochondrial shape. Fzo1p[1] mediate mitochondrial fusion and Dnm1p[2] regulates mitochondrial fission. Loss of Dnm1p function impairs fission resulting in the formation of highly connected networks due to the accumulation of unopposed fusion events. In yeast, two additional proteins Mdv1p and Fis1p are essential components of the fission machinery[3]. Fis1p is an integral mitochondrial outer membrane protein recruiting Dnm1p and Mdv1p to the surface of the outer membrane. *In vivo* studies indicate the intact C-terminal structure of Fis1p is essential for localisation whereas the N-terminal region of Fis1p is necessary for mitochondrial fission. In mammalian cells, the dynamin-like homologue to Dnm1p, Drp1p, is also required for mitochondrial fission. It is distributed predominantly in the cytosol and is transiently associated with mitochondria. The human homologue hFis1 shares 25% sequence identity and 61% sequence similarity with the yeast counterpart. The structures of hFis1 and hFis1/Drp1p complex will help identify the molecular interaction and how specificity is achieved. To this aim, the cytosolic domain of hFis1 has been expressed as a GST-fusion protein and the progress towards the determination of hFis1p X-ray crystal structure will be discussed.

References

1 Rapaport, D., Brunner, M., Neupert, W. and Westermann (1998) *J. Cell. Biol.* **273**, 20150-20155.
2 Otsuga, D. *et al* (1998) *J. Cell. Biol.* **143**, 333-349.
3 Mozdy, A. D., McCaffery, J. M. and Shaw, J. M. (2000) *J. Cell. Biol.* **151**, 376-379.

THE CRYSTAL STRUCTURE OF T84.66FAB AT 2.2 Å RESOLUTION AND MODELLING THE BINDING OF ANTI-CEA ANTIBODY CONSTRUCTS TO THE CEA ANTIGEN

Jennifer A. Carmichael,[a,b] Barbara Power,[a,b] Albert van Donkelaar,[a] Mark Sherman,[c] Paul Yazaki,[c] Anna M. Wu,[d] and Peter J. Hudson[a,b]

[a] CSIRO Health Science and Nutrition 343 Royal Parade, Parkville 3052, Victoria, Australia; [b]CRC for Diagnostic Technologies, 343 Royal Parade, Parkville 3052, Victoria, Australia; [c]Department of Molecular Biology, Beckman Research Institute of the City of Hope, Duarte, CA 91010, USA; [d]UCLA school of medicine, Los Angeles, CA 90095, USA (Jenny.Carmichael@csiro.au)

The crystal structure of the Fab arm of the T84.66 anti-carcinoembryonic antibody (T84.66Fab) was solved to 2.2Å and compared to the previously solved structure of an engineered T84.66 anti-CEA scFv diabody (T84.66Di) previously solved in this laboratory [1]. The CDR loop structure seen in the T84.66Fab supports the novel loop structures observed in the T84.66Di L1 and H3 loops. The same loop structure has now been seen in all three Fv structures (T84.66Fab, T84.66DiAB, T84.66DiBA) determined and indicates that this is unlikely to be the result of crystal packing, a possibility raised when the T84.66Di structure was first solved. The T84.66Fab T84.66Di comparison also revealed flexibility in one of the Fv C domain interface loops that could be a factor in the design of future scFv constructs for immunodiagnostics or therapeutics.

These structures (T84.66Fab, T84.66DiAB, T84.66DiBA) and another engineered anti-CEA scFv, MFE-23 [2], PDB acc., 1QOK, were then used in docking studies with a model of the CEA antigen based on the crystal structure of CEACAM1 [3] PDB acc., 1L6Z. This resulted in models of the potential binding sites of these antibody variants to the CEA antigen. A model of the docked T84.66 structure(s) is presented. The docking of the MFE-23 is also presented and discussed in reference to a previously constructed MFE-23-CEA model [4].

References

1 Carmichael, J. A., Power, B. E., Garrett, T. P., Yazaki, P. J., Shively, J. E., Raubischek, A. A., Wu, A. M. and Hudson, P. J. (2003) *J Mol Biol.* **326**, 341-351.

2 Boehm, M. K., Corper, A. L., Wan, T., Sohi, M. K., Sutton, B. J., Thornton, J. D., Keep, P. A., Chester, K. A., Begent, R. H. and Perkins, S. J. (2000) *Biochem. J.* **346**, 519-528.

3 Tan, K., Zelus, B. D., Meijers, R., Liu, J. H., Bergelson, J. M., Duke, N., Zhang, R., Joachimiak, A., Holmes, K. V. and Wang, J. H. (2002) *EMBO J.* **21**, 2076-2086.

4 Boehm, M. K. and Perkins, S. J. (2000) *FEBS Lett.* **475**, 11-16.

STRUCTURAL STUDIES OF CP PROTEIN AND ITS FRAGMENTS WITH ANDROGEN RECEPTOR-mRNA

Mahjooba Sidiqi,[a] Julian Vivian,[a] Jackie Wilce,[b] and Matthew Wilce[a]

[a]Department of Pharmacology, QEII Medical Centre, Perth, W.A 6009, Australia; [b]Department of Biochemistry, 35 Stirling Hwy, Nedlands, Perth, W.A 6009, Australia (treasures40@yahoo.com)

For some proteins regulation of gene expression can occur post-transcriptionally, at the level of mRNA stability and translational efficiency. This has been shown to differ from one mRNA to another and can be regulated by protein-RNA interactions. mRNA stability can be determined by elements often located at the 3' untranslated region (UTR) of the mRNA. A Variety of proteins have been identified which bind such elements in leading to the stabilization of the mRNA. CP protein specifically binds poly (C) rich regions at the 3' UTR of the androgen receptor mRNA and is thought to lead to its stabilsation and increased androgen receptor expression which plays a critical role in the proliferation of prostate cancer cells. Its characterization may provide important insight into the regulation of androgen receptor expression and potentially assist in the development of drugs aimed to reduce androgen expression in prostate cancer.

CP and CP fragments (containing KH domains representing RNA binding motifs in the sequence) were successfully cloned in bacterial overexpression systems. Milligram quantities of pure protein was successfully prepared and purified for some of the fragments. Preliminary structural studies showed that CP KH domain three is suitable for NMR studies. Small crystals of this fragment were also obtained and we present the structure was determined at a resolution of 1.9Å. In the future crystallization experiments will be conducted in the presence of androgen receptor mRNA which will hopefully shed some light on the stabilisation of androgen receptor mRNA and thus the mechanism of proliferation in prostate cancer cells.

THE SIGNIFICANCE OF INTERACTION BETWEEN O6 HYDROXYL GROUPS OF GLUCOSE RESIDUES OF MALTOORIGOSACCHARIDE AND β-AMYLASE FROM *BACILLUS CEREUS* VER. *MYCOIDES*

Hideo Miyake,[a,b] Genji Kurisu,[a] Masami Kusunoki,[a] Sigenori Nishimura,[b] and Yasunori Nitta[b]

[a]Institute for Protein Research, Osaka University, Suita, Osaka 565-0871, Japan; [b]Graduate School of Agriculture and Biological sciences Osaka Prefecture University, Sakai, Osaka 599-8531, Japan (miyake@protein.osaka-u.ac.jp)

β-Amylase (EC. 3.2.1.2) hydrolyzes the α-1,4-glucosidic linkage of α-1,4-D-glucans such as starch, thereby liberating β-maltose from the non-reducing end of substrate. In the previous study, the X-ray crystal structure of a catalytic site mutant, E172A (Glu172_Ala), in complex with substrate maltopentaose was determined, and maltopentaose was observed at subsites –2 to +3 [1]. Hydrogen bonds between O6 hydroxyl groups of glucose residues located at subsites –2 to +1 and the side chains of Asp49, Arg397, Glu367 and Arg174 were formed.

Three mutants [D49A (Asp49_Ala), R397L (Arg397_Leu), E367A (Glu367_Ala), R174L (Arg174_Leu)] which can not form a hydrogen bond with an O6 hydroxyl group of one of the glucose residues were created, and their crystal structures complexed with maltoorigosaccharide (maltose and maltotriose) were determined at 1.8 to 2.5 Å resolution, respectively by X-ray crystallography. In the case of the crystal structure of the wild-type enzyme complexed with maltose, two maltose molecules bound at subsites -2 to +2 in tandem [1]. In the case of the crystal structure of all mutants complexed with maltose, however, maltoorigosaccharide was not observed at the place of mutation. Also, in the case of D49A complexed with maltotriose, maltoorigosaccharide was not observed at subsites –2 and –1 even though maltotriose is substrate for this enzyme.

On the other hands, the crystal structure of the native enzyme complexed with a substrate analog [(1-4)-*O*-α-D-glucopyranosyl-(1-4)-*O*-α-D-glucopyranosyl-D-xylopyranose (GGX)] was also determined. It ,which bound to subsites +1 to +3, however, could not bind to subsites –2 to +1. Therefore, we conclude that this enzyme strictly recognize the O6 hydroxyl groups of glucose residues and the interactions of O6 hydroxyl group of glucose residues located at subsites –2 to +1 are significant.

Reference

1 Hideo Miyake, Genji Kurisu, Masami Kusunoki, Sigenori Nishimura, Shinichi Kitamura and Yasunori Nitta (2003) *Biochemistry*. in press.

TOWARDS A CATALYTIC MECHANISM OF AMINOPEPTIDASE P

S C Graham,[a] M H Lee,[a] M J Maher,[a] W H Simmons,[b] H C Freeman[a] and J M Guss[a]

[a]School of Molecular and Microbial Biosciences, University of Sydney, Australia; [b]Department of Molecular and Cellular Biochemistry, Loyola University Chicago, USA
(stepheng@usyd.edu.au)

Aminopeptidase P (AMPP) is a proline-specific peptidase that cleaves the N-terminal amino acid residue from a polypeptide chain where the second residue is proline. AMPP is a ubiquitous enzyme that plays an important role in a wide variety of biological processes. Examples include the recycling of cellular proline and, in mammals, the regulation of peptide hormones. Human membrane-bound AMPP is the target of a potential drug, apstatin, which has been shown to regulate blood pressure when used in conjunction with angiotensin-converting enzyme inhibitors. Our previous work on *E. coli* AMPP has shown that it is a member of the family of pita-bread fold enzymes with a dinuclear metal centre in its active site. Other members of this family include methionine aminopeptidase and prolidase. Structures have now been refined in the presence of inhibitors and in several crystal forms at different pH values. While these previous studies provided a putative mechanism of action for AMPP, they left open a number of questions including the basis of specificity for the *N*-terminus of the peptide and for proline as the second residue. We have undertaken further structural studies, including determination of the structures of mutant and inhibitor-bound forms of *E. coli* AMPP, in order to elucidate its mechanism of catalysis. We have shown that, while AMPP and methionine aminopeptidase have similar structures, the chemistry of the secondary amide bond cleaved by AMPP and the nature of the amino acid residues surrounding the active site of AMPP require differences in their mechanisms of catalysis. We have also made a model of the human membrane-bound form of AMPP. This model has permitted us to draw some conclusions about differences in binding affinity of substrates and inhibitors between the *E. coli* and human membrane-bound forms of the enzyme.

CRYSTAL STRUCTURE OF THERMOSTABLE ASPARTASE AND STRUCTURE-BASED EXPLORATION OF FUNCTIONAL SITES IN THE ASPARTASE FAMILY

Yasuo Hata,[a] Tomomi Fujii,[a] Hisanobu Sakai,[a] and Yasushi Kawata[b]

[a]Institute for Chemical Research, Kyoto University, Uji, Kyoto 611-0011, Japan; [b]Department of Biotechnology, Faculty of Engineering, Tottori University, Tottori 680-0945, Japan (hata@scl.kyoto-u.ac.jp)

Aspartase (L-aspartate ammonia-lyase, EC 4.3.1.1) plays an important role in bacterial nitrogen metabolism by catalyzing the reversible conversion of L-aspartate to fumarate and ammonium ion. The crystal structure of the thermostable aspartase from *Bacillus* sp. YM55-1 has been solved and refined for 2.5 Å resolution data with an *R*-factor of 22.1% [1]. The present enzyme is a homotetramer with subunits (M_r= 51,627, 468 amino acid residues) composed of three domains: the N-terminal large domain, the central helix domain, and the C-terminal small domain. It exhibits no allosteric effects, in contrast to the *E. coli* aspartase which is activated by divalent metal cation (Mg^{2+}) and L-aspartate, but is four-times more active than the *E. coli* enzyme. The overall folding of the present enzyme subunit is similar to those of the *E. coli* aspartase [2] and the *E. coli* fumarase C [3], both of which belong to the same superfamily with the present enzyme. A local structural comparison of these three enzymes revealed seven structurally different regions. Five of the regions were located around putative functional sites, suggesting the involvement of these regions into the functions characteristic of the enzymes. Of these regions, the region of Gln96–Gly100 is proposed as a part of the recognition site of the α-amino group in L-aspartate for aspartase and the hydroxyl group in L-malate for fumarase. The region of Gln315–Gly323 is a flexible but well sequence($-G_{317}$–S–S–I–M–P_{322}–)-conserved loop that is suggested to be involved in the catalytic reaction. The region of Lys123–Lys128 corresponds to a part of the putative activator-binding site in the *E. coli* fumarase C. The region in the *Bacillus* aspartase, however, adopts a main-chain conformation which prevents the activator binding. The regions of Gly228–Glu241 and Val265–Asp272, which form a part of the active-site wall, are suggested to be involved in the allosteric activation of the *E. coli* aspartase by the binding of the metal ion and the activator L-aspartate. Moreover, an increase in the numbers of intersubunit hydrogen-bonds and salt-bridges is observed in the *Bacillus* aspartase relative to those of the *E. coli* enzyme, implying a contribution to the thermostability of the present aspartase.

References

1 Fujii, T., Sakai, H., Kawata, Y. and Hata, Y. (2003) *J. Mol. Biol.* (accepted on March 3).
2 Shi, W., Dunbar, J., Jayasekera, M. M. K., Viola, R. E. and Farber, G. K. (1997) *Biochemistry*, **36**, 9136–9144.
3 Weaver, T. and Banaszak, L. (1996) *Biochemistry*, **35**, 13955–13965.

CRYSTAL STRUCTURE OF THE CU-AMINE OXIDASE FROM ARTHROBACTER GLOBIFORMIS IN COMPLEX WITH THE SUICIDE INHIBITOR 4-(2-NAPHTHYLOXY)-2-BUTYN-1-AMINE

David B. Langley,[a] Eric M. Shepard,[b] Anthony P. Duff,[a] Hans Freeman,[a] David M. Dooley,[b] and J. Mitchell Guss[a]

[a]Department of Biochemistry, The Univeristy of Sydney, Australia; [b]Department of Chemistry and Biochemistry, Montana State University, Bozeman, MT, USA (d.langley@mmb.usyd.edu.au)

Cu-containing amine oxidases (CuAOs) are a ubiquitous class of enzyme catalysing the oxidative deamination of primary amines to their respective aldehydes with the release of H_2O_2 and NH_3. One class of CuAO contains the cofactor 2,4,5-trihydroxyphenyl alanine quinone (TPQ), which is a post-translationally modified tyrosine residue. The catalytic cycle can be conceptually split into two halves; reductive and oxidative (**A**). In the reductive half, the primary amine nucleophilically attacks the TPQ to yield a Schiff-base adduct which is subsequently hydrolysed to leave an N-substituted reduced TPQ. The oxidative half involves oxidation of the reduced TPQ by molecular oxygen with the liberation of H_2O_2 and NH_3.

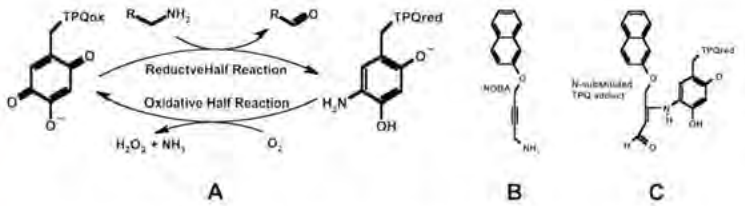

A B C

The inhibitor 4-(2-naphthyloxy)-2-butyn-1-amine (NOBA) has been specifically designed to inhibit CuAOs (**B**). While the primary amine is designed to target the molecule to the active site and allow formation of the Schiff-base, provision of a triple bond is intended to facilitate attack by an adjacent amino-acid nucleophile to yield an adduct stuck in the active site. NOBA is stoichiometrically potent against the enzyme from *Arthrobacter globiformis* (AGAO), while less toxic to CuAOs from other species. We have solved and refined the structure of AGAO co-crystallised with NOBA. Interestingly, the electron density does reveal an adduct attached to the TPQ, but its shape excludes the presence of the Schiff-base adduct expected. A model has been postulated to interpret the density (**C**). We believe that a Schiff-base product is first formed then hydrolysed, as per the usual catalytic cycle. However, the hydrophobic naphthyloxy ring of the product aldehyde prevents its diffusion from the active site. The alkyne moiety of the same product is then attacked by the N-substituted reduced TPQ to yield the product shown in **C**, which is consistent with the density observed. Current investigation is aimed at capturing the postulated initial Schiff-base intermediate, and refining structures of other CuAOs in complex with this inhibitor.

STRUCTURAL GENOMICS OF NOVEL MACROPHAGE PROTEINS ASSOCIATED WITH INFLAMMATORY DISEASE AND CANCER

Pawel Listwan,[a,c] Nathan Cowieson,[a] Anna Aagaard,[a,c] Robert Serek,[a] Carmel Walsh,[a] Timothy Ravasi,[a,c] Christine Wells,[a,c] Thomas Huber,[b] David Hume,[a,c] Jenny Martin,[a,c] and Bostjan Kobe[a,c]

[a] Department of Biochemistry and Molecular Biology, and Institute for Molecular Bioscience, University of Queensland, St.Lucia QLD 4072, Australia; [b] Department of Mathematics, University of Queensland, St. Lucia QLD 4072; [c]CRC for Chronic Inflammatory Diseases (listwan@uq.edu.au)

Most of the potential pathogens that attempt to invade a mammalian cell fail at the very first stage due to the remarkable effectiveness of innate immunity. The presence of the potential pathogens is detected via receptors that recognise generic non-mammalian structures including cell wall components including lipopolisaccharides, peptidoglycans, lipotechoic acids and microbial DNA [1]. The first line of defense is the macrophage, which comprises 15-20% of the cells in the most organs, and is particularly abundant at the routes of pathogen entry such as lung, skin, gut and genitourinary tract [2]. When the potential pathogen is recognised, the macrophage engulfs and attempts to destroy the foreign organism. The knowledge of regulation of macrophage function will form the basis of two classes of therapeutics. Amplification of the toxic function of macrophages to destroy foreign organisms or tumor cells more effectively is one option, the other being the selective suppression of some components of the macrophage activation response. These then can be used to treat conditions like septicaemia and toxic shock, arthritis, atherosclerosis and other chronic inflammatory diseases the other one.

To define the molecular functions of proteins with roles in macrophages, we set out to characterise them structurally using X-ray crystallography. We identify proteins with roles in macrophages through expression profiling using microarray technology. We select and prioritise the proteins for structural analysis according to a number of criteria such as anticipated insight into function and feasibility for structure determination. We have developed protocols for cloning, expression and crystallography that can be adapted for high-throughput approach. To the best our knowledge, this project is the first structural genomics effort in Australia, and the microarray-to-structure pipeline is unique among the structural genomics initiatives worldwide. Our initial list of 40 proteins resulted in 7 soluble proteins, 2 targets are currently in crystallisation trails and one is ready for MAD data measurement. Currently we are optimising this system and here we present our strategy for the selection, prioritisation, cloning, expression and crystallisation of a number of protein targets.

References

1 Hoffman, J.A., Kafatos, F.C., Janeway, C.A., And Ezekowitz, R.A. (1999) Phylogenetic perspectives in innate immunity, *Science* **284**, 1313-1318.

2 Gordon, S., and Hume, D. A. (1986). Localization and function of tissue macro-phages, *Ciba FoundSymp* **118**, 54-67.

A STRUCTURAL GENOMICS APPROACH TO TUBERCULOSIS

Edward N. Baker,[a] Vickery L. Arcus,[a] Kristina Backbro,[a] Graeme L. Card,[a] Jodie M. Johnston,[a] Moyra Komen,[a] Nayden Koon,[a] Simon Li,[a] Andrew A. McCarthy,[a] Rochelle J. Ramsay,[a] Miriam L. Sharpe,[a] and J. Shaun Lott[a]

[a]School of Biological Sciences, University of Auckland, Auckland, New Zealand (ted.baker@auckland.ac.nz)

The availability of ever-increasing numbers of complete genome sequences is revolutionising the biological sciences. A challenge now in this "genomic revolution" is to add value to the sequence data by focusing on the structure and function of gene products. Current initiatives in structural genomics have a number of objectives, both structural and functional, including the discovery of new folds, determination of representative structures for all protein families, discovery of function from structure, and the characterisation of potential drug targets.

We are participants in a worldwide structural genomics consortium focused on *Mycobacterium tuberculosis*, the cause of TB, and one of the world's most devastating pathogens. Around 3 billion people die annually from the disease. Athough drugs exist, resistance is rising and treatment is complicated by the unusual nature of the organism, with its dense, waxy cell wall, and its ability to persist in a dormant state in the lung for long periods.

The TB Structural Genomics Consortium [1] has central facilities for the benefit of all participants, but individual labs pursue their own objectives, with coordination to try to avoid overlap. Our focus is on two types of target, (a) enzymes from key biosynthetic pathways which are potential drug design targets, and (b) proteins of uncertain or unknown function that are implicated in key aspects of TB biology. In the first category we have chosen enzymes involved in the biosynthesis of essential amino acids and of menaquinone and thiamin. In the second category we focus on proteins of unknown function that are implicated by microarray experiments either in antibiotic resistance or in the hypoxic response (and possibly persistence).

The approaches taken in our laboratory to cloning, expression, purification, crystallization and structure determination will be reviewed. The major bottlenecks to date have been in obtaining soluble expression and in crystallization, and we are reviewing our approaches in both these areas. So far from about 100 genes cloned we have 9 protein structures, with more to come. The solved structures include several proteins of unknown function, two others that appear to be good drug targets, and one protein whose structure suggests that it is mis-annotated in this and other genomes.

References

1 TB Structural Genomics Consortium: See http://www.doe-mbi.ucla.edu/TB.

HIGH THROUGHPUT APPROACHES FOR CRYSTALLISATION OF BIOLOGICAL MACROMOLECULES

Christine L. Gee,[a] Richard D. Kidd,[a] Anna Aagaard,[a] Fiona M. McMillan,[a] Niranjali U. Gamage,[a] Paul R. Young,[b] David. A. Hume[b] and Jennifer L. Martin[a]

[a]Institute for Molecular Bioscience; [b]School of Molecular and Microbial Sciences, The University of Queensland, St Lucia, 4072, Australia (c.gee@imb.uq.edu.au).

Structural genomics programs generate hundreds of proteins for structural analysis. To keep pace with this, rapid and economical methods for high throughput screening of crystallisation conditions are required. Here we present a protocol for semi-automated 96 well format screening as a high throughput approach for crystallisation.

We use a Packard multiPROBE II liquid handling robot to dispense solutions into a master 96 deep-well tray. Once solutions are dispensed into 96 well format, multi-channel pipettes are used to dispense aliquots into microtitre plates and to set up hanging drops on plastic sealing film. The plastic film is then sealed over the rims of the individual wells. This method removes the need for grease sealing and individual manipulation of cover slips used in the standard 24 well crystallisation tray, thus saving time. The smaller footprint trays are space saving, occupying almost half the space of the standard 24 well trays. They are inexpensive and also save reagents, as they use one-tenth the reservoir volume of the old 24 well format, thus lowering costs.

The robot is also used to mix solutions for grid optimisation screens. These are generally dispensed in 24 well format into a tissue culture plate and the crystallisation hanging drops are again dispensed with a multi-channel pipette onto sealing film.

Several proteins have been crystallised in our laboratory using these techniques and these will be described in more detail.

THE STRUCTURE AND FUNCTION OF STREPTOLYSIN O

Julian J. Adams,[a] Susanne C. Feil,[a] Rodney K. Tweten,[b] and Michael W. Parker[a]

[a]Biota Structural Biology Laboratory, St Vincent's Institute of Medical Research Fitzroy, Victoria 3065, Australia; [b]Department of Microbiology and Immunology, The University of Oklahoma Health Sciences center, Oklahoma City, Oklahoma 73190, USA (jjadams@medstv.unimelb.edu.au)

Streptolysin O (SLO) is a cholesterol dependant cytotoxin (CDC) secreted by *Streptococcus pyrogenes*. SLO is one of the key virulence factors in *streptococcus* infections of soft tissue e.g. strep throat, impetigo and necrotising fascitis. SLO is also a causative agent in toxigenic or immunopathological disease e.g. Scarlet fever, toxic shock syndrome and rheumatic fever. SLO is the archetype for the CDC super family of pore forming toxins [1], it however differs from the other members of the family as it possesses a 70-75 amino acid N-terminal extension, the function of this extension is unknown. There is some evidence to suggest this difference may have a significant influence on membrane specificity and activity. We hope to be able to shed some light on the function and biological relevance of the N-terminal domain. Our group solved the first structure of the CDC super family: perfringolysin O [2] (PFO). This structure revealed aspects of CDC toxin activity but much more needs to be learned. A structure of another CDC super family member will be invaluable. The results from this project will be used for *in silico* compound screening and possible development of treatments for *streptococcus* infections.

As SLO has approximately 58% sequence identity with PFO it is anticipated that the structure will be amenable to solution by molecular replacement (MR). If MR from the data recently collected in house and at the APS fails to yield a structure, heavy atom soaks and multiple anomalous dispersion techniques will be employed. To this end Pt and Hg derivative crystals have being prepared and data sets collected.

References

1 Palmer, M. (2001) The family of thiol-activated, cholesterol-binding cytolysins. *Toxicon*. **39**, 1681-1689.

2 Rossjohn, et al. (1997) Structure of a cholesterol-binding thiol-activated cytolysin and a model of its membrane form. *Cell*. **89**, 685-692.

HIGH RESOLUTION ANALYSIS OF THE NEW INHIBITOR PGD-042 BOUND HUMAN HEMETOPOIETIC PROSTAGLANDIN D SYNTASE

N. Katsuyama,[a] T. Inoue,[a] Y. Okano,[a] H. Shishitani,[a] N. Okazaki,[a] H. Matsumura,[a] Y. Urade,[b] and Y. Kai[a]

[a]Department of Materials Chemistry, Graduate School of Engineering, Osaka University, 2-1 Yamada-oka, Suita, Osaka 565-0871, Japan; [b]Department of Molecular Behavioral Biology Osaka Bioscience Institute, Osaka 565, Japan (naok@chem.eng.osaka-u.ac.jp)

Prostaglandin (PG) D2 is an allergic and inflammatory mediator produced by human mast cells and Th2 cells in a variety of human tissues. PGD2 is formed from arachidonic acid by successive enzyme reactions: oxygenation of arachidonic acid to PGH2 via PGG2 by PG endoperoxide synthase, cyclooxygenase (COX), followed with isomerization of PGH2 to PGD2 by PGD synthase (PGDS). Hematopoietic PGDS (H-PGDS) is responsible for the biosynthesis of PGD2 by mast cells and Th2 cells. Overproduction of PGD2 exacerbates asthmatic reactions, such as enhancement of eosinophilia and accumulation of Th2 cytokines, as shown by an ovalbumin-challenged athma model in human L-PGDS- or H-PGDS-transgenic mice. On the other hand, these asthmatic reactions are weakened in gene-disrupted mice for the D type of prostanoid (DP) receptor specific for PGD2. The DP receptor is constitutively expressed in human basophils and eosinophils, and is induced in pulmonary and airway epithelial cells by the allergic inflammation.

Recently, PGD2 was also identified as a ligand for an orphan receptor CRTH2, which is preferentially expressed in Th2 cells, eosinophils, and basophils and mediates chemotaxis of these cells for PGD2. Therefore, PGD2 produced by H-PGDS in human mast cells and Th2 cells is considered to accelerate allergic and inflammatory reactions by stimulating both DP and CRTH2 receptors in autocrine and paracrine manners. Thus, the human H-PGDS is a promising target for the anti-allergic drug design.

Cibacron Blue is one of the potent inhibitor for human H-PGDS with IC50 value of 44 nM. However, one of the Cibacron blue derivatives (PGD-042), with only the quinone ring and the sulfonamide, shows 2-order reduction of the inhibition activity. To discuss the correlation between the complex structure and the inhibition activity, we tried to co-crystallization with two compounds. The crystallization with Cibacron blue and PGD-042 were performed by co-crystallization method in the presence of 100mM Cibacron blue or 10μM PGD-042, respectively.

We obtained the complex crstal with inhibitor -042 with co-crystallization method by using hanging-drop vapour diffusion method. We collected the X-ray diffraction data under cryo-temperature using 1.0 Å wavelength X-ray radiation at station BL44XU of the SPring-8 synchrotron radiation source. The crystals diffracted beyond 2.0 Å resolution at the synchrotron radiation source.

THE ROLE OF PROLINE RESIDUES IN THE HINGE REGION OF CDC2 KINASE SUBUNIT PROTEINS

Joyanne A. Kelly,[a,b,c,d] Elizabeth A. Williams,[a,c,d] and Matthew C. J. Wilce[a,b]

[a]School of Pharmacology and Medicine, University of Western Australia, Crawley 6009, W.A., Australia; [b]Crystallography Centre, School of Biomedical and Chemical Sciences, University of Western Australia, Crawley 6009, W.A., Australia; [c]Centre for Applied Cancer Studies, University of Western Australia, Crawley 6009, W.A., Australia; [d]Lions Cancer Institute Inc., Oasis Lotteries House, 37 Hampden Rd, Nedlands 6009, W.A., Australia (joyanne@cyllene.uwa.edu.au)

Cdc2 Kinase Subunit (Cks) proteins are essential for mitosis, however their precise function has eluded researchers for two decades. Two conformations of Cks have been detected crystallographically, a compact monomer with the C-terminal fourth β-strand inserted into the core of the molecule between strands 2 and 3, and a strand-exchanged dimer in which the fourth β-strand is inserted into the core of the dimer partner in an equivalent position. There is an absolutely conserved "hinge" region, consisting of the motif PEP, N-terminal to the fourth β-strand. In the monomer this motif constitutes a β-turn while in the dimeric structure it is extended, allowing strand exchange. The mutant protein, $p13^{suc1P90AP92A}$, in which alanine residues replace both prolines of the turn, provides an opportunity to examine the role of prolines in this conformational plasticity. We have expressed and purified this mutant protein. Two millimolar $p13^{suc1P90AP92A}$ crystallised in 50mM Tris pH7.5, 30% PEG 1500K. Diffraction data were collected at room temperature on a MAR345 image plate using Cu Kα; radiation from a Rigaku RU200 rotating-anode generator source. The structure was solved to 2.7Å in space group *P*6(3); unit cell parameters were found to be $a=b=75.1$, $c=34.9$, $\alpha=\beta=90$, $\gamma=120$.

The three dimensional structure of this mutant suggests that the reduced hydrogen bonding capacity of proline residues is more likely to be responsible for the propensity of Cks proteins to form strand exchanged dimers than backbone strain between prolines 90 and 92 [1].

References

1 Rousseau, F., Schymkowitz, J. W., Wilkinson, H. R. and Itzhaki, L. S. (2001) *Proc. Natl. Acad. Sci. USA* **98**, 5596-5601.

SAD PHASING USING SULFUR ANOMALOUS SCATTERING WITH CHROMIUM RADIATION

K. F. Tesh, C. Yang, J. W. Pflugrath, C. N. Stence, D. A. Courville, and J. D. Ferra

Rigaku/MSC, Inc. 9009 New Trails Dr., The Woodlands, TX 77381, USA (kft@RigakuMSC.com)

Anomalous scattering with soft X-ray radiation opens new possibilities in phasing for macromolecular crystallography. Anomalous scattering from sulfur atoms collected on an in-house chromium radiation (2.29 Å) source was used to phase the X-ray diffraction data of thaumatin (22 kDa), trypsin (24 kDa) and glucose isomerase (40 kDa) crystals. The contribution to the anomalous term, ! f''=1.14 e^-, from sulfur for CrK-alpha radiation is double compared to that for CuK-alpha radiation, ! f''=0.56 e^-. The direct methods program SHELXD successfully found sulfur positions using data sets with the resolution limited to 3.5 Å. The statistical phasing program SHARP was used to produce the electron density maps using the sulfur anomalous signal alone at a low resolution (~3.5 Å). An interpretable electron density map for each structure was obtained solely from these phases derived from single-wavelength anomalous dispersion (SAD) data from CrK-alpha radiation. Much less data, that is lower redundancy, is required for this sulfur SAD phasing procedure compared to the highly redundant data reported in the sulfur SAD phasing procedure with CuK-alpha radiation. CrK-alpha radiation can also improve the strength of anomalous scattering of many other intrinsic elements in macromolecules, like Ca^{2+}, Zn^{2+}, and P, because of the doubled value of ! f''. Furthermore, the anomalous scattering of selenium is increased substantially when CrK-alpha radiation is used, because its ! f'' is increased to 2.28 e^- from 1.14 e^- with CuK-alpha radiation.

In order to measure small Bijvoet differences accurately, several devices were developed for the experiment, including an Osmic Confocal MaxFlux optic optimized for CrK-alpha radiation, a helium path and a beam stop. In the cases studied here, radiation damage to the samples and reduction of anomalous signal were observed in some long data sets. Therefore, an adequate collection strategy to maximize the completeness in a short scan range was used in subsequent data collections. The results show the anomalous signal of sulfur atoms can be quickly collected. Since the absorption of solvent and the loop with CrK-alpha radiation may not be negligible any more, the orientation of the crystal and exposure time were accounted for in order to minimize the effects of radiation damage and absorption. This experimental study shows using CrK-alpha radiation can provide sufficient phasing power from sulfur anomalous signals for routinely phasing protein data in-house.

STRUCTURAL CHARACTERIZATION OF TWO PHOSPHOLIPASE A_2 PROTEINS FROM THE VENOM OF THE AUSTRALIAN BROWN SNAKE, PSEUDONAJA AFFINIS AFFINIS

Roopwant K. Judge,[a,b] Matthew C. J. Wilce[a] and Jacqueline A. Wilce[b]

[a]School of Medicine and Pharmacology; [b]School of Biomedical and Chemical Sciences, University of Western Australia, Crawley 6009, WA, Australia (rjudge@receptor.pharm.uwa.edu.au)

Brown snake envenomation is one of the leading causes of snakebite injury in Australia. In the absence of antivenom treatment, the risk of mortality is high. Though potent and highly lethal, the venom of the brown snake common to the Perth region of Western Australia, *Pseudonaja affinis affinis* (dugite), has not been well characterized. The clinical feature of envenomation is disseminated intravascular coagulopathy (DIC), and a procoagulant protein contributing to this effect has been isolated. The secondary features of envenomation include paralysis, cardiac arrhythmias/arrest and respiratory failure. Protein species involved in these effects have thus far not been characterized.

Based on the current level of understanding in snake venom research, the major classes of venom proteins are neurotoxins, PLA_2 and proteins mediating haemostasis. Of these, the PLA_2 proteins are the most likely candidates for involvement in the secondary features of dugite envenomation. The PLA_2 proteins are the predominant protein species in snake venoms, and possess many diverse pharmacological properties in addition to their enzymatic property. Such functional properties include neurotoxicity, myotoxicity and antiplatelet effects.

Our initial interest in the PLA_2 proteins of dugite venom was assisted by a proteomic study investigating the affinity of brown snake antivenom for venom proteins. The study, carried out in our laboratory, revealed a curious result. While the brown snake antivenom was found to bind to the coagulant proteins, it did not recognize any 12-14 kDa PLA_2 proteins. Such a result may explain why victims of brown snake envenomation require a considerably higher dose of antivenom. This class of protein was therefore of interest as a target for further study, with insight into the structural and functional characteristics of the proteins potentially aiding the development of a new antivenom therapeutic.

In order to structurally characterize the PLA_2 proteins from dugite venom, a novel "reverse" approach was utilised. This approach was based on setting up crystallisation trials for all PLA_2 proteins separable from the crude venom. In the event that good quality diffraction data could be collected, LC-MS/MS analysis or N-terminal sequencing of the original sample provided the basis for extraction of the complete amino acid sequence from venom cDNA using PCR. The data could then be solved using molecular replacement methods and built into using the derived sequence. This approach resulted in two PLA_2 structures which are presented.

X-RAY ANALYSIS OF YEAST LIPOAMIDE DEHYDROGENASE COMPLEXED WITH NAD$^+$

Wataru Adachi,[a] Kaoru Suzuki,[b] Masaru Tsunoda,[c] Takeshi Sekiguchi,[b] Lester J. Reed,[d] and Akio Takenaka[a]

[a]Graduate School of Bioscience and Biotechnology, Tokyo Institute of Technology, Nagatsuta, Midori-ku, Yokohama 226-8501, Japan; [b]Department of Environmental Science, College of Science and Engineering, Iwaki-Meisei University, Chuodai-iino, Iwaki 970-8551, Japan; [c]School of Pharmaceutical Sciences, Showa University, Hatanodai, Shinagawa, Tokyo 142-8555, Japan; [d]Department of Chemistry and Biochemistry, The University of Texas at Austin, Austin, TX78712, USA (wadachi@bio.titech.ac.jp).

Lipoamide dehydrogenase (E_3) is one of the components of 2-oxoacid dehydro-genase complex. This enzyme catalyses the oxidization of a dihydrolipoyl group of E_2 with the help of the cofactors, NAD$^+$ and FAD. E_3 belongs to the pyridine nucleotide-disulphide oxidoreductase family of glutathione reductase, trypanothione reductase, mercuric ion reductase, etc. We already reported the native E_3 structure from *Saccharomyces cerevisiae* [1]. In this study, we co-crystallized yeast E_3 with NAD$^+$ to elucidate the mechanism of substrate binding.

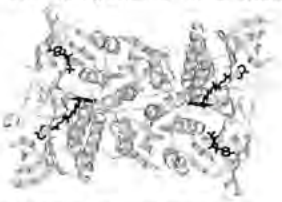

Fig. 1. The overall structure of yeast E_3 with NAD$^+$ and FAD (black lines).

Fig. 2. The binding site of NAD$^+$. The nicotinamide moiety of NAD$^+$ is flipped out in the solvent region. Dots represent the van der Waals surface of E_3.

Diffraction data were collected at 100K and processed at 2.2 Å resolution. The space group and cell parameters are $P2_12_12_1$, a=66.6, b=96.4, and c=160.0Å, respectively. Initial phases were derived by molecular replacement using the native structure. The atomic parameters were refined (the final R=20.3% and R_{free}=24.6%). The overall structure of yeast E_3-NAD$^+$ complex is shown in Fig. 1. When the structure is superimposed on the native one, the overall root- mean-square deviation is 0.62 Å, suggesting no significant difference on NAD$^+$ binding. The final electron density map clearly indicates that the adenosine moiety and the pyrophosphate group of NAD$^+$ are bound to the enzyme, but the remaining nicotinamide moiety is disordered (Fig. 2). It is interesting to note that the binding mode of the nicotinamide moiety is different from those of the related enzymes in the same family. Contrary in the structures of those enzymes complexed with NAD(P)H (reduced form), the nicotinamide moiety is stacked on the isoalloxazine ring of FAD for electron transfer, and the side chain of a Tyr residue near the binding pocket is flip out. In the present enzyme, however, the nicotinamide does not enter the binding site, despite that the Tyr residue is replaced with Ile. It is concluded that the exact positioning of NAD$^+$ on FAD depends on the redox state of the cofactor rather than on the existence of the Tyr side chain.

Reference

1 Toyoda, T., Suzuki, K., Sekiguchi, T., Reed, L. J. and Takénaka, A. (1998) *J. Biochem.* **123**, 668-74.

A NEW METHOD FOR PROTEIN CRYSTALLIZATION: SAMPLING PHASE SPACE IN A MICROFLUIDIC ENVIRONMENT

Kyle Self,[a] Carl L. Hansen,[b] James M. Berger,[c] Stephen R. Quake,[b] Susanna Ng,[a] Shelley Godley,[a] and Joseph Barco[a]

[a]Fluidigm Corporation, 7100 Shoreline Court South San Francisco, California USA; [b]Department of Molecular and Cell Biology, University of California, Berkeley, California USA; [c]Department of Applied Physics, California Institute of Technology, California USA (kyle.self@fluidigm.com)

Protein structure studies have long been the province of the expert crystallographer - too esoteric and expensive for routine use in drug discovery and development. Conventional methods can exhaust many milliliters of starting protein and may only produce a small number of hits. Fluidigm has thus introduced a novel technology that enables a new approach to the identification of crystallization conditions with 100 times less sample.

The Topaz™ Crystallizer has been designed for intensive screening of crystallization conditions using a unique combination of techniques redefined specifically for use within a microfluidic environment. By leveraging fluidic properties in nanoscale geometries, we have created the optimal setting for liquid-liquid diffusion of protein and precipitating reagents.

The keystone of the system is a disposable microfluidic chip, or 'microprocessor', fabricated using a proprietary process known as Multi-layer Soft Lithography—the MSL™ process. We call it a 'Microprocessor' because the metering of fluids takes place within the device, automatically, by way of tiny pneumatically actuated valves. With 432 valves, the Topaz Microprocessor combines nanoliter quantities of a concentrated protein solution with discrete chemical crystallization reagents in three different mixing ratios to screen 144 distinct conditions (48 reagents at 3 protein-reagent ratios) with as little as 3 µL of protein sample.

With the Topaz Crystallizer, one technician can run 5760 diffusion trials per week, with as little as 120 µL of starting protein. Internal and external studies indicate that this system matches or outperforms traditional screening methods in terms of sample conservation, the production of novel crystal hits, and that it can promote the formation of high quality crystals by eliminating convection while maintaining supersaturation conditions. We will describe the crystallization mechanism and the advantages of the Topaz system.

MICROSTRUCTURES OF THE FeSiBNbCu SOFT MAGNETIC MATERIAL STUDIED BY HIGH RESOLUTION ELECTRON MICROSCOPY (HREM)

Vo Vong and Ng.Q.Thang

Laboratory of Electron Microscopy - National Centre for Natural Science and Technology, 18 Hoangquocviet Str., Caugiay Hanoi, Vietnam
(vvemlab@ncst.ac.vn)

Microstructures of the magnetic material $Fe_{76,5-x}Cu_1Nb_xSi_{13,5}B_9$,which was annealed at various temperatures between 500^{0}C and 750^{0}C in Ar-atmotphere and then melt-quenching, has been studied by high resolution electron microscopy.

Changes of the grain sizes, phases and nanocrystalline structure of the alloys under influences of the heat treatments have also been systematically investigated by the JEM-4000EX,which has accelerating voltage 400 kilovolt and resolution 0,17 nanomet .

In the work we present the method for preparation of brittle materials for TEM plan-view investigations.The wide areas , which electron beam can transmite , were received in the work.

The new results ,as well as, the alloys were changed from an amorphous state through a partially crystallized state at 550^0 C and finally to a fully crystallized state at 750^{0}C, will be submitted . Grains were observed when the sample was annealed at750^{0}C, they have size from 60 to 82nm in diameter

The magnetic properties and microstructural evolution of the material have also been investigated.

References

1 Vong, V. (2000) The structural changes of the materials under influence of heat treatments, *World Scientific Publishing*, 670 - 673 Edited by Yeong-Der Yao

2 Hono, K., Hiraga, K., Wang, Q., Inoue, A. and Sakurai, T. (1992) The Microstructure Evolution of A $Fe_{73,5}Si_{13,5}B_9Nb_3Cu_1$ Nanocrystalline Soft Magnetic Material, *Acta Metall. Mater.* **40**(9), 2137 – 2147 , 1992

MICRO-ARRAY CHIP FOR HIGH THROUGHPUT PROTEIN CRYSTALLOGRAPHY

N. Watanabe,[a] I. Tanaka,[a] C. Nishijima,[b] H. Takeuchi,[b] T. Sumi[c] and T. Iseki[b]

[a]Division of Biological Sciences, Graduate School of Science, Hokkaido University, Sapporo, Japan; [b]Chemicals Development Laboratories, Mitsubishi Rayon Co., LTD. Yokohama, Japan; [c]Production Technology Center, Mitsubishi Rayon Co., LTD. Hiroshima, Japan (nobuhisa@sci.hokudai.ac.jp)

Since protein crystallization is influenced by a number of factors, development of a method for high throughput protein crystallization is one of the most important steps for accomplishment of structural genomics. We have been developing a unique device for high throughput screening of protein crystallization condition with nano-volume [1]. The device is micro-array chip utilizing the fiber type DNA chip technology.

In order to hold various precipitant conditions in arrayed hollow fibers on the chip, several kinds of gels are used. We have already fixed types and polymerization conditions of gels for almost all precipitants and wide range of buffer pH. It is possible to make arrayed chip for random conditions such as Crystal Screens of Hampton Research and Wizard Screens of Emerald BioStructures. A property of precipitants in a gel has been confirmed by comparing crystallization results with batch method.

The prototype array has from 12 to 48 different crystallization conditions integrated on a cover glass size chip. Each precipitant solution of 50 nL is kept in a hollow fiber of the arrayed chip separately. One should just put protein solution

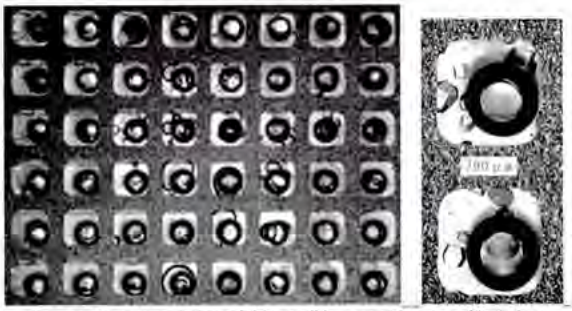

Figure. An arrayed chip of 48 conditions and its magnified view.

onto the chip manually with any single auto-pipetter. Protein and the precipitant solutions are mixed in the micro cell on the chip, and crystallization screening will be performed. Only 50 nL for each crystallization condition, total of about 2 to 10 micro-L protein solution, including loss, is required for screening of conditions on the chip. Using the chip, we can perform many screening conditions without any robotic systems. Our unique screening procedure will make it possible to set up more than 100 different crystallization conditions within a few minutes.

Reference

1 Watanabe, N., Akita, T., Sumi, T., Takeuchi, H. and Tanaka, I. (2002) *Acta Cryst.* **A58**, C94

STRUCTURES AND PHASE TRANSITION IN THE LAYERED PEROVSKITE $La_{0.6}Sr_{0.1}TiO_3$

Christopher J. Howard and Zhaoming Zhang

Materials and Engineering Science, Australian Nuclear Science and Technology Organisation, Private Mail Bag 1, Menai, NSW 2234, Australia
(cjh@ansto.gov.au)

The crystal structure of the layered perovskite $La_{0.6}Sr_{0.1}TiO_3$ at room temperature has been solved by synchrotron X-ray powder diffraction in combination with group theoretical analysis. The structure is orthorhombic in *Cmmm*, on a cell with a = 7.7556(1), b = 7.7349(1), c = 7.7910(1) Å. It is believed that this is the structure also adopted by $La_{2/3}TiO_3$. Pertinent features are the alternation of fully and partly occupied layers of La (Sr) cations, and out-of-phase tilting of the TiO_6 octahedra around an axis perpendicular to the direction of the cation ordering. The compound undergoes a second order transition to a tetragonal structure, the transition temperature being estimated as 360 °C.

STRUCTURE ESTIMATION OF ORBITAL ORDERED THIN FILMS USING SYNCHROTRON RADIATION

Y. Wakabayashi,[a] H. Sawa,[a] M. Nakamura,[b] M. Izumi,[c] K. Miyano,[c] and Y. Murakami[d]

[a]Institute of Materials Structure Science, High Energy Accelerator Research Organization, Tsukuba 305-0801, Japan; [b]Department of Applied Physics, University of Tokyo, Tokyo 113-8586, Japan; [c]Research Center for Advanced Science and Technology, University of Tokyo, Tokyo 153-8904, Japan; [d]Department of Physics, Tohoku University, Sendai 980-8578, Japan (yusuke.wakabayashi@kek.jp)

The series of perovskite Mn oxides $RE_{1-x}AE_xMnO_3$ (*RE*: rare earth, *AE*: alkaline earth metals, *x* denotes hole concentration) attracts great interest because of their unique physical properties. These phenomena are widely noticed for the orbital physics. Thin film technique makes us able to control the orbital state through the lattice distortion and doping ratio. However, it is difficult for conventional x-ray scattering measurement that the whole atomic position determination in thin films because scattering intensity is sensitive to displacements of rare-earth and insensitive to oxygen displacements. In this study, we succeeded to obtain the atomic displacements for various orbital states using the observation of superlattice spots and their photon energy dependence.

We have measured the atomic position in $AMnO_3$ (*A*: $La_{0.6}Sr_{0.4}$, $Pr_{0.6}Sr_{0.4}$ $Nd_{0.6}Sr_{0.4}$ and Sr, we will abbreviate them to LSMO, PSMO, NSMO and SMO, respectively) thin films on $SrTiO_3$ substrate. In the figure, their orbital states expected from their conductivity and hole concentration are summarized. To extract the oxygen position, we examined what element produce the scattering amplitude at superlattice spots using the anomalous dispersion of scattering factor of x-ray.

X-ray diffraction measurements were carried out at BL-1A and 9C, Photon Factory, KEK, Japan. For SMO, we did not observe any displacements. For other three films, we observed several superlattice reflections from oxygen displacement having wave vector (1/2 1/2 1/2). For PSMO and NSMO, we observed additional superlattice reflections from oxygen displacement and *A*-site displacement in *b*-direction. Finally, we obtained the atomic displacements as listed in the table. Mn-O1/Mn-O2 is the ratio of Mn-apical O distance to Mn-in-plane O distance. It is same as *c*/*a* when the atomic displacement is zero.

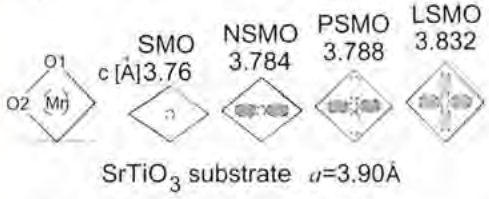

Fig.: Schematic view of the orbital states.

	c/*a*	Mn-O1 / Mn-O2
SMO	0.964	0.964
NSMO	0.970	0.973
PSMO	0.971	0.977
LSMO	0.983	0.985

Table: Results of structure estimation.

THIN-FILM CRYSTAL STRUCTURE DETERMINATION OF $Bi_3Fe_5O_{12}$ MEASURED WITH VCIP METHOD

K. Tanaka, K. Itatsu, N. Adachi, and T. Okuda

Department of Materials Science and Engineering, Nagoya Institute of Technology, Gokiso-cho, Showa-ku, Nagoya 466-8555, Japan (kiyo@tana.mse.nitech.ac.jp)

$Bi_3Fe_5O_{12}$ (BIG) is famous for its gigantic Faraday effect. High quality single-crystal films of BIG was grown for the first time by one of the authors (T.O.) by means of liquid phase epitaxy (LPE) on the substrate of (111) plane of several garnets, $Gd_3(Sc,Ga)_5O_{12}$ (GSGG) in the present study. The crystal structure of BIG is highly important and interesting to investigate the significant property of BIG. However single crystal structure determination has not been done for these thin films because intensities from BIG was too small compared to those from the substrates and the separation of the peaks from BIG and substrates were difficult.

Vacuum Camera Imaging Plate method (VCIP) has been developed by us. Vacuum camera is a cylinder with imaging plate on its inner wall and rotation photograph of a crystal located at the center of the camera are taken under vacuum. It enables us to measure weak X-ray diffraction intensities because the noise due to air-scattering of X-rays is minimum which is two-order less than that without evacuation [1].

Thin film of BIG 3.4 μm thick grown on the GSGG substrate with a thickness of 452.2 μm and 2133x1067 μm wide was glued on a glass rod. Incident X-rays were collimated by a collimator with a diameter of 500 μm. In order to avoid absorption of diffracted beams from BIG, substrate is placed toward the incident beam and the crystals were rotated about ±45 ° with 2 ° overlap of scan with the following film. The peaks of BIG at low angles were well separated from those of substrate. At middle angles only the peaks from GSGG are observed. Separated peaks of Mo Kαdoublet of GSGG were observed at high angles, where scattered X-rays by the substrate produce high background. Intensities were read with Fuji-BAS2500. Total number of observed reflections from BIG was 1588. Overlapped peaks of BIG and GSGG were not used. Reflections were corrected for absorption due to the substrate and BIG itself. Without the correction R-factor would not reduce from 75 %. Measured Bragg peaks were indexed with the program DENZO. Slant incidence of X-rays on the IP was also corrected for.

All the atoms except O atoms were refined assuming anisotropic temperature factors. Final R-factor was 15.9 %. Since the size of the sample is larger than that of the incident X-rays, each peak is large and the setting of integration box accompanies some difficulty. However the integration process can still be improved and much better R-factor is expected to be obtained. The present study opened the door to the thin-film single crystallography.

Reference

1 Zhurova, E. A., Zhurov, V. V. and Tanaka, K. (1999) *Acta Cryst.* B**55**, 917-922.

POLYTYPE POSSIBILITIES ARISING FROM PSEUDO SYMMETRIC CRYSTAL STRUCTURES ALLOWING STACKING FAULTS

Anthony. C. Willis, A. David Rae, Tory N. Cayzer, and Michael S. Sherburn

Research School of Chemistry, The Australian National University, Canberra, ACT 0200, Australia (willis@rsc.anu.edu.au)

Alternative stackings of substructures allows the possibility of polytypes and indeed crystals containing coherent blocks of structure of different space groups and different orientations [1]. Two recent organic structures from service crystallography fit this concept and are described, viz (i) 6-ethyl-3-oxo-1,3,3a,4,7a-hexahydro-isobenzofuran-4-carboxylic acid methyl ester and (ii) the related 6-hydoxymethyl compound.

Each can be described as an occupancy modulation of a 1:1 disordered parent structure of orthorhombic symmetry which is the Fourier transform of the *I* even reflections, *Pnma* for (i) and *Ibm2* for (ii). Ordered layers can be formed but not all symmetry elements of such a layer can be symmetry elements of an ordered crystal structure. This allows alternative origins c/2 apart for each layer. For (i) the layers have $P2_1ca$ symmetry and the ordered structure has $P.2_1/c.$ symmetry in the cell $a_P,b_P,2c_P$. For (ii) the layers have $Pbc2_1$ symmetry and the ordered structure has *C.c.* symmetry in the cell $a_P+c_P,b_P,2c_P$. If every second layer shifts by c/2 we create a different orientation of the structure allowing a twin-disorder mechanism. The third and fourth layers can be related to the first and second by translations that differ by c/2. This allows the possibility of polytypes. For (i) there is the possibility of different orientations of an ordered structure of $A2_1/d.$ symmetry in the cell $a_P,2b_P,2c_P$, ie $P.2_1/c.$ symmetry in the cell $-2b_P,a_P,b_P+c_P$ while for (ii) there is the possibility of different orientations of an ordered structure of $Pbc2_1$ symmetry in the cell $a_P,b_P,2c_P$.

Reference

1 Rae, A. D., and Willis, A. C. (2003) Z. *Krist.* **218**, 221-230.

THE TEMPERATURE DEPENDENCE OF THE CRYSTAL STRUCTURE OF 3,5-DI-T-BUTYLPYRAZOLE

Alexandre N. Sobolev, and Allan H. White

Chemistry, University of Western Australia, Crawley WA 6009, Australia
(ans@chem.uwa.edu.au)

Recent studies [1,2] of the structure of the title compound have suggested it to be temperature dependent, in respect of the impact on disorder in the rotational dispositions of the t-butyl groups, and in the hydrogen-bonded hydrogens. The structure has now been redetermined at 10K, revealing, *en route*, a phase transition at *ca.* 110K from the high-temperature *Pbca* form, Z = 8, to a low-temperature $Pb2_1a$ form, Z = 16, the contents of the asymmetric unit increasing from one molecule, with temperature dependent disorder, to four molecules ('A-D'), all devoid of crystallographic symmetry. At 10K, all species in the structure are ordered, with the molecules partitioned pairwise into '*cis*' and '*trans*' forms (referring to the relative rotational dispositions of the methyl hydrogens.)

Redeterminations of the structure of 3,5-dimethylpyrazole[3], at room-temperature and at 10K are also discussed.

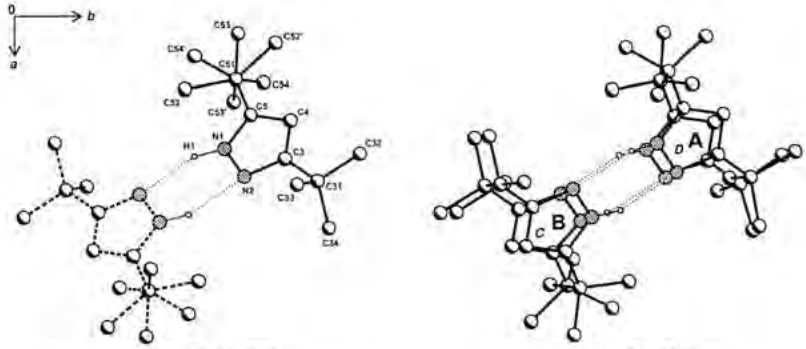

T = 120 K T = 10 K

References

1 Aguilar-Parilla, F., Limbach, H. -H., Foces-Foces, C., Cano, F. H., Jagerovic, N., and Elguero, J. (1995) *J. Org. Chem.*, **60**, 1965-1970.

2 Deacon, G. B., Gitlits, A., Roesky, P., Burgstein, M. R., Lim, K. L., Skelton, B. W., and White, A. H. (2001) *Chem. Eur. J.*, 127-138.

3 (a) Baldy, A., Elguero, J., Fawe, R., Pierrot, M., and Vincent, E. -J. (1985) *J. Amer. Chem. Soc.*, **107**, 5290-5291.
(b) Smith, J. A. S., Wehrle, B., Aguilar-Parrilla, F., Limbach, H. -H., Foces-Foces, M. C., Cano, F. H., Elguero, J., Baldy, A., Pierrot, M., Khurshid, M. M. T., Larcombe-McDouall, J. B. (1989) *J. Amer. Chem. Soc.*, **111**, 7304-7312.

EXPERIMENTAL AND THEORETICAL STUDIES OF THE SULFOXIMINE GROUP [R^1-S(=O)(=N-R^2)R^3]: DETECTION OF POSSIBLE LATTICE EFFECTS

Gerhard Raabe

Institut fuer Organische Chemie, Rheinisch-Westfaelische Technische Hochschule Aachen, Professor-Pirlet-Strasse 1, D-52074 Aachen, Germany (gerd.raabe@thc.rwth-aachen.de)

Sulfoximines of general structure R^1-S(=O)(=N-R^2)R^3 play an important role in stereoselective synthesis. Evaluation of the available structural information obtained by X-ray diffraction methods reveals that especially the values of the bond angles at the sulfur atom cover relatively wide ranges. This rises the question as to the influence of the environment in the crystal lattice on the structure of the sulfoximine group. The easiest way to detect such lattice effects is to perform a quantum-chemical calculation for the isolated unperturbed molecule and to compare its optimized structure with the one obtained experimentally in the solid state. Although state of art methods like conventional *ab initio* and DFT-based methods today can handle relatively large systems the computational efforts increase significantly as the molecule under consideration becomes larger. Thus, the much faster semiempirical methods which also require significantly less memory are still widely used to optimize the structures of larger molecules. The reliability of the structures obtained with these methods critically depends on their parametrizations. Determination of the semiempirical parameters, however, is never a trivial task especially not in the case of an element like sulfur which exists in a variety of valence states. We, therefore, performed semiempirical geometry optimizations for a large number of sulfoximines for which the solid state structures are known from X-ray diffraction studies. In these calculations we employed the most frequently used semiempirical methods (MNDO[1], AM1[2], PM3[3], MSINDO[4]). Comparison of the semiempirical results with those obtained for sample compounds on the conventional *ab initio* and DFT level shows which of the four methods is suited to predict lattice effects in the case of sulfoximines.

References

1 Dewar, M. J. S. and Thiel, W. (1977) *J. Am. Chem. Soc.* **99**, 4899-4907.
2 Dewar, M. J. S., Zoebisch, E. G., Healy, E. F. and Stewart, J. J. P. (1985) *J. Am. Chem. Soc.* **107**, 3902-3909.
3 (a)Stewart, J. J. P. (1989) *J. Comput. Chem.* **10**, 209-220. (b)Stewart, J. J. P. (1989) *J. Comput. Chem.* **10**, 221-264.
4 (a)Ahlswede, B. and Jug, K. (1999) *J. Comput. Chem.* **20**, 563. (b)Ahlswede, B. and Jug, K. (1999) *J. Comput. Chem.* **20**, 572.

THE PDF-4/FULL FILE AND PDF-4/ORGANICS DATABASES: NEW DATA MINING TOOLS FOR STRUCTURAL CRYSTALLOGRAPHY AND MATERIALS CHARACTERISATION

Brian O'Connor,[a] Camden Hubbard,[b] Tim Fawcett,[c] and John Faber[c]

[a]Materials Research Greoup, Department of Applied Physics, Curtin University of Technology, GPO Box U1987, Perth, WA 6845, Australia; [b]Oak Ridge National Laboratory, Oak Ridge, TN 37831-6064, USA; [c]International Centre for Diffraction Data, 12 Campus Boulevard, Newtown Square, PA 18073-3273, USA (B.O'Connor@curtin.edu.au)

The ICDD is a not-for-profit organisation comprising 340 of the world's leading x-ray scientists. It is dedicated to collecting, editing, publishing and distributing powder diffraction data for the characterisation of crystalline materials. The membership of the ICDD consists of worldwide representation from academe, government and industry. It is our mission to continue as the world centre for quality x-ray powder diffraction data to meet the needs of the technical community.

Through the combined efforts of the members and its staff of 40 at ICDD Headquarters, the organisation serves the crystallography and materials science communities (i) by producing the ICDD Powder Diffraction File (PDF) and other data base products for materials characterisation; (ii) through x-ray analysis education programs and conference management (including the Denver X-ray Conference); and (iii) through philanthropic initiatives such as scholarship support for postgraduate students working in the field.

The ICDD has recently released the PDF-4/Full File powder diffraction database which gives powder diffractionists a very sophisticated tool for data mining. PDF-4 contains over 87,000 measured patterns and approximately 49,000 patterns simulated from crystal structure data. Searches may be conducted for metals & alloys, pharmaceuticals, zeolites, superconductors, detergents pigments, ceramics, corrosion products, polymers, cement materials, forensics and explosives sub-files. Common query fields for data mining include elemental composition, formula, common name, colour, melting point, space group, unit cell dimensions, Pearson symbol, mineral classification and statistical quality of the pattern. Algorithms are provided to transform single cystal structural data into powder patterns using 'on-the-fly' calculations which include adjustable experimental effects such as slit configuration and crystallite broadening.

The organisation has recently released PDF-4/Organics which contains data for over 146,000 organic and organometallic phases of which almost 123,000 patterns are calculated from ICDD and CCDC single-crystal structural data. This exciting new tool has awesome data mining capability through searching 30+ separate diffraction fields and physical properties which include formula, chemical name, functional group index, drug activity, space group and unit cell dimensions. Material-type sub-files include organics, pharmaceuticals, polymers, pigments and forensics.

Examples to be described will include:

1. Making use of isomorphous phase information in the data base for structure solution
2. Pharmaceutical polymorph characterisation
3. Unknown identification

HIGH TEMPERATURE LAUE METHOD WITH POLYCHROMATIC SR: ITS APPLICATION TO QUARTZ PHASE TRANSITION

Kazumasa Ohsumi,[a] Yoshikazu Miyata,[b] Katsuhiro Kusaka,[a] Takeshi Nakagawa,[a] and Kenji Hagiya[c]

[a]Photon Factory, Inst. Materials Structure Science, KEK, Tsukuba, 305-0801, Japan; [b]Graduate School for Advanced Studies, KEK, Tsukuba, 305-0801, Japan; [c]Faculty of Science, Himeji Institute of Technology, Hyougo, 678-1297, Japan (kazumasa.ohsumi@kek.jp)

The Laue method is advantageous for obtaining diffraction data from a crystal at both low and high temperatures, because perturbative air-flow around the sample is reduced due to the stationary crystal when using polychromatic SR.

Low and high temperature equipment and a control system for observation through an optical microscope(LK-600PH; Linkam Scientific Instruments Ltd.) was developed and installed vertically on the Laue camera at BL-4B1 of the Photon Factory, KEK, Tsukuba. The Laue camera was originally developed for diffraction studies especially for sub-micrometer sized specimens and/or micrometer sized area of a larger sample[1],[2]. Taking into account the possibility of a thermal gradient within the sample, the Laue camera is suitable for our purpose. The low and high temperature system on the Laue camera was applied to the α–β phase transition of quartz(SiO_2), because it is well known that a modulated structure exists in the narrow temperature range between α–β quartz[3].

Diffraction data were obtained from α- to β-phase through the modulated structure region at 0.1 K steps. Satellite-reflection profiles and intensities around the main spots clearly changed at each temperature, partially shown in the figure below. Refinements of α- to β-quartz were carried out including substructure of the modulated structure region. The result indicates that the changes of positional and anisotropic thermal parameters describe the behavior of the oxygen atom through modulated structure region.

T_{im} : Temperature at maximum intensities of satellite reflections

References

1 Ohsumi, K., Hagiya, K. and Ohmasa, M. (1991) *Jour.Appl.Cryst.* **24**, 340-348.

2 Ohsumi, K., Hagiya, K., Uchida, M., Suda, N., Miyamoto, M., Kitamura, M. and Ohmasa, M. (1995) *Rev. Sci. Instrum.* **66(2)**, 1448-1450.

3 van Tendeloo, G., van Landuyt, J. and Amelinckx, S.(1976) *Phys. Stat. Sol. (a)* **33**, 723-735.

X-RAY EXTENDED-RANGE TECHNIQUE FOR PRECISION MEASUREMENT OF THE X-RAY MASS ATTENUATION COEFFICIENT AND IM(F) FOR MOLYBDENUM USING SYNCHROTRON RADIATION

C. T. Chantler,[a] M. de Jonge,[a] Z. Barnea,[a] C. Q. Tran,[a] B. B. Dhal,[a] and D. J. Cookson[b]

[a]School of Physics, University of Melbourne, Parkville, Vic 3010, Australia; [b]ANSTO, Private Mail Bag 1, Menai, NSW 2234 and Chem-Mat-CARS-CAT (Sector 15, Bldg 434D), Argonne National Laboratory, 9700 S. Cass. Avenue, Argonne, IL 6043 (chantler@ph.unimelb.edu.au)

Complex X-Ray form factors are used in crystallography, material science, medical diagnosis, refractive index studies and XAFS. Determinations of the complex component typically differ by around 10% or 10 standard deviations. This has long been a concern of the International Union of Crystallography, and we have seriously undertaken to determine sources of systematic error in these measurements. We apply the X-Ray Extended-Range Technique [1,2] for accurate measurements of the mass attenuation coefficient and the imaginary component of the atomic form factor. We present our latest experimental results for Molybdenum featuring an absolutely calibrated energy scale, harmonic component determination at a level of 1 photon in 10^4 and sample thickness calibration. The range of the attenuation measurement far exceeds the Nordfors range of $2 < \ln (I_0/ I) < 4$, resulting in an increase of precision and accuracy to below 0.1 % in the range from 13.5 keV to 41.5 keV. The new result challenges available theoretical calculations and suggests that new methods of computation are required to approach the accuracy of the experimental data, while also challenging us to develop a theory of XAFS capable of understanding the absolute magnitude of fine structure oscillations.

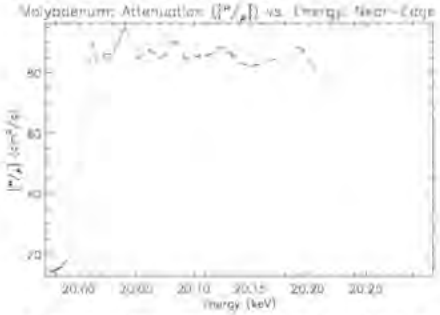

Preliminary results of an absolute measurement of the total attenuation coefficient of Molybdenum showing typical grid densities employed near the fine structure.

References

1 Chantler, C. T., Tran, C. Q., Paterson, D., Cookson, D. and Barnea, Z. (2001) *Phys. Lett.* **A286,** 338-346.

2 Chantler, C. T., Tran, C. Q., Barnea, Z., Paterson, D., Cookson, D. and Balaic, D. X. (2001) *Phys. Rev.* **A64,** 062506-1 – 15.

X-RAY MASS ATTENUATION COEFFICIENT OF SILICON: THEORY VERSUS X-RAY EXTENDED-RANGE TECHNIQUE AND OTHER EXPERIMENTS

C. T. Chantler, C. Q. Tran, and Z. Barnea

School of Physics, University of Melbourne, Parkville, Vic 3010, Australia
(chantler@ph.unimelb.edu.au)

Structural determinations near absorption edges using synchrotron radiation sources, multiple-wavelength anomalous dispersion (MAD) techniques and X-ray absorption fine structure (XAFS) investigations have shown many successes in recent years. They provide information on local electron density distributions, lattice spacings, atomic environments in solids and excited-state occupation levels. However, the X-ray interaction away from edges can be just as revealing about the electronic structure, inner-shell orbitals, and relativistic corrections to atomic structure. We compare new experimental X-ray total mass attenuation coefficients of silicon obtained with the X-ray Extended-Range Technique (XERT) [1, 2] from 5 keV to 20 keV with theoretical calculations and earlier experimental measurements over a 5 keV - 50 keV energy range. The accuracy of between 0.27% and 0.5% of the XERT data allows us to probe alternate atomic and solid state wave-function calculations and to test dominant scattering mechanisms (Laue-Bragg, Rayleigh and TDS assumptions). Discrepancies between experimental results and theoretical computations of the order of 5% are discussed in detail. No single theoretical computation is currently able to reproduce the experimental results over the entire 5 keV - 50 keV energy range investigated.

References

1 Chantler, C. T., Tran, C. Q., Barnea, Z., Paterson, D., Cookson, D. and Balaic, D. X. (2001) *Phys. Rev.* **A64,** 062506-1 – 15.

2 Tran, C. Q., Chantler, C. T., Barnea, Z., Paterson, D., and Cookson, D. J. (2003) *Phys. Rev.* **A** in press.

THE CRYSTAL STRUCTURE OF DOPED PEROVSKITES DERIVED FROM ELECTRON SCATTERING TECHNIQUES

C. J. Maunders,[a] J. E. Etheridge,[a] C. J. Rossouw,[b] and H. J. Whitfield[b]

[a]Department of Physics and Materials Engineering, Monash University, Clayton, Victoria, Australia; [b]CSIRO Manufacturing and Infrastructure Technology, Private Bag 33, Clayton South MDC, Victoria 3169, Australia (christian.maunders@spme.monash.edu.au)

Structural and electronic properties of perovskites can be manipulated through the addition of dopant atoms. For example, stabilisation of high temperature phases at room temperature is possible with the introduction of small concentrations of foreign ions into the structure. The present work considers a certain class of barium titanates, having the perovskite structure, that have been transformed into a hexagonal phase at room temperature that is stabilised by the addition of dopant Ru or Mn atoms. The structure focussed on is the 6 layer (6H) hexagonal $Ba_3(Ru_1,Ti_2)O_9$.

In order to understand how the dopant atoms are accommodated within the 6 layer (6H) hexagonal $Ba_3(Ru_1,Ti_2)O_9$ structure, we are investigating the unit cell configuration using a variety of electron scattering techniques. Space group determination was performed using convergent beam electron diffraction (CBED). Local lattice parameters were determined from intersections of various deficit lines derived from higher order Laue zone(HOLZ) beams. The sublattice site occupancy of Ru dopant atoms was subsequently confirmed using atom location by channelling enhanced microanalysis (ALCHEMI). Transmission electron microscopy has been used to investigate the microstructure at lattice resolution.

The dynamical dispersion surface excitations and spacings were observed in the quantum state line contrast in HOLZ beams. This relates back directly to the predominant eigenstates that are excited under highly symmetric scattering conditions, and these were observed to change with small tilt such that different sets of eigenstates (partial waves) are excited.

EFTEM AND HRTEM STUDIES OF METAKAOLINITE AND METADICKITE

Sujeong Lee,[a] Youn Joong Kim,[b] Hi-Soo Moon,[c] and Won-Seon Seo[a]

[a]Ceramics Reliability Center, Korea Institute of Ceramic Engineering and Technology, Seoul 153-801, Korea; [b]Division of Analysis and Measurement, Korea Basic Science Institute, Daejon 305-333, Korea; [c]Department of Earth System Sciences, Yonsei University, Seoul 120-749, Korea (crystal@kicet.re.kr)

Metakaolinite in the kaolinite-mullite reaction series is microcrystalline or amorphous, which makes it difficult to study by XRD, NMR and conventional TEM analyses. However, a 14Å modulation has been recently reported with the periodicity along the c^*-axis[1]. Several models of metakaolinite are proposed, but suffer from little understanding of structural ordering along the *c*-axis and the fact that the spinel-type phase is formed not by the decomposition of metakaolinite but by a topotactic formation with respect to metakaolinite before the decomposition of metakaolinite[2-6]. We performed EFTEM and HRTEM studies to reexamine metakaolinite and metadickite structures, with a focus on the short-range order. Different lengths of modulations develop along the c^*-axis from the regions where the structures are disturbed due to the OH elimination during the progression of dehydroxylation in kaolinite and dickite. The 14Å modulation is confirmed to be the most common in BF images, which proves that the pattern of vacant octahedral sites in successive layers changes to lose the original symmetry. Mullite crystals are abruptly induced from the kaolinite heated at 630C by electron beam radiation during HRTEM imaging, which indicates the difference of the structural stability between the kaolinite dehydroxylates at 550C and 630C. The periodicity along the c^*-axis, taken together with all the reasonable crystallographic data in earlier works, should be considered to propose the metakaolinite structure.

References

1 Lee, S., Kim, Y. J. and Moon, H. –S. (2003) *J. Am. Ceram. Soc.*, 86[1], 174-176.
2 Brindley, G. W. and Nakahira, M. (1959) *J. Am. Ceram. Soc.*, 42[7], 314-318.
3 MacKenzie, K. J. D., Brown, I. W. M., Meinhold, R. H. and Gowden, M. E. (1985) *J. Am. Ceram. Soc.*, 68[6], 293-297.
4 Rocha, J. and Klinowski, J. (1990) *Phys Chem Minerals*, 17, 179-186.
5 Gualtieri, A. and Bellotto, M. (1998) *Phys Chem Minerals*, 25, 442-452.
6 Lee, S., Kim, Y. J. and Moon, H. -S. (1999) *J. Am. Ceram. Soc.*, 82[10], 2841-2848.

DEPENDENCE OF THE ACCURACY OF A CONTINUOUS PHASE TRANSITION TEMPERATURE ON ANGULAR RESOLUTION IN POWDER DIFFRACTOMETRY

Masatomo Yashima,[a] Mizuki Mori,[a] Roushown Ali,[a] Masahiko Tanaka,[b] and Takeharu Mori[b]

[a]Department of Materials Science and Engineering, Interdisciplinary Graduate School of Science and Engineering, Tokyo Institute of Technology, 4259 Nagatsuta-cho, Midori-ku, Yokohama, 226-8502, Japan; [b]Photon Factory, Institute of Materials Structure Science, High Energy Accelerator Research Organization, 1-1 Oho, Tsukuba, Ibaraki, 305-0801, Japan (yashima@materia.titech.ac.jp)

A number of researchers have studied the structural phase transition in various materials, because it is one of the most important topics in many fields such as physics, chemistry, biology, geoscience and materials science. Near the transition temperature, many materials exhibit interesting and useful properties. Therefore, it is of vital importance to determine accurately the transition temperature and the temperature dependence of unit-cell parameters near the transition point. It is often difficult to determine precise unit-cell parameters near the transition point by conventional laboratory-based X-ray powder diffractometer, due to low angular resolution. On the contrary, the synchrotron radiation powder diffraction has much narrower peak width and no splitting as *K*alpha1 and *K*alpha2 peaks. Therefore we have investigated the unit-cell parameters near transition point by synchrotron radiation powder diffraction technique [1,2]. The precision of unit-cell parameters is improved by higher-resolution diffractometer. Therefore the precision of the transition point would also be improved by using higher-resolution instrument. However, to our best knowledge, the effect of angular resolution on the accuracy of a transition temperature has not been investigated in the literature. We have investigated *in situ* a continuous transition between the orthorhombic and tetragonal phases in double-perovskite-structured $La_{0.64}(Ti_{0.92},Nb_{0.08})O_3$ by three X-ray powder diffractometers with different delta(d)/d resolutions of 0.03%, 0.06% and 0.10% [3]. The d and delta(d) denote the lambda/(2sin(theta)) and peak width where lambda and theta are wavelength of X-ray and Bragg angle. Only the highest-resolution diffractometer of delta(d)/d =0.03% was able to detect the peak splitting between 400 and 040 reflections in the temperature range of 327 to 339 deg C. It was found that the accuracy of the transition temperature is considerably improved with decreasing of delta(d)/d value. The maximum temperature where the peak splitting between 400 and 040 reflections is detectable increases, while the transition temperature determined by a power law decreases with decreasing of delta(d)/d value.

References

1 Ali, R., Yashima, M., Tanaka, M., Yoshioka, H., Mori, T. and Sasaki, S. (2002) *J. Solid State Chem.* **163**, 51-59.

2 Yashima, M., Ali, R., Tanaka, M. and Mori, T. (2002) *Chem. Phys. Lett.* **363**, 129-133.

3 Yashima, M., Mori, M., Ali, R., Tanaka, M. and Mori, T. (2002) *Chem. Phys. Lett.* in press.

A NEW HIGH-TEMPERATURE FURNACE FOR HIGH-RESOLUTION SYNCHROTRON RADIATION POWDER DIFFRACTION STUDY UP TO 1900K

Masatomo Yashima,[a] Masahiko Tanaka,[b] Takeharu Mori,[b] Kenjiro Ohouchi,[a] and Daiju Ishimura[a]

[a]Department of Materials Science and Engineering, Interdisciplinary Graduate School of Science and Engineering, Tokyo Institute of Technology, 4259 Nagatsuta-cho, Midori-ku, Yokohama, 226-8502, Japan; [b]Photon Factory, Institute of Materials Structure Science, High Energy Accelerator Research Organization, 1-1 Oho, Tsukuba, Ibaraki, 305-0801, Japan (yashima@materia.titech.ac.jp)

A number of researchers have studied the structural change and the phase transition in various materials, because they are some of the most important topics in many fields such as physics, chemistry, biology, geoscience and materials science. Near the transition temperature, many materials exhibit interesting and useful properties. Therefore, it is of vital importance to determine accurately the transition temperature and the temperature dependence of unit-cell parameters near the transition point. It is often difficult to determine precise unit-cell and structural parameters near the transition point by conventional laboratory-based X-ray powder diffractometer, due to low angular resolution. On the contrary, the synchrotron radiation powder diffraction has much narrower peak width and no splitting as *K*alpha1 and *K*alpha2 peaks. Therefore we have investigated the unit-cell parameters near transition point by synchrotron radiation powder diffraction technique [1,2]. But the previous furnace developed by Tanaka [3] could not work well above 700 Celsius degree. In the present study we successfully devised and fabricated a new furnace that enabled *in situ* accurate structural study through high-resolution synchrotron powder diffraction. The delta(*d*)/*d* resolution of the present powder diffraction data was estimated to be 0.03% from the full width at the half maximum. It was found that this furnace is quite useful to distinguish a very similar crystal structure from each other. The synchrotron powder diffraction data of calcium titanate measured at about 1300 Celsius degree was analyzed by a combination method of the Rietveld refinement and of a maximum entropy method based pattern fitting where the computer programs *RIETAN-2000*, *ENIGMA*, *PRIMA* and *VENUS* were used [4,5]. Chemical bonding between titanium and oxygen atoms was clearly observed in the electron density map of the calcium titanate at 1300 Celsius degree. This furnace would open a new world of the high-temperature science and technology in a variety of academic fields such as materials science, physics, chemistry and geoscience.

References

1 Ali, R., Yashima, M., Tanaka, M., Yoshioka, H., Mori, T. and Sasaki, S. (2002) *J. Solid State Chem.* **163**, 51-59.
2 Yashima, M., *et al.* (2002) *Chem. Phys. Lett.* **363**, 129-133.
3 Tanaka, M. (2000). *Photon Factory Activity Report 1999* #17, KEK Progress Report 2000-1, edited by Y. Murakami *et al.*, pp.42-44. High Energy Acceleration Research Organization, Tsukuba, Japan.
4 Tanaka, H., *et al.* (2002) *J. Appl. Cryst.* **35,** 282-285.
5 Izumi F., (2002) *J. Cryst. Soc. Jpn.* **44,** 380-388.

SUB-SECOND X-RAY DIFFRACTION MEASUREMENT AND STRUCTURE ANALYSIS BY MSGC

Hidehiro Uekusa,[a] Yuji Ohashi,[a] Y. Tsuji,[b] Y. Nishi,[b] T. Tajima,[b] and S. Adachi[c]

[a]Department of Materials Science, Tokyo Institute of Technology, Tokyo 152-8551, Japan; [b]Rigaku Corporation, Tokyo 196-8666, Japan; [c]HARIMA Institute RIKEN, Hyogo 679-5148, Japan (uekusa@cms.titech.ac.jp)

Rapid X-ray diffraction measurement technique is an essential to realize the time-resolved observations of crystalline-state reactions, unstable species in excited state and reaction intermediates. To achieve time resolution of seconds or sub seconds order, the use of photon counting type two-dimensional detector is required.

Recently, MSGC (Micro Strip Gas Chamber) was developed for the rapid X-ray data collection. MSGC is a gaseous detector having both photon counting and two-dimensional imaging properties. The features of the detector are a large detective area of 10 x 10cm, a fine positional resolution of 100 micrometer and an excellent capability for high counting rate up to 10^7 cps suitable for the synchrotron radiation experiments.

With the measurement system consists of a MSGC detector, one axis goniometer and a laboratory X-ray generator, complete data set from typical organic crystals were recorded within several minutes to seconds range and the results of structure analyses were satisfactory [1]. In the experiment using the synchrotron radiation at SPring-8, structure analysis of three dimensional reflection data from sub-second measurement was successfully achieved. For an application of real-time monitoring of diffraction pattern, the timing resolution of millisecond can be achieved. By utilizing this ability and bright SR at SP8, time-resolved measurement of the cell dimension of photo-irradiated Platinum complex crystal [2] was carried out. The dimensional change caused by photo-excited Platinum complex and thermal expansion of the crystal was clearly observed.

References

1 Ochi, A., Uekusa, H., Tanimori, T., Ohashi, Y., Toyokawa, H., Nishi, Y., Nishi, Y., Nagayoshi, T. and Koishi, S. (2001) *Nucl. Inst. Meth. Phys. Res.* **A467-468**, 1148-1151.

2 Yasuda, N., Kanazawa, M., Uekusa, H. and Ohashi, Y. (2002) *Chem. Lett.* **31**, 1132-1133.

THE BEAMLINE FOR MACROMOLECULAR ASSEMBLIES OF THE INSTITUTE FOR PROTEIN RESEARCH

Masato Yoshimura,[a] Eiki Yamashita,[a] Atsushi Nakagawa,[a] Masaki Yamamoto,[b] Shinya Yoshikawa,[c] and Tomitake Tsukihara[a]

[a]Institute for Protein Research, Osaka University, Suita, Osaka 565-0871, Japan; [b]JASRI/RIKEN Harima Institute, The Institute of Physical and Chemical Research, Sayo-gun, Hyogo 679-5148, Japan; [c]Department of Life Science, Himeji Institute of Technology, Ako-gun Hyogo 678-1297, Japan (yoshimur@protein.osaka-u.ac.jp, atsushi@protein.osaka-u.ac.jp)

Biological macromolecular assemblies play significant roles in many biological reaction systems, including energy transfer, protein synthesis, protein analysis, DNA replication and signal transduction. More than 20,000 protein structures are now known since the first crystal structures of hemoglobin and myoglobin were determined. On the other hand, fewer than 100 structures of macromolecular assemblies, including viruses have been determined by X-ray crystallography. This is because of the difficulties faced in the preparation, crystallization, X-ray diffraction measurement, and crystal structure determination of large molecular assemblies. A beamline for biological macromolecular assemblies at SPring-8, which is specially designed to collect high resolution and high quality diffraction data from crystals of macromolecule assemblies with large unit cells, has been operating since September 1999.

This beamline uses a standard undulator of SPring-8 as a light source, a piece of super mirror as a condensing device and a rotated-inclined double crystal as a monochromator. The wavelength is usually fixed at 0.9 Å, but MAD experiments can also be performed. The size of the X-ray beam can be changed according to the size of the crystal using a slit-system.

We recently developed a new type area detector, which is a hybrid of imaging plates and a CCD. This detector has a CCD detector (Bruker-AXS SMART6500) surrounded by independent six imaging plates. The CCD detector can be used both for diffraction data collection of ordinary protein crystals diffracting below ~2.0 Å resolution and for checking the quality of crystals. Imaging plates are used for diffraction data collection from macromolecular assemblies, because of the large detector area.

The present status of beamline including the new detector system and some diffraction data will be presented.

X-RAY MICRODIFFRACTION SURFACE AREA INVESTIGATIONS OF TUNGSTEN CLAD MAGNESIUM ALLOYS

Natasha Wright,[a] M. Mandagie,[b] and G. Theodossiou[a]

[a]CSIRO Manufacturing and Infrastructure Technology, Private Bag 33, Clayton South MDC, Victoria 3169, Australia; [b]CAST Cooperative Research Center for Cast Metals Manufacturing (Natasha.Wright@csiro.au)

X-ray microdiffraction is a useful tool for fast, non destructive and effective determination of crystalline phase composition in a wide range of materials [1,2]. Technological advancements both in the field of x-ray optics and in particular the development of 2-dimensional area detectors have made surface area crystalline phase mapping possible with laboratory source instruments [3].

This paper discusses one of the many unique applications undertaken using the Bruker GADDS(General Area Detection Diffraction System) instrument situated at CSIRO Manufacturing and Infrastructure Technology. The material investigated was a polished cross section of an Mg Alloy that had undergone laser cladding with a Tungsten material. Each cladding area had undergone different laser parameters to produce different phase compositions, with area of most interest being the interface region between the substrate and cladding.

X-ray microdiffraction maps of the entire cladding area for each laser parameter were undertaken using the GADDS surface area mapping capability. GADDS results indicated structural changes in spots as small as 100 micron in the cladding-substrate interface region; these differences would have been very difficult to detect using conventional powder diffraction techniques [1]. The area was then analyzed using Scanning Electron Microscopy and Energy Dispersive X-ray Spectroscopy (EDXS) so that image morphology and elemental species of the various regions could be obtained and to verify the chemical data provided with phase composition results from GADDS analysis. There was good correlation between chemical data and phase composition. GADDS surface area mapping, in conjunction with SEM and EDXS, was successful in the characterization of crystalline phase composition in Tungsten Clad Magnesium Alloys.

References

1 Hay, D., Scarlett, N. and Wilson, N. (2001) *Proc.Eng2001Mat*, Melbourne, Australia, IMEA press, 99-104.
2 Taylor, R. C., Hinczak, I. (2001) *Rietveld Made Easy*, 188-194.
3 Bruker AXS, *Diffraction Solutions – GADDS. D-76181, (1997)*, Karlsruhe, Germany, FRG press, **B86-E00001.**

ON THE DESIGN FOR A VERSATILE IMAGING AND HARD X-RAY BEAMLINE FOR MATERIALS SCIENCE, BIOMEDICAL, AND MEDICAL APPLICATIONS AT "BOOMERANG"

S. W. Wilkins,[a,b] R. A. Lewis,[b] K. K-W. Siu,[b] A. W. Stevenson,[a] K. A. Nugent,[c] and D. J. Parry[a]

[a]CSIRO, Manufacturing and Infrastructure Technology PB33 Clayton Sth, Vic 3169, Australia; [b]School of Physics & Materials Engineering, Monash University, Clayton, Vic 3168, Australia; [c]School of Physics, University of Melbourne, Vic 3010, Australia (Steve.Wilkins@csiro.au)

The development of medium-sized storage rings with high brightness and of new optics and imaging methods opens up exciting possibilities for materials science, biomedical, clinical medical, and other research at such sources. We outline key design features for a versatile imaging and hard X-ray beamline proposed for "Boomerang", operating in the energy range 10-90 keV and with a number of modalities for imaging including; in-line projection imaging [1,2] with both monochromatic and "pink" beam as well as crystal-based methods [3]. The proposed insertion device for this beamline is a 6T superconducting wiggler in order to give high flux in the hard X-ray regime, small source size and relatively wide divergence in the horizontal plane.

Key features of the beamline are the use of 2 experimental stations (hutches) involving a very long beamline (~150 m) for Station 2 as well as the ability to operate in a variety of imaging and diffraction modes, including; i) scanning microprobe (Station 1), ii) plane wave topography (Station 1 or 2), iii) USAXS using Station 1 for sample and Station 2 for detector iv) full field phase-contrast imaging [1,2] using both simple projection from the source as well as an effective secondary source produced by a focusing device such as a compound refractive lens [4] as well as the double-crystal (DEI) approach.

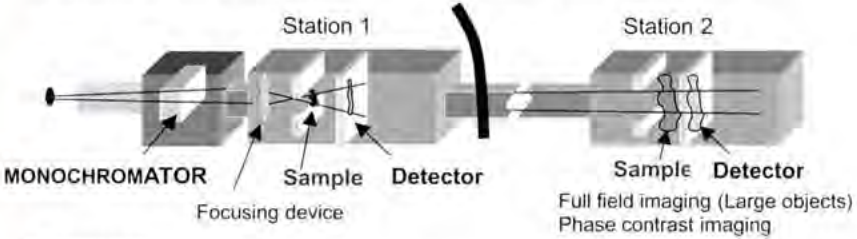

References

1 Snigirev, A., Snigireva, I., Kuznetsov, S., Schelokov, I. and Kohn, V. (1995) *Rev. Sci. Instrum.* **66**, 5486-92.

2 Wilkins, S. W., Gureyev, T. E., Gao, D., Pogany, A. and Stevenson, A.W. (1996) *Nature* **384**, 335-8.

3 Forster, E., Goetz, K. and Zaumseil, P. (1980) *Kristall und Technik* **15**, 937-45.

4 Snigirev, A. et al (1996) *Nature* **384**, 49-51. Snigireva, I. et al (2001) *E. Proc SPIE* Vol **4499**, 64-73.

DIRECT OBSERVATION OF OXYGEN MOLECULES PHYSISORBED IN A MICROPOROUS COORDINATION POLYMER

Yoshiki Kubota,[a] Masaki Takata,[b,c] Makoto Sakata,[b] Ryo Kitaura,[d] Ryotaro Matsuda,[d] Susumu Kitagawa,[d] Tatsuo Kobayashi,[e] Kouichi Kindo,[e] Yoshimi Mita,[f] Akira Matsuo,[e] Michihiro Kobayashi,[f] Ho-Chol Chang,[d] Tadashi Oszawa,[e] and Megumi Suzuki[f]
[a]Dept. of Environmental Sciences, Osaka Women's University, Osaka 590-0035, Japan; [b]Dept. of Applied Physics, Nagoya University; [c]JASRI/SPring-8; [d]Dept. of Synthetic Chemistry and Biological Chemistry, Kyoto University; [e]KYOKUGEN, [f]Dept. of Physical Science, Osaka University, Japan (kubotay@center.osaka-wu.ac.jp)

Recently, various coordination polymers with uniform ordered nanochannels were successfully synthesized by the combination of metal ions and organic molecules. Many of these compounds are found to have extremely high performance gas adsorption and are expected to be promising gas storage materials. So far, adsorbed gas molecules were thought to be trapped in the ordered nanochannels of the material. However, there is no structural evidence for the trapped gas molecule position inside the micropore. Thus, in order to determine the trapped gas molecule position and structure within the material, we have done in-situ synchrotron radiation powder diffraction experiment and revealed the formation of a one-dimensional array of gas molecules along the nanochannels by the MEM/Rietveld analysis.

The sample used in the present study is $[Cu_2(pzdc)_2(pyz)]_n$ (pzdc=pyrazine-2,3-dicarboxylate, pyz=pyrazine), which has a pillared layer structure with one-dimensional nanochannels with dimensions of about 4 x 6 A (CPL-1:coordination ploymer 1 with pillared layer structure). The synchrotron powder diffraction data was collected by the large Debye-Scherrer camera installed at SPring-8 BL02B2. The powder sample was sealed in glass capillary. The gas import tube is attached to the goniometer head to fill O_2 gas in capillary. The gas adsorption is controlled by lowering the temperature not by the gas pressure. The data measurement was carried out from 300K to 90K under 80kPa O_2 pressure. The fundamental crystal structure of CPL-1 had been reported by single crystal X-ray structure analysis. The powder diffraction pattern from 300K to 150K is almost the same with that of the reported structure. However, we investigated the dramatic changes of diffraction pattern at 130K which should be due to the O_2 molecule adsorption. In the first Rietveld analysis of the 90K data, we started the analysis with the fundamental structure of CPL-1 without assuming O_2 molecules. The reliability factors based on the powder pattern, R_{WP} and the integrated intensities, R_I were 18.5% and 54.2%, respectively. However, the MEM charge density visualized the density like O_2 molecules in the middle of the nanochannels. According to the MEM charge density, we determined the structure model of the CPL-1 adsorbing O_2 gas molecule. The R_{WP} and R_I for the Rietveld analysis with the final structure model were improved to be 2.1% and 3.9%, respectively. In the MEM charge density, the dumbbell shaped electron distribution was clearly observed in the middle of the nanochannels. The charge of the distribution was estimated to be almost 16e indicating no charge transfer from the O_2 molecule to CPL-1, which means O_2 gas was physisorbed to CPL-1. And, we found adsorbed O_2 molecules form one-dimensional array along nanochannels. The details of the determined structure and novel characteristic magnetic property caused by O_2 adsorption will be presented.

THE SELF-ASSEMBLED STRUCTURE OF A 2,6 DI(ACYLAMINO)-PYRIDINE: FORMATION THROUGH N-H....N and N-H...O=C INTER MOLECULAR INTERACTIONS

E. Marfo-Owusu and T. Kato

Department of Chemistry and Biotechnology, School of Engineering, The University of Tokyo, Hongo, Bunkyo-ku, Tokyo 113-8656, Japan (emmanuel@chembio.t.u-tokyo.ac.jp)

The 2,6-di(acylamino)pyridines (hereafter, nAPys, where n = 1,2,3,...,5) form self-assembled structures through intermolecular hydrogen bonding network. Knowledge of the hydrogen bond patterns associated with particular donor and acceptor functional groups can be used to synthesize new functional materials of interest. Presently, as part of an initial approach, our research team is employing this concept to investigate the intermolecular hydrogen-bonded network in the nAPys through X-ray single crystal diffraction studies; in order to employ the knowledge to prepare supramolecular complexes of nAPys with alkoxybenzoic acids (hereafter, xOBA) and investigate the single crystal complexes by X-ray diffraction studies. These complexes have potential usefulness for generation of novel materials.

In the present study, we have examined the self assembled structures of nAPys. It was observed that 3APy self assembles through N-H....N and N-H...O=C intermolecular interactions and forms a web-like pattern different from the other nAPys. Interestingly, N-H...N interaction was observed only in 3APy and not in other nAPys. The structural studies revealed that the unique packing modes of the rigid pyridine moiety and flexible alkyl chains contribute significantly to the hydrogen bonded network observed in 3APy. In this poster presentation, the self-assembled structure of 3APy will be exhibited.

Wednesday August 13

AsCA'03/Crystal-23

ABSTRACTS

ORAL SESSIONS

SYSTEMATIC APPROACHES FOR MEMBRANE PROTEIN STRUCTURE DETERMINATION

Ben Hankamer,[a] Rosalba Rothnagel,[a] Alasdair McDowall,[a] Geoff Ericksson,[b] Francis Clark,[b] Jasmine Banks,[b] Bernard Pailthorpe,[b] Charles Sennoga,[c] Andrew Heron,[c] John Seddon,[c] Richard Templer,[c] and David Crout[d]

[a]Institute of Molecular Bioscience, University of Queensland, St Lucia Campus, Brisbane QLD 4072, Australia; [b]Advanced Computational Modelling Centre University of Queensland, St Lucia Campus, Brisbane QLD 4072, Australia; [c]Department of Chemistry, Imperial College London, London SW7 2AY, UK; [d]Department of Chemistry, Warwick University, Coventry CV4 7AL, UK (b.hankamer@ic.ac.uk)

One of the great challenges of structural biology is to increase the rate of producing high-resolution structures of membrane proteins. Membrane proteins form the responsive interface between the cell and the outside world and include specific receptors, signal transducers, channel forming proteins, active transport pumps, electron transport systems and a wealth of other enzymes. The current rate-limiting step in membrane protein structure determination is high quality 2D and 3D crystal production for electron and X-ray crystallography. The development of new approaches for high-resolution structure determination will be described. These include:

1) Single particle analysis: Automation of the new NANO Cryo-EM facility.
2) 2D monolayer crystallization: Production of synthetic lipids for crystallization of His-tag proteins and glycoproteins
3) 2D bilayer crystallization: Production of large 2D crystals [eg. 1]
4) 3D cubic phase crystallization: Development of systematic cubic phase crystallization screens [2]

References

1 Hankamer, B., Morris, E., Nield, J., Gerle, C. and Barber, J. (2001) Three-Dimensional Structure of the Photosystem II Core Dimer of Higher Plants Determined by Electron Microscopy. *J Struct Biol* **135**, 262-9.

2 Sennoga, C., Heron, A., Seddon, J. M., Templer, R. H. and Hankamer, B. (2003) Membrane-protein crystallization in cubo: temperature-dependent phase behaviour of monoolein-detergent mixtures. *Acta Crystallogr D Biol Crystallogr* **59**, 239-46.

STRUCTURAL CHANGES IN AN αβ T-CELL RECEPTOR UPON LIGAND BINDING

Craig S. Clements,[a] Lars Kjer-Nielsen,[b] Anthony W. Purcell,[b] Andrew G. Brooks,[b] James C. Whisstock,[a,c] Scott R. Burrows,[d] James McCluskey,[b] and Jamie Rossjohn[a,c]

[a]The Protein Crystallography Unit Department of Biochemistry and Molecular Biology School of Biomedical Sciences Monash University Clayton, Victoria, 3168, Australia
[b]Department of Microbiology & Immunology, University of Melbourne, Victoria, 3010, Australia; [c]Victorian Bioinformatics Consortium, Monash University, Clayton, Victoria, 3168, Australia; [d]Queensland Institute of Medical Research The Bancroft Centre, Herston, Queensland, 4029, Australia
(craig.clements@med.monash.edu.au)

T-cell antigen receptors (TcRs) are heterodimeric cell-surface receptors that play a pivotal role in the cellular immune response. The TcR interacts specifically with a peptide-laden major histocompatability complex (pMHC). A human TcR has been characterized that interacts with an immunodominant epitope, FLRGRAYGL, from the Epstein-Barr virus, a ubiquitous human pathogen, in complex with HLA-B8. Despite the vast TcR repertoire, this TcR is found in up to 10% of the total T-cell population in seropositive HLA-B8+ individuals. This highly selected TcR was characterized by expressing in *E. coli*, refolding, purifying and crystallizing the receptor. In addition, the HLA-B8 has been expressed in *E. coli*, refolded with the FLRGRAYGL peptide, and shown to be functionally active. The TcR has been crystallized in complex with this pMHC. The crystals of the unliganded and liganded TcR diffract to 1.5 and 2.5 Å respectively.

A comparison of the structures reveals that upon recognising antigen, the TcR undergoes extensive conformational changes in the complementarity determining regions (CDRs), including the disruption of the canonical structures of the germline-encoded CDR1α and CDR2α loops to produce an enhanced fit with the HLA-peptide complex. In addition, engagement of the TcR combining site induces conformational changes in the TcR α constant domain thought to form part of the docking site for the TcR signaling molecule CD3ε. These findings suggest a novel structural link between TcR ligation and intracellular signaling. Further insight may be provided by the structure of the TcR bound to an HLA-B8/antagonist peptide complex.

A NEW MODE OF PORE ASSEMBLY BASED ON THE STRUCTURE OF INTERMEDILYSIN, A TOXIN SPECIFIC FOR HUMAN CELLS

Galina Polekhina,[a] Rodney K. Tweten,[b] and Michael W. Parker[a]

[a]St. Vincent's Institute of Medical Research, 9 Princes Street, Fitzroy, VIC 3065, Australia; [b]Department of Microbiology and Immunology, The University of Oklahoma Health Sciences Center, Oklahoma City, Oklahoma 73104, USA (galinap@medstv.unimelb.edu.au)

The pore-forming cholesterol-dependent toxins have been identified in numerous species from five different genera of Gram-positive bacteria, including *Clostridium*, *Bacillus*, *Streptococcus*, *Listeria* and *Arcanobacterium* [1]. Their toxicity arises from the transition of a monomeric water-soluble form to large self-associated pores in the membrane of target cells. Intermedilysin (ILY), a toxin produced by *Streptococcus intermedius*, is of particular interest due to its exclusive specificity for human cells in contrast to other related toxins and its role in deep-seated abscess formations in brain and liver [2]. Brain abscesses may give rise to meningitis. It has also been shown that ILY interacts with the protein receptor on the target cells [3] unlike other toxins that only require the presence of cholesterol in the target membrane.

We report the crystal structure of ILY that has been determined by combination of single isomorphous replacement and multiple anomalous dispersion techniques and has been refined to 2.3 Å. The structure reveals a profound bend to the rod-shaped molecule compared to the structure of the related toxin from *Clostridium perfringens*, perfringolysin O (PFO). Based on the structure of ILY and the reported fluorescent studies performed on PFO [3] we propose a new mode of pore assembly. We will offer an explanation as to why certain ions are required for stability of ILY and discuss the receptor specificity based on comparison of the structures of ILY and PFO.

References

1 Tweten, R. K., Parker, M. W. and Johnson, A. E. (2002) *Curr. Top. Microbiol. Immunol.* **257**, 15-33.

2 Nagamune, H., Ohnishi, C., Katsuura, A., Fushitani, K., Whiley, R. A., Tsuji, A. and Matsuda, Y. (1996) *Infection and Immunity* **64**, 3093-3100.

3 Ramachandran, R., Heuck, A. P., Tweten, R. K. and Johnson, A. E. (2002) *Nat. Struct. Biol.* **9**, 823-827.

HIGH-THROUGHPUT PROTEIN STRUCTURE VALIDATION ALSO FOR INTEGRAL MEMBRANE PROTEINS

W. Bret Church,[a,b] and Lawrence K. Lee[b]

[a]Molecular Biotechnology Program; [b]School of Molecular and Microbial Biosciences G08, University of Sydney, NSW 2006, Australia (b.church@biotech.usyd.edu.au)

Methods for the prediction of three-dimensional protein structures advanced over the last decade, along with the methods to assess the model validity. The Profiles-3D[1] method is suitable for assessing the validity of structures in soluble proteins and an adaptation allows its application in membrane spanning regions[2].

A program that implements and integrates both the adaptation as well as the original Profiles-3D method has been developed. Both water-soluble regions and membrane spanning regions as well as entire soluble and entire integral membrane proteins can be assessed. An integrated method can assist in the elucidation of membrane spanning domain boundaries. The program implements a novel high-speed method for calculating solvent accessible surface area. This allows efficient analysis of structures and a dedicated tool handling multiple structures permits high-throughput assessment of experimental or other sets of generated structures. 800 structures from a non-redundant data set took less than 22 minutes on a 1.2GHz PC.

Ideally, in this method each residue in the correctly folded protein scores highly. To implement the scoring scheme for such a methodology, a technique that analyses a data set of protein structures is required. The program is able to use its multiple structure handling capabilities to produce scatter plots representing environments at locations in structures or amino acid types. These analyses can assist to identify trends between different family groups, and inconsistencies between scores and correctly folded structures. The user can also create customised probability-based scoring schemes.

The application is currently running on Intel windows-based PC. The graphical user interface was created with the Microsoft foundation class library. All parameters for a calculation are retrievable and the results viewed as spreadsheets or charts as well as displayed on the three-dimensional structure with the basic built-in molecular viewer.

References

1 Bowie, J.U., Luthy, R. and Eisenberg, D. (1991) *Science* **253**, 164-170.
2 Dastmalchi, S., Morris, M.B. and Church, W.B. (2001) *Protein Sci.* **10**, 1529-1538.

CRYSTAL STRUCTURE OF PEA TOC34 - A NOVEL GTPASE OF THE CHLOROPLAST PROTEIN TRANSLOCON

Chwan-Deng Hsiao,[a] Yuh-Ju Sun,[a,b] Farhad Forouhar,[a] and Hsou-min Li[a]

[a]Institute of Molecular Biology, Academia Sinica, Taipei, Taiwan 115, ROC; [b]Institute of Bioinformatics and Structural Biology, National Tsing Hua University, Hsinchu, Taiwan 300, ROC (mbhsiao@ccvax.sinica.edu.tw)

Toc34, a 34-kDa integral membrane protein, is a member of the Toc (translocon at the outer-envelope membrane of chloroplasts) complex that associates with precursor proteins during protein transport across the chloroplast outer membrane [1-3]. Here we report the crystal structure of the cytosolic part of pea Toc34 complexed with GDP and Mg^{2+} at 2.0 Å resolution [4]. In the crystal, the Toc34 molecules exist as dimers with features resembling the ones found in a small GTPase complexed with a GTPase activating protein (GAP). Gel-filtration, however, revealed that dimeric and monomeric forms of Toc34 coexisted in phosphate saline buffer (pH 7.2) solution. Mutation of Arg 128, an essential residue for dimerization, to alanine led to the formation of only a monomeric form whose GTPase activity is significantly reduced compared to that of the wild-type Toc34. These results together with a number of structural features unique to Toc34, suggest that each monomer acts as a GAP on the other interacting monomer.

References

1 Kessler, F., Blobel, G., Patel, H. A. and Schnell, D. J. (1994) *Science* **266**, 1035-1039.
2 Seedorf, M., Waegemann, K. and Soll, J. (1995) *Plant J.* **7**, 401-411.
3 Chen, D. and Schnell, D. J. (1997) *J. Biol. Chem.* **272**, 6614-6620.
4 Sun, Y.J., Forouhar, F., Li, H. M., Tu, S. L., Yeh, Y. H., Kao, S., Shr, H. L., Chou, C. C., Chen, C., and Hsiao, C. D. (2002) *Nature Struct. Biol.* **9**, 95-100.

CHARGE DENSITY STUDY OF AN IRON NITROSYL COMPLEX

Yu Wang,[a] and J. J. Lee[b]

[a]Department of Chemistry, National Taiwan University, Taipei, Taiwan;
[b]National Synchrotron Radiation Research Center, Hsin-Chu, Taiwan
(yuwang@xtal.ch.ntu.edu.tw)

Charge density and bond characterization have been investigated on an Iron-nitrosyl dithiocarbamate complex, [Fe (NO)($S_2CNC_2H_6$)$_2$] in terms of accurate single crystal diffraction at 100K and an open-shell DFT calculation. The iron atom is five- coordinated with four sulfur and one nitrogen atoms in a square pyramidal geometry, the site symmetry is roughly C_{2v}. The iron atom is 0.6261(1) Å above the plane of four sulfur atoms, the nitrosyl group (NO) is in the axial direction perpendicular to the plane. Unfortunately, the oxygen atom exhibits positional disorder.

The complex is related to a potential free radical scavenger, this study may shine some light on how it is so via electron density distribution, especially at the iron site and at the NO group. It is known that NO ligand could be served as a radical neutral species or NO^+, a nitrosyl, or NO^-, a nitroxide group. Thus the unpaired electron can be located either at Fe or at the NO group. According to the electron density distribution based on the multipole model and on the DFT calculation, the electronic configuration of iron atom is $4s^13d^6$, therefore a Fe^I and NO^+ ligand is a nitrosyl group. In other words, the unpaired electron is mostly localized at Fe not on the NO ligand, which is consistent with the conclusion made from single crystal EPR and Moessbauer measurements. Topological analysis on the total electron density will give the bond characterization in terms of topological properties associated with bond critical points. The VSCC of Fe in this five coordinated complex is quite interesting, the detail description and its correlation to the metal ligand bond will be presented.

FINDING HYDROGEN BY SYNCHROTRON POWDER DIFFRACTION

Makoto Sakata,[a] Hitomi Sakai,[a] Eiji Nishibori,[a] and Masaki Takata[a,b]

[a]Department of Applied Physics, Nagoya University, Chikusa, Nagoya 464-8603, Japan; [b]Japan Synchrotron Research Institute, Kouto, Mikazuki-cho, Sayo-gun, Hyougo 679-5198, Japan (sakata@cc.nagoya-u.ac.jp)

It is not well established whether hydrogen can be detected by X-ray diffraction. Most work relating to finding hydrogen by X-rays is carried out using least squares refinement, which relies on only the R-factor by introducing atomic scattering factors of hydrogen. It is reasonable to expect that the nature of chemical bonding nature to hydrogen in different crystals would vary considerably. Therefore, in a rigorous sense, it may not be justified to use an atomic scattering factor for hydrogen in the least squares refinement. In the case of Cytidine ($C_9H_{13}N_3O_5$), for example, atomic positions determined by various authors agreed very well except for hydrogen[1].

Recently, a sophisticated analytical method, which is called imaging of diffraction data by the Maximum Entropy Method (MEM)[2], has been successfully applied to find hydrogen in crystals[3]. MEM does not require atomic scattering factors of any atoms. The previously analysed materials are basically ionic crystals, which should not be extremely difficult to analyse. In this work, we determined charge density distributions of hydrogen in two organic crystals - cytidine ($C_9H_{13}N_3O_5$) and monosodium L-glutamate monohydrate ($C_5H_8NO_4NaH_2O$) by analysing synchrotron powder data, collected using the large Debye-Scherrer camera installed at BL02B2, Spring-8. For cytidine, both RT and low temperature (100K) data have been analysed. It was found that finding charge densities of hydrogen in MEM maps is much easier using low temperature data. For the L-glutamate, therefore, only low temperature (92K) data were analysed.

From the MEM charge density map obtained in this study, we found that: firstly all the charge density of hydrogen can be detected in MEM maps without any ambiguities; secondly charge densities of hydrogen bonds are similar to weak covalent bond; thirdly non-hydrogen bond H shows a lobe shape charge density distribution; fourthly in cytidine, no local maxima is found for the charge density of hydrogen even at low temperature, while in the L-glutamate case, local maxima are very clearly seen. In addition to these results, very interesting charge densities of hydrogen are found for a hydrate water molecule, which does not show slightest sign of lobe shape charge density distribution. This strongly suggests that water molecules of hydrate are in disordered states occupying quite a few crystallographic sites.

References

1 Furberg, S. (1950) *Acta Cryst.* **3,** 325; Furberg, S., Petersen, C. S. and Rømming, C. (1965) *Acta Cryst.* **18,** 313; Ward, D. L. (1993) *Acta Cryst.* **C49,** 1789-92; Chen, L. and Craven, B. M. (1995) *Acta Cryst.* **B51,** 1081-97.

2 Sakata, M. and Sato, M. (1990) *Acta Cryst.* **A46,** 263-70.

3 For example, Noritake, T., Aoki, M., Towata, S., Seno, Y., Hirose, Y., Nishibori, E., Takata, M. and Sakata, M. (2002) *App. Phys. Lett.* **81**, 2008-10.

CHARGE DENSITY STUDIES OF POLYMORPHIC ANTI-ULCER AGENTS. THE APPLICABILITY OF THE ELECTROSTATIC POTENTIAL IN DRUG DESIGN

Jacob Overgaard, Mark P. Waller, and David E. Hibbs

School of Chemistry, University of Sydney, NSW 2006, Australia
(jacobo@chem.usyd.edu.au)

The electrostatic potential (EP) has been extensively employed in the prediction of a variety of condensed phase macroscopic properties from theoretical calculations, and a quantitative approach has recently been suggested based on a range of features of the EP on the molecular surface [1]. However, this method has so far been restricted to the gas-phase, thus excluding the effect of intermolecular interactions. Nonetheless, the EP is of paramount importance in the understanding of drug-receptor interactions. Thus, an experimental determination of the EP including the effects of intermolecular interactions is potentially of great use in rational drug design.

In the present work we will outline the results of a theoretical and experimental charge density (CD) study of both known polymorphs (A and B) of the histamine H_2-receptor antagonist, famotidine (see Figure) [2]. The CD is determined from a combination of X-ray and neutron diffraction data collected at 100 K, using the Hansen-Coppens multipole model [3]. We will focus on a comparison of the experimental and theoretical CDs and describe the similarities in the CDs of the two polymorphic forms of famotidine. In particular, we will discuss the observed differences in the experimental EPs of the two polymorphs, respectively, in relation to their individual abilities to act as anti-ulcer agents. This work represents the preliminary steps towards a more general description of a number of drug types using combined theoretical and experimental charge density studies.

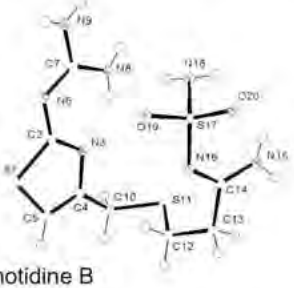

Famotidine B

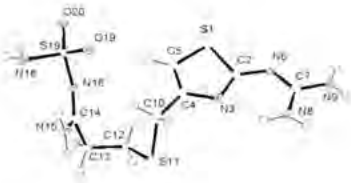

Famotidine A

References:

1 Politzer, P., Murray, J. S. (2002) *Theor. Chem. Acc.* **108**, 134-142.

2 Ferenczy, G. G., Parkanyi, L. J., Angyan, G., Kalman, A., Hegedus, B. (2000) *J. Mol. Struct. (Theochem)* **503**, 73-79.

3 Hansen, N. K., Coppens, P. (1979) *Acta Crystallogr. Sect. A* **39**, 909-921.

ELECTRON DENSITY DISTRIBUTIONS ON WEAK INTERMOLECULAR INTERACTIONS - BR···BR INTERACTIONS

Masanori Yasui,[a] Kouki Tamakawa,[a] Fujiko Iwasaki,[a] and Daisuke Hashizume[b]
[a]Department of Applied Physics and Chemistry, The University of Electro-Communications, Chofu, Tokyo 182-8585, Japan; [b]The Institute of Physical and Chemical Research (RIKEN), Wako, Saitama 351-0198, Japan
(yasui@pc.uec.ac.jp)

Intermolecular halogen-halogen contacts of which interatomic distances are shorter than the normal van der Waals contact are incorporated frequently in organic crystal structures. The geometrical features of Br···Br contacts show anisotropic characters from the CSD retrieval. In this paper, the topological analyses of the experimental electron density distributions of intermolecular Br···Br contacts are carried out to establish the nature of this type of interaction.

Crystals of 4-bromobenzamide show two modifications, one of which, α-form, has structures with linear C-Br···Br contacts (C-Br···Br=166°, Br···Br=3.49Å) and another one, β-form, has bent C-Br···Br contacts (C-Br···Br=92°, Br···Br=3.64Å). X-ray diffraction data of these modifications were collected at the SPring-8 BL04B2 beam-line with wavelength of 0.3282Å upto $\sin\theta/\lambda$ of 1.02Å^{-1} at 100K. The aspherical-atom refinements based on F^2 were carried out using the XD package[1] and converged with $R_1(F)$=0.026 (5219 reflns. with $I>1.5\sigma(I)$) and $R_1(F)$=0.022 (5879 reflns. with $I>1.5\sigma(I)$) for α- and β-form, respectively. Fig.1 shows the Laplacian maps of α- and β-form on the plane of the C-Br···Br. The topological parameters at the BCP of Br···Br interactions and intermolecular NH···O hydrogen bonds are summarized in Table 1. From these results, the Br···Br interactions are revealed to be an electro-static interaction corresponding to the dispersion force. The magnitude of Br···Br interactions can be estimated about a half of those of the NH···O hydrogen bonds according to the dissociation energy, E_{cp}, after Abramov[2].

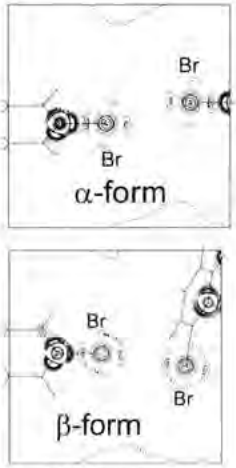

Fig. 1 Laplacian maps on the plane of C-Br···Br

Table 1 Topological parameters

	ρ (eÅ^{-3})	$\nabla^2\rho$ (eÅ^{-5})	E_{cp} (kJmol^{-1})
Br···Br			
α-form	0.085	0.913	-11.1
β-form	0.079	0.747	-7.94
NH···O (averaged value)			
α-form	0.12	2.82	-22.0
β-form	0.14	2.50	-22.9

References

1 Koritsanszky, T., Howard, S. T., Su, Z., Mallinson, P. R., Richter, T., and Hansen, N. K. (1999) *XD, Computer Program Package for Multipole Refinement and Analysis of Electron Densities from Diffraction Data*, Free University of Berlin, Berlin, Germany.

2 Abramov, Y. A., (1997) *Acta Cryst.* **A53**, 264-272.

CHARGE DENSITY ANALYSIS AND DIPOLE MOMENT ENHANCEMENT IN MNA (2-METHYL-4-NITROANILINE)

Andrew Whitten,[a] Mark Spackman,[a] Peter Turner,[b] Wim Klooster,[c] Ross Piltz,[c] and Masaru Tachibana[d]

[a]Chemistry, School of Biological, Biomedical and Molecular Sciences, University of New England, Armidale, NSW 2351, Australia; [b]School of Chemistry, University of Sydney, NSW 2006, Australia; [c]Bragg Institute, Building 58, ANSTO, PMB 1, Menai, NSW 2234, Australia; [d]Department of Physics, Yokohama City University, 22-2, Seto, Kanazawa-ku, Yokohama, 236-0027, Japan (awhitten@une.edu.au)

MNA belongs to a class of substituted benzene derivatives, which possess exceptional non-linear optical properties. Such compounds exhibit large microscopic second order non-linear susceptibilities, and lack a centre of symmetry in the solid state. Another interesting property of these compounds is the apparent enhancement of the dipole moment due to hydrogen bonding and general crystal-field effects. For MNA, *ab initio* calculations of the free molecule give values of the dipole moment of about 8.2 D,[1] while in-crystal estimates obtained from a previous charge density analysis are around 25(8) D,[2] suggesting a three-fold enhancement of this molecular property. This experimental result has been widely cited, but whether the magnitude of the dipole moment enhancement exhibited there is reasonable is of some debate because of difficulties encountered in the analysis of X-ray diffraction data for non-centrosymmetric space groups; the large experimental error associated with the value also raises questions about the ability of the multipole refinement procedure to reliably retrieve such values.

To independently verify this important observation, and hopefully to improve on the results obtained in the previous study, we are making use of experimental data that was unavailable a decade ago, including neutron diffraction data collected on the four-circle diffractometer (2TANA) at HIFAR, as well as charge density quality. X-ray diffraction data collected on the Bruker SMART 1000 CCD system at the University of Sydney, all at 100 K. We are also performing Hartree-Fock CRYSTAL98 calculations to aid in the analysis of the experimental data, and for comparison with experimental results. We will discuss the difficulty in obtaining sensible estimates of one-electron properties for non-centrosymmetric compounds from multipole refinements, and present in detail the results obtained from this study.

References

1 Daniel, C. and Dupuis, M. (1990) *Chem. Phys. Lett.* **171**, 209.
2 Howard, S.T., Hursthouse, M.B., Lehmann, C.W., Mallinson, P.R., and Frampton, C.S. (1992) *J. Chem. Phys* **97**, 5616.

HOW DO TRANSLATION FACTORS CATALYSE PROTEIN SYNTHESIS?

Anders Liljas

Molecular Biophysics, Lund University, Lund, Sweden
(anders.liljas@mbfys.lu.se)

tRNA is the adaptor in protein synthesis. The ribosome has three binding sites for tRNA, the A-, P-, and E-sites. The tRNAs bridge between the ribosomal subunits with the decoding site and the mRNA on the 30S subunit and the peptidyl transfer site on the 50S subunit.

Translation factors are needed to obtain the rate and fidelity required for protein synthesis. They catalyse protein synthesis on the ribosome. Several of the translation factors are GTPases and are structurally and functionally related. They catalyse irreversible steps in the process. Other translation factors operate in conjunction with the GTPases. Several of them bind to the tRNA binding sites on the ribosome and some of them are also tRNA mimics. Some of these tRNA mimics are EF-G, EF-P, SelB, RF1, RF2 and RRF. The range of tRNA mimicking proteins suggest that the shape similarity is not a sufficient criterion for binding to a tRNA binding site. Despite a tRNA similarity some factors bind differently to the ribosome from the tRNAs.

The GTP hydrolysis of the translational GTPases leads to an irreversible step forward in the translation process. The GTPasesare normally inactive enzymes, but at suitable states the ribosome activates their inherent capacity to hydrolyse GTP. This is done by a protein complex ($L10^*L12_4$) whose structure and function is slowly becoming understood.

EVOLUTION OF AN ORGANOPHOSPHATE DEGRADING ENZYME; A COMPARISON OF NATURAL AND DIRECTED EVOLUTION

P. D. Carr,[a] H. Yang,[a] S. Yu M[c]Loughlin,[a] J. W. Liu,[a] I. Horne,[b] X. Qiu,[b] R. J. Russell,[b] J. G. Oakeshott,[b] and D. L. Ollis[a]

[a]Research School of Chemistry, Australian National University, GPO Box 414, Canberra, ACT 2601, Australia; [b]CSIRO Entomology, Canberra, ACT 2601, Australia (pdc@rsc.anu.edu.au)

Organophosphates (OPs) are widely used pesticides both in Australia and globally. The build up of these chemicals in irrigation run-off leads to major environmental management issues. Bioremediation of water contaminated with high levels of OPs by use of enzymes overexpressed in bacteria is an attractive solution to the problem.

We present the X-ray structure of an organophosphate degrading enzyme from *Agrobacterium radiobacter* (OPDA), isolated from contaminated soils located in a cotton farming region of Australia. This structure is compared to another known organophosphate degrading enzyme (OPD) isolated in the USA from *Pseudomonus* bacterium. These enzymes have differing but overlapping substrate specificities.

In vitro directed evolution experiments were used to evolve a series of OPD mutants that had activities similar to OPDA. These mutations tended to cluster in particular regions of the protein which, in most cases, were regions where sequence differences exist between the two proteins. We attempt to explain in structural terms the significance of these regions.

CRYSTAL STRUCTURE OF GLUTAMATE-CYSTEINE LIGASE FROM ESCHERIHIA COLI B WITH SUBSTRATES

T. Hibi, M. Nakayama, H. Nii, and J. Oda

Department of Biochemistry, University of Fukui Prefectural University, Fukui 910-1195, Japan (hibi@fpu.ac.jp)

Glutamate-cysteine ligase catalyzes the ATP-dependent coupling of L-glutamate and L-cysteine to form a glutathione precursor γ-glutamylcysteine. It is the rate-limiting enzyme in glutathione biosynthesis, and the cellular level of glutathione is controlled through the negative feed-back inhibition of GCS by glutathione. GCS is one of targets of potential therapeutic agents such as a parasiticide or a drug suppressing multi-drug resistance of cancer cells.

The GCS used in this study has been isolated from *E. coli* B[1]. This procaryotic enzyme is a single polypeptide with molecular mass of 58,300, unlike the eucaryotic enzymes composed of two nonidentical subunits. However, *E. coli* and rat kidney GCS not only show similar kinetic parameters and substrate specificity but also are inhibited by glutathione[2]. The crystallographic analysis of *E. coli* enzymes will elucidate the mechanism of catalysis and the basis for feed-back inhibition and provide a framework for structure-assisted drug design for any species of GCS. We report the crystallization and structure analysis of the GCS from *E. coli* B and its complex with cysteine and ATP.

Unliganded crystals of GCS were obtained as described before[3], and complex ones were crystallized in the presence with 1 mM ATP and 5 mM L-cysteine using sodium formate as a precipitant. X-ray diffraction data of the crystal were collected at the beamline BL40B2 or BL38B1 (SPring-8, Harima, Japan). Both the crystals were found to index in rhombic lattices corresponding to space group *R*3 with unit-cell parameters $a=b=326.74$, $c=103.96$ Å and $a=b=326.72$, $c=105.01$ Å, respectively. The data of unliganded crystal were 99.8% complete to 2.8 Å resolution, and that of complex crystal were 98.9% complete to 2.8 Å resolution. The unliganded crystals of the selenomethionine substituted enzyme were used for the MAD experiments at the beamline BL41XU, collecting three data sets at different wavelength to 3.0 Å resolution. Structure determination is on going and will be presented at this meeting.

References

1 Watanabe, K., Yamano, Y., Murata, K. and Kimura, A. (1986) *Nuc. Acids Res.* **14**, 4393-4400.

2 Huang, C.-S., Moore, W. R. and Meister, A. (1988) *Proc. Natl. Acad. Sci. USA* **85**, 2464-2468.

3 Hibi, T., Hisada, H., Nakatsu, T., Kato, H. and Oda, J. (2002) *Acta Crystallogr.* **D58**, 316-318.

CRYSTALLOGRAPHIC ANALYSIS OF THE MECHANISM OF HMG-CoA REDUCTASE

Cynthia V. Stauffacher,[a] Nicklaus Steussy,[a] John W. Burgner,[a] Tim Schmidt,[a] and Victor W. Rodwell[b]

[a]Department of Biological Sciences and [b]Department of Biochemistry, Purdue University, West Lafayette, Indiana 47907, U.S.A.
(cyndy@gauguin.bio.purdue.edu)

HMG-CoA reductase (HMGR) catalyzes the first committed step in the isoprenoid biosynthesis pathway that in mammals leads to the production of cholesterol. A highly related enzyme is found in gram-positive pathogenic bacteria, and has been shown to be essential for normal bacterial growth. HMGR is a four electron oxidoreductase, using two molecules of NADPH to convert HMG-CoA to mevalonate. HMGR is the target of the highly effective statin drugs, which mimic the substrate and block the active site pocket in both the classes of the enzyme [1,2].

We have been studying the structure and mechanism of the bacterial HMG-CoA reductase in crystals which both diffract to high resolution and allow the enzyme to catalyze the reaction. Large channels through the crystal allow diffusion of substrates and the closing of a 50 residue flap over the active site during catalysis [3]. Using a slow substrate, dithioHMG-CoA, we have been able to capture a series of catalytic steps in the HMGR mechanism, including an initial "relaxed" binding state for HMG-CoA, the converted "strained" state just before CoA is released and the thiohemiacetal intermediate. These experiments have suggested an explanation why the aldehyde intermediate is not observed in the reaction, as well as an analysis of the stopped-flow kinetics results. Time and exposure experiments indicate that the thioester bond of the substrate is susceptible to breakage in the synchrotron beam, resulting in rearrangement of the substrate in the active site. Initial experiments are also being done to establish the feasibility of a time-resolved x-ray analysis of the HMGR mechanism and the inhibition with statin drugs.

References

1 Istvan, E. S. and Deisenhofer, J. (2001) *Science* **292**, 1160-1164.
2 Tabernero, L., Rodwell, V. W. and Stauffacher, C. V. (2003) *J. Biol. Chem.*: epub Mar03 213006200.
3 Tabernero, L., Bochar, D. A., Rodwell, V. W. and Stauffacher, C. V. (1999) *PNAS.* **96**, 7167-7171.

STRUCTURE AND SIGNALING IN THE EPIDERMAL GROWTH FACTOR RECEPTOR FAMILY

T. P. J. Garrett,[a] M-Z Lou,[a] N. M. McKern,[b] T. E. Adams,[b] G. O. Lovrecz,[b] R. N. Jorissen,[c] E. C. Nice,[c] A.W. Burgess,[c] and C. W. Ward[2]

[a]Walter and Eliza Hall Institute; [b]CSIRO Division of Health Science and Nutrition; [c]Ludwig Institute for Cancer Research, Parkville, Victoria 3050, Australia (tgarrett@wehi.edu.au)

Epidermal growth factor receptor (EGFR) is the cell surface receptor for EGF, a small polypeptide cytokine that stimulates proliferation in a wide variety of epithelial tissues. Upon the binding ligand outside the cell, receptors dimerise into a novel 2:2 complex which then initiates intracellular signaling via cytoplasmic tyrosine kinase domains. The EGFR family contains three other receptors, erbB2 (neu or HER-2), erbB3 and erbB4, with each member having its own identity. For example, erbB2 has no ligand and the erbB3 kinase is inactive. Thus hetero- as well as homo-dimerisation is important in this complex signaling network.

Medically, increased or aberrant signaling via these receptors is characteristic of many cancers. For example, elevated levels of receptor or ligand have been observed in tumours of the brain, head and neck, lung, pancreas and colon. Furthermore, antibodies to EGFR have been shown to inhibit growth of epithelial cell lines in the laboratory and an antibody to erbB2 is currently in clinical trials as a therapy for breast cancer

We have determined the structures of complexed and uncomplexed members of the EGFR family at near atomic resolution and these structures show that the receptors undergo a surprisingly large conformational change upon ligand binding. The structure of erbB2 also shows why it does not bind ligand and, indeed, why it does not need to. Unlike its relatives, it exists in a pre-activated state, ready to interact with potential partners. Closer comparisons of the receptor structures also reveal some more subtle differences. Twists and bends in the dimerisation domains of up to 40˚ hint that different ligands may have some fine specificity in receptor signaling.

Thus, structures of these receptor fragments provide substantial insight into the extracellular events leading to mitogenesis signaling via members of the EGFR family. However they also raise questions about the details of these events. A number of follow-up experiments have confirmed our initial hypotheses and results will be presented about a more detailed understanding of how EGFR family members interact.

SYNCHROTRON X-RAY AND MOLECULAR DYNAMICS STUDIES OF $La_{2-x}Sr_xCuO_4$ WITH x! 1/8

Nobuo Ishizawa, Kenji Suzuki, Katsumi Suda, and Douglas du Boulay

Materials and Structures Laboratory, Tokyo Institute of Technology, 4259 Nagatsuta Midori, Yokohama 226-8503 Japan (nishizaw@n.cc.titech.ac.jp)

Although the tetragonal-orthorhombic structural phase transition in the $La_{2-x}Sr_xCuO_4$ high Tc super conductors has been studied and discussed extensively since their discovery, there is still some mystery about the role played by the Sr dopant in the phase transition mechanism. In our study, the electron density distribution of $La_{2-x}Sr_xCuO_4$ with *x!* 1/8 determined at 297K using single-crystal synchrotron X-ray diffraction revealed not only the d_{x2-y2} orbital hole of Cu but also the disordered nature of the La(Sr) and O constituents, even though the crystal exhibits the archetypal K_2NiF_4 structure with tetragonal I4/mmm symmetry.

Molecular dynamics (MD) calculations were applied to examine the structural disorder in more detail. By averaging related atomic positions across the MD unit cell and across all MD time steps, calculated at 2fs intervals, the Sr and La atoms were found to vibrate harmonically about slightly displaced mean atomic coordinates, with Sr displaced by 0.02Å along the *c* axis with respect to La. In addition, four in-plane O2 atoms localized around Sr were typically displaced by a mean of 0.15Å further along <110> vectors, and the closest apical O2 atom by 0.08Å along <001>, in order to accommodate larger radii Sr cations, as shown in the figure. The directions of these O atom displacements are incompatible with those that facilitate the collective tilting mechanism of the $CuO1_4O2_2$ octahedra in the low temperature orthorhombic form. The local steric hindrance identified around Sr probably impedes the cooperative deformation of the octahedral sheet and helps to explain the experimentally observed decrease in tetragonal-orthorhombic phase transition temperature with increasing Sr content in $La_{2-x}Sr_xCuO_4$.

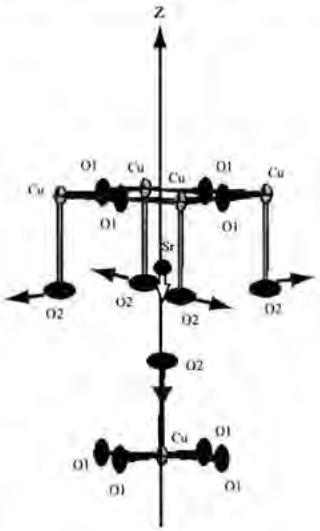

Analysis of the mean La atom positions in the MD study indicates that their equilibrium positions are slightly displaced along <110> from their ideal positions on the *c* axis, indicating that even in the tetragonal archetypal phase they favour a locally orthorhombic distortion.

CORRELATION OF METAPRISM TWIST ANGLE WITH DISEQUILIBRIUM IN CALCIUM-LEAD FLUORO-VANADINITE APATITES

Z.L. Dong and T.J.White

Centre for Advance Research of Ecomaterials, Institute of Environmental Science and Engineering, Innovation Centre, Blk 2, Unit 237, Nanyang Technological University, Singapore 637723 (zldong@ntu.edu.sg)

The synthetic vanadinites $(Pb_xCa_{10-x})(VO_4)_6(F_{2-2y}O_y)$, $0<x<9$ and $0<y<0.35$ adopt the $P6_3/m$ apatite structure with $9.7073(4) \leq a \leq 10.1179(1)$ Å and $7.0153(3) \leq c \leq 7.4021(1)$ Å. For mixed metal compounds (x ! 0) the partitioning of calcium and lead over the $A^I(4f)$ and $A^{II}(6h)$ positions is nonstoichiometric with lead preferentially sequestering to the larger A^{II} site, as determined through the refinement of powder X-ray diffraction data. High resolution electron microscopy, supported by multislice calculations, revealed that samples annealed for 10 hrs at 800°C show great disparity in Ca/Pb partitioning, with domains that are essentially calcium or lead pure co-existing at unit cell scales. Only longer sintering in excess of 2 weeks enabled the metals to order macroscopically. As annealing progresses the lattice parameters adjust first through dilation of a (within 1 week) followed by c contraction (between 1 - 2 weeks). The A^IO_6 metaprism twist angle ϕ is a sensitive measure of disequilibrium and can be used to derive ideal cell parameters from triangular anion networks such that

$$a = t\sqrt{13 - 28\sin^2\left(\frac{\phi}{4}\right) + 16\sin^4\left(\frac{\phi}{4}\right)}$$

$$c = 2\sqrt{h_{\phi=0}^2 - \frac{4t^2}{3}\sin^2\left(\frac{\phi}{2}\right)}$$

where $t = 2.729 + 0.017x$ is the triangle edge, $h_{\phi=0} = 3.576 + 0.017x$ is the metaprism height at $\phi = 0°$, and x is the stoichiometry in $(Pb_xCa_{10-x})(VO_4)_6(F_{2-2y}O_y)$.

NEGATIVE THERMAL EXPANSION IN CYANIDE-BRIDGED COORDINATION FRAMEWORK MATERIALS

Karena W. Chapman, Andrew L. Goodwin, and Cameron J. Kepert

School of Chemistry, University of Sydney, NSW 2006, Australia (chapmank@chem.usyd.edu.au)

The current interest in coordination framework materials derives from the wide range of possible functionalities that can be achieved and the exciting potential to tailor these properties towards specific applications through systematic variation of metal ion, ligand and included guest species. Reported functionalities have included those of a photochemical, mechanical, optical, electronic and magnetic nature, allowing applications in selective sorption, catalysis, sensing, switching and data storage.

We have synthesised and characterised a versatile family of cyanidebridged coordination framework materials that display negative thermal expansion (NTE) behaviour: contracting upon heating. These have diverse potential applications in high precision and low thermal shock materials (in zero thermal expansion composites) where the positive thermal expansion exhibited by the vast majority of materials may be a hindrance.

The thermal expansion in these frameworks have been monitored with variable temperature single crystal and synchrotron powder x-ray diffraction, recording coefficients of thermal expansion ($\alpha = d /dT$) up to 21 x 10^{-6} K^{-1}, more than twice that of the previous record held by zirconium tungstate.

This NTE behaviour arises from a contraction of M...M′ distances due to the increased amplitude of M-CN-M′ transverse vibrations at high temperature. This is crystallographically evident in the atomic displacement parameters of the cyanide ligand perpendicular to the M...M′ axis as shown in the single crystal structural models and powder neutron diffraction.

PHASE TRANSITION AND STRUCTURAL CHANGE OF TRICALCIUM PHOSPHATE AT HIGH TEMPERATURES UP TO 1900 K

Masatomo Yashima,[a] Atsushi Sakai,[a] Keisuke Yamamoto,[a] Yoshisato Kimura,[a] Yoshinao Mishima,[a] Masahiko Tanaka,[b] Takeharu Mori,[b] Kenji Ohoyama,[c] and Yasuo Yamaguchi[c]

[a]Department of Materials Science and Engineering, Tokyo Institute of Technology, 4259 Nagatsuta-cho, Midori-ku, Yokohama, 226-8502, Japan; [b]Photon Factory, Institute of Materials Structure Science, High Energy Accelerator Research Organization, 1-1 Oho, Tsukuba, Ibaraki, 305-0801, Japan; [c]Institute for Materials Research, Tohoku University, Katahira 2-1-1, Aoba-ku, Sendai, 980-8577, Japan (yashima@materia.titech.ac.jp).

Tricalcium phosphates [TCPs: $Ca_3(PO_4)_2$] have been of considerable interest to biologists, mineralogists, and inorganic and industrial chemists, because the TCPs are some of the most important biomaterials as is apatite. The crystal structure-property correlation is one of the most important topics in current science and technology [1]. However, for the TCP materials it has been insufficiently understood and studied, probably due to their complicated crystal structures. In this study, we investigated the α-α' phase transition of TCP using high-temperature powder neutron and synchrotron diffraction and differential thermal analysis (DTA). High-purity α-TCP was prepared by solid-state reactions from $CaHPO_4$ and $CaCO_3$. To investigate the temperature dependence of the crystal structure of TCP, neutron powder diffraction experiments were carried out at high temperatures in air with a 150-detector system, HERMES, installed in the JRR-3M reactor at the Japan Atomic Energy Research Institute, Tokai, Japan. A furnace with $MoSi_2$ heaters was placed on the sample table, and used for the neutron diffraction measurements at high temperatures [1]. The unit-cell and structural parameters of the TCP were refined by Rietveld analysis, using the RIETAN-2000 computer program. High-resolution synchrotron powder diffraction experiments were carried out for the α'-TCP at beam line 3A in the Photon Factory to confirm the space group at 1577 Celsius degree. DTA measurements were also done to determine the precise transition points and transition entropy. The α-α' transition occurs between 1458 and 1508 Celsius degree. Hysteresis is not observed between heating and cooling within the observed temperature interval of 25 Celsius degrees. Structural refinement of the α'-TCP was successfully performed by the trigonal structure with space group $P\bar{3}m$. The temperature dependence of unit-cell parameters of the TCP was determined around the α-α' phase transition point for the first time. At the α-α' phase transition point, the unit-cell parameters a, c, γ angle, and unit-cell volume discontinuously changed, indicating that the transition is of first order.

References

1 Yashima, M., (2002) *J. Am. Ceram. Soc.* **85**, 2925-2930.

IN-SITU STRUCTURE SOLUTION AND PHASE TRANFORMATION STUDIES OF DRUG POLYMORPHS USING HIGH RESOLUTION SYNCHROTRON POWDER DIFFRACTION

W I F David and K Shankland

ISIS Facility, Rutherford Appleton Laboratory, Chilton, Oxfordshire, OX11 0QX, UK (Bill.David@rl.ac.uk)

With third generation synchrotron powder diffractometers, it is possible to collect high resolution diffraction patterns on 50-100 atom structures in a matter of minutes. This enables the rapid scanning of temperature to monitor structural phase transformations and search for new drug polymorphs. We show that it is possible to study the effects of dehydration and to discover new polymorphic forms as a matter of routine. The technique is essentially the structural equivalent of a combination of differential scanning calorimetry and thermo-gravimetric analysis. Three examples will be illustrated that show (i) the subtle effects that occur with the transformation from a hemihydrate to an anhydrous form, (ii) the detailed characterisation of a drug polymorphic phase transformation and (iii) the discovery and crystal structure solution of a new crystal polymorph.

THE ROLE OF NON-MEROHEDRAL TWINNING IN SOME PHASE TRANSITIONS

Victor G. Young, Jr.,[a] Maren Pink,[b] Neil R. Brooks,[c] and William Brennessell[a]

[a]Chemistry Department, University of Minnesota, 207 Pleasant St. S.E., Minneapolis, Minnesota 55455, USA; [b]IUMSC, Chemistry Department, Indiana University, Chemistry Building A421, 800 E. Kirkwood Ave., Bloomington, Indiana 47405-7102; [c]School of Natural Sciences, Bedson Building, University of Newcstle upon Tyne, NewCastle upon Tyne NE1 7RU, United Kingdom (young@chemsun.chem.umn.edu)

We have found numerous examples of materials where the twinning is so intimate that no single twin component can be separated from the other in order to pursue a normal single-crystal, crystallographic investigation. Some of these materials are single crystals at one temperature, but exhibit phase changes associated with the onset of non-merohedral twinning at either lower [1-4] or higher [5] temperatures. A number of these examples will be presented and discussed. The interface between twin components, or composition planes, are of particular interest, because the memory of the symmetry lost in the phase transition is retained within these. Non-merohedral twins pose certain problems not experienced by single crystals or even merohedral twins. Aside from the obvious problem of indexing the reciprocal lattices of competing twin components, non-merohedral twins pose a more serious problem in the acquisition of accurate intensities from interfering reflections. The attribute of partially overlapped reflections acquired from non-merohedral twins has been a significant challenge for crystallographic programmers. However, recent advances in software now provide all the basic tools to index, integrate, and refine data acquired from non-merohedral twins.

References

1 Jazdzewski, B. A., Holland, P. L., Pink, M., Young, Jr., V. G., Spencer, D. J. E. and Tolman, W. B. (2001) *Inorg. Chem.* **40**, 6097.

2 Reger, D. L., Little, C. A., Young, Jr., V. G. and Pink, M. (2001) *Inorg. Chem.* **40**, 2870.

3 Colombo, D. G., Young, Jr., V. G. and Gladfelter, W. L. (2000) *Inorg. Chem.* **39**, 4621.

4 Schweitzer, J. W., Martinson, L. S., Baenziger, N. C., Swenson, D. C., Young, Jr., V. G. and Guzei, I. (2000) *Phys. Rev.* **B62**, 12792.

5 Choe, W., Pecharsky, V. K., Pecharsky, A. O., Gschneidner, K. A., Young, Jr., V. G. and Miller, G. J. (2000) *Phys. Rev. Let.* **84**, 4617.

MECHANISMS OF SELF-ASSEMBLY AND SWITCHING OF THE BACTERIAL FLAGELLUM

Keiichi Namba
Graduate School of Frontier Biosciences, Osaka University Protonic NanoMachine Project, ERATO, JST, & Dynamic NanoMachine Project, ICORP, JST, 3-4 Hikaridai, Seika, Kyoto 619-0237 Japan (keiichi@fbs.osaka-u.ac.jp)

The bacterial flagellum is made of a rotary motor and a long helical filament by means of which bacteria swim. The size of the bacterial cell body is about 1 μm by 2 μm, but the flagellum grows to about 15 μm long. The flagellar motor at its base rotates at around 300 Hz and drives the rapid rotation of each flagellum to propel the cell movements in viscous environments. The diameter of the flagellar motor is 30 to 40 nm, ant it consists of many proteins including membrane spanning proteins: a rotor ring, made of about 25 copies of FliF/FliG complex; about eight stator units, made of MotA/MotB complex; other parts such as the rotation switch regulator, bushing, and drive shaft, all made of different proteins. The long helical filament, which is a tubular structure with a diameter of about 20 nm, is made of 20,000 to 30,000 copies of a single protein flagellin, and yet the filament can form left-handed or right-handed helical forms and switch between these two in response to the twisting force produced by quick reversal of the motor rotation. This allows bacteria to alternate their swimming pattern between running and tumbling, which is essential for their tactic behavior. The flagellum also has a short, highly curved segment that connects the motor and the helical propeller, and this segment is called hook. Its bending flexibility makes it function as a universal joint, while the filament is relatively more rigid to work as a propeller. There is a very short segment called the hook-filament junction, which is made of HAP1 and HAP3. This junction is thought to play a mechanical buffer to connect the two mechanically distinct structures. The flagellum is constructed through various self-assembly processes, in which all the axial structures growing towards the cell exterior are constructed by the flagellar component proteins translocated from the cytoplasm to the distal end of the growing structure, where three cap complexes help efficient self-assembly of these proteins in different stages.

We have been trying to visualize the structure of the flagellum in atomic detail to understand how it self-assembles and works. We solved crystal structures of core fragments of the flagellar axial component proteins by X-ray crystallography. X-ray fiber diffraction gave high-resolution structural information. Electron cryomicroscopy also visualized the structures of the filament, cap and cap-filament complex. All these structures present interesting implications for the function of each molecule, demonstrating the importance of dual nature of protein molecules, flexibility and precision.

Thursday August 14

Biological Structure Workshop

ABSTRACTS

ORAL SESSIONS

CELL FREE PROTEIN SYNTHESIS AND STRUCTURAL/FUNCTIONAL PROTEOMICS

Shigeyuki Yokoyama,[a,b,c] and Takanori Kigawa [a]

[a]RIKEN Genomic Sciences Center; [b]RIKEN Harima Institute at SPring-8; [c]Department of Biophysics and Biochemistry, Graduate School of Science, The University of Tokyo (yokohama@biochem.s.u-tokyo.ac.jp)

The RIKEN Institute has started the Structural Genomics/Proteomics Initiative (RSGI) (http://www.rsgi.riken.go.jp) at the Genomic Sciences Center (GSC) and the Harima Institute at SPring-8. RSGI is now integrated into the Japanese national project, National Project on Protein Structural and Functional Analyses, which studies both structures and functions of proteins in selected biological systems. We have been determining the three-dimensional structures of proteins of sequence families and analyzing molecular and cellular functions of these proteins in order to establish the structure-function relationships. Key technologies are essential to conduct the research in a high-throughput way. In particular, cell-free protein synthesis is highly suitable for high-throughput preparation and screening of protein samples for structural proteomics.

Proteins are expressed from libraries of genes/cDNAs by cell-free protein synthesis methods and/or conventional recombinant methods. In particular, cell-free protein synthesis is highly suitable for high-throughput preparation and screening of protein samples for structural proteomics. The system may produce proteins directly from PCR-amplified linear DNA fragments, requiring no cloning procedures. Hundreds of proteins and protein domains can be expressed from cDNA clones within a day. By using the dialysis method developed by Professor A. Spirin, production of proteins has reached the level of milligram quantities. The system is useful to assess the solubility, productivity, and structural stability of proteins and thus practical for selecting protein samples for larger scale production. ^{1}H-^{15}N HSQC spectra are measured to screen the domain/proteins, suitable for structure determination. His tag removal, changes in domain boundary, and optimization of the solvent condition may improve NMR spectra. After the screening, the selected "excellent" proteins are prepared by cell-free method as labeled protein samples, the uniformly [^{13}C, ^{15}N]-labeled proteins for NMR structure determination. Selenomethionine substituted proteins for X-ray crystallography are also prepared by cell-free method[1].

Reference

1 Kigawa, T., Yamaguchi-Nunokawa, E., Kodama, K., Matsuda, T., Yabuki, T., Matsuda, N., Ishitani, R., Nureki, O. and Yokoyama, S. (2002) *J. Struc. Func. Genomics* **2**, 29-35.

A STRUCTURAL GENOMICS APPROACH TO TUBERCULOSIS

Edward N. Baker, Vickery L. Arcus, Kristina Backbro, Graeme L. Card, Jodie M. Johnston, Moyra Komen, Nayden Koon, Simon Li, Andrew A. McCarthy, Rochelle J. Ramsay, Miriam L. Sharpe, and J. Shaun Lott

School of Biological Sciences, University of Auckland, Auckland, New Zealand (ted.baker@auckland.ac.nz)

The availability of ever-increasing numbers of complete genome sequences is revolutionising the biological sciences. A challenge now in this "genomic revolution" is to add value to the sequence data by focusing on the structure and function of gene products. Current initiatives in structural genomics have a number of objectives, both structural and functional, including the discovery of new folds, determination of representative structures for all protein families, discovery of function from structure, and the characterisation of potential drug targets.

We are participants in a worldwide structural genomics consortium focused on *Mycobacterium tuberculosis*, the cause of TB, and one of the world's most devastating pathogens. Around 3 billion people die annually from the disease. Athough drugs exist, resistance is rising and treatment is complicated by the unusual nature of the organism, with its dense, waxy cell wall, and its ability to persist in a dormant state in the lung for long periods.

The TB Structural Genomics Consortium [1] has central facilities for the benefit of all participants, but individual labs pursue their own objectives, with coordination to try to avoid overlap. Our focus is on two types of target, (a) enzymes from key biosynthetic pathways which are potential drug design targets, and (b) proteins of uncertain or unknown function that are implicated in key aspects of TB biology. In the first category we have chosen enzymes involved in the biosynthesis of essential amino acids and of menaquinone and thiamin. In the second category we focus on proteins of unknown function that are implicated by microarray experiments either in antibiotic resistance or in the hypoxic response (and possibly persistence).

The approaches taken in our laboratory to cloning, expression, purification, crystallization and structure determination will be reviewed. The major bottlenecks to date have been in obtaining soluble expression and in crystallization, and we are reviewing our approaches in both these areas. So far from about 100 genes cloned we have 9 protein structures, with more to come. The solved structures include several proteins of unknown function, two others that appear to be good drug targets, and one protein whose structure suggests that it is mis-annotated in this and other genomes.

References

1 TB Structural Genomics Consortium: See http://www.doe-mbi.ucla.edu/TB.

STRUCTURAL GENOMICS OF NOVEL MACROPHAGE PROTEINS ASSOCIATED WITH INFLAMMATORY DISEASE AND CANCER

Pawel Listwan,[a,c] Nathan Cowieson,[a] Anna Aagaard,[a,c] Robert Serek,[a] Carmel Walsh,[a] Timothy Ravasi,[a,c] Christine Wells,[a,c] Thomas Huber,[b] David Hume,[a,c] Jenny Martin,[a,c] and Bostjan Kobe[a,c]

[a]Department of Biochemistry and Molecular Biology, and Institute for Molecular Bioscience, University of Queensland, St.Lucia QLD 4072, Australia;
[b]Department of Mathematics, University of Queensland, St. Lucia QLD 4072;
[c]CRC for Chronic Inflammatory Diseases (listwan@uq.edu.au)

Most of the potential pathogens that attempt to invade a mammalian cell fail at the very first stage due to the remarkable effectiveness of innate immunity. The presence of the potential pathogens is detected via receptors that recognise generic non-mammalian structures including cell wall components including lipopolisaccharides, peptidoglycans, lipotechoic acids and microbial DNA [1]. The first line of defense is the macrophage, which comprises 15-20% of the cells in the most organs, and is particularly abundant at the routes of pathogen entry such as lung, skin, gut and genitourinary tract [2]. When the potential pathogen is recognised, the macrophage engulfs and attempts to destroy the foreign organism. The knowledge of regulation of macrophage function will form the basis of two classes of therapeutics. Amplification of the toxic function of macrophages to destroy foreign organisms or tumor cells more effectively is one option, the other being the selective suppression of some components of the macrophage activation response. These then can be used to treat conditions like septicaemia and toxic shock, arthritis, atherosclerosis and other chronic inflammatory diseases the other one.

To define the molecular functions of proteins with roles in macrophages, we set out to characterise them structurally using X-ray crystallography. We identify proteins with roles in macrophages through expression profiling using microarray technology. We select and prioritise the proteins for structural analysis according to a number of criteria such as anticipated insight into function and feasibility for structure determination. We have developed protocols for cloning, expression and crystallography that can be adapted for high-throughput approach. To the best our knowledge, this project is the first structural genomics effort in Australia, and the microarray-to-structure pipeline is unique among the structural genomics initiatives worldwide. Our initial list of 40 proteins resulted in 7 soluble proteins, 2 targets are currently in crystallisation trails and one is ready for MAD data measurement. Currently we are optimising this system and here we present our strategy for the selection, prioritisation, cloning, expression and crystallisation of a number of protein targets.

References

1 Hoffman, J.A., Kafatos, F.C., Janeway, C.A., And Ezekowitz, R.A. (1999) Phylogenetic perspectives in innate immunity, *Science* **284**, 1313-1318.
2 Gordon, S., and Hume, D. A. (1986). Localization and function of tissue macro-phages, *Ciba FoundSymp* **118**, 54-67.

ELECTRON CRYOMICROSCOPY OF VIRUS PARTICLES AT SUB-NANOMETER RESOLUTION

Wah Chiu,[a] Z. Hong Zhou,[b] Matthew L. Baker,[a] Wen Jiang,[a] Joanita Jakana,[a] Matthew Dougherty,[a] Brian R. Bowman,[c] Florante A. Quiocho,[c] and Frazer J. Rixon[d]

[a]National Center for Macromolecular Imaging, Baylor College of Medicine, Houston, TX 77030, USA; [b]University of Texas Houston Medical School, Houston, TX 77030; [c]HHMI, Baylor College of Medicine, Houston, TX 77030; [d]MRC, Institute of Virology, Glasgow, G11 5JR, Scotland, UK (wah@bcm.tmc.edu)

Electron cryomicroscopy can resolve three-dimensional structures of large, icosahedral virus particles at sub-nanometer resolution (7-9 Å). At this resolution, we can clearly identify long helices and recognize beta sheets. A combined use of bioinformatics, x-ray crystallography of individual components together with the medium resolution structure of the whole virus can enable us to derive pseudo-atomic model of the virion. We will demonstrate this approach with the human herpesvirus capsid.

The herpesvirus capsid is made up of four proteins (VP5, VP26, VP23 and VP19C) with a diameter of 1250 Å and a total mass of 0.2 billion daltons. The three-dimensional structure of the intact capsid has been determined at 8.5-Å resolution by electron cryomicroscopy. The crystal structure of the upper domain of VP5 has been recently solved. There is an excellent match of the secondary structure elements in the upper domain of VP5 between the crystal structure and the electron cryomicroscope map. The helix bundle in the middle domain of VP5 has been found to be structurally homologous to annexin domain. These helices are located at domains that undergo conformational changes during capsid assembly and DNA packaging. The lower domain of the VP5 forms a floor linking the adjacent capsomere subunits responsible for the stability of the capsid in its mature state. With all the structural and chemical informatics of the VP5, we can conclude that the VP5 is made up of two new folds and one old fold to form the 149kD polypeptide. The graphical segmentation of the triplex from the electron cryomicroscopy map has shown the unique spatial arrangement of the two copies of VP23 and one copy of VP19C. The arrangement of this heterotrimer at the local 3-fold positions accounts for the asymmetric interactions with adjacent capsid components and the unusual co-dependant folding of its subunits.

Acknowledgements: This research has been supported by NCRR and NIAID.

CATCHING CATALYSIS IN THE ACT: PROBING ENZYME MECHANISMS USING SINGLE CRYSTAL MICROSPECTROPHOTOMETRY AND X-RAY CRYSTALLOGRAPHY

Arwen R. Pearson and Carrie M. Wilmot

Biochemistry, Molecular Biology and Biophysics, The University of Minnesota, 6-155 Jackson Hall, 321 Church St SE, Minneapolis, MN 55455, USA, (pears079@umn.edu)

Traditionally X-ray crystallography has provided important insights into the mechanisms of enzyme catalysis. However, X-ray structures often represent reaction starts, endpoints or kinetic deadends, and are not direct visualizations of reaction intermediates formed during turnover. The marriage of spectroscopic techniques and crystallography in the development of single crystal microspectrophotometers has revolutionised the field of structural enzymology [1,2].

Many enzymes have been shown to be catalytically active in the crystalline state and, if there are no major conformational changes associated with catalysis, will often remain crystalline during turnover. If an enzyme reaction involves a chromophore, either as a cofactor or substrate, single crystal microspectrophotometry can be used to monitor the reaction in the crystal. When an intermediate of interest is observed to accumulate in the crystal, it can be flash frozen in a cold nitrogen stream for X-ray structure determination.

I will present an overview of the commercially available 4DX system [3-5], as well as methods used in our laboratory to trap reaction intermediates of methylamine dehydrogenase for structural studies.

References

1 Hajdu *et al.* (2000) *Nature Structural Biology* **7** 1006-1012
2 Wilmot *et al.* (2002) *Met. Enzymol.* **353** 301-318
3 Hadfield & Hajdu (1993) *J. Appl. Cryst.* **26** 839-842
4 Sjögren *et al.* (2002) *J. Appl. Cryst.* **35** 113-116
5 http://www.4dx.se/spectrop.htm

STRUCTURE MODELLING AND VALIDATION

T. Alwyn Jones, Mark Harris, and Gerard J. Kleywegt

Department of Cell and Molecular Biology, Uppsala University, BMC, Box 596, SE- 751 24 Uppsala, Sweden (alwyn@xray.bmc.uu.se)

The recent developments in computer hardware have greatly benefited crystallography in general, and molecular modelling in particular. I will present my most recent developments in the use of secondary structure templates during map interpretation as implemented in the program O [1], and our development of web-based systems of interest to the crystallographic community. The latter include MOLRAY [2], X-TRACK [3] and EDS (to be published, 2003, I hope).

Model coordinates are usually perceived as the final result of a crystallographic experiment. Unfortunately they suffer from a number of inherent problems that are best overcome my direct visualization of the structure with the experimental electron density. This can only be accomplished if the experimental data (the so-called structure factor amplitudes) are also deposited at the public data banks. We have calculated electron densities for all structures at the PDB that also have structure factors deposited. They are made available to users via the world-wide-web, together with derived goodness-of-fit indicators, via the Uppsala Electron Density Server, EDS (http://fsrv1.bmc.uu.se/eds/).

EDS is also useful as a new kind of structure validation resource. Without the diffraction data one is restricted to stereochemical-based indicators that compare a particular structure with expectations based on the analysis of other structures, one's own chemical and biological knowledge, or empirical formulae. Even so, such indicators will often recognize a sloppily refined structure. However, only if an electron density map is available can one properly assess what is wrong and what is more-or-less correct in the deposited model.

References

1 Jones, T. A., Zou, J-Y., Cowan, S. W. and Kjeldgaard, M. (1991) *Acta Crystallographica*, **A47,** 110-119.

2 Harris, M. and Jones, T. A. (2001) *Acta Crystallographica*, **D57**, 1201-1203.

3 Harris, M. and Jones, T. A. (2002) *Acta Crystallographica*, **D58**, 1889-1891.

THE PROTEIN DATA BANK AND STRUCTURAL GENOMICS

Helen M. Berman[a]

Protein Data Bank; Research Collaboratory for Structural Bioinformatics, [a]Rutgers, the State University of New Jersey, Department of Chemistry, 610 Taylor Road, Piscataway, NJ 08854-8087 USA (berman@rcsb.rutgers.edu)

The Protein Data Bank (PDB; http://www.pdb.org/) is involved in several aspects of structural genomics. The PDB developed and currently maintains the Target Registration Database (TargetDB; http://targetdb.pdb.org/), organizes the data dictionaries that will define the specification for the exchange and deposition of data with the structural genomics centers (http://deposit.pdb.org/mmcif/), and creates and maintains software tools to capture data from standard structure determination applications (http://deposit.pdb.org/software/). Our progress in these efforts will be described.

The PDB is supported by funds from the National Science Foundation, the Office of Biology and Environmental Research at the Department of Energy, and two units of the National Institutes of Health: the National Institute of General Medical Sciences and the National Library of Medicine.

Friday August 15

Biological Structure Workshop

ABSTRACTS

ORAL SESSIONS

CASSIOPEIA – A PROGRESS REPORT FROM THE DEVELOPMENT OF FIVE BEAM-LINES AT THE MAX SYNCHROTRON LABORATORY

Anders Liljas

Molecular Biophysics, Lund University, Lund, Sweden
(anders.liljas@mbfys.lu.se)

In a Danish – Swedish collaboration involving many scientists, a new data collection facility has been built up at the synchrotron laboratory at Lund University, MAX. The facility is using the MAX-II storage ring run at 1.5 GeV, where a 3.5 T multipole wiggler provides X-rays of high intensity around 1Å wavelength for the Cassiopeia project. The beam is split into three main directions. The middle beam is used for a MAD station and the two beams on the sides are used for two stations each. The two front stations use diamond monochromators in the Laue mode and the back stations are using Bragg monochromators. The four side stations have essentially fixed wavelengths around 1Å. Details of the project as well as the initial experiences will be reported.

BUILDING A USER-FRIENDLY BEAMLINE

Aina Cohen, and Paul Ellis

Structural Molecular Biology, Stanford Synchrotron Radiation Laboratory, SLAC, MS 69, 2575 Sand Hill Road, Menlo Park, CA 94025, USA (acohen@slac.stanford.edu) (ellis@ slac.stanford.edu)

A user-friendly beamline is one that gives visiting researchers the ability to get maximum value from their synchrotron visit. This means that this beamline will let them conduct a wide variety of experiments as rapidly and easily as possible. The protein crystallography group at SSRL has been working toward this goal in two ways: by building new beamlines optimised for the experiments that users want to do, and by implementing new instrumentation, computers, control systems and software to take maximum advantage of existing stations.

This talk will focus on the expectations of synchrotron users and the ways in which beamline builders can address them. Topics will include the use of advanced control systems to give fixed-wavelength wiggler sidestations MAD and SAD capability, automated screening with a robotic crystal mounting system, fluorescence analysis for SAD and MAD, and some of the new techniques being exploited at SSRL, particularly derivatising with quick soaks in high concentration salts, krypton and xenon pressurisation, SAD phasing, and using low energy x-rays to maximise anomalous signal.

Acknowledgements: SSRL operations are funded by DOE BES, and the SSRL Structural Molecular Biology program by DOE BER, NIH NCRR BTP and NIH NIGMS. The JCSG is funded by the Protein Structure Initiative of the National Institutes of Health, National Institute of General Medical Sciences.

NEW BEAMLINES FOR MACROMOLECULAR CRYSTALLOGRAPHY

Janet L. Smith,[a] Robert F. Fischetti,[b] L. E. Berman,[c] W. Diete,[d] R. Signorato,[d] R. Benn,[b] S. Stepanov,[b] R. Sanishvili,[b] S. Xu,[b] A. Urakhchin,[b] O. Makarov,[b] and W. W. Smith[b]
[a]Dept. of Biological Sciences, Purdue University, West Lafayette, IN 47907 USA; [b]Biosciences Division, Argonne National Laboratory, Argonne, IL 60439 USA; [c]National Synchrotron Light Source, Brookhaven National Lab, Upton, NY 11973 USA; [d]ACCEL Instruments GmbH, Friedrich Ebert Str. 1, 51429 Bergisch-Gladbach, Germany (smithj@purdue.edu)

X-ray crystallography applied to current biological problems is entirely dependent on synchrotron radiation. A greatly improved success rate for biological diffraction experiments with synchrotron radiation transformed the practice of macromolecular crystallography in the 1990s. Today, the vast majority of crystal structures published or deposited in the PDB are determined with data from synchrotron X-ray sources. Technologies large and small contribute to the improved success rate. Compared to 1993, today's synchrotron sources produce X-ray beams that are brighter, more parallel and more stable; today's beamlines are more numerous, user friendly and accessible; today's detectors are faster, more sensitive and well matched to the brighter sources; and today's cryoprotected samples travel more safely and withstand greater radiation doses.

Multiwavelength anomalous diffraction (MAD) is the most frequently employed method of phase determination for structures that are not accessible to molecular replacement. Of all biological diffraction experiments, MAD places the greatest demands on a synchrotron beamline. The beam must be highly monochromatic, stable in position and energy, and rapidly tunable. Although improvements in synchrotron beams, beamline optics and sample stability have made MAD accessible to most crystallographic problems, experimental design still must be done carefully, with an understanding of the likeliest sources of error.

Undulator sources at 3rd-generation synchrotrons are best known for their brightness. However, crystals of biological macromolecules are radiation sensitve, even when frozen, and features beyond simple brightness account for the success of 3rd-generation undulator sources for this experiment. Bright, stable, small, parallel undulator beams are ideal for beamlines that must be robust to changes in beam size, energy and focus. To exploit the special properties of the undulator source, especially for MAD experiments, we are developing a new crystallography facility (GM/CA CAT) at the Advanced Photon Source (APS). Two beamlines will be based on the APS dual canted-undulator geometry, which incorporates two independent, hard X-ray devices in one straight section. The particle beam trajectory through the devices introduces a 1-milliradian horizontal separation between the two X-ray beams. The novel beamline design will provide a 500-mm separation between the beams at the first sample position. A pair of adaptive bimorph mirrors will focus each beam. Beamline controls based on EPICS and Blulce will provide automated beamline setup, and sample mounting and centering. The GM/CA CAT project is sponsored by the National Institute of General Medical Sciences (GM) and the National Cancer Institute (CA) of the US National Institutes of Health for their grantees and the biological research community.

BIOLOGICAL APPLICATIONS AT THE AUSTRALIAN SYNCHROTRON FACILITY

Jose Varghese

CSIRO Health Sciences and Nutrition, 343 Royal Pd. Parkville, Victoria 3052, Australia (Jose.Varghese@csiro.au)

First light at the new Australian synchrotron radiation source, to be located near the Monash University Campus in Melbourne, will appear in 2007. While design work on the machine facility and building have been finalised, planning for the beam-lines is ongoing and offers opportunities for the Australian biological sciences unprecedented access to high brilliance light ranging from the infrared to hard X-rays. This facility will be a great boost to structural biologists who represent the largest single user community. However this facility will also enable biologists to have access to a number of other techniques like circular dichromism spectra, small angle solution scattering, fluorescence spectroscopy, micro probes, biological and medical imaging, radiology, surface scattering, X-ray microscopy and general spectroscopy. Proposals for beam-lines that will support these techniques will be discussed, and the applications to biological sciences that this infrastructure will enable shall be presented.

Thursday August 14

Sagamore XIV

ABSTRACTS

ORAL SESSIONS

BONDING EFFECTS IN LARGE METAL CLUSTER MOLECULES

Piero Macchi, and Angelo Sironi

Dipartimento di Chimica Strutturale e Stereochimica Inorganica, Università di Milano, via Venezian 21 20133, Milano, Italy (piero.macchi@unimi.it)

The chemistry of medium and high nuclearity transition metal clusters [1] is particularly intriguing because of the bonding mechanism that characterizes the metal cages, somewhat intermediate between that of simple metal bonded molecules and that of bulk metals themselves.

In this context, our experimental and theoretical studies on some molecules of general formula $[M_6(CO)_{16-n}]^{-2n}$ (M = Co, Rh; n = 0-2) were carried out [2] with the intent of characterizing the source of stabilization for the cluster cages and the role of different ligands or stereochemical arrangements. The comparison with dimeric species previously studied [3] allows a generalization of the bonding mechanisms.

Moreover, we have investigated the changes occurring upon introducing interstitial species (like hydrides) in the metal cavities. A comparison with simple metal hydrides and metal-metal bonds supported by hydrides is proposed.

References

1 Mingos, D. M. P. and Wales, D. J. *Introduction to cluster chemistry*; Prentice-Hall, London, 1990.

2 Macchi, P., Garlaschelli, L., Sironi, A., work in progress.

3 (a) Macchi, P., Proserpio, D. M. and Sironi, A. (1998) *J. Am. Chem. Soc.* 120, 13429; (b) Macchi, P., Garlaschelli, L. and Sironi, A. (2001) *J. Am. Chem. Soc.* 124, 14173.

EXPERIMENTAL RESULTS ON COUPLED ANALYSIS OF SPIN AND CHARGES DENSITIES OF Y AND Gd COMPLEXES

N. Claiser,[a] B. Gillon,[b] M. Souhassou,[a] C. Lecomte,[a] N. K. Hansen,[a] Y. Pontillon,[c] A. Caneschi,[d] D. Gatteschi,[d] C. Carbonera,[d] A. Bencini,[d] A. Cousson,[b] and E. Lelièvre-Berna[e]
[a]L.C.M.3B., UMR CNRS 7036, Faculté des Sciences, BP 239, 54506 Vandoeuvre-lès-Nancy, France; [b]Laboratoire Léon Brillouin, CEA-CNRS, Centre d'Etude de Saclay, 91191 Gif/Yvette, France; [c]DRN/DEC, Centre d'Etudes Nucléaires de Grenoble, 17 rue des Martyrs, 38054 Grenoble Cedex 9, France; [d]Department of Chemistry, University of Florence, Via Maragliano 77, 50144 Firenze, Italy; [e]Institut Laue-Langevin, 6 rue Jules Horowitz, BP 156, 38042 Grenoble Cedex 9, France (claiser@lcm3b.uhp-nancy.fr)

Within the vast field of molecular magnetism, we have studied two complexes in which the semiquinoato radical (DTBSQ=3,5-di-tertbutyl- semiquinonate, S=1/2) coordinates a heavy atom (Yttrium, S=0 or Gadolinium, S=7/2). Two $HBPz_3$ (hydrotrispyrazolylborate) complete the coordination sphere [1]. On the basis of the experimental electron and spin densities, our aim was to highlight the interactions at the microscopic level that play an important role in the magnetic behaviour observed in these two complexes.

The total electron density, obtained by a high resolution X-ray diffraction experiment, and the spin density, obtained by a polarised neutron diffraction experiment, were determined on the two complexes: Y-SQ and Gd-SQ. The topological analysis of the total electron density [2, 3] was used to characterise quantitatively the interatomic interactions, particularly between the ligands and the central ion. This method gives also access to the net atomic charges, useful for the comprehension of the charge transfer inside the complexes. In this study, we will present the experimental spin density distribution and the topological properties of the electron density in the two complexes and confront them to the DFT calculations results.

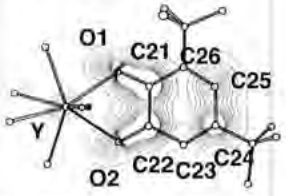

Fig. 1: Projected spin density induced at 1.9 K under 9.5 T on the semiquinoato ring plane of Y-SQ. Contours: ±0.005 with steps of 0.010 $m_B/Å^2$.

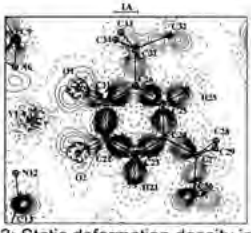

Fig. 2: Static deformation density in the semiquinoato plane of Y-SQ. Contours of 0.05 $eÅ^{-3}$: positive (solid), negative (short dashed) and zero (long dashed).

References

1 Dei, A., Gatteschi, D., Pécaut, J., Poussereau, S., Sorace, L. and Vostrikova, K. (2001) *C.R. Acad. Sci. Paris,* **Chemistry 4**, 135-141.
2 Bader, R. F. W. (1990) *Atoms in molecules: a quantum theory*. The International Series Monographs in Chemistry. Oxford Clarendon Press.
3 Souhassou, M. and H. Blessing, R. (1999) *J. Appl. Cryst.* **32,** 210.

SCATTERING FACTOR CALCULATIONS AND DISPERSION CORRECTIONS FOR HEAVY ATOMS

C. T. Chantler

School of Physics, University of Melbourne, Parkville, Vic 3010, Australia
(chantler@ph.unimelb.edu.au)

Reliable knowledge of the complex X-ray form factor and the photoelectric attenuation coefficient is required for crystallography, deformation density bonding studies and refractive index studies. Dispersion corrections are important in DAFS, MAD analyses, and XAFS. Discrepancies between currently used theoretical approaches of 200% exist for numerous elements from 1 keV to 3 keV X-ray energies, and at higher energies these discrepancies can persist at the 10% level or more. Recent tabulations [1] improve upon the theoretical uncertainty in some of these regions by a factor of 10 and reduce the error of this approach to below one standard deviation. Recent experimental developments [2] have begun to probe alternate theory, providing a tool to investigate the significance of relativistic corrections and convergence criteria across a range of atomic number. In part, this has revealed that more theoretical work will be required in future years.

References

1 Chantler, C. T., Olsen K. and Zucker, D. S. (2003) X-Ray Form Factor, Attenuation and Scattering Tables (version 2.0). [Online] *http://physics.nist.gov/ffast* [2003, March 31]. National Institute of Standards and Technology, Gaithersburg, M D; Chantler, C. T. (2000) *J. Phys. Chem. Ref. Data* **29**(4), 597-1048; Chantler, C. T. (1995) *J. Phys. Chem. Ref. Data* **24**, 71-643.

2 Chantler, C. T., Tran, C. Q., Paterson, D., Cookson, D. and Barnea, Z. (2001) *Phys. Lett.* **A286,** 338-346; Chantler, C. T., Tran, C. Q., Barnea, Z., Paterson, D., Cookson, D. and Balaic, D. X. (2001) *Phys. Rev.* **A64,** 062506-1 – 15.

MULTI-TEMPERATURE EDD MEASUREMENT IN RARE-EARTH HEXABORIDES LB_6 (L=La, Ce, Sm)

K. Tanaka, S. Funahashi, and S. Takagi

Department of Materials Science and Engineering, Nagoya Institute of Technology, Gokiso-cho, Showa-ku, Nagoya 466-8555, Japan
(kiyo@tana.mse.nitech.ac.jp)

Rare-earth hexaborides LB_6 (L=La, Ce, Sm) have cubic crystal structure with metal atoms at body-center and the centers of regular B_6 octahedra at corners with B atoms on edges. They have very interesting physical properties. SmB_6 is a Kondo insulator and Sm^{3+} has formally five 4f-electrons. La^{3+} in LaB_6 has formally no 4f-electrons. CeB_6 is a famous Kondo crystal and its EDD at the four temperatures were analyzed with X-ray AO analysis method exhibiting the electron transfer from Ce-4f and B-2p electrons to the $(B\text{-}B)_{out}$ bonds connecting two B_6 regular octahedra[1]. This causes anharmonic vibration (AHV) at low temperature and entropy increases. Since the entropy increment caused by the 4f-electron donation to $(B\text{-}B)_{out}$ bonds increases entropy it cannot be stopped. Therefore the EDD of the three title compounds were measured at 100, 165, 230 and 298 K to compare the EDD of the three complexes. The relationship between electron transfer and AHV at low temperatures in these complexes with different physical properties is also interesting.

Highly accurate structure factor measurement of EDD of rare-earth complexes is necessary. Especially multiple diffraction (MD) easily affects the diffracted intensities more than 1 % of the observed ones while the number of 4f-electrons is very small compared to the total ones in the unit cell forcing us the measurement with the accuracy less than 1%. Therefore the sample was rotated around the scattering vector (Ψ-scan) and the intensity were measured where intensity perturbation due to MD is calculated to be less than 0.5 %[2].

The deformation density of LaB_6 at 165 K exhibited deep troughs and peaks which alternately distribute spherically around La^{3+}. It was analyzed with the X-ray AO analysis method. A part of the 5p(j=3/2) as well as B-$2p_z$ electrons are transferred to 4f(Γ_8) and 4f(Γ_7) orbitals and both are occupied by 0.09(1) electrons making spherical EDD. The residual density is very small indicating the success of the refinement. The deformation density of SmB_6 at 100 and 165K revealed striking peaks along <100> directions. The 5p(j=3/2) and four-fold 4f(Γ_8) orbitals are fully occupied. However two-fold 4f(Γ_7) orbitals, each of which is supposed to accommodate 0.5 electrons, are occupied by only 0.08(23) and 0.10(2) electrons at 100 and 165 K, respectively. Instead of it Sm-5d(Γ_8, j=5/2) orbitals are occupied fully and B-2p electrons are transferred to Sm atoms. There is no indication of AHV of Sm atoms. The X-ray AO analysis for LaB_6 and SmB_6 at the other temperatures are being done and the variation of B-B bond lengths with temperature are also presented in conjunction with the change in electron configurations.

References

1 Tanaka, K. and Onuki, Y. (2002) *Acta Cryst.* B**58**, 423-436.
2 Tanaka, K. and Saito, Y. (1975) *Acta Cryst.* **A31**, 841-845.

OPPORTUNITIES FOR RESEARCH AT AUSTRALIA'S REPLACEMENT RESEARCH REACTOR

R. A. Robinson

Bragg Institute, ANSTO, Lucas Heights, NSW 2234, Australia
(rro@ansto.gov.au)

The 20-MW Australian Replacement Research Reactor represents possibly the greatest single research infrastructure investment in Australia's history. Construction of the facility has commenced, following award of the construction contract in July 2000, and the construction licence in April 2002. The project includes a large state-of-the-art liquid deuterium cold-neutron source and supermirror guides feeding a large modern guide hall, in which most of the instruments are placed. Alongside the guide hall, there is good provision of laboratory, office and space for support activities. While the facility has "space" for up to 18 instruments, the project has funding for an initial set of 8 instruments, which will be ready when the reactor is fully operational in January 2006. Instrument performance will be competitive with the best research-reactor facilities anywhere, and our goal is to be in the top 3 such facilities worldwide. Staff to lead the design effort and man these instruments have been hired on the international market from leading overseas facilities, and from within Australia, and 6 out of 8 instruments have been specified and costed. At present the instrumentation project carries ~15% contingency. An extensive dialogue has taken place with the domestic user community and our international peers, via various means including a series of workshops over the last 2 years covering all 8 instruments, emerging areas of application like biology and the earth sciences, and computing infrastructure for the instruments.

In December 2002, ANSTO formed the Bragg Institute, with the intent of nurturing strong external partnerships, and covering all aspects of neutron and X-ray scattering, including research using synchrotron radiation.

I will discuss the present status and predicted performance of the neutron-beam facilities at the Replacement Reactor, synergies with the synchrotron in Victoria, in-house X-ray facilities that we intend to install in the Bragg Institute, at Lucas Heights, and the tremendous opportunities that all of this presents for research in Australia.

ENPI - THE EUROPEAN NEUTRON POLARIMETRY NETWORK, A STATUS REPORT

Francis Tasset

Institut Laue-Langevin, BP 156, F-38042 Grenoble Cedex 9, France
(tasset@ill.fr)

Instrumentation for polarised neutron science, including for atomic magnetisation maps measurements, is being renewed and extended in a radical way. Last decade, revolutionary tools were introduced both for the production and the analysis of the neutron beam polarisation as well as for the measurement of the associated 3d-vector quantity. These last three years, such advanced modular tools, like the ^{3}He Neutron-Spin-Filter, and the Zero-field polarimeter Cryopadum, were actively developed and commissioned within the frame of EC-FP5 RTD-Network ENPI. A status report of this successful collaboration involving 8 European neutron groups interested in Polarimetric Neutron Scattering will be presented.

CURRENT STATUS AND FUTURE PLANS AT THE AUSTRALIAN SYNCHROTRON PROJECT

S. W. Wilkins

CSIRO, Manufacturing and Infrastructure Technology PB33 Clayton Sth, Vic 3169, Australia (Steve.Wilkins@csiro.au)

The Australian Synchrotron Light Source, will be a 3 GeV double bend achromat (DBA) ring with low emittance (~8 nm rad) that is scheduled to commence construction works in mid 2003 and to be commissioned in 2007. It will be sited adjacent to the campuses of Monash University and CSIRO in Clayton, Victoria.

The ring will be a medium-sized (216m circumference) one with high brightness such as to approach in performance in the ~10 keV regime (of typical interest to crystallographers) some of the very large third generation rings. The ring will have 14 (12 useable) straight sections and be able to accommodate up to 30 beamlines.

Early stage beamlines under consideration and of interest to crystallographers and materials scientists include those designed for; i) macromolecular crystallography, ii) small molecule and charge-density studies; iii) infrared spectroscopy, iv) high performance scanning microprobe; iv) a microdiffraction microprobe high-resolution powder diffraction, and v) SAXS/WAXS.

References

1 http://www.synchrotron.vic.gov.au/general_info/beamline_proposals.asp
2 Boldeman, J. W., *The Australian Synchrotron Light Source*, paper presented to EPAC 2002.

CHARGE DENSITIES OF PHOSPHORUS CONTAINING COMPOUNDS AT 20 K

Marc Messerschmidt, and Peter Luger

Institute for Chemistry/ Crystallography, Free University Berlin, 14195 Berlin, Germany (mcmesser@chemie.fu-berlin.de)

All measurements are performed on a Huber 4-circle-goniometer with a 2-stage-helium-cryostat and a Bruker-Apex detector. This setup benefits from the low running costs and good temperature stability of the closed cycle Helium cryostat. While these cryostats are normally used with carbon or beryllium vacuum chambers, that produce a lot of powder lines, we have developed a new vacuum chamber, which is constructed from 0.1mm Kapton film. This gives small and unstructured background. The cylinder is stabilized through spanning inside the large Huber Eulerian cradle. This mounting only on top and bottom avoids any shadowing of the beam path. Measurements of some weeks at 20 K are easily possible. The crystal is normally centered optical, because transparent kapton film is used. Charge densities of phosphorus compound have normally high residual densities, when measured at liquid nitrogen temperature. This phenomenon is often explained with inharmonic thermal motion. Our first system is Adenosinemonophosphate and as a model system we want to use Phosphoruspentoxide. Therefore we present results of 20 K measurements and compare it with results from 100K.

EXPERIMENTAL ATTEMPTS TO MEASURE NONCOLLINEAR LOCAL MAGNETISATION

P. J. Brown

Institut Laue Langevin, BP 156, 38042 Grenoble, France (brown@ill.fr)

The representation of atomic magnetic moments as simple vectors, shown as arrows in the pictorial representation of a magnetic structure, has proved a very useful one; but it should not be pushed too far. In a solid, the magnetisation is a continuous function, a property of the electron wave-functions, and there is no requirement that it should be collinear. Nevertheless the assumption of a collinear magnetisation distribution is widely made and one should therefore give some thought to the circumstances in which it might not be valid. The first and most obvious is that of a non-collinear magnetic structure. When the atomic moments themselves are not parallel it would be naive to suppose that there is a well defined boundary between atoms at which the magnetisation changes abruptly from one general direction to another. A second example occurs in anisotropic systems; if the local easy axes of magnetisation of atoms are not parallel to one another then the magnetisation distribution induced by an applied field will be non-collinear. Furthermore even in very simple systems in which the orbital moment is not fully quenched there may be non-collinearity due to spin-orbit interaction. In fact the spin-orbit interaction is by far the most important cause of non-colinearity in magnetic systems, being the principal means by which an atom's spin direction is coupled to the orientation of its ligand environment. In all the examples which will be given, in which a non-collinear magnetisation distribution has been sought or found, this non-collinearity is primarily due to the presence of orbital magnetisation.

Several experimental techniques are available to probe non-collinearity of the magnetisation distribution. The most direct is to measure both the magnitude and direction of the magnetic interation vectors which give its fourier components. Such measurements are now becoming possible for antiferromagnets with the advent of a new generation of neutron polarimeters which will allow both greater geometric flexibility and higher precision. However up to now non-collinear magnetisation distributions have been revealed by more indirect means. Polarised neutron flipping ratio measurements can give only a single component of the magnetic interaction vector directly. However the special geometric properties of the interaction vector and the symmetry breaking properties of an applied field can be exploited to obtain evidence of non-collinearity in the magnetisation distribution even from such limited data.

MAGNETIC EXAFS AS A TOOL TO MEASURE RADIAL DISTRIBUTION OF SPIN AND ORBITAL MAGNETIC MOMENTS

Andrei Rogalev, and José Goulon

European Synchrotron Radiation Facility (E.S.R.F.), BP-220, F-38043 Grenoble Cedex, France (rogalev@esrf.fr)

Over the past decade, X-ray Magnetic Circular Dichroism (XMCD) has developed as a useful *local* probe of magnetic properties in ferro(i)magnetic and paramagnetic compounds. In XMCD experiments, one measures the difference in the X-ray Absorption Spectra recorded with left and right circularly polarized photons while the sample magnetization is kept parallel or antiparallel to the direction of propagation of the incident X-ray beam. What made XMCD attractive is the possibility to access, using magneto-optical sum rules, to orbital-projected magnetic moments both in magnitude and direction with the full benefit of the element selectivity that characterizes X-ray absorption spectroscopy. From the very early work it was realized that magnetic dichroism was not restricted to only the x-ray absorption near edge structure (XANES) region but contributed also to the extended x-ray absorption fine structure (EXAFS) region.

In this presentation we will show that the magneto-optical sum rules in their differential form allow one to extract from the Magnetic EXAFS spectra the radial distribution of spin and orbital magnetic moments around the absorbing atom in ferromagnet. The validity and great potentiality of this approach will be illustrated using Magnetic EXAFS spectra recorded at the $L_{2,3}$-edges of Eu in the ferromagnetic semiconductor EuS. The results can be nicely correlated with those derived from conventional XMCD measurements in the XANES region.

TWISTED STATES OF Fe/Tb MULTILAYERS

Katsuyoshi Takano,[a] Kazuhiro Ikeuchi,[b] Hiroshi Sakurai,[b] Hiromi Oike,[b] and Fumitake Itoh[b]

[a]Satellite Venture Business Laboratory, Gunma University, 1-5-1 Tenjin-cho, Kiryu, Gunma, 376-8515, Japan; [b]Department of Electronic Engineering, Gunma University, 1-5-1 Tenjin-cho, Kiryu, Gunma, 376-8515, Japan (ktakano@el.gunma-u.ac.jp)

The magnetic structures of multilayers have been understood as interface effects. Thus the multilayers with a long artificial period have been thought to have bulk like behaviour. Therefore there are a few investigations about multilayers with the long period. However we found that the Tb magnetic moments in $[Fe(12.4nm)/Tb(15.2nm)]_{25}$ multilayer shows twisted state structures at a low temperature and a certain magnetic field, which are different from bulk Tb metal.

In order to see the local magnetic structures, the magnetic moment of Fe and Tb were measured by x-ray magnetic circular dichroism (XMCD) at the Fe *K*-edge at the Tb $L_{2,3}$-edges. The magnitude and direction of magnetic moments were derived from the XMCD intensities and signs.

We have measured the magnetic field dependence of the XMCD intensity [1], [2]. The sample was at first demagnetized. Then the XMCD intensity was measured at a magnetic field with reversing the field using fixed circularly polarized x-rays. This measurement was repeated by stepwise increasing the magnetic field from 0.2 kG to 6.2 kG. Thus obtained information corresponds to the initial magnetization of each element in the M-H curve [2].

Above 150 K, both Fe and Tb moments increase proportionally with increasing the magnetic field up to 1.5 kG, keeping the coupling ferrimagneticaly. Below 150 K, the Fe moment increases, while the Tb moment decreases with increasing the magnetic field. This behaviour can be explained by a twisted state; the magnetic moments of Fe and Tb align anti-parallel in the low field. But the magnetic moment of Tb begins to turn to the applied field, keeping the Fe moment constant.

References

1 Itoh, F., Nakamura, M., Sakurai, H., Kiriaake, H., Nawate, M., Honda, S. and Kawata, H. (1993) *Proc. 7th Int. Conf. X-Ray Absorption Fine Structure, Kobe*, 1992, *Jpn. J. Appl. Phys.* **32** Sippl. 32-2, 326.

2 Koizumi, A., Takagaki, M., Suzuki, M., Kawamura, N. and Sakai, N. (2000) *Phys. Rev. B* **61**, 14909.

Thursday August 14

Sagamore XIV

ABSTRACTS

POSTER SESSIONS

THE ATOMISTIC ORIGIN OF THE INVERSE PIEZOELECTRIC EFFECT IN α-SiO_2 AND α-$GaPO_4$

Jav Davaasambuu,[a] Vasili Kochin,[a] Andreas Pucher,[a] Semen V. Gorfman,[a] Vladimir G. Tsirelson,[a] Peter Blaha,[b] and Ullrich Pietsch[c]
[a]Quantum Chemistry Department, Mendeleev University, Moscow, Russia; [b]Institute of Materials Chemistry, Technical University of Wien, Austria; [c]Institute of Physics, University of Potsdam, Potsdam, Germany (upietsch@ullipc.physik.uni-potsdam.de)

The inverse piezoelectric effect of α-quartz can be observed applying an external electric field parallel to the non-centrosymmetric [11.0] direction. In a previous paper we have shown that the model of field induced mutual displacement of ionic sublattices fails for the explanation of the atomic origin of the macroscopic measurable effect. Therefore we proposed an alternative model which is based on the rotation of nearly rigid SiO_4 tetrahedra under influence of the external electric field considering the strong covalent bond between silicon and oxygen.

Meanwhile this model has been verified by measuring the changes of integrated intensities of selected Bragg reflection DR/R of α-SiO_2 and the isostructural α-$GaPO_4$ under influence of a periodic external high electric field of E 8 kV/mm. For the first time a similar experiment was performed at low temperatures (50 < T < 300 K).

The received data were interpreted in terms of a semi-empirical structure model and by ab-initio calculations. Nine structural parameters of the semi-empirical model were refined using nine selected Bragg reflections which were measured at different field strength. For the refinement we used the constraint of rigid SiO_4 tetrahedra. In addition, the form factor variation was neglected because the quantum-mechanically predicted field dependence is two orders of magnitude smaller than the experimental data. Our model fits all measured DR/R in a qualitative right manner. At E=3kV/mm the Si-O-Si angle in direction parallel and perpendicular to the applied field change by about 0.05° and 0.02°, respectively. In $GaPO_4$ the Ga-O-P angles parallel to the field alter by about 0.12° reflecting the higher piezoelectric coefficient d_{111} compared to α-SiO_2.

The temperature dependence of DR/R´s was measured down to 50 K. They can be interpreted mainly by the temperature dependence of Debye-Waller factors but an additional contribution caused by the field-induced rotation of SiO_4 and $(Ga,P)O_4$ tetrahedra, respectively.

Ab-initio calculations have been performed using the WIEN2k-package. Here we defined a supercell of reduced symmetry along the [11.0] direction of the quartz structure containing 72 atoms. The external electric field of about 5 kV/mm is modelled by an additional saw-like potential. The relaxed atomic positions within a sub-unit of the supercell with constant field strength were used as input for the semi-empirical model, mentioned above. Although the calculations are not finished yet, the results seem to verify our predictions.

References

1 Tsirelson, V. G., Gorfman, S. V. and Pietsch, U. *Acta Cryst A*. submitted.
2 Davasambuu, J., Kochin, V., Pucher, A. and Pietsch, U. (2002) *Europhys.Lett*. submitted.
3 Stahn, J., Pietsch, U., Blaha, P. and Schwarz, K. H. *Phys.Rev.* B63, 165205.

SIMULATION OF COMPTON DOUBLE SCATTERING

Yukinobu Kakutani, Akihisa Koizumi, and Nobuhiko Sakai

Graduate School and Faculty of Science, Himeji Institute of Technology, Hyogo 678-1297, Japan (yukinobu@sci.himeji-tech.ac.jp)

In 1987, a simulation of magnetic Compton double scattering of circularly polarized photons by magnetic electrons was reported by Sakai[1]. This simulation code was suitable for the magnetic Compton scattering (MCS) experiments using gamma-ray sources, in which no linear polarization of the incident gamma-rays presented.

We have made a new simulation code including both linear and circular polarizations of incident photons, which is suitable for the MCS experiments utilizing synchrotron radiation x-rays.

First, the validity of the present simulation was confirmed by the reproduction of the experimental ratio between Compton double scattering result on Ge measured by Pasic *et al*[2]. The agreement between the simulation and experimental result is good, as shown in Fig. 1. Second, it was confirmed that the intensity of Compton double scattering depends on polarization of incident photons, material, incident energy and sample volume.

Concerning to the spin-dependent Compton double scattering, a result of simulation on Fe (2 mm height, 10 mm wide and 10 mm thickness), showed that the influence of magnetic Compton double scattering on 3d transition metal is negligible for ordinary measurements.

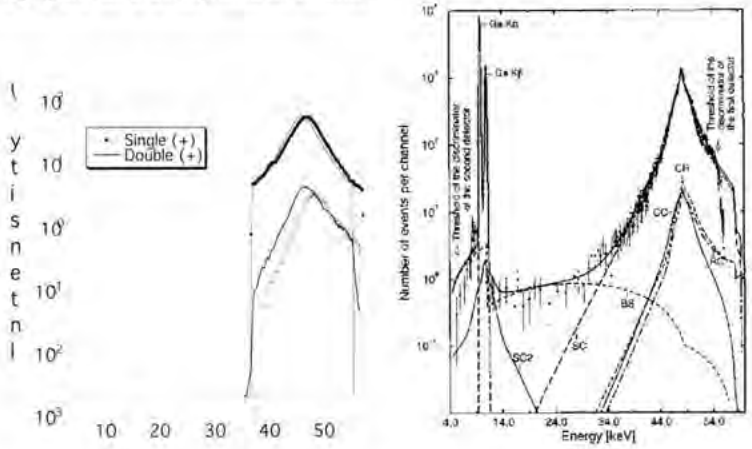

Fig.1: Results of Compton double scattering on Ge. (a) present simulation, a Lorenz type function is assumed to simulate Compton broadening. (b) experiment by Pasic *et al*[2].

References

1 Sakai, N. (1987) *J. Phys. Soc. Jpn.* **56**, 2477-2485.

2 Pasic, S. and Ilakovac, K. (1997) *Phys. Rev.* **A 55**, 4248-4252.

DIRECT PHASE DETERMINATION OF FRACTIONAL REFLECTION IN CHARGE-DENSITY-WAVE CRYSTALS USING X-RAY MULTIPLE DIFFRACTION

Shih-Lin Chang,[a] Chao-Hong Du,[b,c] Mau-Tsu Tang,[c] Yu. P. Stetsko,[c] Yen-Ru Lee,[a] Tsong-Tze Lin,[a] Shih-Chang Wong,[a] and Wen-Shien Sun[a]

[a]Department of Physics, National Tsing Hua University; [b]Department of Physics, Tamkang University; [c]National Synchrotron Radiation Research Centre, Hsinchu, Taiwan, 300, R.O.C. (slchang@phys.nthu.edu.tw)

We report the direct determination of collective phase of charge-density wave (CDW) [1, 2] in a quasi-two-dimensional material 2H-$NbSe_2$ using the multiple diffraction technique. Via the coherent interaction between the X-ray waves propagating in the CDW modulated structure and the host structure, the collective phases of CDW were determined to be either 0° or 180° from the analyses of the asymmetry of the diffraction profiles along the azimuth scans of a CDW fractional reflection. The phases were observed not to vary with changing temperature, suggesting that the phases are pinned. This finding may be useful for the direct observation of the dynamic phenomena caused by the phase of the density waves.

References

1 Thorne, R. E. (1996) *Physics Today*, May 42-43.
2 Overhauser, A. W. (1978) *Advances in Physics* **27**, 343-357.

ELECTROSTATIC PROPERTIES OF THE MOLECULAR SIEVE $AlPO_4$-15

E. Aubert, F. Porcher, M. Souhassou, and C. Lecomte

Laboratoire de Cristallographie et Modélisation des Matériaux Minéraux et Biologiques, CNRS UMR 7036, Université H. Poincaré – Nancy I, BP 239, 54506 Vandœuvre-lès-Nancy, France (aubert@lcm3b.uhp-nancy.fr)

Charge density and electrostatic potential analyses are of special interest in characterizing host / guest systems like zeolites or AlPO systems[1].

Single crystal of $AlPO_4$-15 ($NH_4Al_2(OH)(H_2O)(PO_4)_2 H_2O$) were obtained by hydrothermal synthesis (180°C); the X-ray diffraction data were collected on a Nonius K CCD diffractometer, Mo(Ka) radiation, $P2_1/n$, a=9.556(1) Å, b=9.563(1) Å, c=9.615(1) Å, b=103.58(1)°. The charge density was modeled according to the multipolar formalism of Hansen and Coppens using program MoPro[2]. The final residual indices are R=1.02%, Rw=0.66%, N_{obs}=4725, N_{par}=510, $(\sin\theta/\lambda)_{max}$=0.90Å^{-1}. The analysis of the topology of the electron density was performed on the multipolar and IAM models in order to characterize interactions between framework atoms (P,Al-O) and between framework and guest molecules (hydrogen bonds).

The electrostatic potential (EP) was derived from two representations. The first one consists of point charges placed at atomic positions. The potential was obtained trough a summation in direct space $V(\mathbf{r})=S_i Q_i/r_{i,i}$ using different set of charges (issued from a Pv/K refinement or topological analysis). The second one used the charge density issued from the multipolar model and calculations were performed with summation in direct and reciprocal spaces[3,4]. From these two representations, electrostatic interaction energies were derived. For the second one, it was evaluated for a molecule A as $E_A = V_{t\text{-}A}(\mathbf{r})\rho_A(\mathbf{r})d\mathbf{r}$, where $V_{t\text{-}A}(\mathbf{r})$ is the EP that is felt by molecule A (generated by all the crystal except molecule A) and $\rho_A(\mathbf{r})$ is the charge density of molecule A. Thus, electrostatic interaction energies for water molecules, ammonium cation and hydroxyl group occluded in the molecular sieve are compared with results obtained from a differential scanning calorimetry experiment.

References

1 Lecomte, C. (1999). In *Implications of Molecular and Materials Structure for New Technologies*, pp. 23-44, Kluwer Academic Publishers.

2 Guillot, B., Viry, L., Guillot, R., Lecomte, C. and Jelsch, C. (2001) *J. Appl. Cryst.*, **34**, 214-223.

3 Stewart, R. F. (1979) *Chem. Phys. Lett.* **65**, 335-338.

4 Ghermani, N. E., Bouhmaida, N. and Lecomte, C. (1992) *ELECTROS, STATDENS*. Internal report URA CNRS 809. Université Henri Poincaré, Nancy 1, France.

VIRTUAL EXPERIMENTS FOR THE BUILDUP OF ASPHERICAL ATOM SCATTERING FACTORS OBTAINED BY A NOVEL PARTITIONING SCHEME AND APPLICATION TO A TRIVALINE STRUCTURE

Birger Dittrich,[a] and Dylan Jayatilaka[b]

[a]Freie Universität Berlin, Institut fuer Chemie/Kristallographie, Takustr. 6, 14195 Berlin, Germany, Tel.: +49 30 83853450, Fax.: +49 30 83853464; [b]University of Western Australia, Chemistry, 35 Stirling Highway, Crawley WA 6009, Australia, Tel.: +61 8 93808563, Fax.: +61 8 93801005 (birger@chemie.fu-berlin.de)

Following a route recently described by Koritsanszky et al. [1] we have calculated theoretical data sets for geometry optimized [2] model compounds. The theoretical structure factors are fitted with the Hansen and Coppens multipole model [3] using the XD program package [4] treating the theoretical Fc's as Fo's. Starting from [1] a generalized scheme for a partitioning of any structure into transferable atoms is proposed. These transferable atoms are called invarioms (from **invar**iant a**toms**) and are similar in a transfer process from one molecule to another because they mimic the same chemical environment with respect to the nearest neighbors of the atom of interest. To minimize the size of the model compounds the valences of the nearest neighbors of the atom of interest are saturated with hydrogen atoms. This partitioning scheme is used to build up a library of multipole parameters, in a similar manner as realized by Pichon Pesme et al. [5] and successors for experimental data.

Amino acids and peptides consist of only 30 invarioms. The database used here already contains these 30 invarioms and an application to experimental data as a test of the method will be presented. The test structure, VVV * EtOH * TFA, was recently determined in our lab. It crystallizes in the space group $P2_1$, a = 9.705, b = 19.270, c = 11.820 Å and γ= 100,26° with Z=2 and four independent molecules in the asymmetric unit. The spherical R-factor using the independent atom model is 4.2%. The structure is not suited for a high resolution data collection / multipole refinement due to the four independent molecules in the asymmetric unit and the presence of trifluoracetic acid, but is an ideal test case for the application of a transfer of the theoretically obtained multipole parameters.

The expected outcome is not only a lower R-factor. Using only the spherical structure the electrostatic potential as well as the dipole and multipole moments can be calculated from the transferred aspherical electron density. This approach could, if successful, be generalized to any crystal structure without a limit in the number of atoms.

References

1 Koritsanszky, T., Volkov, A. and Coppens, P. (2002) *Acta Cryst.* **A58**, 464.
2 Gaussian 98, Revision A.11.3, M. J. Frisch et al., Gaussian, Inc., Pittsburgh PA, 2002.
3 Hansen, N. and Coppens, P. (1978) *Acta Cryst.* **A34**, 909.
4 Koritsanszky, T., Howard, S., Richter, T., Su, Z., Mallinson, P. and Hansen, N. K., XD - A program package for Multipole Refinement and Analysis of Electron Densities from Diffraction Data. User Manual. Freie Universität Berlin, 1996.
5 Pichon Pesme, V., Lecomte, C. and Lachekar, H. (1995) *J. Phys. Chem.* **99**, 16.

Help from T. Koritsanszky for structure factor calculation is gratefully acknowledged.

THE NEW QUASI-LAUE DIFFRACTOMETER AT THE REPLACEMENT RESEARCH REACTOR

Wim T. Klooster

Bragg Institute, ANSTO, PMB 1, Menai, NSW 2234, Australia
(wim@ansto.gov.au)

The new single-crystal diffractometer for the Replacement Research Reactor will be a quasi-Laue diffractometer, similar to VIVALDI at ILL, France. It will be competitive with the best instruments currently available. Data collection times for a normal structure determination will be less than a day, a considerable improvement on current data collection times, typically a few weeks at HIFAR. Also, the crystal size needed for an experiment can as small as about 0.1 mm^3, opening up new research areas where it has proved difficult to grow crystals sufficiently big (several mm^3) which are currently needed. Another area of research opening up will be multiple temperature and/or pressure measurements.

This new instrument will be a useful tool to obtain structural information in a timely fashion, where x-rays do not provide enough detail.

The instrument will be on the end of a thermal supermirror guide, and we are exploring the possibility of enhancing the flux further by using a converging guide section immediately before the instrument itself.

More detailed information on the instrument will be presented.

NEW IONIC MODEL POTENTIAL FOR SEMICONDUCTORS WITH APPLICATION TO Si

Teiji Kobayasi,[a] and Hisashi Nara[b]

[a]General Education, College of Medical Sciences, Tohoku University, Sendai, Miyagu Prov. 980-8575, Japan; [b]Department of Systems and Information, Hachinohe Institute of Technology (cobalt@clg.niigata-u.ac.jp)

A new ionic model potential for semiconductors is proposed, which consists of a set of continuous exponential functions. Introduced damping and amplitude parameters into the model potential are to be treated as adjustable. Unlike the ionic model potentials of the Heine-Abarenkov and Topp-Hopfield types, the proposed model potential has no artificial sharp cut-off parameter for the repulsive core-orthogonality condition and has continuous derivatives of arbitrary orders. The reasons of the proposition are discussed in relation with light metals where the ionic model potentials with the cut-off parameter work successfully. In particular, an unphysical and artificial oscillation of the potential form factor in high momentum region, which is introduced by the potential discontinuity, will be discussed. The proposed model potential is applied to constructing crystal potential of Si semiconductor and the adjustable parameters are determined so as to be consistent with the Si crystal pseudo potential of high quality by taking a valence electron dielectric screening effect into account. The effectiveness of the proposed model potential is discussed by (1) comparing the calculated ionic energy levels of Si with experiments, (2) checking the consistency between the ionic and crystal potentials for Si, and so on.

EFFECTS OF ELECTRON CORRELATION ON MAGNETIC COMPTON PROFILES OF Ni IN THE GW APPROXIMATION

Yasunori Kubo

Department of Physics, College of Humanities and Sciences, Nihon University, Tokyo 156-8550 (kubo@chs.nihon-u.ac.jp)

The magnetic Compton profiles (MCP's) are studied with the conventional band theory based on the local-density approximation(LDA) and so-called GW approximation (GWA) connected band theory. In the GWA, the basis sets, eigen-energies and eigen-states generated by the full-potential linearized augmented-plane wave method(FLAPW), are used.

Since the magnetic moment of Ni is 0.6 μ_B, which is about 4 times smaller than that of Fe, it is not easy to measure MCP with good statistical accuracy. However, recent MCP's [1,2] using Storage-Ring have demonstrated discrepancies between the experiments and conventional band calculations using LDA in lower momentum region, where the Fermi surface structures and the hybridization between the 3d- and s,p- electrons predominantly influence the momentum distributions of magnetic electrons. The discrepancies are examined from the point of view of electron correlation effects. The occupation number densities $N(k)$'s are evaluated from a first-principle calculation of the spectral function within the GWA. The MCP's are calculated using the $N(k)$'s.

References

1 Dixon, M. A. G., Duffy, J. A., Gardelis, S., McCarthy, J. E., Cooper, M. J., Dugdale, S. B., Jarlborg, T. and Timms, D. N. (1998) *J. Phys.: Condens. Matter* **10**, 2759-2771.

2 Kakutani, Y., Kubo, Y., Koizumi, A., Sakai, N., Ahuja, B. L. and Sharma, B. K. (2003) *J. Phys. Soc. Jpn.* **72,** in print.

CHARGE DENSITY ANALYSIS AND DIPOLE MOMENT ENHANCEMENT IN MNA (2-METHYL-4-NITROANILINE)

Andrew Whitten,[a] Mark Spackman,[a] Peter Turner,[b] Wim Klooster,[c] Ross Piltz,[c] and Masaru Tachibana[d]

[a]Chemistry, School of Biological, Biomedical and Molecular Sciences, University of New England, Armidale, NSW 2351, Australia; [b]School of Chemistry, University of Sydney, NSW 2006, Australia; [c]Bragg Institute, Building 58, ANSTO, PMB 1, Menai, NSW 2234, Australia; [d]Department of Physics, Yokohama City University, 22-2, Seto, Kanazawa-ku, Yokohama, 236-0027, Japan (awhitten@une.edu.au)

MNA belongs to a class of substituted benzene derivatives, which possess exceptional non-linear optical properties. Such compounds exhibit large microscopic second order non-linear susceptibilities, and lack a centre of symmetry in the solid state. Another interesting property of these compounds is the apparent enhancement of the dipole moment due to hydrogen bonding and general crystal-field effects. For MNA, *ab initio* calculations of the free molecule give values of the dipole moment of about 8.2 D,[1] while in-crystal estimates obtained from a previous charge density analysis are around 25(8) D,[2] suggesting a three-fold enhancement of this molecular property. This experimental result has been widely cited, but whether the magnitude of the dipole moment enhancement exhibited there is reasonable is of some debate because of difficulties encountered in the analysis of X-ray diffraction data for non-centrosymmetric space groups; the large experimental error associated with the value also raises questions about the ability of the multipole refinement procedure to reliably retrieve such values.

To independently verify this important observation, and hopefully to improve on the results obtained in the previous study, we are making use of experimental data that was unavailable a decade ago, including neutron diffraction data collected on the four-circle diffractometer (2TANA) at HIFAR, as well as charge density quality X-ray diffraction data collected on the Bruker SMART 1000 CCD system at the University of Sydney, all at 100 K. We are also performing Hartree-Fock CRYSTAL98 calculations to aid in the analysis of the experimental data, and for comparison with experimental results. We will discuss the difficulty in obtaining sensible estimates of one-electron properties for non-centrosymmetric compounds from multipole refinements, and present in detail the results obtained from this study.

References

1 Daniel, C. and Dupuis, M. (1990) *Chem. Phys. Lett.* **171**, 209.

2 Howard, S. T., Hursthouse, M. B., Lehmann, C. W., Mallinson, P. R., and Frampton, C. S. (1992) *J. Chem. Phys.* **97**, 5616.

MOLECULAR ELECTRIC PROPERTIES USING HIRSHFELD SURFACES: A NOVEL APPLICATION OF SURFACE INTEGRALS

Mark Spackman,[a] Andrew Whitten,[a] Joshua McKinnon,[a] Xiaoxiong Meng,[a] and Christopher Radford[b]

[a]Chemistry, School of Biological, Biomedical and Molecular Sciences, University of New England, Armidale NSW 2351, Australia; [b]School of Mathematics, Statistics and Computer Sciences, University of New England, Armidale NSW 2351, Australia. (mspackma@une.edu.au)

The Hirshfeld surface was originally devised [1] as a novel partitioning of molecules in crystals, for the purpose of providing a simpler route to estimating electric properties, especially dipole moments, of molecules in crystals. In that original communication dipole moments were presented for three small molecules in crystals, using a rather crude numerical integration over the volume inside the surfaces. We have recently taken advantage of the trangulated nature of these surfaces to convert volume integrals to surface integrals, using standard methods in vector calculus.

The method is based on that of Popelier, who has described in some detail the computation of the atomic charge inside surfaces defined by the quantum theory of atoms in molecules (QTAM) [2]. This is quite a straightforward property to compute, and the relevant expression is (in atomic units):

$$q = \iiint_V \rho(\mathbf{r})dV = \frac{1}{4\pi}\iint_S (\mathbf{E}\ \ \mathbf{n})dS$$

In this manner the net charge within the relevant surface can be obtained by integration of the electric field projected onto the surface normal, summed over the oriented surface. In a similar manner the dipole moment of the charge distribution within the surface can be expressed in terms of two surface integrals, one involving the electrostatic potential, and the other the electric field; second moments also require a volume integral, which is directly related to the average of the electrostatic potential within the enclosed volume.

For integration over QTAM surfaces, Popelier employed a parametric representation of the various surfaces. However, all of our work on Hirshfeld surfaces [3] has taken advantage of their description as smooth isosurfaces of a readily defined weight function, and from this, their representation as triangulated surfaces. A triangulated surface automatically provides a set of surface points and their connectivity as triangles on the surface. From this information, relevant electric properties are readily computed at all points on the surface (from either theoretical – Gaussian98 or Crystal98 – or experimental – Valray or XD – charge distributions), and surface normals are obtained trivially.

Results will be presented for dipole moments of a variety of molecules in molecular crystals, and compared with relevant QTAM results.

References

1 M. A. Spackman and P. G. Byrom (1987) *Chem. Phys. Lett.*, **267**, 215.
2 P. L. A. Popelier (2001) *Theor. Chem. Acc.*, **105**, 393.
3 J. J. McKinnon, A. S. Mitchell & M. A. Spackman (1998) *Chem. Commun.*, 2071; J. J. McKinnon, A. S. Mitchell & M. A. Spackman (1998) *Chem. Eur. J.*, **4**, 2136; M. A. Spackman & J. J. McKinnon, *CrystEngComm*, **4**, 378.

STUDY OF ANISOTROPY IN MOMENTUM DENSITY OF COBALT

B. K. Sharma,[a] B. L. Ahuja,[b] S. S. Asawat,[a] V. Purvia,[a] Y. Kakutani,[c] A. Koizumi,[c] and N. Sakai[c]

[a]Department of Physics, University of Rajasthan, Jaipur 302015, India; [b]Department of Physics, College of Science Campus, M. L. Sukhadia University, Udaipur 313001, India; [c]Graduate School and Faculty of Science, Himeji Institute of Technology, Ako-gun, Hyogo 678-1297, Japan (bkrish@sancharnet.in)

The directional Compton profiles of hcp cobalt have been measured at 0.42 a.u. momentum resolution using synchrotron radiation at SPring8, Japan. The measurement is compared with the available APW calculation of Matsumoto et al [1]. It is seen that the APW calculation describes qualitatively the anisotropy of the electron momentum distribution, which is influenced by the Fermi surface topology. The lack of quantitative agreement between theoretical and experimental anisotropies may be due to insufficient treatment of the momentum component above 6.5 a.u. and electron-electron correlation effect. The data points to the need for a better theoretical calculation incorporating the above mentioned features.

References

1 Mastumoto, M., Tomimoto, K. and Wakoh, S. (1993) *J. Phys. Soc. Jpn* **62**, 2734.

THE STUDY OF THE PHASES OF CDWs UNDER THE APPLICATION OF ELECTRIC FIELDS USING MULTIPLE X-RAY DIFFRACTION

Chao-Hung Du,[a] Mau-Tsu Tang,[b] Yuri P. Stetsko,[b,c] Yen-Ru Lee,[c] J. -J. Lee[b] and Shih-Lin Chang[b,c]

[a]Department of Physics, Tamkang University, Tamsui 25137, Taiwan; [b]Synchrotron Radiation Research Center, Hsinchu Science-Based Industrial Park, Hsinchu 30077, Taiwan; [c]Department of Physics, National Tsing Hua University, Hsinchu 30043, Taiwan (chd@mail.tku.edu.tw)

We report the electric field effects on the CDWs' (charge density waves) phases in a quasi-one dimensional material $K_{0.3}MoO_3$ using multiple x-ray diffraction. $K_{0.3}MoO_3$ undergoes a metallic-insulator transition due to the formation of charge density waves (CDWs) at temperature $T_{CDW} \sim 180$ K. Conventionally, the dynamic behavior of the CDWs have been widely studied using the transport measurements, and the non-linear response to the application of electric fields exceeding the threshold value has been known to be due to the deformation of the CDWs' phases. The use of the multiple x-ray diffraction allows us to directly probe the phases of the CDW modulation, further, we observed that the CDWs' phases shifted under the application of an electric field. We demonstrate that the use of multiple diffraction and the application of electric fields allow the direct observations of the deformation of the CDWs' phases.

CHARGE DENSITY STUDIES OF POLYMORPHIC ANTI-ULCER AGENTS. THE APPLICABILITY OF THE ELECTROSTATIC POTENTIAL IN DRUG DESIGN

Jacob Overgaard, Mark P. Waller, and David E. Hibbs

School of Chemistry, University of Sydney, NSW 2006, Australia
(jacobo@chem.usyd.edu.au)

The electrostatic potential (EP) has been extensively employed in the prediction of a variety of condensed phase macroscopic properties from theoretical calculations, and a quantitative approach has recently been suggested based on a range of features of the EP on the molecular surface [1]. However, this method has so far been restricted to the gas-phase, thus excluding the effect of intermolecular interactions. Nonetheless, the EP is of paramount importance in the understanding of drug-receptor interactions. Thus, an experimental determination of the EP including the effects of intermolecular interactions is potentially of great use in rational drug design.

In the present work we will outline the results of a theoretical and experimental charge density (CD) study of both known polymorphs (A and B) of the histamine H_2-receptor antagonist, famotidine (see Figure) [2]. The CD is determined from a combination of X-ray and neutron diffraction data collected at 100 K, using the Hansen-Coppens multipole model [3]. We will focus on a comparison of the experimental and theoretical CDs and describe the similarities in the CDs of the two polymorphic forms of famotidine. In particular, we will discuss the observed differences in the experimental EPs of the two polymorphs, respectively, in relation to their individual abilities to act as anti-ulcer agents. This work represents the preliminary steps towards a more general description of a number of drug types using combined theoretical and experimental charge density studies.

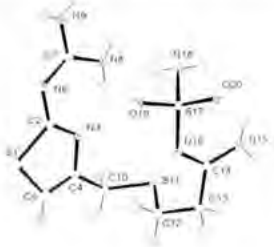

Famotidine B

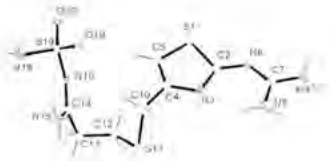

Famotidine A

References

1 Politzer, P. and Murray, J. S. (2002) *Theor. Chem. Acc.* **108**, 134-142.
2 Ferenczy, G. G., Parkanyi, L. J., Angyan, G., Kalman, A. and Hegedus, B. (2000) *J. Mol. Struct. (Theochem)* **503**, 73-79.
3 Hansen, N. K. and Coppens, P. (1979) *Acta Cryst. Sect. A* **39**, 909-921.

CHARGE DENSITY ANALYSIS OF β-Si_3N_4

Doug du Boulay,[a] Nobuo Ishizawa,[a] and Victor Streltsov[b]

[a]Materials and Structures Laboratory, Tokyo Institute of Technology, Nagatsuta, Midori-Ku Japan; [b]CSIRO HSN, 343 Royal Parade, Parkville VIC 3052, Australia (ddb@R3401.msl.titech.ac.jp)

β-Si_3N_4 is important in both electronics and mechanical fabrications industries because of its intrinsic hardness and resistance to oxidation. Despite widespread use its structure is still somewhat controversial. The controversy concerns the existence, or not, of mirror planes normal to the hexagonal 6_3-screw axes which decide the issue of centricity versus acentricity.

Using BL-14A of the Photon Factory synchrotron, Tsukuba, Japan, three largely absorption and extinction free 0.75Å data sets were measured at three different temperatures, 295K, 200K and 150K. We found no compelling, reproducible evidence to support the acentric model and therefore believe that the $P6_3/m$ symmetry is preferable, despite earlier conflicting reports[1-3]. An electron microscopy study has subsequently supported these conclusions[4]. With greater faith in our experiments we have applied multipole population and topological analyses[5]. These analyses agree largely with more theoretical modeling derived from Density Functional Theory using the Linear Augmented Plain Wave approach as implemented in Wien2k[6].

The results of these analyses are consistent regarding the magnitude and topography of the charge density along the interatomic interactions. The coordination geometries of two independent NSi_3 groups is trigonal planar, while that of the SiN_4 group is tetrahedral. The three symmetry distinct Si-N bonds exhibit pronounced charge density accumulation near the bond midpoints, characteristic of covalent sp^2 and sp^3 hybridization schemes for N and Si respectively.

Topological analysis of the electron density revealed the existence of additional (3,-1) critical points at the high symmetry (*-6*) sites midway along the 2.9Å N-N contacts. This feature was also reproduced by DFT calculations. The magnitude of the Laplacian of the density at the N-N critical point is around 20 times smaller than for the other (3,-1) critical points along the N-Si shared electron interactions, with the local electron density at that point around $^1/_4$ of that appearing in the N-Si bonds. This could be interpreted as evidence of weak N-N shared electron interactions, i.e. partial covalent bonding. By comparison, all other N and Si bonds are of order 1.73Å in length.

References

1 Bando, Y. (1983) *Acta Cryst.* B**39**, 185-189.
2 Grun, R. (1979) *Acta Cryst.* B**35**, 800-804.
3 Schneider, J., Frey, F., Johnson, N. and Laschke, K. (1994), *Zeit. fur Krist.* **209**, 328-333.
4 Tsuda, K. (2002) *private communication.*
5 Blaha, P., Schwarz, K., Madsen, G. K. H., Kvasnicka, D. and Luitz, J., WEIN2k, (Karlheinz Schwarz Tech. Universitat Wien, Austria (2001) ISBN 3-9501031-1-2.
6 Stewart, R. F., Spackman, M. A. and Flensburg, C. (1998) VALRAY98.

CHARGE DENSITY STUDY UNDER HIGH PRESSURE

Makoto Sakata,[a] Takafumi Itsubo,[a] Eiji Nishibori,[a] Yutakata Moritomo,[a] Norimichi Kojima,[b] Yasuo Ohishi,[c] and Masaki Takata[a,c]

[a]Department of Applied Physics, Nagoya University, Chikusa, Nagoya 464-8603, Japan; [b]Graduate School of Arts and Science, University of Tokyo, Tokyo 153-8902, Japan; [c]Japan Synchrotron Research Institute, Kouto, Mikazuki-cho, Sayo-gun, Hyougo 679-5198, Japan (sakata@cc.nagoya-u.ac.jp)

It is very well known that physical properties of materials can be drastically changed by applying pressure, such as emergence of superconductivity of ladder compounds. It is also very common that materials undergo structural phase transitions when they start to show very different physical properties under high pressure. It is, therefore, highly desirable to determine structural changes accurately, preferably at electron density level, under high pressure. It is, however, not easy task to carry out accurate structure analysis under high pressure because of experimental restrictions, which prevent from the collection of an accurate X-ray diffraction data. The present state-of-art of structure refinements under high pressure is far from matured.

In order to produce high-pressure conditions, we have to use high-pressure cell, such as diamond anvil cell (DAC), which limit the amount of specimen to be used in the X-ray diffraction experiment to micro-gram order. Under such a condition, there is no doubt that third generation SR source has a great advantage. In this study, an accurate structural analysis of $Cs_2Au_2Br_6$ by using SR powder data collected at BL10XU, Spring-8 will be described. Gold atoms in $Cs_2Au_2Br_6$ are a mixed valence state at ambient pressure.

In this study, a DAC with large culet is used to have the powder specimen as much as possible. Because of this, the highest pressure to be reached by the DAC has to be limited to a few tenth GPa. The specimen was oscillated about 3.5 degree at all the pressure points, where the experiments were done. The oscillation was very effective to have homogeneous intensities along Debye ring, which is essential for the accurate structure analysis like charge density study. The collected data at 2.2GPa and 8.1Gpa are analysed by MEM/Rietveld analysis[1] to obtain the experimental charge density distributions.

In the Rietveld refinements, which is done as a preliminary analysis before MEM, the R-factors based on integrated Bragg intensities became as small as 1.28% and 1.05% at 2.2GPa and 8.1% GPa, respectively. It has to be admitted that the refinements is done satisfactorily to proceed further MEM analysis. From the MEM charge density map obtained in this study, it is revealed that the network structure is formed by covalency between Au and Br atoms at 8.1GPa, while at 2.2GPa Au and Br atoms form clusters. It is also recognised that the mixed valence state of Au at 2.2GPa transfers to the charge order states of Au+ and Au3+ at 8.1GPa. The present results may represent the present state-of-art of charge density studies under high pressure.

References

1 Takata, M., Nishibori, E. and Sakata, M. (2001) *Z. Kristallogr.* **216**, 71.

FERMI SURFACE OF A SHAPE MEMORY ALLOY OF TiNi

N. Shiotani,[a] I. Matsumoto,[a] H. Kawata,[a] J. Katsuyama,[b] M. Mizuno,[b] H. Araki,[b] and Y. Shirai[b]

[a]Photon Factory, KEK, Tsukuba, Ibaraki 305-0801, Japan; [b]Department of Materials Science and Engineering, Osaka University, Suita, Osaka 565-0871, Japan (shiotani@post.kek.jp)

The TA_2 [110] phonon anomaly observed in the pre-martensitic phase of the equiatomic intermetallic compound, TiNi, by inelastic neutron scattering has suggested nesting of the Fermi surface. So far, however, no direct observation of the Fermi surface has been reported.

We study the Fermi surface of $Ti_{48.9}Ni_{51.1}$ via high resolution Compton scattering. The Compton profiles are measured along 28 directions in the irreducible orientation triangle of cubic symmetry. Using Fourier-Bessel reconstruction scheme the 3-dimensional electron momentum density is obtained. The LCW-folding procedure is employed to map out the occupation number density in **k**-space. The results are compared with band theoretical predictions by Kakeshita et al. [1] and Zhao and Harmon [2].

References

1 Kakeshita, T., Fukuda, T. and Saburi, T. (2000) *Sci. Tech. Adv. Mat.* **1**, 63.
2 Zhao, G. L. and Harmon, B. N. (1993) *Phys. Rev.* B**48**, 2031.

PRECISE CHARGE DENSITY STUDY OF CYTOCHROME *c*-553 BY MAXIMUM ENTROPY METHOD

Masaki Takata,[a,b] Kenichi Kato,[b] Hiroshi Tanaka,[c] Atsushi Nakagawa,[d] and Makoto Sakata[a]

[a]Department of Applied Physics, Nagoya University, Nagoya 464-8603, Japan; [b]Japan Synchrotron Radiation Research Institute, Hyogo 679-5198, Japan; [c]Department of Material Science, Shimane University, Mtasue 690-8504, Japan; [d]The Institute for Protein Research, Osaka University, Suita 565-0871, Japan (takatama@spring8.or.jp)

Structures of various protein molecules are now studied extensively to explore the structural basis of the protein function. Therefore, the several experimental and analytical techniques have been developed in order to get a high-resolution crystallographic structure of protein crystal. However, most of the studies have been carried out for the atomic arrangement. In order to have a better and deeper understanding for functions and properties of the protein molecule, a precise charge density study is required to reveal bonding nature of molecule especially for an active segment. Recently, we have developed a new program of the Maximum Entropy Method, ENIGMA(Electron and Nuclear Image Generator by Max-ent Analysis)[1], for the charge density study of huge systems, such as proteins and polymers. By ENIGMA, we tackled charge density study of cytochrome *c*-553, and revealed precise charge density showing characteristic bonding nature of Heme group.

In the present study, we have employed synchrotron radiation single crystal data of cytochrome c-553, of which structure was solved by the multiple wavelength anomalous diffraction method [2]. The reliability factor of the obtained charge density is 2.4%, which is far beyond the value, 19.6%, of the previous conventional structure determination. The obtained charge density clearly exhibits the covalent bonding networks of atoms and the characteristic anisotropy of the Fe-N coordinate bonds in the heme group. Furthermore, the ability of the structure prediction by MEM revealed the solvent water molecule image in the crystal without assuming the existence of water molecule. The present result shall open the door to an accurate charge density study for the structure-function relationship of proteins.

References

1 H.Tanaka, et al. (2002) *J.Appl. Cryst.* **35**, 282-286.
2 A.Nakagawa, et al. (1990) *J.Biochem.* **108**, 701-703.

AN EXPERIMENTAL CHARGE DENSITY STUDY OF SINGLE-COMPONENT MOLECULAR METALS, $Ni(TMDT)_2$ AND $Au(TMDT)_2$.

E. Nishibori,[a] Y. Fujishiro,[a] M. Takata,[a] M. Sakata,[a] A. Kobayashi,[b] W. Suzuki,[b] E. Fujiwara,[b] H. Tanaka,[c] and H. Kobayashi[d]

[a]Department of Applied Physics, Nagoya University, Nagoya 464-8603, Japan; [b]Research Centre for Spectro-chemistry, Graduate School of Science, The University of Tokyo, Hongo, Bunkyo-ku, Tokyo 113-0033, Japan; [c]Nanotechnology Research Institute, National Institute of Advanced Industrial Science and Technology, Umezono, Tsukuba 305-8568, Japan; [d]Institute for Molecular Science and CREST, Myodaiji, Okazaki 444-8585, Japan (eiji@mcr.nuap.nagoya-u.ac.jp)

Recently, the molecular conductors, which consist of single-component molecules, have been attracted much interests, because of metallic behavior under certain circumstances. First metallic single-component molecule confirmed by the conductivity measurement was $Ni(tmdt)_2$ (tmdt: tri-methylene-tetra-thiafulvalence-dithiolate), which showed metallic behavior at very low temperature, i.e. below 0.6K[1]. After discovery of this material, similar single-component molecules with same extended-TTF (tetra-thiafulvalene) ligands were synthesized, such as $Cu(tmdt)_2$ and $Au(tmdt)_2$. Surprisingly enough, $Au(tmdt)_2$ showed metallic behavior at room temperature. The conductivity of $Au(tmdt)_2$ was $15Scm^{-1}$ at room temperature[2]. This value was over ten times smaller than that of $Ni(tmdt)_2(200Scm^{-1})$[1]. $Au(tmdt)_2$ and $Ni(tmdt)_2$ are iso-structure substances[1,2]. It would, therefore, be very important to study the electron density level structure to have better understanding of the difference of conductivity. In this study, the experimental charge density distributions of both $Au(tmdt)_2$ and $Ni(tmdt)_2$ were derived by the Maximum Entropy Method(MEM) using synchrotron radiation(SR) powder data.

SR powder experiment were carried out by the large Debye-Scherrer camera installed at BL02B2, Spring-8 for both $Ni(tmdt)_2$ and $Au(tmdt)_2$. The wavelength of incident X-ray was 1.0Å, which is rather long wavelength as third generation SR source. The reason for choosing this wavelength is to try to have better peak-separations of Bragg reflections. The collected data were analysed by MEM/Rietveld method[3] to derive experimental charge densities, which allows us to investigate the difference of charge densities of these compounds. From the comparison of obtained charge densities, it was found that there are distinct differences in Metal-S bond. The minimum electron density between Au-S bond were 0.18[e/ $Å^3$] in $Au(tmdt)_2$, which is much lower than that of Ni-S in $Ni(tmdt)_2$, i.e. 0.33[e/$Å^3$]. It was also found that electron density of TTF ligands in $Au(tmdt)_2$ was elongated toward the direction of adjacent molecule. This tendency was not seen in the case of $Ni(tmdt)_2$. These differences of charge density level structures would be related to the different behaviours of the electronic conductivity of these compounds.

References

1 Tanaka, H. et al. (2001) *Science* **291**, 285-287.
2 Suzuki, W. et al. (2003) *J. Am. Chem. Soc.*, **125**, 1486-1487.
3 Takata, M. et al. (1995) *Nature* **377**, 46-49.

MULTIPOLE REFINEMENTS WITH RIGID-BOND AND LINK CONSTRAINTS

T. Koritsanszky

Department of Chemistry, Middle Tennessee State University, TN, USA
(tkoritsa@mtsu.edu)

Controlling an often over-parametrized multipole refinement is an ultimate but seldom achieved goal. In this respect, model restrictions supporting the physically most significant least-squares solution, are always helpful. While preconceptions on the static density are routinely invoked (chemical and local symmetries), atomic anisotropic displacement parameters (ADP) are usually treated as free variables disregarding supportive information accessible from spectroscopic data and theoretical calculations.

This presentation describes easy-to-handle constraints applied to the shifts of ADP's that result in a linear least-squares cycle. The core property considered is the difference mean-squares displacement amplitude (DMSDA) matrix[1] corresponding to the intra-molecular vibrational modes that are readily obtained from theoretical force fields for geometry-optimized, isolated molecules:

$$\ddot{\mathbf{A}}_{AB} = \mathbf{r}_{AB}(\mathbf{U}_A - \mathbf{U}_B)\mathbf{r}_{AB}$$

where A and B refers to the nuclei linked and $\mathbf{r}_{AB}$ is the interatomic unit vector.

The refinement starts with the calculated intra-molecular ADP's (transformed to the crystal system) whose shifts are constrained, after each least-squares cycle, to yield a vanishing DMSDA matrix (all links are assumed to be rigid). The linearly independent links are derived via singular value decomposition of the matrix of constraints. This means, in general, 6N-M constraints, where N is the number of atoms in the molecule and M is the number of independent tensor elements of the rigid-body model[2]. The procedure described corresponds to a fit of the T, L and S tensors against the structure factors in the course of which the contributions of the intra-molecular modes to the ADP's are preserved. The method has several extra features: it provides rigid-body ADP's free of contaminations from intra-molecular vibrations, eliminates singularities and assigns ADP's also to hydrogen atoms.

An alternative approach starts the refinement with a set of rigid-body ADP's (yielding vanishing DMSDA matrix) and invokes a partial set of rigid-link constraints, only those that are consistent with a desired segmentation of the molecule into rigid atomic groups. This refinement corresponds to a fit of ADP's of the segmented rigid-body model to the structure factors.

Both options have been implemented into the new release of XD. Results from small molecule refinements are presented.

References

1 Hirshfeld, F. L. (1976) *Acta Crystallogr.* **A32**, 239.
2 Schomaker, V. and Trueblood, K. N. (1968) *Acta Crystallogr.* **B24**, 63.

STRUCTURAL RELATIONSHIP OF β-SODIUM (X=0.33) AND β′-COPPER (X=0.65) VANADIUM BRONZES $M_XV_2O_5$

Ruslan Ozerov,[a] Victor Streltsov,[b] and Alexander Sobolev[b]

[a]Mendeleev University of Chemical Technology of Russia, 125047 Moscow, Russia; [b]Crystallography Centre and Department of Chemistry, The University of Western Australia, Nedlands 6907, Western Australia, Australia (RPOzerov@www.mail.ru) and (Victor.Streltsov@csiro.au)

The β′-copper vanadium bronze single crystal structure $Cu_{0.65}V_2O_5$ has been studied at room, 75, and 9K temperatures and compared with the β-sodium vanadium bronze $Na_{0.33}V_2O_5$ structure (Ozerov et al 2001).

Temperature changes have not significantly affected the crystal structure. The centrosymmetric space group C2/m was accepted for the crystal structure studied. However, there are three space groups with the same extinction laws: centrosymmetric C2/m and two non-centrosymmetric Cm and C2. To our knowledge there are no information on possible ferroelectricity in this compound allowing to make the choice between them.

It was found that the copper atoms in the C2/m space group, contrary to the sodium compound, occupy three positions: Cu1 is in 4(i) position with coordinates x=0.541, y=0 and z =0.344 and Cu2 atoms in 8(j) position with coordinates x=0.529, y=0.038 and z =0,358. In the sodium compound, the Na atoms occupy only half of 4(i) positions in ordered or disordered manner while in the copper compound Cu atoms are distributed over three positions. Similar triple splitting of the copper atoms positioning in ED maps in copper bronze has been found by Kato et al, (1989). However these authors attributed it to the anharmonicity of the thermal vibration of the copper atoms. The splitting of the Cu position observed presently has been well confirmed at 9K in our studies. This suggests that distribution of copper atoms among three positions (one Cu1 and two Cu2) is rather static than dynamical one.

References

1 Kato, K., et al. (1989) *Acta Cryst.* **C45**, 1845-1847.
2 Ozerov, R.P., et al. (2001) *Acta Cryst.* **B57**, 244-250.

VALENCE STATE OF VANADIUM ATOMS IN β-$Na_xV_2O_5$ BRONZE

Ruslan P. Ozerov,[a] Alexandra A. Alexa,[a] and Victor A. Streltsov[b]

[a]Mendeleev University of Chemical Technology, Miusskaya Sq. 9, Moscow 125047, Russia; [b]CSIRO HSN, Parkville Vic 3052, Australia (rpozerov@mail.ru)

There are three types of vanadium atoms (V1, V2 and V3) in the crystal structure of β-phase of alkali vanadium bronze $M_{0.33}V_2O_5$ (M=Na, K and some other ions) [1-2]. They form a rigid oxygen-vanadium framework with alkali atoms disposed in the channels. It is well known that the two types of oxygen polyhedra around V1 and V2 atoms are nearly regular octahedra, however the third, around V3 atom, is strongly deformed resembling a trigonal bi-pyramid.

There is an intriguing question concerning the valence states of the V atoms in the structure which determine many properties of this crystal. It is suggested that one electron of the alkali atom is moved over to vanadium atom(s) influencing the change of their valence state. The question is to which vanadium atom(s) the electron is transferred. An attempt has been made recently to use the multipole model in the accurate crystal structure investigation of the Na-V-bronze [3]. However, the precision was not enough to make a definite conclusion.

The aim of this study is to apply the band-valence method to the problem. This method suggests the definite valence state to the central atom of the oxygen polyhedron on the base of the examination of the Me-O distances [4-5]. Using the valence band theory the valence state of all three vanadium atoms for $Na_{0.286}V_2O_5$ have been calculated and the results be discussed.

There were no unambiguous evaluations of the method accuracy. Moreover, one should notice that the results strongly depend on some values chosen *a priory*. Therefore, we can conclude that in this respect the most useful are the relative valences values of several ions in the same compound (see table 1) but not their absolute values.

References

1 Wadsley, A. D. (1955) *Acta Cryst.* **8**, 695-699.
2 Ozerov, R. P., Gol'der, G. A., and Zhdanov, G. S. (1957) *Kristallogr.* **2**, 217-225.
3 Ozerov, R. P., Streltsov, V. A., Sobolev, A. N., Figgis, B. N. and Volkov, V. L. (2001) *Acta Cryst.* **B 57**, 244-250.
4 Brese, N. E. and O'Keeffe, M. O. (1991) *Acta Cryst.* **B47**, 192-197.

DEVELOPMENT OF MEASURING MAGNETIC COMPTON PROFILES BY GRAZING INCIDENT GEOMETRY

Hiroshi Sakurai,[a] Fumitake Itoh,[a] Minoru Ota,[a] Katsuyoshi Takano,[b] Xioxi Liu,[b] and Hiroshi Kawata[c]

[a]Dept. Electronic Engineering, Gunma University, Kiryu, Gunma 376-8515, Japan; [b]SVBL, Gunma University, Kiryu, Gunma 376-8515, Japan; [c]Inst. Material Structure Science, KEK, Tsukuba, Ibaraki 305-0801, Japan (sakuraih@el.gunma- u.ac.jp)

Recent nano-structure in magnetic thin films becomes important for data storage devices such as MR head and perpendicular anisotropic media. A magnetic Compton profile (MCP) is agood candidate to measure the wavefunction of nano-structured films. However, it is difficult to measure the MCP's of the thin film because of strong scattering from substrates.

We have suggested to measuring MCP's by grazing incident geometry, and succeeded in measuring a thin Fe film with thickness of 200nm on a thick glass substrate as shown in Figure.

MCP measurements of a multilayer (Pd/Fe) and granular materials(MgF_2/Fe) are under way.

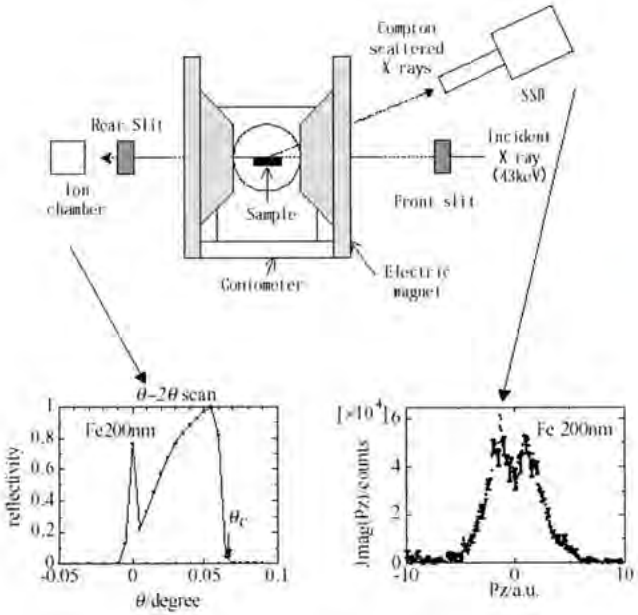

Figure

MAGNETIC COMPTON PROFILES OF MAGNETIC THIN FILMS AND ANISOTROPY OF Co/Pd MULTILAYER

M. Ota,[a] H. Sakurai,[a] F. Itoh,[a] M. Itou,[b] and Y. Sakurai[b]

[a]Department of Electronic Engineering, Gunma Univ., Japan, [b]SPring-8, Japan
(harasawakoike@excite.co.jp)

Magnetic Compton scattering is a good candidate to probe the electronic structures. However there are few measurements of thin films because of strong scattering from substrate. In this study we have succeeded in observing the magnetic Compton profile of magnetic thin film with substrate and the anisotropy of Co/Pd multilayer for the first time.

Fe 1μm was sputtered on the polyethylene terephtalate (PET) film with 4μm thickness. (Co(0.8*nm*)/Pd(1.6*nm*))417 multilayer with 1μm was also fabricated on the PET film. The films were folded in 16 to increase the effective volume. Magnetic Compton profiles of these samples were measured at the high-energy beamline BL08Wat the SPring-8, Japan. The incident X-ray energy was 174*keV* and the scattering angle was 175.8 *degree*. The incident beam and applied field (2.5T) were parallel or perpendicular to the sample plane.

Figure (1-a) shows magnetic Compton profiles of Fe 1μm sample on PET substrate together with Fe 10μm reference sample. Figure (1-b) shows differential profile of Figure (1-a). The difference is close to about 0. This result demonstrates that the measurement of magnetic Compton profiles in magnetic thin films is possible.

Figure (2-a) shows anisotropy of magnetic Compton profiles on (Co(0.8*nm*)/Pd(1.6*nm*))417 multilayer sample. Figure (2-b) shows differential profile of Figure (2-a). The difference is remarkable in the region of Pz<2(a.u.). This suggests that the dā states of Co 3d-band is responsible for the anisotropy. Further theoretical calculations are in progress.

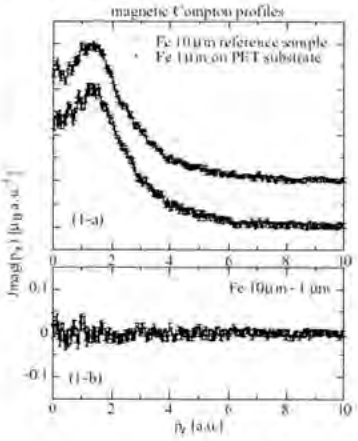

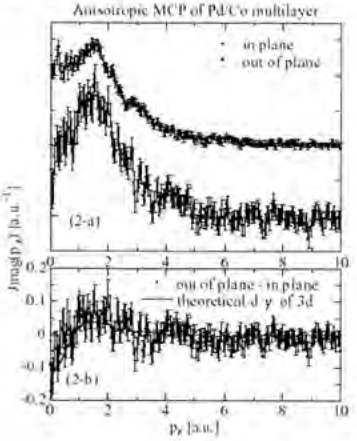

THE ELECTRON DENSITY TOPOLOGY CHANGES DUE TO THE PHASE TRANSITION IN $KmNF_3$

Yury V. Ivanov, and Kiyoaki Tanaka

Department of Material Science and Engineering, Nagoya Institute of Technology, Gokiso-cho, Showa-ku, Nagoya 466-8555, Japan
(yury@tana.mse.nitech.ac.jp)

Three high-precision X-ray diffraction experiments (MoK_{α}, T=190, 240 and 298K) for cubic perovskite potassium manganese trifluoride, $KMnF_3$, were carried out. The data obtained were approximated by Hansen-Coppens multipole model expanded up to hexadecupoles [1], the anharmonicity of atomic displacements up to 4-th level was considered. Figures of merit were: $R(|F|)$=0.0060, $R_w(|F|)$=0.0086, S=0.99 (for T=190K); $R(|F|)$=0.0065, $R_w(|F|)$=0.0089, S=1.00 (for T=240K); $R(|F|)$=0.0053, $R_w(|F|)$=0.0071, S=0.99 (for T=298K).

The maps of the model total static electron densities (ED) were calculated, and ED topological analysis was performed. At room temperature the ED exhibits 6 symmetry-equivalent bond critical points (CPs) on Mn-F lines and 12 on K-F lines. Thus, geometrical and topological coordination numbers of Mn and K atoms are the same: 6 and 12, correspondingly. The shapes of atoms in $KMnF_3$ defined by zero-flux surfaces in the gradient of ED are far from spherical. The ED basin of Mn atom separates the basins of neighboring F atoms in spite of the fact that F-F distance is the same as the K-F one. So, fluorine atom forms the bond paths with two Mn and four K atoms. Thus, it's topological coordination number is six, whereas geometrical coordination number is 12. At lower temperature the formation and strengthening of a new Mn-K bond path is observed. The topological coordination numbers become 20 and 14 for K and Mn, respectively. The weakening of K-F interaction is simultaneously observed.

The consideration of atomic displacements detects that the probability density function (PDF) of the F atom has single maximum at 298K and four maxima at 190K. So, fluorine position is split towards structural holes with the shift of 0.2Å. These pictures are in a good agreement with existence of point of phase transition at 186K. The crystal structure changes from *Pm3m* to *I4/mcm*, it can be described as a tilting of MnF_6 octahedron about *c* axis.

The ED values and curvatures at the bond CPs in $KMnF_3$ indicate the closed-shell type interactions between pairs K-F and Mn-K, whereas Mn-F bond can be considered as an intermediate type.

The topology of the electrostatic potentials (ESP) was studied as well. The pattern of (3,-1) CPs doesn't depend on temperature. These CPs were found on Mn-F, K-F, Mn-K, and K-K lines. Three of them correspond to the bond CPs in the ED, while the last appeared on the same points, where the global minimum in the ED exists. The bonded radii of K and Mn on cation-anion bonds derived from the ESP are vastly larger than those derived from ED. The fluorine anions show reverse picture. Thus, in terms of ESP the conventional concept of crystal structures depicting arrangement of small cations in cavities between large adjoining anions isn't justified. The notion about a cationic grid as a basis of structure is more adequate here.

Reference

1 Hansen, N. K. and Coppens, P. (1978) *Acta Cryst.* **A34**, 909-921.

STRUCTURE ANALYSIS OF GAS MOLECULES ADSORBED IN THE NANOCHANNEL OF A COORDINATION POLYMER BY THE MEM/RIETVELD METHOD

Yoshiki Kubota,[a] Masaki Takata,[b,c] Makoto Sakata,[b] Ryo Kitaura,[d] Ryotaro Matsuda,[d] Susumu Kitagawa,[d] Tatsuo Kobayashi,[e] Kouichi Kindo,[e] Yoshimi Mita,[f] Akira Matsuo,[e] Michihiro Kobayashi,[f] Ho-Chol Chang,[d] Tadashi Oszawa,[g] and Megumi Suzuki[f]

[a]Dept. of Environmental Sciences, Osaka Women's University, Osaka 590-0035, Japan; [b]Dept. of Applied Physics, Nagoya University; [c]JASRI/SPring-8; [d]Dept. of Synthetic Chemistry and Biological Chemistry, Kyoto University; [g]KYOKUGEN; [f]Dept. of Physical Science, Osaka University, Japan (kubotay@center.osaka-wu.ac.jp)

Recently, various coordination polymers with uniform ordered nanochannels were successfully synthesized by the combination of metal ions and organic molecules. Many of these compounds are found to have extremely high performance gas adsorption and are expected to be promising gas storage materials. So far, adsorbed gas molecules were thought to be trapped in the ordered nanochannels of the material. However, there is no structural evidence for the trapped gas molecule position inside the micropore. Thus, in order to determine the trapped gas molecule position and structure within the material, we have done in-situ synchrotron radiation powder diffraction experiment and revealed the formation of a one-dimensional array of gas molecules along the nanochannels by the MEM/Rietveld analysis.

The sample used in the present study is $[Cu_2(pzdc)_2(pyz)]_n$ (pzdc=pyrazine-2,3-dicarboxylate, pyz=pyrazine), which has a pillared layer structure with 1D nanochannels with dimensions of about 4 x 6 A (CPL-1:coordination ploymer 1 with pillared layer structure). The synchrotron powder diffraction data was collected by the large Debye-Scherrer camera installed at SPring-8 BL02B2. The powder sample was sealed in glass capillary. The gas import tube is attached to the goniometer head to fill O_2 gas in capillary. The gas adsorption is controlled by lowering the temperature not by the gas pressure. The data measurement was carried out from 300K to 90K under 80kPa O_2 pressure. The fundamental crystal structure of CPL-1 had been reported by single crystal X-ray structure analysis. The powder diffraction pattern from 300K to 150K is almost the same with that of the reported structure. However, we investigated the dramatic changes of diffraction pattern at 130K which should be due to the O_2 molecule adsorption. In the first Rietveld analysis of the 90K data, we started the analysis with the fundamental structure of CPL-1 without assuming O_2 molecules. The reliability factors based on the powder pattern, R_{WP} and the integrated intensities, R_I were 18.5% and 54.2%, respectively. However, the MEM charge density visualized the density like O_2 molecules in the middle of the nanochannels. According to the MEM charge density, we determined the structure model of the CPL-1 adsorbing O_2 gas molecule. The R_{WP} and R_I for the Rietveld analysis with the final structure model were improved to be 2.1% and 3.9%, respectively. In the MEM charge density, the dumbbell shaped electron distribution was clearly observed in the middle of the nanochannels. The charge of the distribution was estimated to be almost 16e indicating no charge transfer from the O_2 molecule to CPL-1, which means O_2 gas was physisorbed to CPL-1. And, we found adsorbed O_2 molecules form one dimensional array along nanochannels. The details of the determined structure and novel characteristic magnetic property caused by O_2 adsorption will be presented.

MOMENTUM TRANSFER DEPENDENCE OF X-RAY RAMAN SCATTERING AT THE BERYLLIUM K-EDGE

M. Volmer,[a] C. Sternemann,[a] J. A. Soininen,[b,c] H. Nagasawa,[d] M. Paulus,[a] H. Enkisch,[a] G. Schmidt,[e] M. Tolan,[a] and W. Schülke[a]

[a]Institute of Physics, University of Dortmund, D-44221 Dortmund, Germany; [b]Department of Physics, University of Washington, Seattle, Washington 98195, USA; [c]OpticalTechnology Division, National Institute of Standards and Technology, Gathersburg, Maryland 20899, USA; [d]Faculty of Economics, Seikei University, Tokyo, 180-8633, Japan; [e]DELTA, University of Dortmund, D-44221 Dortmund, Germany
(schenkel@physik.uni-dortmund.de)

We studied the Beryllium K-edge using non-resonant x-ray Raman scattering at different momentum transfers, thus probing the unoccupied density of states with access to different symmetries of the final states of the excited electrons. We measured data for a Be polycrystal as well as for a single crystal with momentum transfer both parallel and perpendicular to the c-axis. The measurements have been carried out at the superconducting wiggler beamline SAW2 of the DELTA synchrotron [1] making use of the standard IXSS setup [2]. Energy loss spectra were measured at momentum transfers q=0.64 (1.27) a.u. where the dipole approximation is appropriate to describe the excitation process so that 1s→p transitions dominate the x-ray Raman scattering cross section. By changing the scattering angle, q has been increased up to 4.78 a.u. making 1s→s transitions possible, resulting in a strong change in shape of the K-edge energy loss spectra. Additionally the single crystal spectra show distinct differences for a momentum transfer parallel and a momentum transfer perpendicular to the c-axis at low q. This directional dependence vanishes at higher q.

The experimental data are compared with first principles calculations modeling x-ray Raman scattering and its momentum transfer dependence [3-4].

References

1 Dortmund Electron Accelerator (DELTA), University of Dortmund, Maria-Goeppert-Mayer-Str. 2, D-44221 Dortmund, Germany (*www.delta.uni-dortmund.de*).
2 Berthold, A., Mourikis, S., Schmitz, J. R., Schülke, W. and Schulte-Schrepping, H. (1992) *Nucl. Instr. Methods A* **317**, 373.
3 Soininen, J. A. and Shirley, E. L. (2001) *Phys. Rev. B* **64**, 165112.
4 Soininen, J. A., Hämäläinen, K., Caliebe, W. A., Kao, C. -C. and Shirley, E. L. (2001) *J. Phys.: Condens. Matter* **13**, 8039.

CONSTRAINED DENSITY FUNCTIONAL THEORY USING X-RAY DIFFRACTION DATA

Daniel J. Grimwood

Chemistry, School of Biomedical & Chemical Sciences, University of Western Australia, Crawley, WA 6009, Australia (reaper@theochem.uwa.edu.au)

A constrained density functional method using X-ray diffraction data is developed. The method is applied to N_2O_4. A comparison is made with the constrained Hartree-Fock method [1], to determine which method is better suited to reproduce experimental structure factors.

References

1 Jayatilaka, D. and Grimwood, D. J. (2001) *Acta Cryst.* A**57**, 76-86.

A WAVEFUNCTION CONSTRAINED JOINTLY TO X-RAY AND POLARISED NEUTRON DIFFRACTION DATA FOR THE Cs_3CoCl_5 CRYSTAL

Dylan Jayatilaka

Chemistry, School of Biomedical & Chemical Sciences, University of Western Australia, Crawley, WA 6009, Australia (dylan@theochm.uwa.edu.au)

The experimental wavefunction technique [1,2] is extended, to implement the joint refinement of X-ray and Polarised Neutron Diffraction (PND) data. Results are presented for the $CoCl_4^{2-}$ ion in the Cs_3CoCl_5 crystal.

References

1 See, e.g., Grimwood, D., Bytheway, I. and Jayatilaka, D. (2003) *J. Comp. Chem.* **24**, 470-483.

2 Grimwood, D. and Jayatilaka, D., *TONTO: A System for Computational Chemistry,* www.theochem.uwa.edu.au/tonto/index.html.

CRYSTAL EXPLORER: A GRAPHICAL USER INTERFACE FOR DISPLAYING AND MANIPULATING HIRSHFELD SURFACES AND FINGERPRINTS FOR CRYSTAL ENGINEERING APPLICATIONS

Dylan Jayatilaka, Daniel Grimwood and Stephen Wolff

Chemistry, School of Biomedical & Chemical Sciences, University of Western Australia, Crawley, WA 6009, Australia (dylan@theochem.uwa.edu.au).

The Hirshfeld surface is a region enclosing a moeity in a crystal, within which more than 50% of the electron density comes from that moeity [1]. The surface can be coloured in a number of ways, to highlight local packing interactions in the crystal [2,3]. In addition, a fingerprint of the surface can be made which quickly and clearly displays in a 2D format inter-moeity interactions - thus making comparison of crystalline interactions in different crystal structures straightforward [4].

Crystal Explorer is a graphical user interface (GUI) for manipulating Hirshfeld surfaces [5] and the associated fingerprints. Examples demonstrating the use of the GUI will be presented.

References

1 Spackman, M.A., Byrom, P.G. (1997) *Chem. Phys. Lett.*, **267**, 215-220.
2 McKinnon, J.J., Mitchell, A.S., Spackman, M.A., (1998) *Chem. Eur. J.*, **4**, 2136-2141.
3 McKinnon, J.J., Mitchell, A.S., Spackman, M.A., (1998) *Chem. Comm.*, **4**, 2071-2072.
4 Spackman, M.A., McKinnon, J.J, (2002) *Cryst. Eng. Comm.*, 378-392.
5 *Crystal Explorer: A GUI for manipulating Hirshfeld Surfaces*, www.theochem.uwa.edu.au/crystal_explorer.

STUDY OF METAL-INSULATOR TRANSITION IN Rb_4C_{60} BY COMPTON SCATTERING, UNDER PRESSURE

Genevieve Loupias,[a] A. A. Sabouri-Dodaran,[a] M. Marangolo,[a] Ch. Bellin,[a] F. Mauri,[a] S. Rabii,[a,b] Th. Buslaps,[c] M. Mezouar,[c] and W. Crichton[c]

[a]Laboratoire de Minéralogie-Cristallographie de Paris, Univ. Paris VI, case 115, 4 pl. Jussieu, F-75252 Paris Cedex 05, France; [b]Dept. of Elect. Eng., Univ. of Pennsylvania, Philadelphia, PA 19104-6390, USA; [c]European Synchrotron Radiation Facility (ESRF), BP 220, F-38043 Grenoble-Cedex, France (loupias@lmcp.jussieu.fr)

LDA band structure calculations on the bct Rb_4C_{60} [1] claim a metallic behavior for this material but they are strongly at odds with the NMR and photoemission finding of an insulating ground state.

Compton scattering was used to measure the ground state momentum density in Rb_4C_{60} and theoretical directional Compton Profiles, obtained from wave-function calculations, was used for comparison [2]. In this molecular solid, the Jahn-Teller distortion of the C_{60} molecules was not taken into account by previous LDA calculations and was assumed to be responsible of the mismatch between theoretical and experimental Compton Profile of A_4C_{60} (A=Rb and K) compounds. In particular, this effect – which has not yet been clearly experimentally observed – is invoked to be responsible of the Mott insulating phase in A_4C_{60}.

In order to switch off the Jahn Teller effect, we have performed new measurements of Rb_4C_{60} Compton Profiles below and above the metal-insulator transition at 0.8 GPa (respectively 0.1 and 1.9 GPa). The difference of Compton Profiles will be compared with corresponding calculated results, obtained from our recent ab-initio energy band structure calculations. In particular, these calculations allowed us to quantitatively discriminate kinetic energy effect induced by pressure and Jahn-Teller effect, on momentum densities.

As a consequence, a new model will be presented to explain metal-insulator transition, supported by both new experimental and theoretical Compton results.

References

1 Erwin, S. C. and Bruder, C. (1994) *Physica B* **199**, 600.

2 Marangolo, M., Bellin, Ch., Loupias, G., Rabii, S., Erwin, S. C. and Buslaps, T. (1999) *Phys. Rev. B*, 17084.

ARE ELECTRON CORRELATION EFFECTS OBSERVABLE IN ELASTIC X-RAY SCATTERING EXPERIMENTS?

Graham Chandler, Ian Bytheway, Brian Figgis, and Dylan Jayatilaka

Chemistry, School of Biomedical & Chemical Sciences, University of Western Australia, Crawley WA 6009, Australia (gsc@chem.uwa.edu.au)

Difference density maps clearly show shifts in the density when Hartree-Fock calculations are compared with those incorporating correlation effects [1]. However,as pointed out by Wiberg *et al.* for many stable molecules the charge redistribution from electron correlation should be a small correction compared with the accuracy of experimental observations[2]. Are they large enough to be detectable?

To test this matter X-ray structure factors which include thermal smearing effects taken from experimental measurements, have been calculated for a range of small-molecule molecular crystals from spherical atom procrystal electron densities, and Hartree-Fock, QCISD, and density functional (B3LYP) electron densities using the superposition of independent molecules method. These calculations were carried out to assess whether the effects of electron correlation on the electron density cause sufficient change in structure factors when compared with those from Hartree-Fock to enable the correlation effect to be experimentally detectable.

The spherical atom procrystal calculations have been used in showing the magnitude of the effect which chemical bonding makes on structure factors. X-ray data was shown to be capable of distinguishing the effects of chemical bonding long ago [3]. However, the specific effect of bonding on structure factors has not been examined before. It was included in our calculations for the added insights it may give to the determination of bonding effects from X-ray data and also to demonstrate the great difference in magnitude of the changes in structure factors generated by correlation when compared to the changes caused by bonding.

The results of this investigation will be presented.

References

1 Boyd, R. and Wang, L. (1989) *J. Comput. Chem.* **10**, 367.

2 Wiberg, K., Hadad, C., LePage, T., Breneman, C. and Frisch, M. (1992) *J. Phys. Chem.* **96**, 671.

3 Coppens, P. (1997) *X-ray Charge Densities and Chemical Bonding*, (Oxford University Press, New York); Dawson, B. (1967) *Proc. Roy. Soc.* **A298**, 255.

Friday August 15

Sagamore XIV

ABSTRACTS

ORAL SESSIONS

INELASTIC MAGNETIC X-RAY SCATTERING FROM HIGHLY CORRELATED ELECTRON SYSTEMS

P. A. Montano,[a,b] Y. Li,[b,c] J. F. Mitchell,[c] P. E. Mijnarends,[d,e] S. Kaprzyk,[d,f] B. Barbiellini,[d] and A. Bansil[d]

[a]Materials Sciences and Engineering, SC-13Germantown Bldg. U.S. Department of Energy, 1000 Independence Ave. SW, Washington DC 20585, USA; [b]Department of Physics, University of Illinois, Chicago IL 60680, USA; [c]Materials Science Division, Argonne National Lab., 9700 South Cass Ave. Argonne IL 60439,USA; [d]Department of Physics, Northeastern University, Boston, MA 02115, USA; [e]Delft University of Technology, Delft, The Netherlands; [f]Academy of Mining and Metallurgy, al. Mickiewicza 30, 30-059 Cracow, Poland (pedro.montano@science.doe.gov)

We have used the magnetic Compton scattering (MCS) technique to determine the spin distribution in highly correlated electronic systems. These systems have extremely interesting physical properties such as their electronic transport and magnetic behavior as well as their interrelationship. We report MCS experiments on colossal magneto resistance (CMR) perovskite manganite $La_{0.7}Sr_{0.3}MnO_3$, bilayered perovskite manganite $La_{1.2}Sr_{1.8}Mn_2O_7$, and magnetite Fe_3O_4. The experiments were carried out at various temperatures along different crystallographic directions and at different magnetic fields. Spin moments are calculated and their changes with temperature along different directions at different external magnetic fields are presented. For this purpose magnetic Compton profiles (MCP) along low-index crystallographic directions were measured using the elliptical multipole wiggler (EMW) installed at beamline 11-ID-B of the Advanced Photon Source (APS). The line shapes of the Magnetic Compton profiles are analyzed using a simple approximation with atomic d orbitals and free electron gas model. The modeling was used to investigate the electron distribution in the ground state. The band structure of the $La_{1.2}Sr_{1.8}Mn_2O_7$ was computed semi-relativistically within the conventional local-spin-density approximation based band theory framework and spin self-consistent KKR framework. The experimental MCPs were compared with the corresponding first-principles computations and a very good overall level of accord was found. Within the resolution of the experimental data, some Fermi surface signatures in the MCPs could be identified in accord with theoretical predictions. Our analysis indicates that the MCPs are well-explained in terms of spin contribution and that orbital effects are negligible for $La_{1.2}Sr_{1.8}Mn_2O_7$. It is observed that in $La_{0.7}Sr_{0.3}MnO_3$, the spin moment changes insignificantly from 5K to 100K and then drops rapidly at temperatures above 100K. At the same time, an itinerant electron feature observed at 5 K disappears for temperatures higher than 100K. The magnetite Fe_3O_4 MCP show an itinerant electron feature at all temperatures from 10K up to 300K. This result suggests a significant role for the itinerant electrons even in the low temperature region, which is in disagreement with a simple charge ordering picture. The spin moment behavior of magnetite also shows correlation with the conductivity around Verwey transition temperature.

This work was supported by the US DOE.

ELECTRON CORRELATION EFFECTS IN NOVEL MATERIALS: RECENT STUDIES OF CUPRATES, MANGANITES AND 3D QUANTUM DOTS

Arun Bansil

Department of Physics, Northeastern University, Boston, MA 02115, USA
(bansil@neu.edu)

Electron correlation effects are becoming an increasing focus of attention in understanding the behavior of wide classes of novel materials. This talk presents some of our recent work concerning several systems of current interest. In connection with the cuprate superconductors, we show how the Fermi surface evolves with electron doping in $Nd_{2-x}Ce_xCuO_{4-\delta}$ as the Mott pseudogap collapses, in the light of recent high resolution ARPES experiments and related mean field Hartree-Fock and self-consistent renormalization computations within the framework of the one-band t-t'-t''-U Hubbard model Hamiltonian. We also discuss how the ARPES matrix element via its selectivity properties can be exploited to focus on interesting physics in the cuprates (e.g. the issue of coherence effects and bilayer splitting in Bi2212). In connection with quantum dots, we discuss an exactly solvable model Hamiltonian for describing the interacting electron gas in a quantum dot. Results for a spherical square well confining potential are presented. The ground state is found to exhibit striking oscillations in spin polarization with dot radius at a fixed electron density. These oscillations are shown to induce characteristic signatures in the momentum density of the electron gas, providing a novel route for direct experimental observation of the dot magnetization via spectroscopies sensitive to the electron momentum density. Finally, brief comments are made on recent magnetic Compton scattering measurements on $La_{1.2}Sr_{1.8}$Mn_2O_7 from which we adduce that orbital effects on the momentum density in this CMR material are quite small.

SUPERCONDUCTIVITY AND FERROMAGNETISM OF $ZrZn_2$

Zs. Major,[a] S. B. Dugdale,[a] R. Watts,[a] G. Santi,[a] M. A. Alam,[a] S. M. Hayden,[a] J. A. Duffy,[b] J. W. Taylor,[b] T. Jarlborg,[c] E. Bruno,[d] D. Benea,[e] and H. Ebert[e]

[a]H.H. Wills Physics Laboratory, University of Bristol, Tyndall Avenue, Bristol BS8 1TL, UK; [b]Department of Physics, University of Warwick, Coventry CV4 7AL, UK; [c]DPMC, University of Geneva, 24 quai Ernest Ansermet, CH-1211 Geneva 4, Switzerland; [d]Deparment of Physics, Univeristy of Messina, Salita Sperone 31, 98166 Messina, Italy; [e]Institute for Physical Chemistry, Ludwig-Maximilians University, Butenandtsrasse 5-13, 81377 Munich, Germany (zs.major@bristol.ac.uk)

The discovery of the ferromagnetism co-existing with superconductivity in the compound UGe_2 [1], followed by similar discoveries in $ZrZn_2$ [2] and URhGe [3], has re-opened the debate about the relationship between magnetism and superconductivity. At the centre of this debate is the question of the pairing mechanism for the superconductivity, with the speculation that it is magnetically rather than phonon-mediated.

Knowledge of the topology of the Fermi surface (FS) is vital to an understanding of the superconductivity. Furthermore, such measurements are a stringent test of electronic structure calculations, on which our models for the superconductivity rely. Our recent quantum oscillatory measurements of the FS of ferromagnetic $ZrZn_2$ [4] have revealed a FS topology that is in agreement with our LMTO band structure calculations; however, the quasiparticles are strongly renormalized, to such a degree that there is no clear experimental evidence of the heaviest sheet. This sheet is important because it contributes about half of the density-of-states at the Fermi level. Also, there is some indication that FS nesting could be important, both in terms of the possibility of a Fulde-Ferrell-Larkin-Ovchinnikov (FFLO) superconducting state [5], and also in terms of spin-fluctuations and magnetically mediated pairing [6,7]. Given its likely dominance in determining physical properties, information about this unobserved sheet is vital.

We present the results of our investigation into these specific aspects of the superconductivity and ferromagnetism in $ZrZn_2$ using two different momentum density measurements. First, our positron annihilation study of the (paramagnetic) FS, and our search for signatures of the heavy sheet, is discussed. Secondly, we have used magnetic Compton scattering to address the issue of the delocalisation of the magnetic moment as an additional insight into the electronic structure. Both these measurements are supported by first-principles electronic structure calculations, and their implications discussed in terms of possible mechanisms for the superconducting pairing.

References

1 Saxena, S. S., *et al.* (2000) *Nature (London)* **406,** 587.
2 Pfleiderer, C., *et al.* (2001) *Nature (London)* **412,** 58.
3 Aoki, D., *et al.* (2001) *Nature (London)* **413,** 613.
4 Yates, S. J. C., *et al.* (2003) *Phys. Rev. Lett.* **90,** 057003.
5 Singh, D. J. and Mazin, I. I. (2002) *Phys. Rev. Lett.* **88,** 187004.
6 Santi, G., *et al.* (2001) *Phys. Rev. Lett.* **87,** 247004.
7 Fay, D. and Appel , J. (1980) *Phys. Rev. B* **22,** 3173.

WAVE-FUNCTION-BASED AB INITIO METHODS FOR ELECTRONIC STRUCTURE CALCULATIONS ON INSULATORS

Alok Shukla

Physics Department, Indian Instititute of Technology, Powai, Mumbai 400076, India (shukla@phy.iitb.ac.in)

Traditionally, the *ab initio* electronic structure calculations for crystalline systems have been performed within the framework of density functional theory (DFT). However, it is a well-known fact that the DFT does not perform satisfactorily for systems in which electron correlations are strong. As far as excited state properties are concerned, DFT-based approaches systematically underestimate the band-gaps and band-widths of even weakly correlated systems such as semiconductors. Additionally, DFT-based approaches are not amenable to systematic improvements. Therefore, there is a need to go back to the basics and investigate the feasibility of computing the electronic structure of solids via the wave-function route, i.e., by directly solving the Schroedinger equation. The advantages of such an approach are obvious - one can perform both the mean-field (Hartree-Fock) as well as many-body calculations (CI, coupled-cluster etc.) within the same formalism.

Over last several years we have pursued such an approach for crystalline insulators using the Wannier-functions (as against the Bloch orbitals) as the single-particle orbitals, and have performed both Hartree-Fock and the correlated calculations on several ionic and covalent systems. In our talk, we will describe our approach whose implementation resulted in the computer program WANNIER [1,2] and also present results concerning electronic and lattice properties of several crystalline insulators [3,4]. We will argue that such an approach can also be extended to metallic systems, provided one uses a nonorthogonal set of localized orbitals.

References

1 Shukla, A., Dolg, M., Fulde, P. and Stoll, H. (1998) *Phys. Rev. B* **57**, 1471.
2 Shukla, A., Dolg, M., Fulde, P. and Stoll, H. (1999) *Phys. Rev. B* **60**, 5211.
3 Shukla, A. (2000) *Phys. Rev. B* **61**, 13277.
4 Abdurahman, A., Shukla, A. and Dolg, M. (2002) *Phys. Rev. B* **65**, 125204.

THE SIESTA METHOD: PRESENT STATUS AND FUTURE PROSPECTS

Julian D. Gale,[a] Emilio Artacho,[b] Alberto Garcia,[c] Javier Junquera,[d] Pablo Ordejón,[e] Daniel Sánchez-Portal,[f] and José M. Soler[g]

[a]Department of Chemistry, Imperial College London, South Kensington, SW7 2AZ, U.K.; [b]Department of Earth Sciences, University of Cambridge, Downing Street, Cambridge, CB2 3EQ, U.K.; [c]Departamento de Fisica de la Materia Condensada, Universidad del País Vasco, Apt. 644, 48080 Bilbao, Spain; [d]Institut de Physique, Bâtiment B5, Université de Liège, B-4000 Sart-Tilman, Belgium; [e]Institut de Ciència de Materials de Barcelona, CSIC, Campus de la UAB, Bellaterra, 08193 Barcelona, Spain; [f]Dep. de Física de Materiales and DIPC, Facultad de Química, UPV/EHU, Apt. 1072, 20080 Donostia, Spain; [g]Dep. de Física de la Materia Condensada, C-III, Universidad Autónoma de Madrid, E-28049 Madrid, Spain (j.gale@imperial.ac.uk)

In order to achieve the goal of being able to perform *ab initio* electronic structure calculations on very large molecular and condensed matter systems it is necessary to address the issue of the calculation scaling with increasing system size. Here the details of the SIESTA method [1,2] will be presented, which makes it possible to perform calculations that scale linearly with increasing numbers of atoms, both in computational expense and memory usage. This is achieved through the use of radially confined basis functions that lead to sparse matrices, in combination with an auxillary basis of a real space mesh for the evaluation of the Hartree and exchange-correlation potentials. In addition, linear scaling requires the use of functional minimization approaches to solve for self-consistency, though conventional matrix diagonalisation is also available. Through the use of parallel computing, and the above methodology, it is now quite feasible to perform *ab initio* calculations on thousands of atoms.

Many standard observables of electronic structure theory may be obtained including electron and spin densities, optimized structural configurations, phonons, as well as dynamical information. Examples will be given of the application of the technique, as well as possible directions for future advancement.

References

1 Artacho, E., Sánchez-Portal, D., Ordejón, P., García, A., and Soler, J. M. (1999) *Phys. Stat. Sol. B* **215**, 809-817.

2 Soler, J. M., Artacho, E., Gale, J. D., Garcia, A., Junquera, J., Ordejón, P. and Sánchez-Portal, D. (2002) *J. Phys.: Condens. Matter* **14**, 2745-2779.

SOME NEW DEVELOPMENTS WITH WAVEFUNCTIONS CONSTRAINED TO EXPERIMENTAL SCATTERING DATA

Dylan Jayatilaka

Chemistry, School of Biomedical and Chemical Sciences, University of Western Australia, Crawley, WA 6009, Australia (dylan@theochem.uwa.edu.au)

Over the last few years we have developed methods to constrain *ab initio* Hartree-Fock wavefunctions to reproduce observed X-ray structure factors for molecular crystals [1,2]. In the talk I will outline some new developments under way in our group:

1. The estimation of errors in derived properties obtained from the constrained wavefunctions, due to errors in the experimental measurements.
2. The use of constrained density functional theory (DFT) wavefunctions.
3. The use of X-ray and Polarised Neutron Diffraction (PND) structure factors to jointly constrain the wavefunctions.
4. An idea of how to constrain non-variational wavefunctions, such as the coupled cluster type wavefunctions, to reproduce experimental scattering data.

References

1 See, e.g., Grimwood, D., Bytheway, I., Jayatilaka, D., (2003) *J. Comp. Chem.* **24**, 470-483, and references therein.

2 Grimwood, D., Jayatilaka, *TONTO: A System for Computational Chemistry* www.theochem.uwa.edu.au/tonto/index.html.

Saturday August 16

Sagamore XIV

ABSTRACTS

ORAL SESSIONS

POSITION AND MOMENTUM DENSITIES COMPLEMENTARITY AT WORK, REFINING A QUANTUM MODEL FROM DIFFERENT DATA SETS

J. -M. Gillet, S. Ragot, and P. J. Becker

Laboratoire Structures, Propriétiés et Modélisation des Solides, CNRS/UMR8580, Ecole Centrale Paris, Grande Voie des Vignes 92295 Chatenay-Malabry Cedex, France (gillet@spms.ecp.fr)

Although Bragg and Compton scattering are well-established techniques, very few attempts to combine information originating from those experiments have been made so far. This remark also holds for Bragg magnetic scattering.

We propose a quite general procedure to refine a quantum model from different data sets using basic Bayesian statistics. As an illustration, different results for extracting chemical information such as charge transfer in ionic-covalent compounds will be given.

Influence of correlation in data, as introduced in momentum density reconstruction, will be explored and extension to other combinations of experiments will be suggested.

At a different level of interpretation and accuracy, a simultaneous approach of position and momentum representations of the One electron Density Matrix (1DM) requires, at least, a possibility of working beyond the straight path of "independent electrons" scheme in a perfect 3D lattice. We will describe an ab-initio computational strategy to the calculation of the 1DM that reproduces infinite lattices results with a good accuracy but that enables for the of defects in the structure as well as a fair account for electron correlation energy. This Cluster Partitioning Method (CPM) will be shown to be efficient for studies ranging from intra-atomic correlation mechanisms in ionic solid to analysis of hydrogen bond in ice and, with few compromises, an extension to more complicated structures.

ELF: FOR THE GOOD AND FOR THE BAD

Andreas Savin

Laboratoire de Chimie Théorique, CNRS et Université Pierre et Marie Curie, Paris, France (andreas.savin@lct.jussieu.fr)

The electron localization function (ELF) of Becke and Edgecombe [1] is a tool to analyze chemical bonding in molecules and solids. After a decade of applications, this talk is a view back, about the soundness of its definition, its advantages and limitations, its perspectives, but also about some of its competitors.

Reference

1 Becke, A. D. and Edgecombe, K. E. (1990) *J. Chem. Phys.* **92**, 5397.

SINGLE-PARTICLE ORBITALS AND MANY-BODY COMPTON SCATTERING

Bernardo Barbiellini

Department of Physics, Northeastern University, Boston, MA 02115, USA
(bba@neu.edu)

Single particle orbitals continue to play a useful role even when one considers properties of correlated electron systems. The natural orbitals introduced by Löwdin, which form an orthonormal basis set, are a particularly suitable set of one-particle functions to use for ground-state electron momentum density (EMD) computation [1]. In the independent particle model (IPM), the occupancy of a natural orbital can only be 1 or 0. The introduction of correlations then yields occupation numbers with values which differ from 0 or 1, with most high energy states being nearly unoccupied. We also discuss the so-called Dyson orbitals, which are a different set of one-particle orbitals associated with many-body states and related spectral functions. These orbitals however are in general not normalized and can be linearly dependent. We show how Dyson orbitals can be used to express the Compton scattering cross-section beyond the constraints of the commonly invoked framework of the impulse approximation (IA) [2]. Our goal is to develop computationally tractable schemes for obtaining Compton scattering cross-section beyond the IPM and IA. Illustrative results on Li, Al, Be and Cr are presented.

References

1 Barbiellini, B. and Bansil, A. (2001) *J. Phys. Chem. Solids* **62**, 2181.
2 Kaplan, I.G., Barbiellini, B. and Bansil, A., preprint cond-mat/0304294.

CHEMICAL INFORMATION FROM THE SOURCE FUNCTION

C. Gatti, F. Cargnoni, and L. Bertini

CNR-ISTM, Istituto di Scienze e Tecnologie Molecolari, via Golgi 19. 20133 Milano, Italy (c.gatti@istm.cnr.it)

Recently it was shown [1] that one may view the electron density at any point **r** within a molecule to consist of contributions from a source $G(\mathbf{r}, \mathbf{r}')$ operating at all other points $\mathbf{r}'$. By evaluating the source over regions bounded by surfaces that satisfy the topological definition of an atom[2], the density at **r** may be equated to a sum of atomic source contributions $S(\mathbf{r},\Omega)$

$$\tilde{n}(\mathbf{r}) = -(1/4\pi)\int \frac{\nabla'^2 \tilde{n}(\mathbf{r}')}{|\mathbf{r}-\mathbf{r}'|} d\mathbf{r}' = -(1/4\pi)\sum_\Omega \int_\Omega G(\mathbf{r},\mathbf{r}')d\mathbf{r}' \equiv \sum_\Omega S(\mathbf{r},\Omega)$$

Such a decomposition enables one to view the properties of the density from a new perspective and establishes the source function (SF) as a potentially interesting tool to provide chemical information.

This study [3] is aimed at widening up the limited spectrum of applications of the SF [1,4] so as to increase the knowledge of properties and usefulness of the SF. We examine a number of cases, including (a) the effect of the X substitution on the source contribution from A to the electron density at bond critical point (BCP) in AX diatomics and the extent to which the near transferability of the integral properties of A, when present, is reflected in the source contribution from A to the BCP density; (b) the relative weight of the internal and external contribution to the density at a (3,-3) critical point when this is a non-nuclear maximum, rather than a maximum associated to a nuclear-cusp; (c) the relative weight of source contributions from the atoms of H-bond complex to the density at the H-bond CP, in a series of complexes of increasing strength. The correspondence between the H-bond classification provided by the ELF topological approach and by the SF is also highlighted.

The figure on the right, where circles are proportional to the $S(\mathbf{r},\Omega)$ from different atoms Ω and with negative sources in light grey, clearly shows how the SF discriminates among very strong, intermediate and weak H-bond complexes.

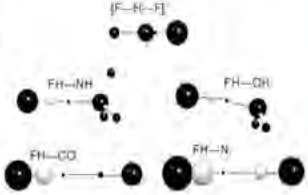

It is concluded that the SF appears as a practical tool to unravel the local and non local character of the electron density distributions and to quantify such a locality and nonlocality in terms of a physically sound and appealing chemical partitioning.

References

1 Bader, R. F. W. and Gatti, C. (1998), *Chem. Phys. Lett.* **287**, 233-238.
2 Bader, R. F. W. in *Atoms in Molecules: A Quantum Theory*, International Series of Monographs on Chemistry, Oxford, University Press, (1990), **22**.
3 Gatti, C., Cargnoni, F. and Bertini, L. (2003), *J. Comput. Chem.* **24**, 422-436.
4 Overgaard, J., Schiøtt, B., Larsen, F. K. and Iversen, B. B. (2001) *Chem. Eur. J.* **7**, 56-3767.

THERMAL MOTION ANALYSIS, A MOLECULAR MEAN FIELD MODEL

Hans-Beat Bürgi

Laboratory of Crystallography, University of Berne, Freiestr. 3, CH-3012 Bern, Switzerland (hans-beat.buergi@krist.unibe.ch)

Atomic displacement parameters (ADPs) are a by-product of crystal structure analysis that is largely ignored although they encompass about two thirds of the numerical information from such an analysis. Reasons for this include: (1) poor quality of ADPs due to systematic errors arising from the diffraction experiments and (2) no information on the correlation of motion between different atoms. The quality of ADPs has improved significantly due largely to the availability of synchrotron radiation and CCD area detectors [1]. Due to the low dispersion of synchrotron radiation, the magnitude of ADPs is largely independent of the details of data processing, contrary to what is found for sealed tube data, and with He- and N2-cooling devices it is relatively easy to collect data from ~10 to 300 K within 2-3 days of beam time.

The rigid body model of Schomaker and Trueblood is the most popular way of interpreting ADPs [2]. It has been extended to include soft intramolecular motion, albeit at a penalty: the distinction between internal and external motions is partially lost [3]. Both approaches assume correlations implicit in a rigid or semi-rigid body. If a structure is determined at several temperatures, each set of ADPs is analysed seperately, thus ignoring the information contained in the temperature dependence of the ADPs.

We have developed a physical model that improves several of these shortcomings: (1) the model explicitly accounts for the temperature dependence of the ADPs and provides for temperature independent contributions to the ADPs; (2) the correlation of atomic motion is obtainable from the model provided ADPs are available over a sufficient range of T, preferably from ~10 K to the melting temperature of the substance; (3) the ADPs from all experiments are analysed simultaneously; (4) the model is expressed and programmed in terms of chemical coordinates to facilitate comparison with results from vibrational spectroscopy and ab initio calculations [4]. Multi-temperature analysis of ADPs gives access to several new types of information. For rigid molecules the amplitudes of intramolecular zero-point motions are determined simultaneously with those of libration and translation. The T,L,S matrices are thus improved compared to the classical analyses. A Grueneisen parameter may be introduced to account for the lowering of vibration frequencies due to thermal expansion of the crystal (anharmonicity). The specific heat c_V is obtainable from the vibration frequencies (c_P if combined with measurements of dV/dP). Multi-temperature analysis is a powerful way to distinguish between motion and positional disorder of atoms that is too small to be resolved by most structure analysis (~< 0.7 Å) [5].

References

1 A.T.H. Lenstra, J.F.J. Van Loock, B. Rousseau, S.T. Maes, Acta Cryst., 2001, A57, 629.
2 V. Schomaker, K. N. Trueblood,. Acta Cryst., 1968, B24, 63.
3 V. Schomaker, K. N. Trueblood,. Acta Cryst., 1998, B54, 507
4 H.-B. Bürgi, S. C. Capelli, Acta Cryst., 2000, A56, 403. H. B. Bürgi, M. Förtsch, J. Mol. Struct., 1999, 485-486, 457.
5 H.-B. Bürgi, Annu. Rev. Phys. Chem., 2000, 51, 275. H.-B. Bürgi, Faraday Discussion, 122 (2002) 41.

PSEUDOATOM RADIAL FUNCTIONS FROM THEORETICAL MOLECULAR DENSITIES

T. Koritsanszky,[a] and A. Volkov[b]

[a]Department of Chemistry, Middle Tennessee State University, TN, USA;
[b]Department of Chemistry, State University of New York at Buffalo, NY, USA
(tkoritsa@mtsu.edu)

Recent experimental and model electron density (ED) studies[1] have presented convincing evidences for the limited adequacy of the deformation radial functions (RF) applied in popular pseudoatom models. These functions are routinely taken as Slater-type functions whose parameters are deduced from ground-state atomic Hartree-Fock calculations utilizing single-zeta basis sets[2].

In this contribution we present a simple method for deriving pseudoatomic RF's for chemically bonded atoms. The approach, following Stewart's suggestion[2], is based on the least-squares projection technique, however, instead of the total molecular ED, we use its component stockholder- atoms[4] (ρ_S) as individual target functions in the fit. ρ_S represents the most localized bonded atom, satisfies the nuclear cusp condition and exhibits the proper long-range behavior.

The least-squares conditions lead to stockholder-atom RF's (γ_{lm_z}) defined as

$$\tilde{a}_{lm_z}(r) = P_{lm_z}^{-1}\int_{\Omega}\tilde{n}_S(\mathbf{r})d_{lm_z}(\vartheta,\varphi)d\Omega, \qquad P_{lm_z} = \int_{-\infty}^{+\infty}\tilde{n}_S(\mathbf{r})d_{lm_z}(\vartheta,\varphi)d\mathbf{r}$$

where, d_{lm_z}'s are density normalized real spherical harmonics, P_{lm_z}'s are multipole populations and the integration, taken over the angular variables (ϑ,φ), is performed numerically. The multicenter three-dimensional problem of projecting the molecular ED into its constituent pseudoatoms can thus be reduced to a one-center one-dimensional problem of projecting normalized stockholder-atom RF's to linear combinations of primitive basis functions.

Preliminary results for H-, C- and O-atoms show that the molecular ED can be reconstructed with an accuracy of 0.05 eÅ^{-3} if the RF's are represented in terms of two Slater functions, at least. While the χ-refinement works well for the monopole RF's, it fails for the higher order functions, just as it often does in experimental studies. The method has the potential not only for reducing the bias in parameter estimates of the multipole model and thus providing reliable topological details of the static experimental ED, but also in density construction of large molecules.

References

1 Koritsanszky, T. and Coppens, P. (2001) *Chem. Rev.* **101**, 1583 and references therein.
2 Clementi, E. and Raimondi, D. L. (1963) *J. Chem. Phys.* **38**, 2686.
3 Stewart, R. F. (1977) *Isr. J. Chem.* **16**, 12.
4 Hirshfed, F. L. (1977) *Theoret. Chim. Acta* **44**, 129.

MULTIPOLAR REFINEMENT OF PROTEINS : SUCCESS AND PITFALLS

B. Guillot,[a] C. Jelsch,[a] A. Podjarny,[b] and C. Lecomte[a]

[a]LCM[3]B, Faculté des Sciences, BP239, 54506 Vandoeuvre-les-Nancy, France; [b]LGBS, IGBMC, 1, rue Laurent Fries, BP10142, 67404 Illkirch, France (bguillot@lcm3b.uhp-nancy.fr)

The constant advances in synchrotron radiation and crystallogenesis methods, and the impulse of structural genomics projects have bought bio-crystallography in a context favorable to subatomic resolution protein or nucleic acid structures. Thus, as soon as such precision can be frequently obtained, the amount of information available in the precise electron density should also be easily and naturally exploited, similarly to the field of small molecules charge density studies.

Indeed, in addition of a better modeling of thermal motion and stereochemistry, allowing a deeper understanding of the structure – function relationship, subatomic resolution leads to a parameterized description of the deformation density, if an adequate atomic model like the multipole formalism, is used during the refinement[1]. From this description, it becomes possible to derive experimental atomic charges and more generally experimental electrostatic properties: in other words a new point of view to chemical reactivity, molecular recognition processes and host-guest mechanism.

However, proteins are not small molecules. There are specific methods for both fields and prior to get valuable information from a charge density study of a biological macromolecule, we have to extend multipolar refinement methods to proteins and in parallel adapt some bio-crystallography techniques to the small molecules world!

This is the topic of the present talk. We will present, on one hand the methods implemented in our program MoPro[2], designed to allow non spherical (multipolar) electron density refinement of all sized molecules, in reasonable amounts of CPU time, and, on the other hand, some applications, especially based on the 0.66Å structure of Human Aldose Reductase[3], to show both successes and limits of these methods.

References

1 Jelsch, C., Teeter, M. M., Lamzin, V., Pichon-Pesme, V., Blessing, R. H. and Lecomte, C. (2000). *Proc. Natl. Acad. Sci. (USA)*. **97**, 3171-3176.

2 Guillot, B., Viry, L., Guillot, R., Lecomte, C. and Jelsch, C. (2001). *J. Appl. Cryst.* **34**, 214-223.

3 Muzet, N., Guillot, B., Jelsch, C., Pichon-Pesme, V. and Lecomte, C. (2003) submitted.

CHARGE DENSITY STUDIES OF Z' = 2 MOLECULES. POSSIBILITIES AND LIMITATIONS

Dai Hibbs, Mark P. Waller, and Jacob Overgaard

School of Chemistry, University of Sydney, NSW 2006, Australia
(hibbs_d@chem.usyd.edu.au)

Experimental X-ray charge density (CD) studies of molecules with more than one molecule in the asymmetric unit are relatively rare [1]. On the contrary, such occurrences are abundant in structural chemistry, evidenced by the 22015 hits of Z' 2 in CCDC, corresponding to 8% of all published structures [2]. Thus, it is apparent that such compounds have been avoided by the CD community. This is due to several factors. Firstly, the increase in the number of parameters is a significant drawback, since a successful multipole model in most cases requires more than 300 reflections per non-hydrogen atom. Secondly, one of the molecules often experiences a rather weak crystal field; hence the thermal motion of this molecule can be severe and the molecule may even be disordered. Thirdly, there can exist significant correlations between multipole parameters from different molecules. All in all, CD studies of this type of crystal structures offer a range of problems that need to be addressed.

There are, however, large potential benefits of studying the CD in such molecules. In the case of rigid molecules, it allows the determination of multipole parameters of identical atoms in slightly different environments without the presence of systematic errors intrinsic in a comparison of different experiments. Hence, it is important in the evaluation of transferability of atomic multipole parameters [3].

This presentation will outline the details of experimental and theoretical charge density studies of three organic molecules all having two molecules in the asymmetric unit (see Figure). Besides a discussion of the prospects of giving an independent description of the two molecules in the same study, each of the three systems represents interesting chemical and theoretical issues that will be addressed.

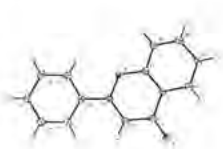

FLAVONE

FLUORENOL

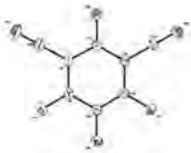

TFIPN

References

1 Gatti, C., May, E., Destro, R. and Cargnoni, F. (2002) *J. Phys. Chem. A.* **106**, 2707; van Reeuwijk, S. J., van Beek, K. G. and Feil, D. (2000) *J. Phys. Chem. A.* **104**, 10901.

2 CCDC search 13/3/03 gave 22015 hits equalling Z' 2 out of 272066.

3 Pichon-Pesme, V., Lecomte, C. and Lachekar, H. (1995) *J. Phys. Chem.* **99**, 6242.

SPIN DENSITIES IN MOLECULE-BASED MAGNETIC COMPOUNDS: FIRST STUDY OF A PHOTO-INDUCED MAGNETIC STATE

B. Gillon

Laboratoire Léon Brillouin (CEA-CNRS), C.E. Saclay, 91191 Gif-sur-Yvette, France (gillon@llb.saclay.cea.fr)

Molecule-based magnets attract growing attention because of their specific optical and mechanical properties, which do not present classical magnets. Photo-switchable molecule-based magnetic materials, like spin crossover compounds, are of particular interest for future data storage at the molecular level.

The understanding of the mechanisms which are involved in magnetism of molecule-based compounds is essential for the design of new systems. The spin density determination by polarized neutron diffraction (PND) provides direct information on the nature and the origin of the intra- and inter-molecular magnetic interactions. A short review of spin density studies in different types of molecule-based magnetic compounds will be given: a molecule-based magnet, with an ordering temperature of 39K, in which Mn^{II} and Mo^{III} transition metal ions interact through cyano bridges[1], a paramagnetic Ti^{IV} complex in which two semiquinonato radicals interact ferromagnetically via the non magnetic transition metal ion [2] and a high spin cyano-bridged molecular cluster $Ni^{II}_9W^{V}_6$ (S =12).

In a second part, the determination of the photo-induced magnetisation density and high spin Fe^{II} magnetic form factor in a spin crossover Fe^{II} complex will be reported[3]. A new experimental set-up on the polarised neutron diffractometer 5C1 at the LLB allows in situ light illumination of the crystal. A complete photo-process was achieved for the Fe^{II} complex. Large possibilities of PND in providing information on the magnetic coupling scheme, the spin density distribution and spin delocalisation effects could be useful for other photo-magnetic crystals.

References

1 Stride, J. A., Gillon, B., Gukasov, A., Larionova, J., Clérac, R. and Kahn, O. (2001) *C. R. Acad. Sci. Paris, Chem.* **4**, 105-112.

2 Pontillon, Y., Bencini, A., Caneschi, A., Dei, A., Gattteschi, D., Gillon, B., Sangregorio, C., Stride, J. A. and Totti, F. (2000) *Angew. Chem. Int. Eng. Ed.* **39**, 1786-1788.

3 Jeftic, J., Gillon, B., Goujon, A., Nau, Q., Gukasov, A., Codjovi, E. and Varret, F. *Polyhedron*, in press.

ENSEMBLE REPRESENTABLE DENSITIES FOR ATOMS AND MOLECULES: ANALYSIS OF POLARISED NEUTRON EXPERIMENTS WHEN SEVERAL ZEEMAN LEVELS ARE POPULATED

P. Cassam-Chenaï[a,b]

[a]LETMEX, Physique Recherche, Faculté des Sciences, Université de Nice-Sophia Antipolis, Parc Valrose, Nice, F-06100, France; [b]Department of Chemistry, University of Western Australia, Nedlands, WA 6009, Australia (cassam@unice.fr)

Polarised neutron diffraction experiments conducted at 4.2 K on Cs_3CoCl_5 crystals are analysed by using a 4-dimensional model Hilbert space made of *ab initio* n-electron wave functions of the $CoCl_4^{2-}$ molecular ion. The magnetic structure factors given by the best ensemble density operator that is representable in our model space are fitted to the experimental ones by optimizing two spin-orbit mixing coefficients of the embedded $CoCl_4^{2-}$ ions and several configuration interaction coefficients. The optimized density operator can in turn be used to calculate any observable. Here we present density maps of the spin density, and the orbital current density. The method, which is general, gives a goodness of fit, χ^2, less then 1 with fewer parameters optimised than other methods employed so far. It provides a new way of gaining information about spin-orbit coupling and the relative contributions of spin and orbital motion to the magnetic properties of an atomic or molecular system. Another interesting finding is that a χ^2 less then 1, can be obtained with a spin density of the same sign everywhere in space, leading to the conclusion that spin polarisation is within the experimental error. The so-called "collinear approximation" has been avoided in this work although it has been found to be justified for this system. A direct comparison is made between calculated and experimental flipping ratios [1].

References

1 Cassam-Chenaï, P. (2002) *J. Chem. Phys.* **116**, 8677-8690.

OBSERVATION OF ORDERED ORBITAL OF $YTiO_3$ BY THE X-RAY MAGNETIC DIFFRACTION EXPERIMENTS

Masahisa Ito,[a] Naruki Tuji,[a] Fumitake Itoh,[a] Hiromichi Adachi,[b] Etsuo Arakawa,[c] Kazumichi Namikawa,[c] Hironori Nakao,[d] Youichi Murakami,[d] Yasujiro Taguchi,[e*] and Yoshinori Tokura[e]

[a]Faculty of Engineering, Gunma University, Aramaki-machi 4-2, Maebashi, Gunma 371-8510, Japan; [b]Materials Research Institute, KEK, Oho 1-1, Tukuba, Ibaraki 305-0801, Japan; [c]Tokyo Gakugei University, Nukuikita-machi 4-1-1, Koganei, Tokyo 184-8501, Japan; [d]Graduate School of Science, Tohoku University, Aramaki, Aoba-ku, Sendai 980-8578, Japan; [e]Department of Applied Physics, The University of Tokyo, Hongo 7-3-1, Bunkyo-ku, Tokyo 113-0033, Japan; *present address, Institute for Materials Research, Tohoku University, Katahira 2-1-1, Aoba-ku, Sendai 980-8577, Japan (itom@fs.aramaki.gunma-u.ac.jp)

The orbital degree of freedom is recognized to be an important factor that determine the solid state properties of some perovskite compounds such as $YTiO_3$ together with the charge degree and the spin degree of freedom. Orbital ordering of $YTiO_3$ has been intensively researched both theoretically[1,2] and experimentally[3-6]. The 3d electrons of Ti atoms in a t_{2g} orbital are thought to be ordered. Ordered orbitals of $YTiO_3$ have been observed by NMR[3], neutron diffraction[4], and the resonant X-ray scattering[5]. The model wave functions of the ordered orbitals were based on the assumption that the orbital moments are quenched. In the present study we made the X-ray magnetic diffraction (XMD) measurement of ferromagnetic $YTiO_3$ in order to measure the orbital (L) and the spin(S) magnetic form factors utilizing the ability of LS separation of the XMD.

The experiment is divided into two part; (1) the measurement of the orbital magnetic form factor to check the orbital moments is quenched or not, and (2) the measurement of the spin magnetic form factor to observe the ordered orbital directly. XMD could be a tool to observe directly the orbitals of the orbital ordering systems.

References

1 Mizokawa, T. and Fujimori, A. (1996) *Phys. Rev. B* **54**, 5368-5380.
2 Sawada, H. and Terakura, K. (1998) *Phys. Rev. B* **58**, 6831-6836.
3 Itoh, M., Tsuchiya, M., Tanaka, H. and Motoya, K. (1999) *J. Phys. Soc. Jpn.* **68**, 2783-2789.
4 Ichikawa, H., Akimitsu, J., Nishi, M. and Kakurai, K. (2000) *Physica B* **281&282** 482-484.
5 Nakao, H., Wakabayashi, Y., Kiyama, T., Murakami, Y., Zimmenrmann, M. V., Hill, J. P., Gibbs, D., Ishihara, S., Taniguchi, Y. and Tokura, Y. (2002) *Phys. Rev. B* **66**, 184419 1-7.
6 Ulrich, C., Khaliullin, G., Okamoto, S., Reehuis, M., Ivanov, A., He, H., Taguchi, Y., Tokura, Y. and Keimer, B. (2002) *Phys. Rev. Lett.* **89** 167202 1-4.

Sunday August 17

Sagamore XIV

ABSTRACTS

ORAL SESSIONS

ELECTRON MOMENTUM SPECTROSCOPY OF SINGLE CRYSTAL SILICON AND NICKEL TARGETS

M. Vos, C. Bowles, C. Chen, A. S. Kheifets, V. A. Sashin, and E. Weigold
Research School of Physical Sciences and Engineering, Australian National University, Canberra 0200 ACT, Australia (maarten.vos@anu.edu.au)

In Electron Momentum Spectroscopy (EMS) an incoming electron ionizes a target and the scattered and ejected electrons are measured in coincidence. By comparing the energies and momenta of both outgoing electrons with that of the incoming electron, we can determine the energy and momentum transferred to the target, i.e. we measure the energy-resolved momentum densities including lifetime broadening and other correlation effects. Here we present data for single crystal silicon and nickel along high-symmetry directions. Clear anisotropies in the electronic structure were found for both materials. For an infinitely thin crystal one can determine directly the magnitude of the contribution of different plane waves to the Bloch function at a given binding energy. However, for a crystal of finite thickness diffraction may occur for the incoming and/or outgoing electron beams and this complicates the interpretation. By varying measurement geometry one can vary the diffraction conditions, and hence extract valuable information on the contribution of different plane waves to the Bloch function.

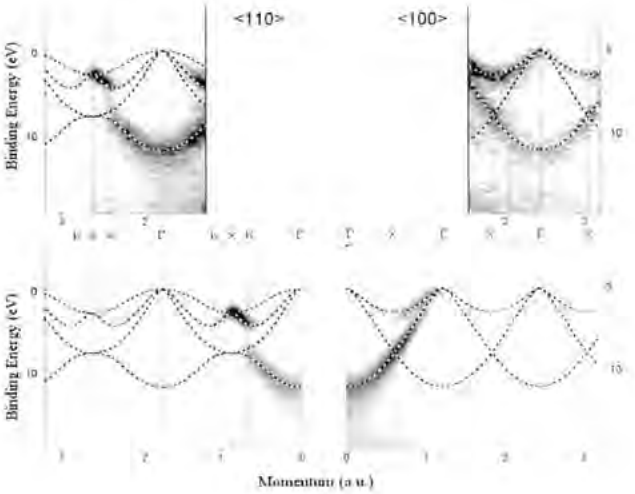

Fig.1 Measured spectral momentum density of Si along <110> and <100> directions. The dotted line is the calculated band structure. The top half shows the high momentum part on an expanded grey scale. The anisotropy is clearly resolved, and the influence of diffraction is evident as well.

ORBITAL MOMENTUM DENSITIES OF CHEMICALLY SIMILAR MOLECULES USING HREMS AND DFT

M. J. Brunger,[a] K. L. Nixon,[a] L. Campbell,[a] F. Wang,[b] B.Appelbe,[b] M. Hamilton,[c] and D. A. Winkler[d]

[a]School of Chemistry, Physics and Earth Sciences, Flinders University, GPO Box 2100, Adelaide, SA 5001, Australia; [b]Victorian Partnership for Advanced Computing, PO Box 201, Carlton South, Vic 3053, Australia; [c]School of Computer Science and Information Technology, RMIT, Melbourne, Vic 3000, Australia; [d]Division of Molecular Sciences, CSIRO, Private Bag 10, Clayton South MDC, Vic 3169, Australia (Michael.Brunger@flinders.edu.au)

We report on results from our High-Resolution Electron Momentum Spectroscopy (HREMS) studies[1] and Density Functional Theory (DFT) calculations[2] into the complete valence electronic structures of the chemically similar molecules norbornadiene (C_7H_8), norbornene (C_7H_{10}) and norbornane (C_7H_{12}). Representative examples of our measured and calculated orbital momentum densities for each of these molecules are presented and systematically discussed. In addition some of their important physico-chemical properties (particularly their respective structures), as derived from our studies, are also presented. These latter results are compared against corresponding values from independent measurements and calculations.

References

1 Brunger, M. J. and Adcock, W. (2002) *J. Chem. Soc., Perkins Trans.* **2**, 1-22.

2 Wang, F., Brunger, M. J., Winkler, D. A., Hamilton, M. and Appelbe, B. (2003) *J. Comput. Chem.*, submitted.

PROBING ELECTRON MOMENTUM DENSITIES IN MOLECULES USING A NEW MULTICHANNEL (e,2e) SPECTROMETER

Masahiko Takahashi and Yasuo Udagawa

Institute of Multidisciplinary Research for Advanced Materials, Tohoku University, Sendai 980-8577, Japan (masahiko@tagen.tohoku.ac.jp)

Electron momentum spectroscopy (EMS), based on the (e,2e) reaction under the Bethe ridge conditions, has been developed as a powerful means for investigations of electronic structure of atoms and molecules [1]. Within the plane-wave impulse approximation (PWIA), the EMS cross section for a gaseous target is directly related to the spherically averaged momentum density or momentum profile of the Dyson orbital for the ionization transition. Furthermore, EMS can give unique and versatile information for the detailed study of electronic structure, such as symmetries, binding energies and pole strengths of the states involved.

Nevertheless, the potential of EMS has not been fully achieved as yet due mainly to the small cross sections involved, which cause large statistical uncertainty and poor energy resolution. Very recently, we have developed a new spectrometer that employs a spherical analyzer and position sensitive detectors [2]. By taking an advantage of simultaneous detection in energy and momentum, collection efficiency for the two outgoing electrons has been significantly improved compared with our previous apparatus [3], opening up the possibility of considerably more precise measurements.

In this contribution we report details and performance of the newly developed spectrometer. Our recent studies of several targets will also be presented. Applications to be discussed involve (1) electron momentum profiles for the complete valence shell of CO and (2) simultaneous ionization excitation processes of H_2, together with comparison between experiment and theory. Finally, prospects for probing directional momentum densities or looking at molecular orbitals in the three-dimensional momentum-space will be discussed for gaseous targets.

References

1 Weigold, E. and McCarthy, I. E. *Electron Momentum Spectroscopy* (Kluwer Academic/Plenum Publishers, New York, 1999).
2 Takahashi, M., Saito, T., Matsuo, M. and Udagawa, Y. (2002) *Rev. Sci. Instrum.* **73**, 2242-2248.
3 Takahashi, M., Nagasaka H. and Udagawa, Y. (1997) *J. Phys. Chem.* A **101**, 528-532.

CHARGE DENSITY MEASUREMENTS OF TRANSITION-METAL OXIDES USING CONVERGENT-BEAM ELECTRON DIFFRACTION

K. Tsuda, Y. Ogata, and M. Tanaka
Institute of Multidisciplinary Research for Advanced Materials, Tohoku University, Sendai 980-8577, Japan (k_tsuda@tagen.tohoku.ac.jp)

We have developed a method to refine crystal structural parameters using convergent-beam electron diffraction (CBED) [1], [2]. The method is applicable to *nanometer-size* crystal structure refinement because CBED patterns can be obtained from specimen areas of a few nm in diameter. The method is based on the least-squares fitting between full dynamical calculations and experimental intensities of energy-filtered *two-dimensional* CBED patterns of zeroth-order Laue-zone (ZOLZ) reflections and higher-order Laue-zone (HOLZ) reflections. For this purpose, we developed an energy-filter transmission microscope *JEM-2010FEF* [3], and our own analysis program *MBFIT* [1] to refine structural parameters.

The method can be applied to the determination of charge-density distribution because the low-order Fourier coefficients of the electrostatic potential (low-order crystal structure factors for electron diffraction), which are very sensitive to valence electrons, can be refined together with the atom positions and Debye-Waller factors. Through Poisson's equation, the structure factors for electron diffraction are related to those for X-ray diffraction, or the Fourier coefficients of the charge density. According to the nature of Poisson's equation, a small change in the low-order structure factors for X-rays causes a large change in those for electrons. Thus, the present method has a high potential to determine charge-density distribution more sensitively than X-ray diffraction.

We applied the present method to the rhombohedral phase of $LaCrO_3$ [3]. Clear anisotropy of thermal vibration of the oxygen atoms was successfully determined by CBED for the first time. The deformation electrostatic potential and deformation charge-density map were constructed from the refined structural parameters, revealing clear charge transfer from the metal atoms to the oxygen atoms.

The present method can be extensively applied to the charge-density determination of the perovskite and related transition-metal oxides revealing charge- ordering and orbital-ordering phenomena, which are closely related to the colossal magnetoresistance and the high-T_c superconductivity. Though the materials are frequently composed of very small domains owing to twin structures and/or characteristic phase separations, the CBED technique allows us to obatain diffraction intensity data from a single domain. We have already obtained a preliminary result of the anisotropic charge density of the orbital-ordering phase of $LaMnO_3$, for which the ordering of e_g orbitals of the Mn 3*d* electrons was observed using the resonant X-ray scattering technique [4]. More detailed analyses using several CBED patterns with different beam incidences are now in progress.

References

1 Tsuda, K. and Tanaka, M. (1999) *Acta Cryst.*, **A55**, 939-954.
2 Tsuda, K., *et al.* (2002) *Acta Cryst.*, **A58**, 514-525.
3 Tanaka, M., *et al.* (1999) *J. Microsc.*, **194**, 219-227.
4 Murakami, Y., *et al.* (1998) *Phys. Rev. Lett.*, **81**, 582-585.

CALCULATIONS OF ELECTRON ATOMIC SCATTERING FACTORS AND TEMPERATURE DEPENDENT DEBYE-WALLER FACTORS

Lian-Mao Peng

Department of Electronics, Peking University, Beijing 100871, China
(plm@ele.pku.edu.cn)

Electron atomic scattering factors and Debye-Waller factors are two types of important parameters that an electron crystallographer must have before conducting any quantitative electron crystallography work. While numerical values of electron atomic scattering factors are available for all free neutral atoms and most commonly occurring ions[1], Debye-Waller factors are more difficult to find and most of the time the existing Debye-Waller factors are given only at few fixed temperatures and it is not always clear as to how to interpolate these values to other temperatures. In this lecture we will be concerned with the advantages of using an alternative analytical expression [2] for the electron atomic scattering factors, especially those for ions and for reflection high-energy electron diffraction (HREED) and surface calculations [3-5]. We will also present results on lattice dynamics calculations on a range of compounds, especially oxides, and the evaluation of temperature dependent Debye-Waller factors from these calculations, their parameterization [6-8] and computation of absorptive scattering factors of electrons [9].

References

1 J.M. Cowley (1999) *International Tables for Crystallography*, Volume C, p259, Kluwer Academic Publishers
2 J.M. Cowley, L.-M. Peng, G. Ren, S.L. Dudarev and M.J. Whelan (1999) *International Tables for Crystallography*, Volume C, p262 (1999) Kluwer Academic Publishers
3 L.-M. Peng, G. Ren, S.L. Dudarev and M.J. Whelan (1996) *Acta Cryst.* **A52**, 257
4 L.-M. Peng, S.L. Dudarev and M.J. Whelan (1998) *Phys. Rev.* **B57**, 7259
5 L.-M. Peng (1998) *Acta Cryst.* **A54**, 481
6 H.X. Gao, L.-M. Peng and J.M. Zuo (1999) *Acta Cryst.* **A55**,1014
7 H.X. Gao and L.-M. Peng (1999) *Acta Cryst.* **A55**, 926
8 H.X. Gao and L.-M. Peng (2000) *Acta Cryst.* **A56**, 519
9 L.-M. Peng, G. Ren, S.L. Dudarev and M.J. Whelan (1996) *Acta Cryst.* **A52**, 456

THE "COMBINATION METHOD" OF QUANTITATIVE CBED AND X-RAY DIFFRACTION APPLIED TO CORUNDUM.

Philip N.H. Nakashima,[a] Victor A. Streltsov,[b] and Andrew W.S. Johnson[c]

[a]School of Physics and Materials Engineering, Monash University, Clayton Vic 3800, Australia; [b]Structural Biology, CSIRO Division of Health Sciences and Nutrition, Parkville Vic 3052, Australia; [c]Centre for Microscopy and Microanalysis, University of Western Australia, Crawley WA 6009, Australia (philip.nakashima@spme.monash.edu.au)

Corundum, or α-Al_2O_3, has a great tendency to form perfect crystals. A lot of theoretical and experimental charge density research has been conducted with corundum as a benchmark compound because experimental results should, in principle, be very reproducible from this highly ideal material. However, very high crystal perfection often leads to significant extinction in the integrated intensity measurements of strong, lower order reflections (those most sensitive to the bonding charge density distribution) by conventional single crystal X-ray diffraction due to the increased likelihood of multiple scattering. In addition, the data lacks an absolute scale, the relativity of the structure factor measurements resulting from the application of kinematic scattering theory. The conventional least squares methods of refining extinction and scale simultaneously are heavily compromised in the presence of significant extinction due to the strong correlation between the two quantities. Different approaches to applying extinction and scale corrections can result in great variability in the experimentally determined charge densities [1, 2]. Such variability eliminates the possibility of making a reliable comparison of experimentally measured charge density with that computed by theoretical models.

The "combination method" overcomes the problems discussed above by using quantitative convergent beam electron diffraction (QCBED) to measure the lower order structure factors to high precision (uncertainty of order 0.1%) on an absolute scale. The technique fully accounts for multiple scattering and measures the structure factors from the angular distribution of intensity within the corresponding reflections on or near the Laue circle. This negates the issues of scale and extinction. QCBED is less accurate in measuring higher order structure factors and therefore, a combination of the low order QCBED data with the higher order X-ray data is required to optimise charge density measurements. An overlap of the QCBED data set with the valid, extinction free portion of the X-ray data allows the latter to be scaled to the QCBED data. A similar approach was used successfully by Zuo et al [3] to measure charge density in Cu_2O.

We will present comparisons of our experimental results with DFT (GGA/FPLAPW) and PHF calculations.

References

1 Streltsov, V. A. and Maslen, E. N. (1992) *Acta Cryst.* **A48**, 651.

2 Streltsov, V. A., Nakashima, P. N. H. and Johnson, A. W. S. (2001) *J. Phys. chem. Solids* **62**, 2109.

3 Zuo, J. M., Kim, M., O'Keeffe, M. and Spence, J. C. H. (1999) *Nature* **401**, 49.

Monday August 18

Sagamore XIV

ABSTRACTS

ORAL SESSIONS

RECENT MOMENTUM DENSITY STUDY OF NOVEL MATERIALS

Y. Sakurai, and M. Itou

Japan Synchrotron Radiation Research Institute (JASRI), SPring-8,
1-1-1 Kouto, Mikazuki, Sayo, Hyogo 679-5198, Japan (sakurai@spring8.or.jp)

Recent progress of the high-resolution Compton scattering project at SPring-8 will be reported.

The Cauchois-type x-ray spectrometer[1] has been upgraded by installation of an x-ray image intensifier (X-II) as a position sensitive detector (PSD). The new PSD system consists of a X-II (HAMAMATSU V7339P-MOD) and a CCD camera (HAMAMATSU C4742-95-12ER). The x-ray entrance window has a diameter of 4 inches which covers the focal positions corresponding to the x-ray energies between 70 and 90 keV for the incident x-ray energy of 115 keV and the scattering angle of 165 degrees. The X-II PSD detects these x-rays under the photon-counting operation mode. The overall momentum resolution is 0.12 atomic unit (a.u.) at present, and should be better than 0.10 a.u. in future. The improvement makes it possible to measure a set of Compton profiles within a reasonable beam-time for a tomographical reconstruction of three- or two-dimensional momentum density or a systematic investigation under various sample conditions.

Currently, many research subjects are running with the spectrometer. Among them, the followings will be presented in this conference;

(1) Fermi surface topology of the spin-triplet superconductor Sr_2RuO_4 [2],
(2) Cohesion mechanism of Al-based and Cd-based quasicrystals [3],
(3) Hydrogen-induced change in momentum density for metal-hydrides [4],
(4) Charge transfer in Si clathrates.

The authors would like to express their many thanks to Y. Maeno, J. Tamura-Okada, Y. Watanabe, S. Nanao, S. Mizusaki, I. Yamamoto, M. Yamaguchi, H. Fukuoka, S. Yamanaka, N. Hiraoka, A. Koizumi, and N. Sakai, whom they have been collaborating on the high-resolution Compton scattering project at SPring-8. They also acknowledge the support by the SPring-8 Joint Research Promotion Scheme under the auspices of the Japan Science and Technology Corporation.

References

1 Hiraoka, N., Itou, M., Ohata, T., Mizumaki, M., Sakurai, Y. and Sakai, N. (2001) *J. Synchrotron Rad.* **8**, 26-32.
2 Hiraoka, N., Deb, A., Itou, M., Sakurai, Y., Mao, Z. Q. and Maeno., Y. (2003) *Phys. Rev. B*, in press.
3 Tamura-Okada, J., Watanabe, Y., Yokoyama, Y., Hiraoka, N., Itou, M., Sakurai, Y. and Nanao, S. (2002) *J. Phys.: Condens. Matter* **14**, L43-L48.
4 Mizusaki, S., Hiraoka, N., Yamamoto, I., Itou, M., Sakurai, Y. and Yamaguchi, M. (2003) *J. Phys. Soc. Jpn*, in press.

SPIN DENSITIES IN MOMENTUM SPACE

J. A. Duffy

Department of Physics, University of Warwick, Coventry, CV4 7AL, United Kingdom (j.a.duffy@warwick.ac.uk)

Magnetic Compton scattering is a technique whereby the spin dependent electron momentum density in ferromagnets can be probed. The spin-polarised Compton profile is a 1-dimensional integral of the momentum space spin density. The total spin moment can be directly obtained via the integrated scattering cross section, whilst the lineshape is determined by the nature of the electronic orbitals or bands on which the magnetism resides. Spin-polarised Compton scattering is closely related to the magnetic form factor measurements with the neutron and x-ray diffraction methods. The method is particularly useful for studying both itinerant moment systems, and materials where there is a combination of localised and itinerant moments.

A set of examples will be given, covering in particular, rare earth systems, the hexaborides and the study of the spin density in ferromagnetic superconductors.

Magnetic Compton scattering is particularly suited to the study of rare-earth systems, since it can distinguish between the localised *4f* moments and other more delocalised contributions to the spin moment. For example, in Gd, the itinerant moment can be easily distinguished from the localised *4f* magnetism, and furthermore so can the change in itinerant moment on alloying with yttrium. In materials such as $SmMn_2Ge_2$, it is possible to separate the *4f* and *3d* contributions. It sensitivity to the spin moment only has enabled the ferromagnetism in the $Sm_{1-x}Gd_xAl$ system, where the spin and orbital moments cancel giving little or no net moment, to be investigated.

The doped hexaboride $Ca_{1-x}La_xB_6$ appears to exhibit weak ferromagnetism, with a moment of $0.07\mu_B$ for $x = 0.005$, with a Curie temperature of ~600K. However, the real nature of the magnetism observed is controversial, and is sometimes considered to arise from Fe impurities. Magnetic Compton scattering has revealed a very delocalised moment, not representative of that found for a *3d* system, providing evidence in favour of the ferromagnetism being intrinsic.

Recently, the technique has been applied to the study of ferromagnetic moments in superconducting materials. It has been used in $ZrZn_2$, in the normal state, to study the *4d* moment, and for comparison with electronic structure calculations. It has also been used in $ErNi_2B_2C$, to measure the spin density in the superconducting state, where it is not prohibited by the diamagnetism present. $ErNi_2B_2C$ is a so-called magnetic superconductor, where magnetic Compton scattering measurements show clear evidence for the existence of a weak ferromagnetic state below 2.3K, within the superconducting state.

Finally, present developments of the method, including use of higher magnetic fields, and high pressures, will be discussed.

COMPTON-SCATTERING STUDIES ON ATOMIC AND MOLECULAR SYSTEMS

S. Huotari, M. Hakala, Sz. Galambosi, S. Manninen, and K. Hämäläinen

Division of X-ray Physics, Department of Physical Sciences, P.O.B. 64, FIN-00014 University of Helsinki, Finland (simo.huotari@helsinki.fi)

Recent advances in Compton-scattering spectroscopy have revealed a range of phenomena not yet fully understood. Systematic studies on simple metals [1-4] have provided us with information on the final-state effects in the scattering process and on the ground-state correlation effects in the electron gas. Separating these effects would be essential in understanding the electron-gas properties. It is possible to minimize the final-state effects partly by using an incident-photon energy high enough, but the separation of correlation and e.g. finite-temperature effects in solids [5,6] is not straightforward.

To build up the understanding of these properties of electronic systems, we have conducted high-accuracy Compton-scattering studies on simple systems starting from noble-gas atoms and continued to simple molecules. It is well-known that correlation effects in closed-shell atoms are small and especially so in the helium atom. Using the Hartree-Fock approximation and by constructing the two-electron He wave function from 1*s* orbitals as a Slater determinant, it is possible to calculate the 1s momentum-space wave function from the measured momentum density. Using this wave function, we have computed the charge density of He as well. Using LCAO methods and correlation corrections based on second-order perturbation theory, we can show how the correlation effects increase when going from rare-gas atoms to simple molecules.

Due to the absence of complications that arise in solid-state (thermal disorder, high-momentum components, etc.), the analysis of atomic and molecular data gives important insight on the applicability of Compton scattering as a probe for e.g. correlation and bonding.

References

1 Hämäläinen, K., Manninen S., Kao, C. -C., Caliebe, W., Hastings, J. B., Bansil, A., Kaprzyk, S. and Platzman, P. M. (1996) *Phys. Rev. B.* **54**, 5453-5459.

2 Schülke, W., Stutz, G., Wohlert, F. and Kaprolat, A. (1996) *Phys. Rev. B* **54**, 14381-14395.

3 Sternemann, C., Hämäläinen, K., Kaprolat, A., Soininen, A., Döring, G., Kao, C. -C., Manninen, S. and Schülke, W. (2000) *Phys. Rev. B* **62** R7687-R7690.

4 Huotari, S., Hämäläinen, K., Manninen, S., Kaprzyk, S., Bansil, A., Caliebe, W., Buslaps, T., Honkimäki, V. and Suortti, P. (2000) *Phys. Rev. B* **62** 7956-7963.

5 Sternemann, C., Buslaps, T., Shukla, A., Suortti, P., Döring, G. and Schülke, W. (2001) *Phys. Rev. B* **63**, 094301.

6 Huotari, S., Hämäläinen, K., Manninen, S., Sternemann, C., Kaprolat, A., Schülke, W. and Buslaps, T. (2002) *Phys. Rev. B* **66**, 085104.

COMPTON SCATTERING ON ALKALI-METAL-DOPED SILICON CLATHRATES

M. Volmer,[a] C. Sternemann,[a] J. S. Tse,[b] D. D. Klug,[b] M. Paulus,[a] C. L. Bull,[c] T. Buslaps,[d] N. Hiraoka,[d] and M. Tolan[a]

[a]Institute of Physics, University of Dortmund, D-44221 Dortmund, Germany; [b]Steacie Institute for Molecular Sciences, National Research Council of Canada, Ottawa, Ontario, Canada K1A 0R6; [c]Davy Faraday Research Laboratories, Royal Institution of Great Britain, 21 Albemarle Street, London W1S 4BS, England; [d]European Synchrotron Radiation Facility, B.P. 220, F-38000 Grenoble, France
(schenkel@physik.uni-dortmund.de)

Silicon clathrates are guest-host materials in which a dopand is trapped in cage-like structures built up from covalently bonded, four-coordinate Si atoms [1,2]. There are two structual types of the clathrates which are analogous to the well known gas hydrate structures I and II [3]. The macroscopic physical properties of these semi-conductor clathrates like electrical conductivity, glasslike thermal conductivity, or superconductivity are crucially influenced by the different inclusion compounds. Therefore, the guest-host interactions of the Silicon clathrates are of special importance to reach a deeper understanding of the electronic properties of these candidates for thermoelectric applications. Compton scattering gives a valuable tool at hand to investigate how the electronic ground state along with the electronic wave functions of the host lattice is changed by the different alkali-metal guests.

Compton profiles of the empty caged Si_{136} structure II clathrate and of the alkali-metal-doped M_8Si_{46} (M = Na, K, Rb) structure I calthrates as well as polycrystalline Si have been measured at the Compton scattering beamline ID15B of the ESRF using an incident photon energy of 56.4 keV with a momentum space resolution of 0.25 a.u. at the elastic line. The Compton profile differences between the alkali-metal doped Si clathrates and the empty caged structure are compared with GGA-LDA calculations [4] of these systems and discussed in terms of charge transfer between the guest and the host lattice. Furthermore, small differences between the Compton profiles of the empty caged Si clathrate and the polycrystalline Si sample are found as well for the valence electron Compton profiles.

References

1 He, J., Klug, D. D., Uehara, K., Preston, K. F., Ratcliffe, C. I. and Tse, J. S. (2001) *J. Phys. Chem. B* **105**, 3475.
2 Moewes, A., Kurmaev, E. Z., Tse, J. S., Geshi, M., Ferguson, M. J., Trofimova, V. A. and Yarmoshenko, Y. M. (2002) *Phys. Rev. B* **65**, 153106, and references therein.
3 Bowron, D. T., Filliponi, A., Roberts, M. A. and Finney, J. L. (1999) *Phys. Rev. Lett.* **81**, 4164.
4 Tse, J. S. and Klug, D. D. (2003) *private communication.*

TOPOLOGICAL ANALYSIS OF 3D GRIDDED ELECTRON DENSITIES

P. Rabiller,[a] M. Souhassou,[b] C. Katan,[c] S. Dahoui,[b] and C. Lecomte[b]

[a]Groupe Matière Condensée et Matériaux, Université de Rennes 1, Rennes UMR CNRS 6626, F35042, France; [b]Laboratoire de Cristallographie et de Modélisation des Matériaux Minéraux et Biologiques UMR CNRS 7036, Université Nancy 1, Vandoeuvre lès Nancy, F54506, France; [c]Synthèse électrosynthèse Organiques UMR CNRS 6510, Université de Rennes 1, Rennes, F35042, France
(philippe.rabiller@univ-rennes1.fr)

Obtaining topological properties of electron densities – following AIM approach[1] –getting rid of basis set dependence is something than can be asked for. The InteGriTy software package[2] has been developed in this spirit and works with electron densities given on regular 3D grids corresponding to either isolated or periodic systems. An interpolation method is used to get at any point the density, its gradient and hessian. Then critical points (CP) can be located and characterized on one hand. On the other hand atomic basins surfaces can be searched for and charge integration be performed over the basins. The conditions and performances of InteGriTy will be first presented, before discussing two applications. In the case of an inorganic compound (Ammonium Dihydrogen Phosphate), a comparison is made between the topological properties derived analytically from the experimental multipolar expansion with the help of NewProp[3] and those obtained with the same density calculated on a 3D grid. The second application deals with organic charge transfer complexes and neutral to ionic phase transition[5].

References

1 Bader, R. F. W. (1995) Atoms in Molecules – A Quantum theory, *Int. Series of Monographs on Chemistry* 22, Clarendon Press - Oxford.
2 Katan, C., Rabiller, P., Lecomte, C., Guezo, M., Oison, V., Lecomte C. and Souhassou, M. (2003) *J. Appl. Cryst.* **36**, 65-73.
3 Pérès, N., Boukhris, A., Souhassou, M., Gavoille, G. and Lecomte, C. (1999) *Acta. Cryst.* **A55**, 1038-1048.
4 Souhassou, M. and Blessing, R. H. (1999) *J. Appl. Cryst.* **32**, 210-217.
5 Oison, V., Katan, C., Rabiller, P., Souhassou, M. and Koenig, C. (2003) *Phys. Rev.* **B67**, 035120, 1-11.

CHARGE-DENSITY STUDY OF THE NON-LINEAR OPTICAL MATERIAL: ZINC (TRIS)THIOUREA SULPHATE

Jacqueline M. Cole,[a] Shamus L. G. Husheer,[a] Dima S. Yufit,[b] Judith A. K. Howard,[b] and Garry J. McIntyre[c]

[a]Department of Chemistry, University of Cambridge, CB2 1EW, UK; [b]Department of Chemistry, University of Durham, DH1 3LE, UK; [c]Institut Laue Langevin, B. P. 156, 38042 Grenoble Cedex 9, France (jmc61@cam.ac.uk)

A charge-density study of the non-linear optical (NLO) material, zinc (tris)thiourea sulphate is presented. The interest lies in the efficiency of the first-order non-linear term, second harmonic generation (SHG), where the laser penetration through the material affects the frequency doubling of light. This work represents one in a series of charge-density studies that we have undertaken in order to unravel and understand the relationships between structure and optical properties [1,2]. In these studies charge-density analysis was used to (i) conduct topologically-based bond-length-alternation type calculations using values of ellipticity, (ii) perform polarization mapping to investigate the nature of intramolecular charge-transfer, and (iii) evaluate the solid-state molecular dipole moment and relate this to the crystal field forces. All of these features play an important role in governing the SHG activity and so structure / property relationships have been built up from this work.

All of these previous investigations have concentrated on organic materials. However, with the subject study, we now extend this type of analysis our investigations to an organometallic compound, zinc (tris)thiourea sulphate, which represents one of few examples of promising organometallic SHG-active materials, many otherwise viable organometallic candidates suffering from reactivity towards air. There is much impetus to study organometallic SHG-active materials since they possess both the major optical advantages of organic materials (eg. very fast optical response and ease of molecular design) *and* those of inorganic materials (principally thermal stability which is the single-most common problem with organics). The results derive from a suitable combination of complementary 100K X-ray and neutron diffraction data, the latter being important for locating the hydrogen atoms precisely. The X-ray data were collected in the laboratory at Durham, UK, on a Bruker SMART diffractometer, whilst the neutron data was collected on the Laue Diffractometer, VIVALDI, at the ILL, Grenoble, France. The results pertaining to the aforementioned analysis methods (i)-(iii) are presented.

References

1 Cole, J. M., Goeta, A. E., McIntyre, G. J. and Howard, J. A. K. (2002) *Acta Crystallogr. B* **58**, 690-700.

2 Cole, J. M., Copley, R. C. B., McIntyre, G. J., Howard, J. A. K., Szablewski, M. and Cross, G. H. (2002). *Phys. Rev. B*, **65**, 125107(1-11).

TOPOLOGICAL CHARACTERIZATION OF INTERMOLECULAR INTERACTIONS

Yu Wang,[a] Chi-Rung Lee,[b] and Chih-Chieh Wang[c]

[a]Department of Chemistry, National Taiwan University, Taipei, Taiwan; [b]Department of Chemical Engineering, Ming-Hsin University of Technology, Hsin-Fong, Taiwan; [c]Department of Chemistry, Soochow University, Taipei, Taiwan (wangyu@ntu.edu.tw)

Topological properties associated with bond critical points (BCP) are applied to intermolecular interactions in order to analyze the role of such interactions in the solid state. One of the important interactions is H-bond, where a very strong symmetric one is similar to a covalent bond, however a very weak one for instance the di-hydrogen bond is also known. The work presented will cover the whole spectrum of these H-bonds with comparison between experiment and theory. In addition, directional interactions between molecules, for example C...S, S...N, N...O interactions, will also be presented. Atomic graph of each atom will be applied to illustrate such directional weak interactions. Packing effects on the chemical bond is investigated through a systematic computation on the designed clusters. In general, the density ρ_b, the total energy density H_b and the Laplacian, $\nabla^2\rho_b$, at the BCP will be the main indices for the characterization of the intermolecular interactions.

TOPOLOGICAL FEATURES OF THE ELECTRON DENSITY AND THE BASIN PROPERTIES IN SOLIDS

A. Martín Pendás

Departamento Quimica Fisica y Analitica, Universidad de Oviedo, 33006 Oviedo. Spain (angel@fluor.quimica.uniovi.es)

The application of the Theory of Atoms in Molecules (AIM) to condensed phase systems [1,2] displays interesting peculiarities, emerging from the necessarily finite size of atomic basins that leads to unambiguous atomic volumes and atomic radii [3]. It also facilitates the introduction of a number of simple indices to characterize different chemical interactions [4]. Our ability to manipulate interatomic distances in such systems by means of external constraints (stress, pressure, temperature), opens a vast field that connects atomic properties with thermodynamic variables. In this work we will present some of these ideas taken from our experience in solids. We will also show how our conventional chemical intuition developed within the molecular realm may fail far from equilibrium configurations, and how the systematic study of the electron density in solids may help us develop new ideas [5].

References

1 Martín Pendás, A., Costales, A. and Luaña, V. (1997) *Phys. Rev. B* **55**, 4275.

2 Luaña, V., Costales, A. and Martín Pendás, A. (1997) *Phys. Rev. B* **55**, 4285.

3 Martín Pendás, A., Costales, A. and Luaña, V. (1998) *J. Phys. Chem. B* **102**, 6937.

4 Mori Sánchez, P., Martín Pendás, A., and Luaña, V. (2002) *J. Am. Chem. Soc.* **124**, 14721.

5 Mori Sánchez, P., Martín Pendás A. and Luaña, V. (2001) *Phys. Rev. B* **63** 125103-1; Martín Pendás, A., Costales, A., Blanco, M. A., Recio, J. M. and Luaña, V. (2000) *Phys. Rev. B* **62**, 13970.

AD HOC

WORKSHOP

PROGRAMS

Australian Synchrotron Project Workshop
Monday August 11
Room A 14:00 – 16:00

Convener: Richard Garrett

Australia's national 3GeV third-generation synchrotron, to be completed in 2007, will be located at Monash University. With a circumference of 216.0m, the storage ring will have twelve straight sections available for insertion devices. An initial suite of 9 beamlines is planned, with the facility eventually accommodating over 30.

Crystallographic research in the protein, powder and small-molecule fields should be catered for at the Australian Synchrotron. The preliminary requirements of crystallographic beamlines were identified at a synchrotron workshop in Melbourne earlier this year. This workshop will be used to fine-tune these specifications and identify key scientific reasons why beamlines supporting crystallographic applications should be part of the initial suite.

The workshop format will be:

- An overview of the status of the ASP and of the synchrotron facilities currently available to researchers via the ASRP.

- Presentation of the draft scientific cases for the crystallography beamlines.

- Break-out groups will review the scientific cases and ensure these are compatible with the technical features of the proposed beamline.

This workshop is supported by the Australian Synchrotron Program, DIIRD, Government of Victoria.

Twinning Workshop
Monday August 11
Room B 14:00 – 16:00

Convener: Victor G Young

A 2-hour workshop will cover aspects of twinning from the basics of identification to the advanced topics of how to handle the refinement of merohedral, pseudo-merohedral and non-merohedral twins.
A number of short presentations will be given on the various subtopics, and a workbook will be provided. The presentations will be interspersed with short assignments in the workbook. Some examples will be provided on CD-ROM for further work once the attendees return to their home laboratories.
There is no participation fee, however the number of participants will be limited.

Modulated Structures Workshop
Tuesday August 12
Room A 14:00 – 16:00

Convener: Siegbert Schmid

Systems that form modulated structures are a fascinating class of materials that lack conventional lattice periodicity but are still perfectly long-range ordered. Such systems exist across the whole range of chemical disciplines from organic conductors and minerals to ceramic materials like high-T_c superconductors and ferroelectrics.

A workshop will investigate many of the basic features of modulated structures. In particular we will examine the types of modulated structures, how to recognise them and what to do about data collection, structure solution and refinement strategies. This introductory workshop is aimed at scientists that have limited or no experience with modulated structures. There is no participation fee but numbers are limited, so registration is essential.

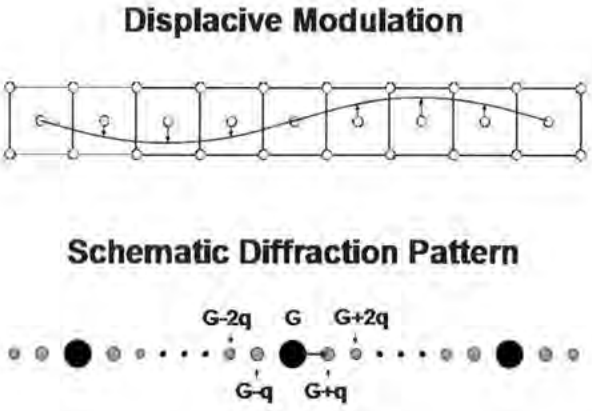

Figure 1: Schematic representation of a displacive modulation and a corresponding diffraction pattern. The structure can either be described as an 8-times superstructure of the basic two-atom unit cell or with that basic structure and the modulation wave parameters. The diffraction pattern indicates a clear intensity hierarchy between main

CCP4 Workshop
Thursday August 14
Room A 14:00 – 18:00

14:00 Introduction and Welcome **(Alun Ashton)**

14:05 CCP4 the organisation, the package (installing etc), General Overview
CCP4i **(Alun Ashton)**

14.45 Data Processing and Scaling with Mosflm and Scala.
(Harry Powell)

15.30 Overview of Molecular Replacement in CCP4
(Katherine McAuley)

16:00 Break

16.15 Advanced and Future strategies for MR
Advanced and Future strategies for Experimental Phasing
(Airlie McCoy)

17.00 Refinement with CCP4/Refmac **(Airlie McCoy)**

17.45 CCP4 and its future projects

18.00 Close

AUTHOR

INDEX